

canadian acoustics

acoustique canadienne

Journal of the Canadian Acoustical Association - Journal de l'Association Canadienne d'Acoustique

SEPTEMBER 2006

Volume 34 -- Number 3

SEPTEMBRE 2006

Volume 34 -- Numéro 3

EDITORIAL / EDITORIAL

3

PROCEEDINGS OF THE ACOUSTICS WEEK IN CANADA 2006/ ACTES DE LA SEMAINE CANADIENNE D'ACOUSTIQUE 2006

Table of Contents / Table des matières

4

Conference Calendar

9

Plenary Session

14

Hearing Conservation I

16

Musical Cognition/ Musical Acoustics I

22

Noise Control I

28

Musical Cognition/ Musical Acoustics II

34

Noise Control II

42

Underwater Acoustics

50

Hearing Conservation II

60

Bio-Acoustics I

70

Cooling Fan Acoustics

74

Bio-Acoustics II

84

Architectural Acoustics

86

Speech and Hearing Sciences I

94

Sensors, Probes and Arrays

98

Speech and Hearing Sciences II

106

High Frequency Acoustics/Communications

112

Abstracts for Presentations without Summary Papers

120

Other Features / Autres Rubriques

News / Informations

128

PROCEEDINGS

ACOUSTICS WEEK IN CANADA

SEMAINE CANADIENNE D'ACOUSTIQUE

ACOUSTICS WEEK IN CANADA

SEMAINE CANADIENNE D'ACOUSTIQUE

ACOUSTIC WEEK IN CANADA

SEMAINE CANADIENNE D'ACOUSTIQUE

ACOUSTICS WEEK IN CANADA

SEMAINE CANADIENNE D'ACOUSTIQUE

CAHIERS DES ACTES

canadian acoustics

THE CANADIAN ACOUSTICAL ASSOCIATION
P.O. BOX 1351, STATION "F"
TORONTO, ONTARIO M4Y 2V9

CANADIAN ACOUSTICS publishes refereed articles and news items on all aspects of acoustics and vibration. Articles reporting new research or applications, as well as review or tutorial papers and shorter technical notes are welcomed, in English or in French. Submissions should be sent directly to the Editor-in-Chief. Complete instructions to authors concerning the required camera-ready copy are presented at the end of this issue.

CANADIAN ACOUSTICS is published four times a year - in March, June, September and December. The deadline for submission of material is the first day of the month preceeding the issue month. Copyright on articles is held by the author(s), who should be contacted regarding reproduction. Annual subscription: \$20 (student); \$60 (individual, institution); \$250 (sustaining - see back cover). Back issues (when available) may be obtained from the CAA Secretary - price \$10 including postage. Advertisement prices: \$600 (centre spread); \$300 (full page); \$175 (half page); \$125 (quarter page). Contact the Associate Editor (advertising) to place advertisements. Canadian Publication Mail Product Sales Agreement No. 0557188.

acoustique canadienne

L'ASSOCIATION CANADIENNE D'ACOUSTIQUE
C.P. 1351, SUCCURSALE "F"
TORONTO, ONTARIO M4Y 2V9

ACOUSTIQUE CANADIENNE publie des articles arbitrés et des informations sur tous les domaines de l'acoustique et des vibrations. On invite les auteurs à soumettre des manuscrits, rédigés en français ou en anglais, concernant des travaux inédits, des états de question ou des notes techniques. Les soumissions doivent être envoyées au rédacteur en chef. Les instructions pour la présentation des textes sont exposées à la fin de cette publication.

ACOUSTIQUE CANADIENNE est publiée quatre fois par année - en mars, juin, septembre et décembre. La date de tombée pour la soumission de matériel est fixée au premier jour du mois précédant la publication d'un numéro donné. Les droits d'auteur d'un article appartiennent à (aux) auteur(s). Toute demande de reproduction doit leur être acheminée. Abonnement annuel: \$20 (étudiant); \$60 (individu, société); \$150 (soutien - voir la couverture arrière). D'anciens numéros (non-épuisés) peuvent être obtenus du Secrétaire de l'ACA - prix: \$10 (affranchissement inclus). Prix d'annonces publicitaires: \$600 (page double); \$300 (page pleine); \$175 (demi page); \$125 (quart de page). Contacter le rédacteur associé (publicité) afin de placer des annonces. Société canadienne des postes - Envois de publications canadiennes - Numéro de convention 0557188.

EDITOR-IN-CHIEF / RÉDACTEUR EN CHEF

Ramani Ramakrishnan
Department of Architectural Science
Ryerson University
350 Victoria Street
Toronto, Ontario M5B 2K3
Tel: (416) 979-5000; Ext: 6508
Fax: (416) 979-5353
E-mail: rramakri@ryerson.ca

EDITOR / RÉDACTEUR

Chantai Laroche
Programme d'audiologie et d'orthophonie
École des sciences de la réadaptation
Université d'Ottawa
451, chemin Smyth, pièce 3062
Ottawa, Ontario K1H 8M5
Tél: (613) 562-5800 # 3066; Fax: (613) 562-5428
E-mail: claroche@uottawa.ca

ASSOCIATE EDITORS / REDACTEURS ASSOCIES

Advertising / Publicité

Jason Tsang
RWDI AIR Inc.
650 Woodlawn Road
Guelph, Ontario N1K 1B8
Tel: (519) 823-1311, #2277
Fax: (519) 823-1316
E-mail: Jason.Tsang@rwdi.com

News / Informations

Steven Bilawchuk
aci Acoustical Consultants Inc.
Suite 107, 9920-63rd Avenue
Edmonton, Alberta T6E 0G9
Tel: (780) 414-6373
Fax: (780) 414-6376
E-mail: stevenb@aciacoustical.com



CAA Halifax 2006

Citadel Halifax Hotel

1960 Brunswick St., Halifax, Nova Scotia

11-13 October 2006

ORGANIZING COMMITTEE

Nicole Collison, Conference Chair
Francine Desharnais, Technical Chair
Joe Hood and Derek Burnett, Exhibit Coordinators
Dave Chapman, Treasurer
Dave Stredulinsky, Webmaster
Cheryl Munroe, Registration and All-round Logistics
Jim Milne, Audiovisual and Technical Logistics

Sponsors

JASCO Research Ltd.
Bruel & Kjaer North America Inc.
Akoostix Inc.
Jade Acoustics Inc.

Exhibitors

JASCO Research Ltd.
Bruel & Kjaer North America Inc.
Scantek Inc.
H. L. Blachford Ltd.
Eckel Industries of Canada Ltd.
SounDivide Inc.
Owens Corning Canada

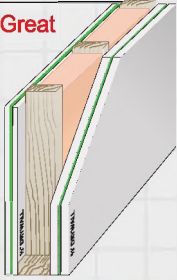
The organizing committee extends a grateful acknowledgment to Marie-Noel Matthews for French translation assistance.

SUPERIOR SOUND ISOLATION

Visit greengluecompany.com to learn more

Green Glue Assembly

Low Frequency: Great
56 STC Rating
39 OITC



Soundboard

Low Frequency: Poor
46 STC Rating
32 OITC

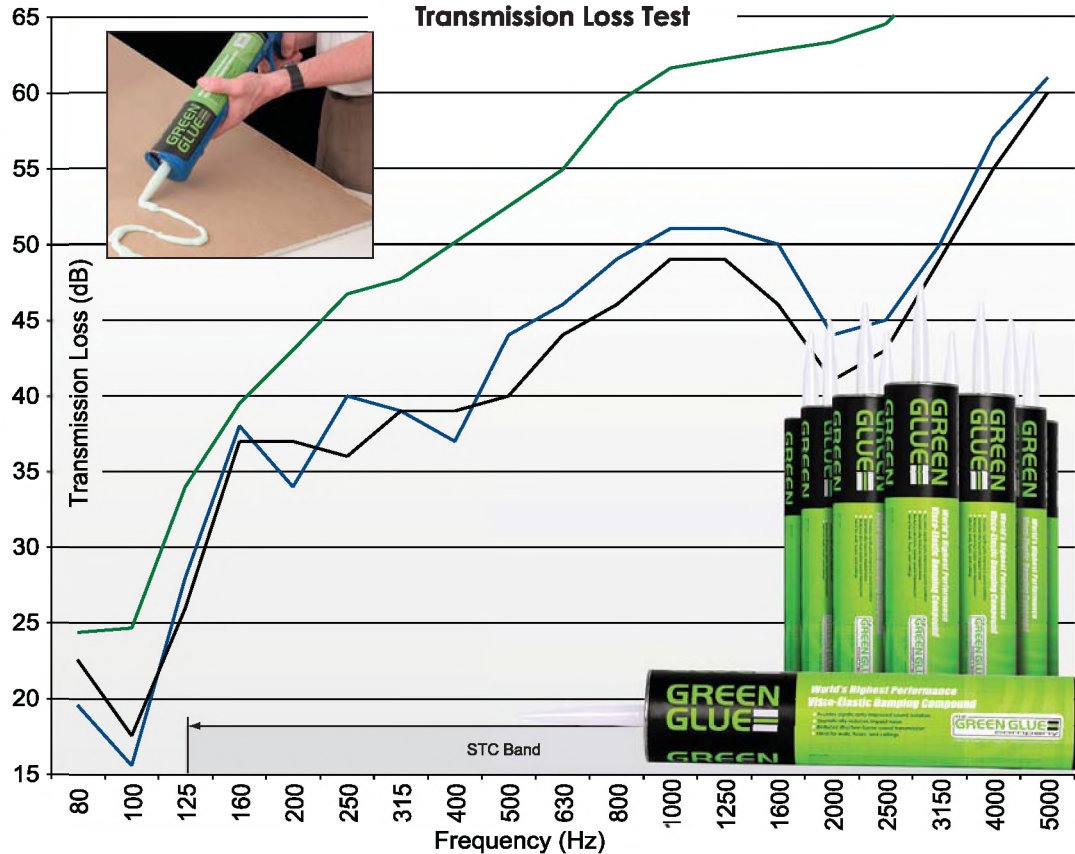


Conventional Drywall

Low Frequency: Poor
44 STC Rating
33 OITC



■ Green Glue Assembly OL 05-0414
 ■ Soundboard Assembly OL 05-1056
 ■ Conventional Drywall OL 05-1059



FOR SUPERIOR WALLS & FLOORS

GREEN GLUE

THIRD PARTY
NVLAP
ACCREDITED LAB
results are available at
greengluecompany.com

Large commercial job?
Green Glue is available in large
55 gallon drum and 5 gallon
pails for commercial use.



Sound isolation problems are low frequency problems

Most sound isolation problems occur at frequencies below 125 Hz. Sources include subwoofers, auto and air traffic. Unfortunately the common STC system does not consider performance below 125 Hz. and that's where most of your problems are.

www.greengluecompany.com
info@greengluecompany.com
Sales: (989) 832-1602

- Superior Low Frequency Isolation
- Low Cost per square foot
- Easy Application
- Can be used over existing walls
- Dramatically reduces impact noise
- Reduces structure-borne sound transmission
- Ideal for walls, floor, and ceiling
- Third party NVLAP accredited lab results are available online.

THE
GREEN GLUE
company

EDITORIAL / EDITORIAL

Welcome to the proceedings of the CAA Halifax 2006 conference. It has been four years since the annual meeting has been in the Maritimes, and much longer since it was held in Halifax. We are very excited to be hosting this year's meeting and want to thank you for contributing to this acoustically diverse event.

There are two plenary speakers, Dennis Jones and Michael Kiefte, and eleven special sessions on a range of acoustical topics. There is no single theme to this year's meeting; the sessions include papers on many aspects of acoustics, such as architectural, hearing and speech, biological, physical, musical, and underwater acoustics, as well as communications, noise control, and sensors, probes and arrays. We are thrilled about the diversity of the topics and look forward to the interaction of so many people from the various disciplines. We believe that one of the best aspects of the annual CAA meeting is the opportunity for all of us to learn from each other!

My thanks to everyone that has assisted in making this conference a success so far: my excellent organizing committee, our exhibitors and sponsors, the special session chairs, the paper contributors, and everyone that has been so enthusiastic about meeting in Halifax!

We are looking forward to seeing you here,

Nicole Collison

Bienvenue au congrès annuel 2006 de l'ACA à Halifax. Il y a déjà quatre ans que les provinces maritimes ont accueilli ce congrès et plus longtemps encore la ville d'Halifax. Nous sommes très heureux d'être les hôtes cette année et nous voulons vous remercier pour votre contribution à cet événement acoustique.

Il y a deux conférenciers invités, Dennis Jones et Michael Kiefte, et onze sessions spéciales portant sur différents sujets reliés à l'acoustique. Le congrès de cette année ne cible aucun thème particulier. Les sessions incluent des présentations et des textes qui touchent plusieurs aspects de l'acoustique comme: l'audition et la parole, l'acoustique architectural, biologique, physique, musicale, sous-marine, la communication, le control du bruit, ainsi que sur senseurs, sondes et réseaux. Nous sommes ravis de la diversité des sujets et des possibilités d'interactions entre les gens de disciplines différentes. Nous croyons que l'un des plus beaux aspects de cette rencontre annuelle de l'ACA est l'opportunité que nous avons d'apprendre de chacun.

Je voudrais remercier toutes les personnes qui ont participé à faire de ce congrès un succès jusqu'à maintenant: mon comité organisateur, nos exposants et commanditaires, les présidents des sessions spéciales, les gens qui ont contribué aux articles et tous ceux qui ont été si enthousiastes au sujet de cette rencontre à Halifax!

Nous avons hâte de vous voir,

Nicole Collison

WHAT'S NEW ??

Promotions
Deaths
New jobs
Moves

Retirements
Degrees awarded
Distinctions
Other news

Do you have any news that you would like to share with Canadian Acoustics readers? If so, send it to:

Steven Bilawchuk, aci Acoustical Consultants Inc., Edmonton, Alberta, Email: stevenb@aciacoustical.com

QUOI DE NEUF ?

Promotions
Décès
Offre d'emploi
Déménagements

Retraites
Obtention de diplômes
Distinctions
Autres nouvelles

Avez-vous des nouvelles que vous aimeriez partager

TABLE OF CONTENTS/TABLES DES MATIÈRES

Organising Committee, Sponsors and Exhibitors	1
Editorial/Éditorial	3
Table of Contents/Tables des matières	4
Conference Calendar	9
Plenary Session	
Voice-Printing the Hermit Thrush (<i>Catharus guttatus</i>) Dennis Jones	14
Hearing Conservation I	
Impulse Noise Hazard: What Do We Know? Alberto Behar	16
Impulse Measurement Considerations in Setting Occupational Noise Criteria Tim Kelsall	18
“AlarmLocator”: A software tool to facilitate the installation of acoustic warning devices in noisy work plants Rida Al Osman, Christian Giguère, and Chantal Laroche	20
Musical Cognition/Musical Acoustics I	
Perceived Holistic Health Effects of Three Levels of Music Participation Betty A. Bailey	22
The Emotionality of Music: Death Metal to Amazing Grace Elysia Iversen and Jane F. MacNeil	24
Investigating the Sound of an African Thumb Piano (Kalimba) David M. F. Chapman	26
Noise Control I	
A Critical Analysis of Loudness Calculation Methods Jeff Defoe, Colin Novak, and Helen Ule	28
A Critical Analysis of Loudness Calculation Methods Jérémie Voix, Lee D. Hager, and Jean Zeidan	30
Classification and Comparison of methods for characterising sound absorbing porous materials Yacoubou Salissou and Raymond Panneton	32
Musical Cognition/Musical Acoustics II	
The affect of short musical sequences with different melodic contours Joshua Salmon and Bradley Frankland	34
An Initial Exploration of Parallelism in Music: Equi-Temporal Three-Tone Diatonic Sequences B. W. Frankland	36

Can Silence Affect Perception?: Duration and Frequency of Occurrence in Perceived Pitch Structure Michael E. Lantz and Lola L. Cuddy	38
The Role of Music, Sound Effects & Speech on Absorption in a Film: The Congruence-Associationist Model of Media Cognition Annabel J. Cohen, Kelti MacMillan, and Robert Drew	40
Noise Control II	
Error Bounds, Uncertainties and Confidence Limits of Outdoor Sound Propagation Nicholas Sylvestre-Williams and Ramani Ramakrishnan	42
Acoustic Performance Investigation of Perforated Muffler Design using a One Dimensional Segment Model Jun Zuo, Collin Novak, Helen Ule, and Robert Gaspar	44
Experimental Evaluation of Automotive Cabin Noise using Various Noise and Vibration Measurement Techniques Neb Radic, Colin Novak, and Helen Ule	46
The Use of Environmental Noise Standards and Guidelines in Canada Bill Gastmeier	48
Underwater Acoustics	
Automatic classification of impulsive-source active sonar echoes using perceptual signal features from musical acoustics Victor W. Young, Paul C. Hines, and Sean Pecknold	50
Geoacoustic inversion in a range-dependent environment under the assumption of range independence Michael G. Morley, Stan E. Dosso, and N. Ross Chapman	52
Quantifying ocean acoustic environmental sensitivity Stan E. Dosso, Diana F. McCammon, Peter M. Giles, Sean Pecknold, and Paul C. Hines	54
Acoustic source localization with environmental uncertainty Stan E. Dosso and Michael J. Wilmut	56
Sound pressure and particle velocity measurements from marine pile driving with bubble curtain mitigation Alex MacGillivray and Roberto Racca	58
Hearing Conservation II	
An Acoustical Study of iPod Output: Effects of Headsets and Control Settings Desiree Pereira, Shaun Sharma and Kathy Pichora-Fuller	60
Relating Use of Portable Audio Devices to Audiometric Thresholds in University Students Brenda Garrido, Andrew Gross and Kathy Pichora-Fuller	62
A Survey of the Use of Portable Audio Devices by University Students Shazia Ahmed, Matthew King, Timothy W. Morrish, Ewelina Zaszewska, and Kathy Pichora-Fuller	64
An Acoustical Study of iPod Use by University Students in Quiet and Noisy Situations Sina Fallah and Kathy Pichora-Fuller	66
Bio-acoustics I	
Localization of Right Whales using Matched Correlation Processing Gordon R. Ebbeson and Francine Desharnais	70

Utility of acoustic location technology for studying avian dawn choruses: social dynamics of male black-capped chickadees
Jennifer Foote, Daniel Mennill, and Laurene Ratcliffe 72

Cooling Fan Acoustics

Design and Testing of a Thermoacoustic System for Thermal Management 74
Masoud Akhavanbazaz, M. H. Kamran Siddiqui, and Rama B. Bhat

Computational Aeroacoustics for Electronics Coolers 76
Jeff Defoe and Colin Novak

Graphics Processing Unit Cooling Solutions: Acoustic Characteristics 78
Matt Nantais, Colin Novak, and Jeff Defoe

The Effect of Varying Heat Sink Fin Distances from Cooling Fan Blade Tip on Noise Emissions 80
Helen Ule, Colin Novak, and Robert Gaspar

Comparative Study of Noise and Vibration Measurements of Computer Cooling Fans 82
Colin Novak, Helen Ule, and Robert Gaspar

Bio-acoustics II

Automated detection of white whale (*Delphinapterus leucas*) vocalizations in St. Lawrence estuary and occurrence pattern
Catherine Bédard and Yvan Simard 84

Architectural Acoustics

The effect of localized sound leaks on the speech privacy of closed rooms 86
Bradford N. Gover and John S. Bradley

Guide for flanking sound transmission in wood framed construction 88
J. David Quirt, Trevor R.T. Nightingale, and Frances King

On Estimating Sound Power from A Few Single Point Measurements 90
Werner Richarz

The Effect of Ancillary Volume on Sound Transmission Measurements Using ASTM Standard Test Method E336 92
Frances King and Trevor R.T. Nightingale

Speech and Hearing Sciences I

A Cross-language Vowel Normalisation Procedure 94
Geoffrey Stewart Morrison and Terrance M. Nearey

Conversational Speech Intensity under Different Noise Conditions in Hypophonia and Parkinson's Disease 96
Scott Adams, Allyson Dykstra, Kayla Abrams, Jennifer Winnell, Mary Jenkins, and Mandar Jog

Sensors, Probes, and Arrays

Directivity Patterns for a Short Line Array of Barrel-stave Flextensional Transducers 98
Dennis F. Jones

Underwater Communications Testing of the Multi-Mode Pipe Projector 100
Richard Fleming, Donald Mosher, Joe Hood, Sean Spears, and Charles Reithmeier

Effect of Cardioid and Limaçon Directional Sensors on Towed Array Reverberation Response Dale Ellis	102
Spherical Microphone Arrays for Analysis of Sound Fields in Buildings Bradford N. Gover	104
Speech and Hearing Sciences II	
The Effect of Sentence Repetition on Speech Intelligibility in Noise Roxanne Larose, Isabelle Mercille, Christian Giguère, Chantal Laroche, Véronique Vaillancourt	106
The Role of Formant Amplitude in the Perception of /i/ and /u/ in Normal Hearing Listeners Lacey Marshall, Teresa Enright, and Michael Kieffe	108
Hearing and Cognitive Performance in Low-Frequency Noise Ann M. Nakashima, Sharon M. Abel, Matthew Duncan and David Smith	110
High Frequency Acoustics/Communications	
Radiated noise and wake acoustic measurements around a maneuvering ship Mark Trevorror, Boris Vasiliev, and Svein Vagle	112
Modelling Pulse-to-pulse Coherent Doppler Sonar Len Zedel	114
High Frequency Broadband Acoustic Channel Estimation Error Analysis for St. Margaret's Bay during the Unet06 Demonstrations Paul Gendron and Garry Heard	116

SOUND SOLUTIONS FROM



Integrated Solutions from World Leaders

- Precision Measurement Microphones
- Intensity Probes
- Outdoor Microphones
- Hydrophones
- Ear Simulation Devices
- Speech Simulation Devices
- Calibrators
- Array Microphones
- Sound Quality
- Sound Intensity
- Sound Power
- Room Acoustics
- Noise Monitoring
- Dynamic Signal Analyzers
- Multi Channel Dynamic Analyzer/Recorders
- Electro Dynamic Shaker Systems
- Advanced Sound & Vibration Level Meters
- Doppler Laser Optical Transducers (Laser Vibrometers)



MetroLaser, Inc. 



Ottawa

200-440 Laurier Ave. West, K1R 7X6
 613-598-0026 fax: 616-598-0019
 info@noveldynamics.com



Toronto

RR#2 13652 4th Line. Acton, Ont. L7J 2L8
 519-853-4495 fax: 519-853-3366
 metelka@aztec-net.com

CONFERENCE PROGRAM – CAA HALIFAX 2006

TUESDAY, 10 OCTOBER 2006

1700 – 2100	CAA Board of Directors Meeting – Salon 7
1700 – 1900	Opening Registration

WEDNESDAY, 11 OCTOBER 2006

0800 – 1530	Conference Registration		
0845 – 0900	Conference Opening		
0900 – 1000	Plenary Session in Terrace Room: Voice-Printing the Hermit Thrush (<i>Catharus guttatus</i>) Dennis Jones		
1000 – 1040 Coffee Break – Terrace Patio			
Terrace Room East		Terrace Room West	
Hearing Conservation I, Chair: Behar		Musical Cognition/Musical Acoustics I, Chair: Cohen	
1040	Impulse Noise Hazard: What Do We Know? – Behar	1040	Perceived Holistic Health Effects of Three Levels of Music Participation – Bailey
1100	Impulse Measurement Considerations in Setting Occupational Noise Criteria – Kelsall	1100	The Emotionality of Music: Death Metal to Amazing Grace – Iversen and MacNeil
1120	In-depth Analysis of Workplace Noise Utilizing a Computer-based Process – Whitehead	1120	Agerian music: Genre classification – Fergani and Houacine
1140	"AlarmLocator": A software tool to facilitate the installation of acoustic warning devices in noisy work plants – Al Osman <i>et al.</i>	1140	Investigating the Sound of an African Thumb Piano (Kalimba) – D. Chapman

1200 – 1300 Lunch – Cavalier Room			
Noise Control I, Chair: Sherry		Musical Cognition/Musical Acoustics II, Chair: Cohen	
1300	Atténuation effective apportée par l'utilisation d'une double protection auditive – Voix <i>et al.</i>	1300	The affect of short musical sequences with different melodic contours – Salmon and Frankland
1320	A Critical Analysis of Loudness Calculation Methods – Defoe <i>et al.</i>	1320	An Initial Exploration of Parallelism in Music: Equi-Temporal Three-Tone Diatonic Sequences - Frankland
1340	Experimental Validation of the Objective Measurement of Individual Custom Earplug Field Performance – Voix <i>et al.</i>	1340	Can Silence Affect Perception?: Duration and Frequency of Occurrence in Perceived Pitch Structure – Lantz and Cuddy
1400	Classification and Comparison of methods for characterising sound absorbing porous materials – Salissou and Panneton	1400	The Role of Music, Sound Effects & Speech on Absorption in a Film: The Congruence-Associationist Model of Media Cognition – Cohen <i>et al.</i>
1420 – 1500 Coffee Break – Terrace Patio			
Noise Control II, Chair: Sherry		Underwater Acoustics, Chair: Pecknold	
1500	Error Bounds, Uncertainties and Confidence Limits of Outdoor Sound Propagation - Sylvestre-Williams and Ramakrishnan	1500	Automatic classification of impulsive-source active sonar echoes using perceptual signal features from musical acoustics – Young <i>et al.</i>
1520	Acoustic Performance Investigation of Perforated Muffler Design using a One Dimensional Segment Model – Zuo <i>et al.</i>	1520	Geoacoustic inversion in a range-dependent environment under the assumption of range independence – Morley <i>et al.</i>
1540	Experimental Evaluation of Automotive Cabin Noise using Various Noise and Vibration Measurement Techniques – Radic <i>et al.</i>	1540	Quantifying ocean acoustic environmental sensitivity – Dosso <i>et al.</i>
1600	CSA Z107.10 Acoustical Standards in Canada – Sherry	1600	A Preliminary Study on the Geoacoustic Parameters of Gassy Sediments in St. Margaret's Bay, Nova Scotia. – R. Matthews <i>et al.</i>
1620	The Use of Environmental Noise Standards and Guidelines in Canada – Gastmeier	1620	Acoustic source localization with environmental uncertainty – Dosso and Wilmut
1640	Exact acoustical analysis of sound radiation from free vibration of rectangular Mindlin plates – Khorshidi <i>et al.</i>	1640	Sound pressure and particle velocity measurements from marine pile driving with bubble curtain mitigation – MacGillivray and Racca
1715-2230	CSA Standards Meeting – open to all interested persons in Salon 7, with field-trip to Ice Breaker		
1800-2000	CAA Halifax 2006 Ice Breaker at Ginger's featuring Gypsophilia		

THURSDAY, 12 OCTOBER 2006

0800 – 1530	Conference Registration		
0830 – 1700	Exhibits Open in Terrace Patio		
0900 – 1000	Plenary Session: Variability in speech production and consequences for theories of speech perception Michael Kieffe		
1000 – 1040 Coffee Break – Terrace Patio			
Terrace Room East		Terrace Room West	
Hearing Conservation II, Chair: Behar		Bio-acoustics I, Chair: Laurinolli	
1040	An Acoustical Study of iPod Output: Effects of Headsets and Control Settings – Pereira <i>et al.</i>	1040	Localization of Right Whales using Matched Correlation Processing – Ebbeson and Desharnais
1100	Relating Use of Portable Audio Devices to Audiometric Thresholds in University Students – Garrido <i>et al.</i>	1100	Utility of acoustic location technology for studying avian dawn choruses: social dynamics of male black-capped chickadees – Foote <i>et al.</i>
1120	A Survey of the Use of Portable Audio Devices by University Students – Ahmed <i>et al.</i>	1120	A remotely-piloted acoustic array for studying sperm whale vocal behaviour – Schulz <i>et al.</i>
1140	An Acoustical Study of iPod Use by University Students in Quiet and Noisy Situations – Fallah and Pichora-Fuller	1140	Estimating the Acoustic Exposure of Marine Mammals to Underwater Noise – Carr and Frankel
1200 – 1300 Lunch – Cavalier Room			
Cooling Fan Acoustics, Chair: Novak		Bio-acoustics II, Chair: Laurinolli	
1300	Design and Testing of a Thermoacoustic System for Thermal Management – Akhavanbazaz <i>et al.</i>	1300	Comparing cricket ears – Morris
1320	Computational Aeroacoustics for Electronics Coolers – Defoe and Novak	1320	Automated detection of white whale (<i>Delphinapterus leucas</i>) vocalizations in St. Lawrence estuary and occurrence pattern – Bédard and Simard
1340	Graphics Processing Unit Cooling Solutions: Acoustic Characteristics – Nantais <i>et al.</i>	1340	Comparison of algorithms for the automatic recognition of Balaenopterid whale calls in noisy environment – Mouy <i>et al.</i>
1400	The Effect of Varying Heat Sink Fin Distances from Cooling Fan Blade Tip on Noise Emissions – Ule <i>et al.</i>	1400	ROCCA: A new tool for real-time acoustic species identification of delphinid whistles – Oswald <i>et al.</i>
1420	Comparative Study of Noise and Vibration Measurements of Computer Cooling Fans – Novak <i>et al.</i>		
1440 – 1520 Coffee Break – Terrace Patio			

Architectural Acoustics, Chair: Quirt		Physical Acoustics, Chair: Mastikhin	
1520	The effect of localized sound leaks on the speech privacy of closed rooms – Gover and Bradley	1520	An environmental noise impact assessment and forecasting tool for military training activities – Carr <i>et al.</i>
1540	Guide for flanking sound transmission in wood framed construction – Quirt <i>et al.</i>	1540	Magnetic Resonance Imaging of Acoustic Streaming in Gases – Newling <i>et al.</i>
1600	On Estimating Sound Power from A Few Single Point Measurements - Richarz	1600	Dynamics of the sonoluminescing bubble – Djurkovic <i>et al.</i>
1620	The Effect of Ancillary Volume on Sound Transmission Measurements Using ASTM Standard Test Method E336 – King and Nightingale	1620	Molecular dynamics simulation of the response of a gas to a spherical piston: Implications for sonoluminescence – Ruuth <i>et al.</i>
1640	Noise Control Provisions in Canada's Building Codes – Quirt and Nightingale	1640	Spatially resolved NMR relaxation of cavitating liquid – Mastikhin and Newling
1715 – 1815	CAA/ACA Annual General Meeting – Terrace Room		
1830 – 1930	Banquet Reception/Cocktails – Cavalier Room featuring pianist Harry Bentham		
1930 ⇒	Conference Banquet and Awards Ceremony – Cavalier Room featuring pianist Harry Bentham		

FRIDAY, 13 OCTOBER 2006

0800 – 1030	Conference Registration		
0800 – 1200	Exhibits Open in Terrace Patio		
Terrace Room East		Terrace Room West	
Speech and Hearing Sciences I, Chair: Adams		Sensors, Probes, and Arrays, Chair: Gover	
0820	A cross-language vowel normalisation procedure – Morrison and Nearey	0820	Directivity patterns for a short line array of barrel-stave flextensional transducers – Jones
0840	An acoustic study of the African Nova-Scotian English vowel systems in North Preston and North Halifax – Moloissa <i>et al.</i>	0840	Underwater Communications Testing of the Multi-Mode Pipe Projector – Flemming <i>et al.</i>
0900	Objective Speech Quality Evaluation Using Markov Chain Monte Carlo Methods – Chen and Parsa	0900	Effect of cardioid and limaçon directional sensors on towed array reverberation response – Ellis
0920	Conversational Speech Intensity under Different Noise Conditions in Hypophonia and Parkinson's Disease – Adams <i>et al.</i>	0920	Spherical microphone arrays for analysis of sound fields in buildings – Gover
0940 – 1000 Coffee Break – Terrace Patio			

Speech and Hearing Sciences II, Chair: Adams		High Frequency Acoustics/Communications, Chair: Crawford	
1020	The effect of sentence repetition on speech intelligibility in noise – Larose <i>et al.</i>	1020	Radiated noise and wake acoustic measurements around a maneuvering ship – Trevorrow <i>et al.</i>
1040	Pitch perception of young cochlear implant users and normal hearing peers – McKinnon	1040	Modelling Pulse-to-pulse Coherent Doppler Sonar – Zedel
1100	The role of formant amplitude in the perception of /i/ and /u/ in normal hearing listeners – Marshall <i>et al.</i>	1100	High frequency broadband acoustic channel estimation error analysis for St. Margaret's Bay during the Unet06 demonstrations – Gendron and Heard
1120	Making young ears old (and old ears even older): Simulating a loss of synchrony – MacDonald <i>et al.</i>	1120	High frequency acoustic observations of episodic mixing events in Lunenburg Bay – Schillinger and Hay
1140	Hearing and Cognitive Performance in Low-Frequency Noise – Nakashima <i>et al.</i>	1140	High-frequency acoustic imaging of bio-degradation of wave-formed sand ripples on the inner continental shelf – Hay
1200 – 1300 Lunch and Student Presentation Awards– Cavalier Room			

VOICE-PRINTING THE HERMIT THRUSH (*CATHARUS GUTTATUS*)

Dennis F. Jones

Scientific Consultant, 38 Columbo Drive, Dartmouth, NS, Canada B2X 3L8

1. INTRODUCTION

Each spring many migratory birds return to the woodlands of Nova Scotia. Among them is the secretive Hermit Thrush (*Catharus guttatus*), one of the most gifted songbirds in North America. Arriving in April, this bird sings well into the summer and migrates south as late as October. The Hermit Thrush is more often heard than seen, preferring to hide under the cover of leaves. The male shown in Fig. 1 was observed prior to foliation.

Sixty years ago, when spectrographic analysis of sound was in its infancy, Koenig et al. [1] published one of the first spectrograms of a Hermit Thrush song, along with several other bird vocalizations. In later years, Stein [2] noted that songs of individual Hermit Thrushes were quite different, Borror [3] found that each male had a repertoire of up to thirteen songs, and Rivers and Kroodsma [4] compared the songs of Arizona and New England birds.

Motivated by these earlier works, the author recorded and analyzed Hermit Thrush songs of birds living in and around the city of Halifax. The objective was to develop a database of voice-prints for individual birds and use it to acoustically identify them from one breeding season to the next.

2. RECORDING METHOD

From the outset, the modus operandi was to obtain audio recordings from birds in the most non-intrusive way possible. To this end, only birds located adjacent to roads or park trails were recorded. None of the birds were banded, marked, stalked or flushed out of hiding.

All of the audio recordings were made using Sony digital video camera recorders. A DCR-TRV525 was used in 2003 but in 2004 the author upgraded to a DCR-VX2100. The sampling rate was 48 kHz with 16 bit quantization. The more sophisticated DCR-VX2100 camera had a recording level meter for adjusting the input audio level. When the bird was not visible, the camera was simply pointed in the direction of the sound source.

Audio files in 'wav' format were extracted from Digital 8 and Mini DV video cassettes used by the DCR-TRV525 and DCR-VX2100 cameras, respectively. Spectral analysis was carried out using the Raven 1.2.1 interactive sound analysis software developed at the Cornell Lab of Ornithology.



Fig. 1. Video frame image of a Hermit Thrush recorded at Shubie Park in Dartmouth, Nova Scotia in April 2003.

3. STUDY SITES

Six woodland areas known to attract Hermit Thrushes were chosen based on easy access to birds from established roads or trails. These areas are listed below along with their locations relative to downtown Halifax. Within these areas, specific study sites were restricted to approximately 100 m of gravel road or trail. Currently eleven sites are monitored, four in A5, two in A1 and A4, and one in each of the others.

- A1. Lewis Lake Provincial Park (22 km WNW)
- A2. Hemlock Ravine Park (8 km NW)
- A3. Oakfield Provincial Park (30 km N)
- A4. Shubie Park (7 km NNE)
- A5. Lake Eagle (15 km NE)
- A6. Bissett Road Trail (10 km E)

4. RESULTS AND DISCUSSION

From April 2003 through July 2006, more than 4000 Hermit Thrush songs from 17 individual birds were recorded and analyzed at the 11 sites. Their repertoires ranged from 8 to 13 songs and a total of 165 unique songs were identified, with no two birds having a single song in common. Their song frequency band was 1.4 to 8.6 kHz.

A typical Hermit Thrush song recorded at Lake Eagle in May 2004 is shown in Fig. 2. The song begins with an introductory note (α) followed by a series of flute-like body notes, with the most significant ones labeled in temporal

order (β to κ). Many songs also contain structures like the upsweeps to ϵ and ι . The bird that sang the song in Fig. 2 had an 11-song repertoire that contained about 350 notes and structures (i.e., upsweeps and downsweeps).

The study had a promising start in 2003 with five birds voice-printed, one in each of A1, A2, and A3, and two at the same site in A4. The bird in A1 was recorded in July and 12 days later in August. Its 9-song repertoire, including all notes and structures, remained unchanged. One of the birds in A4 was recorded in April and 91 days later in July with no significant change to its 11-song repertoire. It was now a matter of waiting until the spring of 2004 to acoustically re-identify one or more of these birds at the same sites.

In the meantime, Hurricane Juan made landfall about 25 km southwest of downtown Halifax on 29 September 2003 [5]. This Category 2 storm caused extensive tree damage to sites A2, A3, and A4, all in the path of the high-wind eastern eyewall. The damage was less extensive at A1 just west of the track. Further damage occurred on 19 February 2004 during a record-setting blizzard that paralyzed the province of Nova Scotia with heavy snowfall and high winds.

If the five Hermit Thrushes recorded in 2003 survived the hurricane, they didn't return to the study sites in 2004. Furthermore, no Hermit Thrushes have maintained territories at these sites in 2005 or 2006. Consequently, seven additional sites were included in the study.

The breakthrough came at Lake Eagle (A5) in 2006, when the voice-prints of two Hermit Thrushes at different A5 sites matched those of two birds in 2005 at the same A5 sites. Both birds had 12-song repertoires which had not changed. An example of one of these songs is shown in Fig. 3 for May 2005 and Fig. 4 for May 2006. With its distinctive trio of downsweeps, this song was first recognized by ear.

It is important to note that these birds were never visually observed in 2005 or 2006. Since there was no definitive non-acoustic verification that they were the same birds,

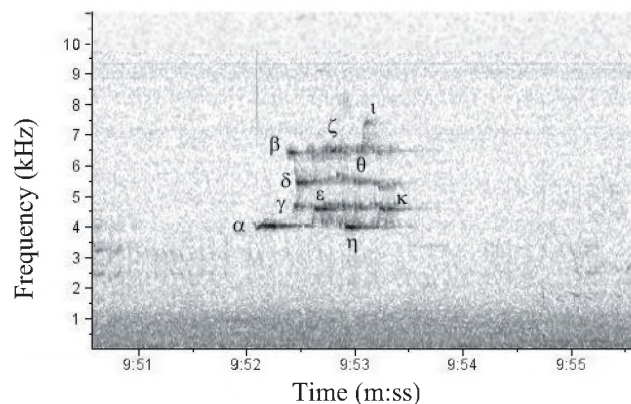


Fig. 2. Hermit Thrush song recorded at Lake Eagle in May 2004. (512-point FFT, 62 Hz filter bandwidth, Hanning window).

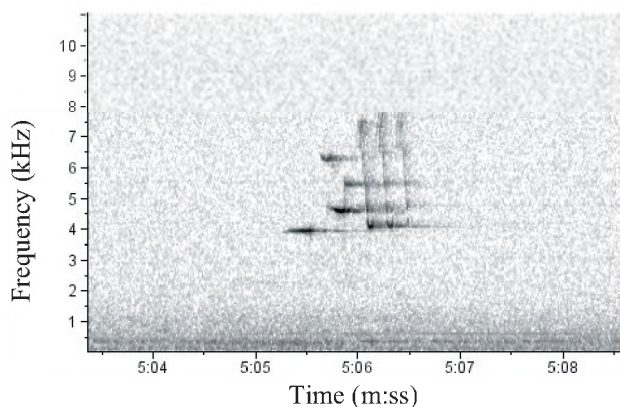


Fig. 3. Hermit Thrush song recorded at Lake Eagle in May 2005. (512-point FFT, 62 Hz filter bandwidth, Hanning window).

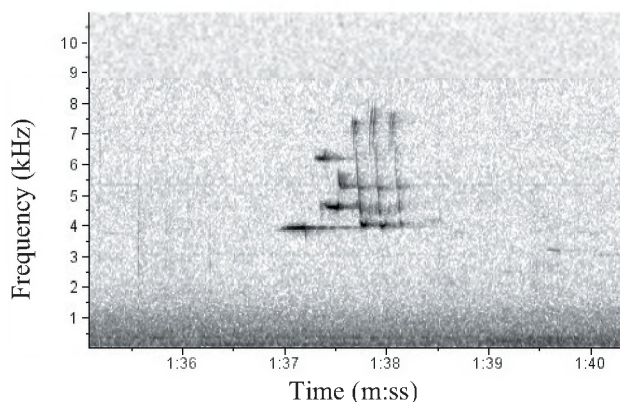


Fig. 4. Hermit Thrush song recorded at Lake Eagle in May 2006. (512-point FFT, 62 Hz filter bandwidth, Hanning window).

the conclusion that they were likely the same birds is based on voice-print matches and the fact that both birds were recorded at the same 100 m sites, in the same month, in two consecutive breeding seasons. It will be interesting to see if these birds return in the spring of 2007.

REFERENCES

- [1] Koenig, W., Dunn, H.K., and Lacy, L.Y. (1946). The sound spectrograph. *J. Acoust. Soc. Am.* 18(1), 19-49.
- [2] Stein, R.C. (1956). A comparative study of "advertising song" in the *Hylocichla* thrushes. *Auk*, 73(4), 503-512.
- [3] Borror, D.J. (1964). Songs of the thrushes (*Turdidae*), wrens (*Troglodytidae*), and mockingbirds (*Mimidae*) of eastern North America. *Ohio J. Sci.*, 64(3), 195-207.
- [4] Rivers, J.W. and Kroodsma, D.E. (2000). Singing behavior of the Hermit Thrush. *J. Field Ornithol.*, 71(3), 467-471.
- [5] Jones, D.F. and Fogarty, C. (2005). The acoustic heartbeat of Hurricane Juan. *Acoustics Research Letters Online*, 6(2), 85-91.

ACKNOWLEDGEMENTS

I would like to thank Ernie Nauffts for allowing me to use his Lake Eagle property. I am also grateful to Art Collier and Carol Smeraldo for monitoring Hermit Thrushes at Lake Eagle and providing a parking spot.

IMPULSE NOISE HAZARD – WHAT DO WE KNOW ABOUT IT?

Alberto Behar

IBBME, University of Toronto, Toronto, ON, Canada. behar@sympatico.ca

INTRODUCTION

There is no definition for impulse noise. It is generally accepted that its duration is of less than 0.5s and that is separated from other noises by more than 0.5s. If generated by collision of material bodies, it is called impact noise. Otherwise it can be generated by a sudden expansion/contraction of the air due to a spark or an explosion.

Although impulse noises are of short rise time, the decay time is a function of the acoustical environment: if in the open or in location with highly absorbent boundaries, it is also very short. However, in a reverberant location, such as most enclosed workplaces are, the decay time can be long enough as to blend with subsequent impulses in such a way that they are not separated in time and, as a result, they lose the impulse characteristic.

HEARING AND IMPULSE NOISE

To describe a continuous noise, it is sufficient to know its sound level, duration and frequency content. This is not the case with the impulse noise, whose characteristics are many more: rise time, decay time, peak value, pulse duration, repetition rate, number of impulses and kurtosis. However, historically, for the assessment of the hearing hazard only the peak value, some measure of duration, and the number of impulses have been considered as of importance.

That is why attempts to set Damage Risk Criteria (DRC) for impulse noise to avoid damage to the hearing have taken into account only those characteristics. The first one was prepared by the Committee on Hearing, Bioacoustics and Biomechanics (CHABA) in 1968. It was done for noise from gunfire and the limits were set in terms of duration of the impulse, peak value and number of impulses. Limits were derived from studies where TTS₂ (temporary threshold shift 2 min after the end of the exposure) measurements were performed on subjects

In 1972 many studies done mainly in UK following epidemiological surveys, came to the conclusion that, when integrating the sound level using 3 dB exchange rate, there should be no difference between the different types of noises, whether they are continuous, interrupted or impulsive. By accepting this principle, known as the Equal Energy Principle, the measurement as well as the assessment of the noise of any kind becomes a very simple exercise: just use a sound integrating device, such as a dosimeter or a dosimeter and if the result is lower than the accepted limit, then there is no hazard to the hearing of the exposed person.

However, further research, especially with very high noise levels, had shown that the linear relation between noise exposure levels and hearing loss, as stated by the Equal Energy Principle is not valid for high noise levels, such are

those found in the military environment. The linearity exists only up to levels around 140 dBA. It was found also, that the damage to the hear cells, that is purely metabolic becomes mechanical above those levels. That is when the concept of “critical level” was introduced, as been the level above which, the mechanical damage starts. In other words, it was confirmed that for those levels, the peak pressure level is not a sufficient indicator of auditory hazard. However, energy alone is not a sufficient indicator either. As an example, it was found that the same energy applied to the ear could be more or less damaging, depending of its frequency content. Very high levels generated by large gun fire resulted in lower TTS₂ than gun fire from small arms that generate lower sound levels. This fact could not be explained even when the measured noise was A-weighted.

AHAAH

The auditory Hazard Assessment Algorithm for Human (AHAAH) was created by Price and Kalb in 1995 and was improved since. It is the first attempt to explain the above-mentioned abnormalities and, at the same time, to provide a tool that could allow for the assessment of the hearing hazard from impulse noise of levels in excess of 150 dBPeak. To do so, the authors created a mathematical model of the entire ear – external, middle and inner including muscles and bones. In the model the ultimate receptor of the noise, the basilar membrane, was divided into 23 locations. When the impulse is entered in the model, the basilar membrane oscillates. For each of the 23 locations the upward flexes are tracked, their amplitude in microns is squared and the sum maintained for each location. The units are called Auditory Hazard Units (AHUs) that is the sum of microns squared.

The model operates on a PC in WINDOWS environment. The waveform of the signal to be assessed is entered in the program as an ASCII file. The output is the number of AHU units. 500 AHUs are the upper limit for a single exposure, with more than 500 AHUs producing an immediate permanent hearing loss.

The AHAAH method has been tested in animals and validated in humans. It has proven to be correct in 95% of the tests with protected hearing and 96% of the instances for all tests.

In an evaluation performed in 2001, the American Institute of Biological Sciences concluded that the method is basically sound for frequencies < 5KHz, not so for higher frequencies¹. They also found that the program is not easy to run from the point of view that is not easy to change variables and algorithms. However, as a bottom line they concluded that for the time being it is the best available instrument but it has to be improved.

Presently the method is used by the Society of Automotive

Engineers (SAE) Committee on Inflatable Restraints for the evaluation of airbag design and safety. Also, the US Army Center for Health Promotion and Preventive Medicine (USA-CHPPM) is using it for evaluating hazard to unprotected ears and is working to produce a version that includes hearing protection. Finally, the US Army military standard MIL-STD-1474D, that includes the AHAH method, is presently sent for comments to the interested bodies.

WHAT ABOUT THE INDUSTRY? (See Footnote 1)

Noise levels in the industry are usually much lower than those from military operations, rarely above 120 dBA Peak. Therefore, the Equal Energy Principle applies with no restrictions. Therefore an integrating instrument such as an Integrating Sound Level Meter or a dosimeter will process the impulse as well as the continuous noise existing in the premises. As a consequence, the final reading on the instrument will provide the information on the total of the acoustical energy, independently of the duration, shape and number of impulses. Most occupational hygiene standards and regulations worldwide stipulate that no unprotected ear should be exposed to sound levels in excess of 140 dBA_{Peak} or dBC_{Peak}. Using the well known formula for the calculation of noise exposure as a function of the sound level and duration:

$$L_{ex} = 85 - 10\text{Log}(X/28,800)$$

Where L_{ex} is the resulting exposure and X, the exposure duration in seconds, it can be found that after only 1-second

exposure to 130 dB the exposed person will reach the maximum allowed 85 dB. In other words using an integrating instrument just one impulse of 130 dBA (well below the critical level) will result in a reading higher than 85 dBA, indicating overexposure.

CONCLUSIONS

From the above it can be concluded that:

- For impulse noises below the critical level, (accepted to be higher than 140 dB_{Peak}), commonly found in the industry, the Equal Energy Principle is valid and any integrating measuring instrument can be used to assess the hearing hazard in the workplace. Keeping L_{ex} at or below the 85 dBA limit should ensure a safe environment where hearing of the exposed personnel is not compromised.
- No unprotected ears should be exposed to noise with peak levels higher than 140 dB. Special care should be taken when dealing with military environment. There, a thorough study should be performed to assess the noise level of the protected ear, eventually using the AHAH Method.

Footnote 1

"The panel opined that the middle ear of the model might not be good for frequencies >5kHz; but they cited no evidence that the model wasn't accurate there. To the contrary, the model reproduced Loeb and Fletcher's data for spark gap noise exposures that peaked at 3 kHz and higher" – R. Price – Personal Communication.

Why Purchase from a Single Manufacturer... ...When You Can Have the Best in the Industry From a Single Supplier?

Scantek is the company to call when you want the most comprehensive assortment of acoustical and vibration equipment. As a major distributor of the industry's finest instrumentation, we have the right equipment at the right price, saving you time and money. We are also your source for instrument rental, loaner equipment, product service, technical support, consulting, and precision calibration services.

Scantek delivers more than just equipment. Since 1985, we have been providing solutions to today's complex noise and vibration problems with unlimited technical support by acoustical engineers that understand the complex measurement industry.

Suppliers of Instruments and Software:

- Norsonic
- RION
- CESVA
- DataKustik (Cadna & Bastian)
- KCF Technologies
- BSWA
- Castle Group
- Metra
- RTA Technologies
- G.R.A.S.

Scantek
Sound and Vibration
Instrumentation and Engineering

Applications:

- Building Acoustics & Vibration
- Occupational Noise and Vibration
- Environmental and Community Noise Measurement
- Sound Power Testing
- Calibration
- Acoustical Laboratory Testing
- Loudspeaker Characterization
- Transportation Noise
- Mechanical Systems (HVAC) Acoustics

IMPULSE MEASUREMENT CONSIDERATIONS IN SETTING OCCUPATIONAL NOISE CRITERIA

Tim Kelsall

Hatch, 2800 Speakman Drive, Mississauga, ON L5K 2R7 tkelsall@hatch.ca

The most common occupational noise limits are 85 dBA Leq and 140 dBZpeak for 100 impulses. Simple arithmetic shows that 100 high frequency pulses at 140 dBZ for 0.9 msec each will give 85 dBA (assuming the A-weighting has little effect due to the frequencies involved), i.e. in practical terms the Leq limit will usually be exceeded before the impulse limit. To check this in practice over 400 measurements were reviewed from a smelting and casting facility and from an ore milling operation. These measurements included impulse noise from jack hammers, pneumatic motors and exhausts, heavy scrap dropping into bins, etc. In no case was 140 dB exceeded, although 85 dBA was exceeded in many cases. More important, in every case the 85 dBA Leq limit would be exceeded well before the 140 dBZpeak limit. It is well known that noise dosimeters are unreliable in measuring impulse noise due to false impulses caused by rubbing the microphone and cable. As a result, routine assessment of impulse noise is much more difficult (expensive) than assessments using just Leq. It is concluded that in practice there is little advantage, and some decided disadvantages, to doing routine assessment (or regulation) of impulse noise exposure in industry.

1. INTRODUCTION

Almost every occupational criterion or regulation in the world controls two items: Leq and impulse noise, the latter usually measured as Lpeak with either a C or Z (linear) weighting. Now that many occupational noise assessments are done with noise dosimeters this tends to cause a concern. Modern high crest factor dosimeters, while able to measure impulse noise and also to correctly measure Leq of sound including impulses are often subject to false readings due to high impulses produced by the cable or microphone rubbing on clothing. This has been noted in explicit warnings in CSA Z107.56¹ and ISO 9612². Impulse measurements using an attended impulse sound level meter are needed by both standards to confirm any impulse measurements. This extra measurement is time consuming and inefficient, regardless of whether impulses are found.

There is considerable question as to whether this extra complication actually helps establish whether workers are being over exposed to noise since it clearly takes very little impulse noise in an 8 hour shift before both the Leq limit and the Lpeak limit are both exceeded. If the Leq limit is exceeded anyway, then there is little point in knowing whether the Lpeak limit is exceeded as well, especially if it complicates the overall assessment.

Table 1 (Reference 3) summarises the noise regulations across Canada. Most regulations include, as limits for over exposure, both Leq > 85 dBA and Lpeak > 140 dB (for 100 impulses). Assuming that most impulses contain considerable high frequency sound one can expect the A weighted and linear sound levels to be of similar magnitude. It is then simple arithmetic to show that 100 impulses

0.9msec long will contain sufficient energy to reach 85 dBA Leq over an 8 hour shift. These are sufficiently short impulses to justify the assumption that they contain significant high frequencies to make A-weighted and linear measurements similar. Impulses containing more low frequencies will, of necessity, be longer in duration and thus again probably will cause the 85 dBA Leq limit to be exceeded. This argument indicates that in practice the 140 dB Peak limit rarely, if at all, is exceeded before the 85 dBA Leq limit has already been exceeded.

Table 1 Noise Regulations in Canada (Ref. 3)

Jurisdiction (federal, provincial, territorial)	Continuous Noise		Impulse / Impact Noise	
	Maximum Permitted Exposure Level for 8 Hours: dB(A)	Exchange Rate dB(A)+	Maximum Peak Pressure Level dB(peak)	Maximum Number of Impacts
Canada (Federal)	87	3	-	-
British Columbia	85	3	140	-
Alberta	85	3	-	-
Saskatchewan	85	3	-	-
Manitoba	85	3	-	-
Ontario	90	5	-	-
Quebec	90	5	140	100

New Brunswick	85	5	140	100
Nova Scotia	85	3	140	100
Prince Edward Island (references ACGIH TLVs)	85	3	-	-
Newfoundland	85	3	-	-
Northwest Territories	85	5	140	100
Nunavit	85	5	140	100
Yukon Territories	85	3	140	90

2. Measurements

To check this argument in practice, over 400 measurements were examined from two large industrial plants: a smelting and casting facility and an ore milling operation. These included measurements of impulse noise from many different sources, including jack hammers, pneumatic motors, pneumatic exhausts and heavy scrap dropping into bins. Most measurements were taken at potential operator locations, or 1m from the equipment being measured.

For each measurement, Figure 1 compares the difference between L_{eq} and L_{peak} to the difference between the two limits: 140 dB and 85 dB. It is calculated by subtracting each measurement from its appropriate limit and then taking the difference between the two results. A positive value indicates the L_{eq} is closer to exceeding the 85 dBA limit than the L_{peak} is to exceeding the 140 dB limit.

It is clear from the results that in none of these measurements will the L_{peak} measurement have any effect on determining whether the criteria are exceeded. Indeed in most cases the L_{eq} is 30 dB closer to its limit than L_{peak} . The two measurements with the lowest difference were a pneumatic tamping machine at 11.9 dB (probably with some rattling parts) and an empty steel scrap bin (at 16.8 dB) with a cubic foot of scrap being dropped into it from a height of over a metre.

Amount by Which Leq Criterion Exceeds Lpeak Criterion
(Positive Number = Leq Limit Exceeded Before Lpeak Limit)

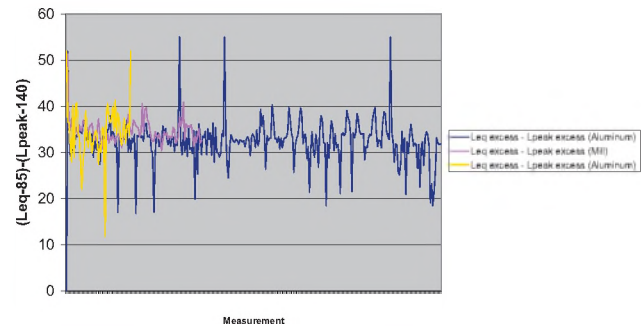


Figure 1 Extent to which Leq is more important than Lpeak in determining excess over occupational limits

3. Conclusions

It is clear both from time considerations and from the measurements examined that the L_{peak} measurement used in most occupational criteria and regulations has little practical effect. In view of the difficulties this measurement poses to the use of noise dosimetry for assessment and its lack of usefulness, it is recommended that provinces and other regulators consider dropping the use of impulse criteria or limiting its use to very specific cases. In practice there appears to be little point in measuring L_{peak} even when it is regulated. It should only be measured in exceptional cases since its measurement is unlikely to have any effect on the outcome of assessments in the vast majority of cases.

REFERENCES

1. Canadian Standard Z107.56, Procedures for the Measurement of Occupational Noise Exposure, 2006
2. ISO/CD 9612, Acoustics -- Guidelines for the measurement and assessment of exposure to noise in a working environment, 2006
3. http://www.ccohs.ca/oshanswers/phys_agents/exposure_can.html National Guidelines for Environmental Noise Control, ISBN: 0-662617014-8, 1989

ALARMLOCATOR: A SOFTWARE TOOL TO FACILITATE THE INSTALLATION OF ACOUSTIC WARNING DEVICES IN NOISY WORK PLANTS

Rida Al Osman, Christian Giguère, and Chantal Laroche
Audiology/SLP Program, University of Ottawa, Ontario, K1H 8M5

1. INTRODUCTION

In many workplaces, acoustic warning signals are necessary to promptly alert workers of events that can compromise safety. Unfortunately, the use of warning signals is poorly regulated and submitted to intuitive installation practices with little regard to the many factors contributing to an efficient use. There exists a very complex interaction between the noise characteristics, hearing protector attenuation and hearing status, so that the perception of warning signals for a given workplace by an individual worker or group of workers is difficult to predict without a suitable analysis [1].

A psychoacoustic software tool, *Detectsound*, was developed to determine whether an acoustic warning signal satisfies the constraints for optimal detection and recognition by the attending workers [2]. *Detectsound* is particularly useful when assessing the level and spectrum of existing alarm systems at given workstations. Warning devices, however, are typically installed on walls or on the ceiling at a certain distance from the targeted workstations. In order to design alarm systems for new plants and to forecast modifications to existing systems, the sound transmission path from the warning devices to the workstations must be considered.

This paper presents the development of a complementary software tool, *AlarmLocator*, to automate the process of installing auditory warning devices in a given setting, in terms of the characteristics of the devices to use and their optimal location in the plant. The software tool produces a solution to two practical installation problems: (1) selecting a suitable number of warning devices and their acoustic power for a given work area, and (2) specifying the location of the devices in the plant in such a way that the signals emitted are clearly audible by all workers at all workstations. A solution to the problem of installing warning devices is thus provided in a format that can be easily understood and used in the workplace.

2. GENERAL FRAMEWORK

The general modeling framework proposed for the optimal installation of warning devices is illustrated in Figure 1. The method consists of the integration of two software tools, *Detectsound* and *AlarmLocator*. As shown in Figure 1, the psychoacoustic tool *Detectsound* [2] requires four inputs:

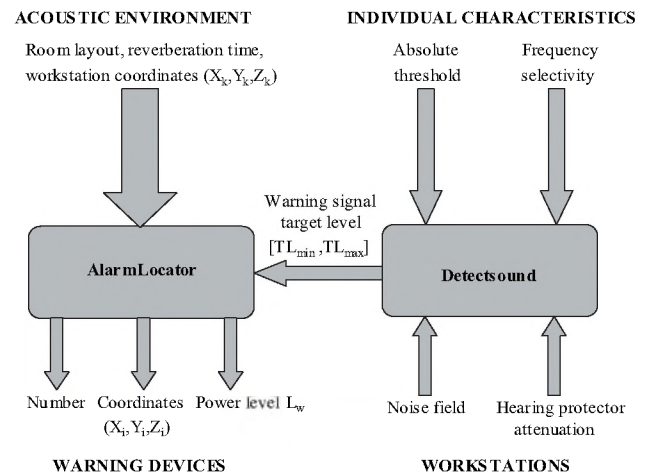


Fig. 1: *AlarmLocator* in interaction with *Detectsound*

- (1) The noise field at the workstation;
- (2) The attenuation of hearing protectors, if used;
- (3) The absolute hearing thresholds of the individual worker attending the workstation;
- (4) The frequency selectivity of the worker.

The last 2 inputs can be obtained through clinical measurements or by predictive tools within *Detectsound* [2].

The output of *Detectsound* is the predicted optimal range (Design window) of warning signal levels at each workstation for various frequencies as shown in Figure 2.

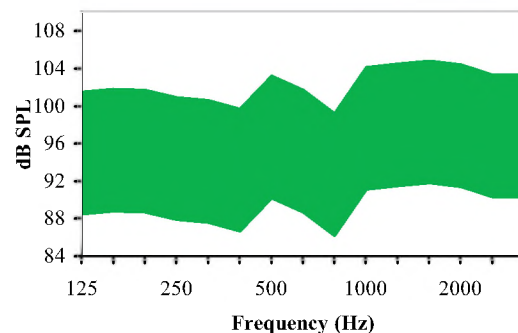


Fig. 2: Example warning signal design window

The left side of Figure 1 represents the model of acoustic propagation in the work plant, *AlarmLocator*. This tool accounts for the sound propagation of warning signals from the physical device location (on walls or ceiling) to the position of individual workers or workstations [3]. The

model takes into account the direct field from the alarm devices and the reverberant field due to wall, ceiling, floor and other reflections. Source directivity effects due to alarm placement are computed using the mirror image method by considering the first three orders of room reflections.

As shown in Figure 1, *AlarmLocator* has 2 major inputs:

- (1) The target warning sound levels ($[TL_{min}, TL_{max}]$) at each workstation produced by *Detectsound*;
- (2) The characteristics of the work area (room layout, reverberation time or sound absorption, number and location of workstations in the room).

The objective of *AlarmLocator* is to search for warning device configurations that will globally satisfy the design window produced by *Detectsound* at all workstations.

The outputs produced by *AlarmLocator* are the following:

- (1) The minimum number of warning devices needed;
- (2) The optimum location of the warning devices;
- (3) The optimum sound power level for each device.

Together, these three outputs constitute a complete solution to the problem of installing acoustic warning devices in the workplace. The “minimum number of warning devices” and the “optimum power level for each device” specifications are required at the purchasing phase, while the “optimal location of each device” specification is needed during the installation phase.

3. CASE STUDY

A case study in a hypothetical work area illustrates the use of *AlarmLocator*. The work area is 14m×21m×8m (W×L×H) and it includes 5 workstations (W1-W5). The spatial coordinates of the workstations are presented in Table 1, together with the target warning sound levels from *Detectsound* after an analysis of the noise field in the room and the hearing characteristic of the individual workers [2]. The reverberation time in the room is assumed to be 0.9 s.

Table 1: Workstation spatial coordinates and target levels ($[TL_{min}, TL_{max}]$) in the work area (Z Coord = 1.5 m).

Workstation Index	X Coord [m]	Y Coord [m]	TL_{min} [dB]	TL_{max} [dB]
1	5.0	5.0	69.0	82.0
2	8.0	2.0	73.0	86.0
3	3.0	7.0	75.0	88.0
4	13.0	19.0	82.0	95.0
5	2.0	3.0	81.0	94.0

Using *AlarmLocator*, a set of possible solutions for installing warning devices can be found. Each solution describes the number, locations and power levels of the necessary warning device(s). For this example, 163 possible solutions are found involving two alarm devices (D_1 and D_2). One of the solutions is shown in Table 2. All the other

solutions have the same power level requirements, but they differ in alarm location.

Table 2: One possible solution of alarm configuration.

Alarm Index	XCoord [m]	Y Coord [m]	ZCoord [m]	Power Level [dB]
1	10.0	21.0	8.0	90.0
2	0.0	0.0	8.0	100.0

The warning sound level distribution in the work area can be constructed for each solution at any desired height level (Z coordinate) in the room. A representation of the warning sound distribution for the solution in Table 2, intended at a height of 1.5 m (ear level) in the room, is shown in Figure 3.

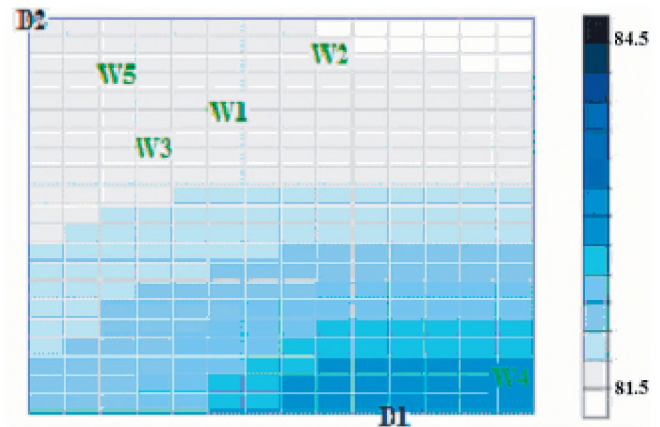


Fig. 3: Noise map for the solution presented in Table 2. “D” represents the alarm devices. “W” represents the workstations.

4. DISCUSSION

A new optimization tool, *AlarmLocator*, was introduced to facilitate the process of installing acoustic warning devices in a given setting. Integrated with *Detectsound*, this new tool provides an optimized possible solution to the complex problem of installing warning devices in a noisy work plant. More specifically, this research revealed a new method for predicting the optimum number, location and sound power of acoustic warning devices. Our goal is to achieve more valid and accurate solutions for the installation of warning devices in the workplace. [Work was funded by a research grant provided by the Workplace Safety and Insurance Board (Ontario)].

REFERENCES

- [1] ISO 7731-2003: Ergonomics: Danger signals for public and work areas-Auditory danger signals (Int. Org. for Standardization).
- [2] Zheng Y., Giguère, C., Laroche C. et al. (2006). “A psychoacoustic model for specifying the level and spectrum of acoustic warning signals in the workplace”. *J. Occup. Environ. Hyg.* (in press).
- [3] Al Osman, R., Giguère, C. & Laroche, C. (2006). “Optimal installation of acoustic warning devices in the workplace”, IEA 16th World Congress on Ergonomics, Maastricht, Netherlands.

PERCEIVED HOLISTIC HEALTH EFFECTS OF THREE LEVELS OF MUSIC PARTICIPATION

Betty A. Bailey

PEI Health Sector Council, 141 Grafton Street, Charlottetown, Prince Edward Island, Canada , C1A 1K9
bbailey@pei.sympatico.ca

1. INTRODUCTION

In previous research, with members of 2 choirs for homeless and disadvantaged singers with little or no music training (Bailey & Davidson, 2002; Bailey, 2002), interpretative phenomenological analysis (IPA) of in-depth semi-structured interviews indicated that group singing positively affected emotional, social, cognitive and physical processes. As well, comments from several participants suggested that many of the positive effects of group singing did not occur while listening to music.

Recent physiological studies have utilized measurements of salivary immunoglobulin A (sIgA) and cortisol to investigate the effects of active and passive participation in music. IgA is an endocrine defense against bacterial infection in the upper respiratory tract (Tomasi, 1972). Increases in levels of sIgA have been associated with pleasurable social (Miletic et al., 1996) and emotional events (Dillon et al., 1985). Cortisol is a measure of stress (Kirschbaum & Hellhammer, 1994). Increases in cortisol levels have been associated with unpleasant and stressful activities (Buchanan et al., 1999).

In an investigation with a professional chorale, Beck et al. (1999) found a significant increase in sIgA between pre and post group singing following 2 practices and a performance. Additionally, cortisol significantly decreased after practices but significantly increased following the performance. In research with members of an amateur choir, Kreutz et al. (2003) found a significant increase in sIgA between pre and post group singing but not pre and post group listening, and a significant decrease in cortisol between pre and post group listening but not pre and post group singing. In a study with undergraduates, Kuhn (2002) found that sIgA levels were significantly increased following an active group music activity which involved singing and playing percussion instruments than listening to a live musical performance in a group.

While the results of the above studies suggest positive effects for both group singing and group listening, there is considerable ambiguity surrounding differences and similarities in the effects of active and passive participation in music. One drawback of the Kreutz et al. and Kuhn studies was the artificiality of the listening conditions. An additional issue, not addressed in the above, is differences between social and segregated listening. Research with adolescents suggests that the majority of the time spent listening to music occurs in isolation (Larsen & Kubey, 1983). Although there appears to be no comparable adult data, it appears that much adult listening also occurs in seclusion. Bull (2000) has proposed that the personal stereo is often used to avoid unwanted affiliation and to escape the realities and responsibilities of everyday life. Therefore,

isolated listening may be more beneficial than social listening.

A survey was designed to determine differences in participants' perceived holistic health effects of differing levels of music participation, including: (1) group singing, (2) isolated listening and (3) group listening.

2. METHOD

Members of 3 choirs participated in the survey. In order to determine perceptions of the general population rather than those of musicians, amateur choirs in which the majority had low levels of music training were targeted.

The members of the 3 choirs were asked to participate in a survey investigating effects of experiences with music. In order to camouflage the purpose of the study, the items related to the 3 levels of participation were interspersed among other items related to choir practices, performances, voice quality and conducting techniques. Items were completely randomized into two survey orders. Of the 100 items included in the survey, 72 items equally investigated the holistic health effects of the 3 participation categories. For example: (1) Singing in a choir usually improves my mood, (2) Listening to music alone usually improves my mood; and (3) Listening to music with others usually improves my mood. Because of the length of the survey, 3 items (1 from each category) were included twice as a check of concentration and consistency. There were an equal number of positively and negatively worded items. The items were classified under 6 dimensions of holistic health: emotional (6 items), physical (7 items), cognitive (5 items), spiritual (1 item), social (1 item), life-satisfaction (4 items). Participants were instructed to rate items using a 5-point rating scale.

3. RESULTS

A repeated measures ANOVA with one within-subjects factor (music participation) with three levels indicated that there was a significant difference between the overall means (mean of 23 items) of the three participation categories, $F(2, 240) = 50.88, p < .001$. Pairwise comparisons with a Bonferroni adjustment indicated that the mean of each participation level was significantly different from the others (all p values $< .001$), providing evidence of an overall differential effect of type of participation with group singing being considered the most beneficial and group listening the least beneficial. On an item by item basis, group singing received the highest mean ratings for 16 of the 23 items and isolated listening received the highest mean ratings for 7 items.

Repeated measures ANOVA with one within-subjects factor (music participation) with three levels and one between-subjects factor was computed for: (1) years of group singing - 4 levels, (2) years of music lessons - 4 levels, (3) age - 3 levels, (4) education - 4 levels, and (5) gender). The results indicated that there were no significant interaction effects of level of music participation on the above variables suggesting that the effects of differing levels of music participation may be quite global.

4. DISCUSSION

The differences in the ratings of the items of the 3 music involvement categories suggest that active participation in choral singing was more holistically beneficial than isolated or group listening. Also, isolated listening was perceived to be more holistically beneficial than social listening.

The physiological studies reviewed in the introduction consistently reported increases in sIgA in the active participation conditions. In Beck et al.'s (2000) work, increases in sIgA were detected even when self report measures indicated increased levels of stress in a performance condition. They assert that choral performance may be both an "anxious and highly stimulating experience that leads adaptively to levels of positive feelings and satisfaction" (p. 104). In the present study, many of the items which received the highest ratings in the group singing category were related to heightened arousal and items which received the highest ratings in the isolated listening category were related to stress reduction and restoration of a homeostatic state.

In this survey, although the holistic health effects of group listening were generally positive, they were weaker than those of isolated listening. Yet, in the Kreutz et al. study, cortisol was found to significantly decrease during group listening. However, in Kreutz et al., even though the listening condition was social, it was quite different from many social listening situations in everyday life, where mental engagement with the music must compete with background noise and conversational interruptions. Therefore, effects of group listening in many commonplace contexts may have fewer stress reduction properties than in the controlled group listening condition in Kreutz et al.

Similarities between the results of the physiological and psychological studies reported above suggest that different levels of music participation have differential effects which appear to be dependent on physical and social factors. As well, the results of these studies indicate that participants' perceptions can mirror physiological effects.

5. REFERENCES

Bailey, B. & Davidson, J. (2002). Adaptive characteristics of group singing: Perceptions from members of a choir of homeless men. *Musicae Scientiae*, 6 (2), 221-256.

Bailey, B. (2002, April). *Empowering the poor and mentally ill through choral performance*. Paper presented at the meeting of the Society for Research in Psychology of Music and Music Education, London, UK.

Beck, R., Cesario, T., Yousefi, S. & Enamoto, H. (2000). Choral singing, performance perception and immune system changes in salivary immunoglobulin and cortisol. *Music Perception*, 18 (1), 87-106.

Buchanan, T., al'Absi, M. & Lovallo, W. R. (1999). Cortisol fluctuates with increases and decreases in negative affect. *Psychoneuroendocrinology*, 24 (2), 227-241.

Bull, M. (2000). *Sounding out the city*. New York: Berg.

Dillon, K. M., Minchoff, B. & Baker, K. H. (1985). Positive emotional states and enhancement of the immune system. *International Journal of Psychiatry in Medicine*, 15, 13-17.

Kirschbaum, C. & Hellhammer, D. H. (1994). Salivary cortisol in psychoneuroendocrine research: Recent developments and applications. *Psychoneuroendocrinology*, 19, 313-333.

Kreutz, G., Bongard, S., Rohrmann, S., Hodapp, V. & Grebe, D. (2004). Effects of choir singing or listening on secretory immunoglobulin A, cortisol, and emotional state. *Journal of Behavioral Medicine*, 27 (6), 623 - 635.

Kuhn, D. (2002). The effects of active and passive participation in musical activity on the immune system as measured by salivary immunoglobulin A (sIgA). *Journal of Music Therapy*, 39 (1), 30-39.

Larsen, R. & Kubey, R. (1983). Changing channels: Early adolescent media choices and shifting investments in family and friends. *Youth and Society*, 15, 13-33.

Miletic, I., Schiffman, S., Miletic, V. & Sattely-Miller, E. (1996). Salivary IgA secretion rate in young and elderly persons. *Physiology and Behaviour*, 60, 243-248.

Tomasi, T. B. (1972). Secretory immunoglobulins. *New England Journal of Medicine*, 7, 500-506.

THE EMOTIONALITY OF MUSIC: DEATH METAL TO AMAZING GRACE

Elysia Iversen¹, and Jane F. MacNeil²

¹University of Calgary at Red Deer College, Red Deer., AB, Canada, T4N 5H5, elysia_iversen@hotmail.com

²Dept. of Psychology; University of Calgary, Red Deer College, Red Deer., AB, Canada, T4N 5H5, jane.macneil@rdc.ab.ca

1. INTRODUCTION

Music is a multidimensional medium that influences one's physical, psychological, and emotional levels of consciousness. It is commonly acknowledged that music can express and arouse emotions (see Juslin & Sloboda, 2001, for a recent review). Given the ubiquitousness of music in the Western world, be it through radio, recordings, television or recorded background music played in public places it is important to gain more understanding regarding the effects of music on our behavior and cognitive processing. Though it has been shown that music can affect an individual, the emotional and psychophysiological mechanisms that account for these effects are not well established (e.g., Juslin & Zentner, 2002).

The research so far has been relatively unsystematic and much of it has been inconclusive, in part because music is processed in different ways. The purpose of this study was to evaluate the effects of preferred versus nonpreferred background sound conditions on the cognitive and emotional responses of healthy young adults. In addition the effect of duration was also considered as a contributing factor.

2. METHOD

2.1 Participants

A sample of 171 female (74.35%) and 59 male (26.65%) college students (N = 230) enrolled in introductory psychology courses participated in this study with a total of 95 (25 males and 70 females) in phase one and 135 (34 males and 101 females) in phase two. Table 1 shows the age ranges of participants.

Table 1. Age ranges of participants.

Total	Phase 1	Phase 2	Total
Under 21	57 (60.00%)	99 (73.33%)	156 (67.83%)
21-25	22 (23.16%)	21 (15.56%)	43 (18.70%)
25-30	8 (8.42%)	8 (5.93%)	16 (6.96%)
30-40	5 (5.26%)	5 (3.70%)	10 (4.35%)
Over 40	3 (3.16%)	2 (1.48%)	5 (2.17%)

2.2 Instruments

Cognitive and Emotional Performance Tests (CEPT) consisted of both traditional general knowledge

questions and questions assessing emotional responses and was compiled from online IQ tests. Version one of the CEPT was composed of 15 multiple choice questions consisting of ten traditional questions, and five emotional questions. Version two of the CEPT was comprised of 30 multiple choice questions, with 20 traditional questions and ten emotional questions. Three different editions (A,B and C) were created for each version of the CEPT that contained the same proportion of questions.

2.3 Procedure

In phase one, participants completed Version 1 A through C of the CEPT under three different background sound conditions, which were randomly selected. Music selections were determined based upon answers to an Individualized Music Preference Questionnaire. Appealing and irritating selections of music were determined by the most frequently identified genre. Participants completed test A in the silent control condition, test B in an appealing sound condition (rock music), and test C in an irritating sound condition (heavy metal). The appealing sound condition consisted of 5 minutes of rock music (e.g., "Hard to Handle" by the Black Crowes) and the irritating sound condition consisted of 5 minutes of heavy metal music (e.g., "Bound to Violence" by Hatebreed). A randomized visual pattern was projected onto a screen located at the front of the room for all three sound conditions. Music was played through the internal audio systems built into the lecture halls. There would have been some variance in the sound levels from the front of the room compared to the back, but independent listeners reported very little difference in sound level quality or experience.

To determine if the duration of the music was an important factor, in phase two the musical background was 10 minutes in duration and sound levels were comparable to those in phase 1. In phase two participants completed the three editions of Version 2 of the CEPT. The presentation of the three background sound conditions was randomly presented. The appealing sound condition consisted of 10 minutes of rock music and the irritating sound condition consisted of 10 minutes of heavy metal music. As in phase one, a randomized visual pattern was projected on a screen that was located at the front of the room.

3. RESULTS

A repeated measures ANOVA was completed on percentage correct scores for all responses. The mean percentage correct scores for the three background sound conditions were compared using paired t-tests with a

Bonferroni correction. Only comparisons significant at the .0167 level will be considered for discussion. For the traditional question test scores over a 5 minute duration the effect of condition was significant $F(2,188)=3.609$, $p=.029$. No significant difference was found between the mean test percentage score during the quiet condition ($M=67.37$, $SD=22.084$) and the appealing condition ($M=72.95$, $SD=15.837$), $t(94)=-2.229$, $p=0.028$. There was also no significant difference between the quiet condition and the irritating condition ($M=67.47$, $SD=17.683$), $t(94)=-0.042$, $p=0.966$. A significant difference was found between the appealing and irritating condition ($t(94)=2.588$, $p=0.011$).

For the traditional question test scores over a 10 minute duration the assumption of sphericity was violated ($p=.004$), therefore the Greenhouse-Geisser correction was used. The effect of condition was found to be significant $F(1.852,248.226)=7.527$, $p=.001$. No significant difference was found between the mean test percentage score during the quiet condition ($M=71.07$, $SD=11.676$) and the appealing condition ($M=70.15$, $SD=13.396$), $t(134)=0.951$, $p=0.343$. There was a significant difference found between the quiet condition and the irritating condition ($M=74.33$, $SD=12.781$), $t(134)=-2.823$, $p=0.005$. A significant difference was also found between the appealing and irritating condition ($t(134)=-3.340$, $p=0.001$).

For the emotional question test scores over a 5 minute duration the assumption of sphericity was violated ($p=.016$), therefore the Greenhouse-Geisser correction was used. The effect of condition was found to be significant $F(1.843,173.245)=70.301$, $p=.000$. A significant difference was found between the mean test percentage score during the quiet condition ($M=23.541$, $SD=24.143$) and the appealing condition ($M=56.459$, $SD=19.708$), $t(94)=-11.652$, $p=0.000$. There was also a significant difference found between the quiet condition and the irritating condition ($M=51.053$, $SD=25.439$), $t(94)=-8.143$, $p=0.000$. No significant difference was found between the appealing and irritating condition ($t(94)=2.015$, $p=0.047$).

For the emotional question test scores over a 10 minute duration the assumption of sphericity was violated ($p=.000$), therefore the Greenhouse-Geisser correction was used. The effect of condition was found to be significant $F(1.791,240.039)=58.616$, $p=.000$. A significant difference was found between the mean test percentage score during the quiet condition ($M=34.9630$, $SD=23.79998$) and the appealing condition ($M=55.615$, $SD=24.836$), $t(134)=-11.096$, $p=0.000$. There was also a significant difference found between the quiet condition and the irritating condition ($M=55.467$, $SD=26.320$), $t(134)=-8.168$, $p=0.000$. No significant difference was found between the appealing and irritating condition ($t(134)=0.068$, $p=0.946$).

4. DISCUSSION

The aim of this study was to determine the effect of preferred versus nonpreferred genres of music on the cognitive and emotional performance of healthy young adults. It was also hypothesized that healthy young adults would show impaired cognitive and emotional performance in the absence of background stimuli. The results of this

study lend support to this hypothesis in that healthy young adults performed better cognitively and emotionally in the presence of background music regardless of whether it was preferred or nonpreferred music when compared to the absence of background stimuli. This may be explained in part due to the fact that an increased number of adolescents are studying at home with either music or the television playing at the same time (Patton et al., 1983; Kotsopoulou, 1997).

No support was found for the prediction that healthy young adults would perform better cognitively and emotionally in an appealing background sound condition compared to an irritating background sound condition. For the emotional IQ questions there was no difference found between percentage correct scores for the appealing background sound condition versus the irritating background sound condition in either the 5 or 10 minute duration.

The most important finding of this study is that the mere presence of music, regardless of preferred or nonpreferred, is beneficial to the cognitive and emotional performance of healthy young adults. These findings have important implications for the structure of the classroom environment in terms of background stimuli. More research needs to be completed to determine what affects the volume, meter, tempo, and rhythm of music have on the cognitive and emotional performance of students in a classroom setting.

Indeed, for most people, music expresses emotion, but only recently has the topic begun to attract serious attention from neuroscientists (Zattore, 2005).

REFERENCES

- Juslin, P. & Sloboda, J. (2001). *Music and Emotion. Theory and Research*. Oxford University Press: Oxford.
- Juslin, P., & Zentner, M. (2002). Current trends in the study of music and emotion: Overture. *Musicae Scientiae. Special Issue 2001-2002*, 3-21.
- Kotsopoulou, A. (1997). *Music in students' lives*. Unpublished MA dissertation, Institute of Education, University of London.
- Patton, J.E., Stinard, T.A., & Routh, D.K. (1983). Where do children study? *Journal of Educational Research*, 76(5), 280-286.
- Zattore, R. (2005). Music. The food of neuroscience? *Nature*, (434), 312-315.

INVESTIGATING THE SOUND OF AN AFRICAN THUMB PIANO (KALIMBA)

David M.F. Chapman

Scientific Consultant, 8 Lakeview Avenue, Dartmouth, Nova Scotia, B3A 3S7 dave.chapman@ns.sympatico.ca

1. INTRODUCTION

The African thumb piano, or kalimba (also called by other names) is an unusual percussion instrument consisting of a number of thin metal blades (keys) mounted on a soundbox or soundboard. (See Figure 1) The keys are mounted with different lengths to produce different notes, and they are typically struck at the end by the performer's thumbs while the soundbox is held by the fingers.

The individual notes of a small kalimba were recorded and frequency-analysed to determine the overtone structure. The notes have a definite pitch, a sharp attack, and a rapid decay; the quality of the note could be described as a "sproing". The dominant tones of a note are: a strong fundamental (f_0) and a single anharmonic overtone (f_1) whose frequency ratio f_1/f_0 is about 5.3-5.9. (There are also higher-frequency, less significant, overtones.)

Using these facts, one can construct a synthetic kalimba waveform from the sum of two exponentially damped sinusoids. By aurally comparing true and synthetic waveforms, it is possible to adjust the few model parameters to produce a realistic-sounding synthetic waveform.

Unlike the modes of a vibrating string or organ pipe, the modes of vibration of a thin bar produce anharmonic overtones (i.e. non-integer-multiples), which provide a mild harshness to the tone quality owing to the discordant musical intervals produced. The principal thrust of this



Figure 1: The small kalimba used for the measurements.

investigation is to investigate the overtone structure of the kalimba notes, and to understand how the key-mounting method affects the f_1/f_0 ratio. Although this task is incomplete, initial results suggest that the overtone structure on this particular kalimba is sensitive to the details of the mounting geometry. Photographs and sound files associated with this project can be found at the web page:

<http://homepage.mac.com/chapmandave/Kalimba/>

2. MEASUREMENT

The kalimba notes were individually recorded and analysed on an Apple Macintosh iMac Intel Core Duo computer, using the built-in microphone and A/D converter, controlled by the freeware audio software AUDACITY. It was decided that this arrangement was sufficient to study the overtone structure of the kalimba, and that a calibrated microphone was unnecessary; by the same token, no special means of exciting the notes was devised: some care was taken to produce uniformly loud notes with the thumbs as one would in a typical performance.

The files produced were common .wav audio files, which were imported into MATHEMATICA 5.2 for analysis. The imported waveforms were plotted and replayed using standard functions. The frequency spectra of the waveforms were computed using the Fourier function (with no averaging) and plotted for inspection. Using the cursor within the MATHEMATICA plot, f_0 and f_1 were measured for all notes.

Referring back to Figure 1, notice that the keys have a peculiar mounting arrangement: essentially the keys are thin bars that are free at one end (the striking end) and clamped at the opposite end; however, partway along from the clamped end, the keys are supported by a fulcrum and held in place by a restraining bar. Through simple experimentation, it was discovered that the low-amplitude motion of the short length between the fulcrum and the bar is not inconsequential and should be taken into account. (If one presses on this portion while a key is struck, the sound is noticeably damped.) By the same token, the portion between the bar and the fixed end was considered to be entirely clamped, and irrelevant to the acoustics. Accordingly, the individual key lengths free-fulcrum (a) and fulcrum-bar (b) were measured.

Nominally (by comparing with a piano) the kalimba notes form a pentatonic scale starting at the D in the third octave: D3 E3 G#3 A#3 D4. Table 1 shows the nominal note name, nominal note frequency, lengths a and b , ratio a / b , fundamental frequency f_0 , overtone frequency f_1 , and frequency ratio f_1/f_0 for all the notes. Figure 2 shows the waveform of the D3 note and Figure 3 shows the corresponding spectrum. In Table 1, note that the ratio f_1/f_0 is not fixed, but is different for each note, and systematically decreases with the a / b ratio (although G#3 is an anomaly).

Table 1. Kalimba note measurements.

note ^(a)	f ^(b) (Hz)	a (cm)	b (cm)	a/b	f_0 (Hz)	f_1 (Hz)	f_1/f_0
D3	293.7	5.4	1.4	3.9	304	1780	5.86
E3	329.6	5.0	1.3	3.8	336	1890	5.63
G#3	415.3	4.6	1.4	3.3	415	2390	5.76
A#3	466.2	4.2	1.3	3.2	462	2590	5.61
D4	587.3	3.7	1.3	2.8	581	3080	5.30

^(a) the nominal note, i.e. the piano note closest to the kalimba note

^(b) the frequency of the nominal note

3. SIMULATION

By inspecting both the measured waveforms and the spectra of the notes, it was decided that a fair representation of the note would be the sum of a pair of sine waves at frequencies f_1 and f_0 , with exponentially decaying envelopes. The frequency parameters are estimated from the spectra; the decay time of the fundamental is estimated from the waveform (and validated by listening). This leaves the overtone/fundamental amplitude ratio and the overtone decay time to be determined. It was assumed that the overtone would decay quicker than the fundamental, and this is supported by detailed examination of the waveform, although it is difficult to precisely estimate this decay time. (Filtering might help.) The same comment holds for the overtone amplitude, although some idea of the overtone

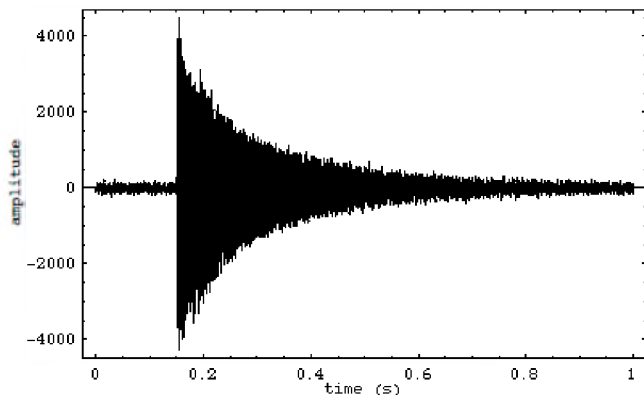


Figure 2: Waveform of note D3. Notice the sharp attack and exponential decay of the waveform.

amplitude ratio can be drawn from the spectrum. The overtone amplitude ratios and decay times were estimated by guesswork and listening. Casual listening by non-experts confirms that the synthetic notes are a fair representation of the real tones. Work continues on this aspect, with a view to determining the model parameters objectively.

4. THEORY

Lord Rayleigh (1896) performed the classic analysis of the modes of a thin vibrating bar. The wave equation for transverse vibrations is a fourth-order linear differential equation whose solutions are combinations of sin, cos, sinh, and cosh functions. Generally, the overtone structure is anharmonic (a fact that is underappreciated) with the precise spacing determined by boundary conditions on the displacement and its first three spatial derivatives. Rayleigh considered the cases of a free end, a clamped end, and a supported end. When the appropriate boundary conditions are applied, the determination of the frequencies of vibration reduces to finding the zeros of a transcendental equation, which is tackled numerically. For the clamped-free bar, which is the closest simple system to the kalimba keys, Rayleigh found $f_1/f_0 = 6.2669$.

Applied to the kalimba in question, the analysis is somewhat complicated by the additional support in the middle, but this will be accommodated by considering the key to be composed of two bars on either side of the fulcrum (one clamped at the end, the other free), with matching conditions where they join. The hypothesis is that the ratio f_1/f_0 for each key is governed by the a / b ratio of the key, and an explanation for the reduced f_1/f_0 ratio will be sought.

The modeling of this vibrating system and the numerical determination of overtone frequencies is ongoing work.

REFERENCES

Rayleigh, John William Strutt (1896). *The Theory of Sound, Volume One*, Chapter 8 (Dover Publications Inc., New York)

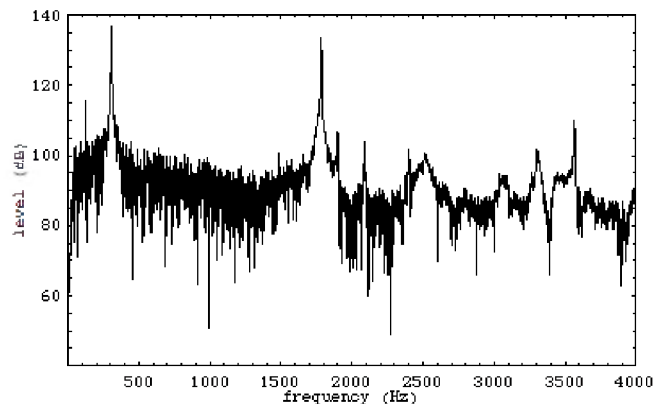


Figure 3: Spectrum of note D3. Notice the fundamental at 304 Hz, the first overtone at 1780 Hz, and a second overtone at 3560 Hz (highly attenuated).

A CRITICAL ANALYSIS OF LOUDNESS CALCULATION METHODS

Jeff Defoe¹, Colin Novak, and Helen Ule

Dept. of Mechanical, Automotive and Materials Engineering, University of Windsor, 401 Sunset Ave., Windsor, Ontario, Canada, N9B 3P4 ¹Corresponding author: defoe2@uwindsor.ca

1. INTRODUCTION

Loudness aims to quantify how loud a sound is perceived to be in comparison to a standard sound [1]. It accounts for both the frequency-sensitivity of the ear and masking effects. The loudness of a sound is most commonly computed from 1/3 octave band sound pressure levels measurements of the source. However, the calculation procedure is poorly understood despite having been standardised in ISO 532B (1975) and DIN 45631 (1991). There exist commercial software packages to determine loudness. In this paper, the 01dB software packages dBFA and dBsonic were considered. For this investigation, four noise sources are used in comparing the software packages to a public domain code and two codes written by the present authors – one based on ISO 532B, the other on DIN 45631. A 1-kHz tone, pink noise, a six-cylinder spark-ignition engine and a six-cylinder diesel engine were used. The purpose of this comparison is to evaluate the validity of the results obtained, as well as to gain insight into the shortcomings of the relevant standards. In addition, comparisons of results amongst the different sound types will serve to illustrate the differences between sound pressure level (SPL) and loudness.

2. THE DEFINITION OF LOUDNESS

In general, a sound will prevent other sounds of lower sound pressure level but with similar frequency content from being heard. This is known as masking. Typically, sound level meters and frequency analysers will present the frequency content of a measured signal in terms of fractional octave bands. The human hearing system does not use fractional octave band filtering: the major range of human hearing is more properly divided into 24 “critical bands” based on the frequency ranges in which masking will occur – that is, if two sounds occur with frequency content within one band of each other, masking will take place [1]. The critical band representation of a sound is its *excitation* [1] – some excitation occurs outside of the critical band in which the sound occurs. So, “similar” frequency content means that one sound’s critical-band spectrum is overshadowed by the masking sound’s critical-band spectrum. Loudness is “the sensation that corresponds most closely to the sound intensity of the stimulus” [1]. The loudness of a 1-kHz tone at an SPL of 40 dB is 1 sone. The concept of “specific loudness” is employed to mean the

contribution to the total loudness of a specific slice of the critical band spectrum. Critical-band filtering is not widely available, so a procedure was developed for use with 1/3 octave band data [1, 4]. Determining the actual loudness of a sound involves several steps. The procedure is a graphical one, standardised in ISO 532 B [2] and DIN 45631 [3]. It is somewhat tedious to use and so two computer programs were written to automate it. One was written by Paulus and Zwicker [4, 5]. The other was developed as part of DIN 45631 [3, 6]. The calculation process is outlined in [4].

3. SOUNDS TESTED AND PROCESSING SYSTEMS USED

A comparison of the results for loudness computed from various methods was investigated in this study. Two basic sources of input data were available: a sound level meter (SLM) and a 01 dB data acquisition system (DAQ). The SLM directly gives 1/3 octave band levels while the data from the DAQ can be filtered to give them. This process was accomplished in several ways. The 01dB software dBFA filters according to EIC 1260. The 01dB software dBsonic uses an unknown filtering algorithm. The MATLAB program [7], uses ANSI S1.11. Five processing methods were used for this study. These were: a Visual Basic (VB) program adapted from [5], a VB program adapted from [6], dBFA, dBsonic, and a MATLAB program [7] based on [6]. The two VB programs were adapted by the present authors. In order to efficiently compare the processing methods and input data, eight combinations were developed, listed in Table 1. For the 1-kHz tone, combinations 1 & 3 were not considered because of SLM hardware limitations.

4. RESULTS AND DISCUSSION

The loudness results for the four types of sounds are shown in table 2. For the 40 dB tones, only the Excel (ISO) method using EIC 1/3 octave data from dBFA, dBsonic, and the Hastings (DIN) method using ANSI 1/3 octave data give the correct result of exactly 1 sone_{GF}. For the 80 dB tones, no combination gives exactly 16 sone, which is the theoretical loudness for this sound. However, dBFA, dBsonic and Hastings with ANSI filtering give results closest to the theoretical value: 16.7, 16.5 and 16.4 sone_{GF} respectively. Only dBsonic and DIN with ANSI filtering give consistently accurate loudness values for the

tones. Based on the results from the tones, dBsonic and DIN with ANSI filtering will be taken as “correct” values of loudness.

Table 1: Combinations used

Combination	Input Data	Processing Method
1	SLM 1/3 oct.	VB from [4, 5] (ISO)
2	dbFA 1/3 oct. (EIC)	VB from [4, 5] (ISO)
3	SLM 1/3 oct.	VB from [6] (DIN)
4	dbFA 1/3 oct. (EIC)	VB from [6] (DIN)
5	dBFA 1/3 oct. (EIC)	dBFA
6	dBsonic 1/3 oct.	dBsonic
7	MATLAB 1/3 oct. (ANSI)	MATLAB (DIN)
8	dbFA 1/3 oct. (EIC)	MATLAB (DIN)

By looking at the results of the DIN loudness calculations using 1/3 octave data filtered via EIC 1260, ANSI S1.11, or using the SLM, it becomes apparent that there is more than just the calculation routine that affects the value obtained: the filtering method plays a significant. There is no mention of the method whereby the 1/3 octave band levels used should be acquired in ISO 532 B [2], nor in the numerical methods described in [4], [5] and [6]. This is a significant oversight in the specification of these standards.

All the sounds gave an A-weighted SPL of 80 dBA, while the loudness values for these sounds are highly varied: the pink noise has a loudness about three times that of the 1-kHz tone! It is also interesting to compare results for ISO and DIN given the same 1/3 octave band inputs. The error varies from 2.63% to 7.95%. Finally, it may not be meaningful to report loudness values with great precision. Consider the 80 dB tone. With an SPL of 80 dB, the loudness is about 16.5 sone_{GF}. According to the power law described in [1], a just-perceptible change to 83 dB would result in a new loudness of 19.7 sone_{GF}. This is a change of 3.7 sone! So, here the practical accuracy limit would be a range of this magnitude, ±1.8 sone.

5. CONCLUSIONS

The physical meaning of and calculation procedures for determining loudness were reviewed. 1-kHz tones at 40 and 80 dB(A), and pink noise, gasoline and diesel engine idle noise at 80 dBA were used to compare eight combinations of loudness calculation methods and 1/3 octave band filtering techniques. It was determined that the only two combinations to give accurate results were dBsonic and DIN with ANSI filtering methods. The program based on ISO does not seem to be accurate. The calculation of loudness from 1/3 octaves cannot be separated from the filtering process, as different methods all result in different values even when processed using a single calculation method. This dependence is largely ignored in the literature [1, 2, 4, 5, 6]. The results also highlight the difference between SPL and loudness. While all the sounds tested had an SPL of 80 dBA, their loudness varied from 16.5 to 50.1 sone_{GF}. Finally, when dealing with loudness, the error will be in the range of ±1.8 sone.

REFERENCES

- Zwicker, E. and Fastl, H., *Psychoacoustics: Facts and Models* (2nd Ed.), 1999, Berlin, Germany : Springer.
- ISO 532B, “Acoustics – Method for calculating loudness level,” 1975.
- DIN 45631, “Berechnung des Lautstärkepegels und der Lautheit aus dem Geräuschspektrum, Verfahren nach E. Zwicker,” 1990.
- Paulus, E. and Zwicker, E., “Programme zur automatischen Bestimmung der Lautheit aus Terzpegeln oder Frequenzgruppenpegeln,” *Acustica*, Vol. 27 253-266, 1972.
- Zwicker, E., Fastl, H. and Dallmayr, C., “BASIC-Program for calculating the loudness of sounds from their 1/3 oct band spectra according to ISO 532 B,” *Acustica*, Vol. 55 63-67, 1984.
- Zwicker, E. et al., “Program for calculating loudness according to DIN 45631 (ISO 532B),” *Journal of the Acoustical Society of Japan (E)*, Vol. 12 39-42, 1991.
- Hastings, Aaron, “*Program to calculate loudness based on DIN 45631*”, 2003.

Table 2: Measurement results (sone_{GF})

Combination	Pink Noise 1	Pink Noise 2	Diesel 1	Diesel 2	Diesel 3	Gasoline 1	Gasoline 2	Gasoline 3	Tone 40 dB 1	Tone 40 dB 2	Tone 80 dB 1	Tone 80 dB 2
1	54.9	54.0	24.0	24.0	23.9	27.5	27.2	26.5				
2	52.6	51.8	24.0	23.8	23.8	27.0	26.3	25.7	1.0	1.0	14.8	14.8
3	53.5	52.5	22.7	22.5	22.4	26.2	25.9	25.2				
4	51.1	50.3	22.7	22.4	22.5	25.8	25.3	24.5	0.9	0.9	14.3	14.3
5	54.0	53.1	24.5	24.2	24.2	27.7	27.0	26.2	1.1	1.1	16.7	16.7
6	50.8	49.9	22.2	22.0	22.1	25.3	24.7	24.0	1.0	1.0	16.5	16.5
7	50.4	49.4	22.4	22.1	22.1	25.3	24.8	24.2	1.0	1.0	16.4	16.4
8	51.1	50.3	22.7	22.4	22.5	25.8	25.3	24.5	0.9	0.9	14.3	14.3

EXPERIMENTAL VALIDATION OF THE OBJECTIVE MEASUREMENT OF INDIVIDUAL CUSTOM EARPLUG FIELD PERFORMANCE

J r mie Voix, Lee D. Hager, Jean Zeidan

Sonomax Hearing Healthcare Inc. Montreal (QC), H4P 2E2, Canada jvoix@sonomax.com

INTRODUCTION

To address the current issues [1] of discomfort (from both a physical and perceptual perspective) and unknown performance of existing Hearing Protection Devices (HPD), a new concept of a re-usable earplug has been recently developed [2,3,4]. For physical comfort this earplug is instantly custom-fitted with soft biocompatible silicone rubber. A sound bore through the earplug is used in two ways: first, for the measurement of the sound pressure level inside the earplug (see [3] for the assessment of the earplug attenuation) and, second, for the filtering of the earplug with passive acoustical dampers (see [2] for the customization of the attenuation to limit speech and warning signals degradation following CSA Z94.2 recommendations [5]). The expandable earplug is illustrated in Fig. 1. with the dual microphone probe and the sound source for field performance measurement.

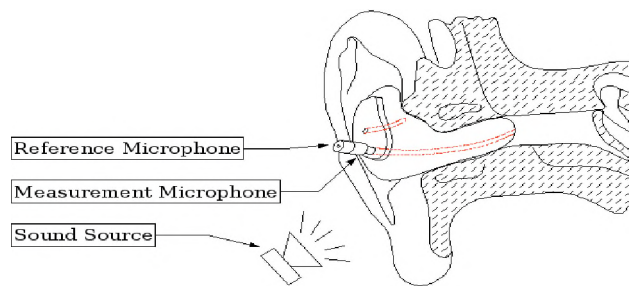


Fig. 1. The expandable custom earplug instrumented.

Once the fitted earplug has cured in the user's ear, a Noise Reduction (NR) measurement is performed on the earplug: a loud pink noise is generated with the reference sound source and the Transfer Function (TF) between the two microphones is computed including the corrections from the daily calibration TF and

the sound bore length correction. A so-called Field-MIRE (Microphone In Real Ear) method presented by the first author [3] is used to predict, from this octave-band NR measurement, the Real Ear Attenuation at Threshold (REAT) i.e. the difference between open and occluded-ear hearing thresholds as reported by human subjects.

From this octave-band REAT prediction, a single number value representing the overall HPD attenuation is computed: the Predicted Personal Attenuation Rating (P-PAR). The P-PAR is computationally similar to the Noise Reduction Rating (NRR), but it is obtained from an objective F-MIRE measurement (not from a subjective evaluation of the attenuation), on a particular user (not on a population sample), under realistic wearing conditions for the hearing protector (not under laboratory conditions), as opposed to standard REAT attenuation rating of HPD [5,6].

EXPERIMENTAL VALIDATION

2.1 Experimental protocol

The prediction method has been validated using results of tests conducted by an independent third-party research laboratory [7]: the P-PAR measured by the dedicated measurement device (dubbed SonoPass™) is compared side-by-side, for the same earplug on the same individual, to the attenuation that is measured using the REAT method. A group of twenty "naive" (as per ANSI S12.6 "Method B" requirements [6]) subjects were used. Each of the twenty subject tests included two parts:

1. Two determination of the REAT of two fits of the same earplug. Each test subject had been instructed prior to the entering of the REAT test room, to not remove/touch his earplug after final REAT testing.

2. A first measurement on the test subject in the same earplug fitting condition of the NR and prediction of the octave-band attenuation. This NR measurement is performed only once the subject exits the test room following the two sets of REAT measurements (because "Method B" requires the subject to stay isolated in the test chamber for the two REAT tests). A second measurement on the test subject of the F-MIRE attenuation, after the earplug has been removed and re-fitted by the subject himself, outside the REAT test room.

2.2 Experimental results

Fig. 2. presents the comparison between REAT and F-MIRE of the overall attenuation values of the twenty subjects, using three frequency ranges (125-2000, 125-4000 and 125-8000 Hz). The best predictions errors (overall prediction error is always less than 10 dB for each of the twenty cases tested) are actually obtained when using only the low-frequency octave-bands. This observation confirms that the low-frequency octave-band attenuation could be a good predictor of the overall attenuation [8], since most earplugs do anyway attenuate very well in high frequency. This observation also suggest that the high-frequency attenuation prediction is not -at least in that studied case- adding much information and appears to actually disturb the prediction capabilities of the measurement system.

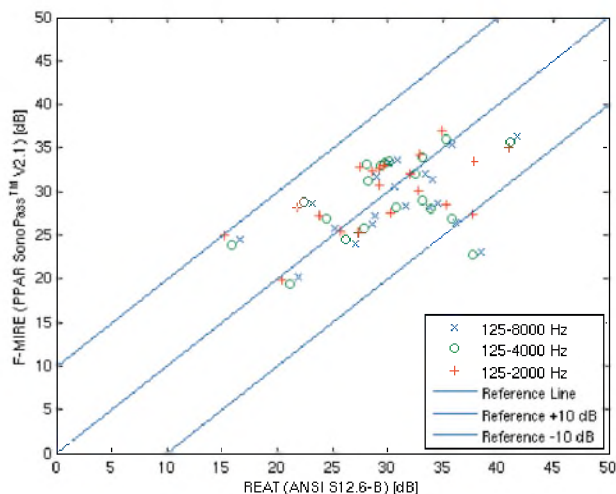


Fig. 2. Comparison between REAT and F-MIRE of the overall attenuation values of the twenty subjects, using the 125-2000 Hz (red '+'), 125-4000 Hz (green 'o') and 125-8000 Hz (blue 'x') ranges.

CONCLUSIONS

The presented approach was developed to meet the need to improve earplug field performance prediction accuracy by changing from average group performance prediction to individual performance prediction. The individual earplug field performance is objectively measured by a Field-MIRE method: the individual attenuation is predicted from the field measurement of the Noise Reduction through the earplug. The individual attenuation is first obtained as a set of values for each octave band center frequency and these values are then combined in a single number, the Predicted Personal Attenuation Rating (P-PAR). This P-PAR is the equivalent to the individual NRR obtained from the classical REAT attenuation testing. The method has been validated experimentally by an independent third party laboratory and the overall prediction error has been found perfectly suitable for improved hearing conservation practices.

ACKNOWLEDGEMENTS

The support of the ETS (University of Quebec), IRSST (Quebec Occupational Health and Safety Research Institute) and NSERC (Natural Sciences and engineering Research Council of Canada) is gratefully acknowledged.

REFERENCES

- [1] NIOSH. Criteria for a Recommended Standard. (1998)
- [2] Voix J., Laville F. and Zeidan J. Filter Selection to Adapt Earplug Performances to Sound Exposure. *Journal of the Canadian Acoustical Association* (2002) 30: p. 122
- [3] Voix J., Laville F. Expandable Earplug with Smart Custom Fitting Capabilities. *InterNOISE*, Dearborne, MI (2002).
- [4] Voix J., Laville F. New Method and Device for Customizing in-situ a Hearing Protector. *Journal of the Canadian Acoustical Association* (2004)
- [5] CSA Z94.2-02, Hearing Protection Devices.
- [6] ANSI S12.6-1997 (r2002), American National Standard Methods for Measuring the Real-Ear Attenuation of Hearing Protector. (1997)
- [7] Auditory System Laboratory, Virginia Tech, "SonoPass and Matlab Output for Sonomax ANSI S12.6B (r2002) Testing". (2006)
- [8] Berger E. Exploring procedures for field testing the fit of earplugs. *Industrial Hearing Conservation Conference*, University of Kentucky, Lexington, Kentucky. (1989)

COMPARISON OF METHODS FOR CHARACTERIZING SOUND ABSORBING MATERIALS

Yacoubou SALISSOU and Raymond PANNETON

GAUS, Department of mechanical engineering, Université de Sherbrooke, Québec, Canada, J1K 2R1
Yacoubou.Salissou@USherbrooke.ca , Raymond.Panneton@USherbrooke.ca

1. INTRODUCTION

Open-cell porous materials are widely used as acoustic absorbent media in the transport industry. In order to have a prior knowledge of their acoustic behaviour, different models have been developed [1-4]. Among all these models, the Johnson-Champoux-Allard [2, 4] is widely used because of its simplicity and accuracy. This model uses five parameters (open porosity, static airflow resistivity, tortuosity, viscous characteristic length and thermal characteristic length) which describe the internal structure of porous materials at the macroscopic scale. Different methods have been developed in order to characterize those parameters. Some of them are based on the physical and mathematical definition of the parameters. However, these methods, qualified as direct methods, require dedicated equipments. The second approach is based on the acoustical model from which analytical expressions linking the material parameters to acoustical measurements are derived. The methods using this approach are qualified as analytical inversion or indirect methods. Finally, the last approach is based on an optimisation problem where the material parameters are adjusted in the acoustic model to reproduce acoustical measurements. The methods of this group are qualified as inverse methods.

In this paper, three samples of metal foam are characterized using direct, indirect and inverse methods. The objective is to highlight that the methods may yield large variability in the found parameters. A discussion is given to explain the observed variability and the limitations of the methods.

2. CHARACTERIZATION METHODS

Direct measurement of the open porosity is performed using the Archimedes principle following the in-air missing mass method [5]. This method gives a direct measured value of open porosity through measurement of sample weight in vacuum and in air, and predicts the measurement error. In this study, because of the lack of material, the three samples will be put together (as one sample) to satisfy the minimum material volume required by the method. The direct method used to measure the static airflow resistivity is based on the method proposed by Stinson & Daigle [6].

The indirect method (IM) used in this work is based on the technique developed by Panneton & Olny [7,8]. Assuming dynamic density, dynamic bulk modulus, and open porosity

known, analytical solutions are used to determine the static airflow resistivity, tortuosity, viscous characteristic dimension (VCD), and thermal characteristic dimension (TCD) of the material.

The inverse method is based on an optimization problem where unknown parameters are adjusted to fit measured acoustic data (ex.: sound absorption coefficient) [9]. This method is first applied to find the tortuosity and the two characteristic lengths by assuming porosity and static resistivity known from direct measurements. Second, the algorithm is applied to find simultaneously the five parameters assuming that none of the parameters are known. The acoustical measurements required for the indirect and inverse methods were obtained using an impedance tube following ASTM E 1050 and ISO 10534-2 standards.

3. RESULTS AND DISCUSSION

The dimensions of the samples are summarized in table 1. Direct measured porosity is 0.89 ± 0.03 . Using this value, the four other parameters obtained from indirect method are summarized in table 2. In general, the parameters values are in good agreement from one sample to another and the deviation from mean values are acceptable. The deviation of tortuosity and characteristic length may appear a little bit high, but since these parameters are difficult to measure with an accurate precision, these deviations are acceptable. Table 3 shows that the method yields stable results inside the accepted values of porosity, and finally, the static airflow resistivity given by this method fits well with those measured directly (table 4). Using the directly measured porosity and mean value of airflow resistivity, the three-parameter inverse method (3-PIM) yields results summarized in table 5. As the indirect method, the results fit quite well from one sample to another and this method yields stable results inside the accepted values of porosity (table 6) and airflow resistivity (table 7), but seems to depend on frequencies range (table 8). In terms of behaviour, the five-parameter inverse method (5-PIM) yields similar results as the three-parameter method (see tables 9 and 10).

Table 11 presents a comparison of the results obtained from the different methods. We observe a significant difference between the porosity value given by the direct and inverse methods. Moreover, the airflow resistivity obtained by inverse method seems to be over estimated. Finally, the

results of the 3-PIM and IM compare well; however they diverge slightly from those giving by the 5-PIM. As 3-PIM and 5-PIM rely only on acoustical measurements, their accuracy exclusively depends on their quality and reproducibility. Usually because of experimental conditions (room temperature, sample fixing, etc), those measurements present a small deviations. The 5-PIM may be strongly vulnerable to those deviations and this may explain its variability. The two other methods (3-PIM and IM) are also affected by acoustical measurement deviations (this may explain their small variability), but less strongly than the 5-PIM since they use some known parameters. Furthermore, because both indirect and inverse methods rely on acoustical measurements, they are less accurate than the direct method. Finally, since both are based on the Johnson-Champoux-Allard model which supposes a motionless frame, they may yield wrong parameters when this condition is not satisfied. These results support the need of: 1) developing non-acoustical and direct methods (mainly for tortuosity and characteristic lengths), or 2) developing more accurate measurements in impedance tube for inverse and indirect characterization purposes.

ACKNOWLEDGEMENTS

N.S.E.R.C. supported this work.

REFERENCES

- [1] Biot, J. Acoust. Soc. Am. **28**, 179-191 (1956).
- [2] Johnson, Koplik, Dashen, J. Fluid. Mech. **176**, 379-402 (1987).
- [3] Champoux, Allard, J. Appl. Phys. **70**, 1975-1979 (1991).
- [4] Lafarge, Lemarinier (P.), Allard (J.F.), Tarnow (V.), J. Acoust. Soc. Am. **102**, 1995-2006 (1997).
- [5] Panneton, Gros, Acta Acustica **91**, 342-348 (2005).
- [6] Stinson, Daigle, J. Acoust. Soc. Am. **83**, 2422-2428 (1988).
- [7] Panneton, Only, J. Acoust. Soc. Am. **119**, 2027-2040 (2006).
- [8] Olny, Panneton, Proc. of Forum Acusticum 2002, 16-20 sept.
- [9] Atalla, Panneton, Can. Acoust. **33**, 11-23 (2005)

Table 1: Samples dimensions

Sample	Thickness (mm)	Diameter (mm)
1	18.83	29.0
2	19.12	29.0
3	19.31	29.0

Table 2: Results from indirect method.

The porosity value was 0.89 ± 0.03 measured with missing mass method [5] on the three samples at a same time. Uncertainty is predicted by method.

Sample	Tortuosity	Resistivity (Ns/m ⁴)	VCD (μm)	TCD (μm)
1	1.38	51 290	21.9	109.5
2	1.31	49 887	20.5	114.7
3	1.18	48 516	18.2	122.3
Mean	1.29	49 898	20.2	115.5

Table 3: Effect of porosity precision on indirect method

Porosity	Tortuosity	Resistivity (Ns/m ⁴)	VCD (μm)	TCD (μm)
0.88	1.28	49 840	20.2	106.0
0.89	1.29	49898	20.2	115.5
0.90	1.30	49927	20.3	132.0

Table 4: Static airflow resistivity from direct method

Sample	1	2	3	Mean
Resistivity (Ns/m ⁴)	51 325	50 034	48 670	50 010

Table 5: Results from 3-PIM

Porosity: 0.89 ± 0.03 , resistivity: 50010 Ns/m⁴, frequency: 800-6000 Hz

Sample	Tortuosity	VCD (μm)	TCD (μm)
1	1.45	24.8	119.9
2	1.45	24.88	122.58
3	1.26	21.2	162.9
Mean	1.39	23.6	135.1

Table 6: Effect of porosity precision on 3-PIM

Porosity	Tortuosity	VCD (μm)	TCD (μm)
0.88	1.42	24.8	122.4
0.89	1.39	23.6	135.1
0.90	1.34	22.1	149.0

Table 7: Effect of resistivity precision on 3-PIM

Resistivity (Ns/m ⁴)	Tortuosity	VCD (μm)	TCD (μm)
49000	1.31	21.7	142.9
50010	1.39	23.6	135.1
51000	1.43	24.5	136.0

Table 8: Frequency range effect on 3-PIM

Frequency range (Hz)	Tortuosity	VCD (μm)	TCD (μm)
800-6000	1.39	23.6	135.1
800-4000	1.37	22.6	153.5
300-6000	1.66	31.3	112.2
300-4000	-	-	-
1000-3000	1.40	23.0	146.3
2000-6000	1.32	21.5	125.7

Table 9: Results from 5-PIM

Frequency range: 800-6000 Hz

Sample	Porosity	Resistivity (Ns/m ⁴)	Tortuosity	VCD (μm)	TCD (μm)
1	0.84	55 135	1.54	28.2	85.1
2	0.84	54 688	1.53	28.30	85.65
3	0.81	53 112	1.42	28.0	85.1
Mean	0.83	54 312	1.50	28.2	85.3

Table 10: Frequencies range effect on 5-PIM

Frequency range (Hz)	Porosity	Resistivity (Ns/m ⁴)	Tortuosity	VCD (μm)	TCD (μm)
800-6000	0.83	54 312	1.50	28.2	85.3
300-6000	0.82	52 045	1.36	24.7	84.1
300-4000	-	-	-	-	-
1500-6000	0.89	54 050	1.47	26.5	117.8
2000-6000	0.91	55 520	1.56	26.7	128.0

Table 11: Comparison of results from the different methods

Method	Resistivity (Ns/m ⁴)	Tortuosity	VCD (μm)	TCD (μm)	Resistivity (Ns/m ⁴)
Direct	0.89	50 010	-	-	-
Indirect	-	49 898	1.29	20.2	115.5
3-PIM	-	-	1.39	23.6	135.1
5-PIM	0.83	54 312	1.50	28.2	85.3

THE AFFECT OF SHORT MUSICAL SEQUENCES WITH DIFFERENT MELODIC CONTOURS

Joshua Salmon and Bradley Frankland

Dept. of Psychology, Dalhousie University, 1355 Oxford St., Nova Scotia, Canada, B3H 4J1

1. INTRODUCTION

The relationship between musical structures and affect (emotion) has been of ongoing interest since at least Hevner (1935, 1936a, 1936b). Hevner explored the relationship between musical structure and affect by manipulating one aspect of musical structure at a time, and having participants rate the affect. For example, Hevner manipulated pitch height by taking pieces written in the high key and transposing them down an octave to a lower key, and vice versa (1936a). Two groups of participants then rated either the modified or original version. Differences in ratings were considered the “affect” or emotion conveyed by the musical structure. For pitch height, for example, high pitch was rated as “graceful” and “sparkling” and low pitch was rated as “sad” and “heavy”. Hevner repeated this procedure for manipulations of mode (major vs. minor), tempo, harmony, rhythm, and melodic contour (ascending versus descending melodies). Hevner’s results indicated a significant relationship between affect and all musical structures except melodic contour. That is, Hevner results for melodic contour were “not clear-cut, distinct or consistent” (1936b, p. 268). Hevner, however, did observe a trend for ascending and descending melodies to be rated differently (1936b).

Reporting “trends” for melodic contour is quite common. For example, Schubert (2004) reported a trend for ascending sequences to be rated as more happy than descending sequences. However, research reporting a significant and reliable relationship between contour and affect is rare. A possible reason for this lack of significant results is that most research has employed long, complex (“ecologically valid”) musical pieces. That is, often the stimuli chosen is a classical composition written by a famous composer (e.g. Mozart or Bach). However, in pieces like these, many attributes are changing: rhythms, tempos, harmonies, et cetera. It can become difficult to tease the influence of the musical structure of interest from all the background variation. Additionally, in long pieces it becomes increasingly difficult to establish which musical event is producing which response. Thus, melodic contour may be best studied under conditions in which most other structures of music are kept constant, and musical pieces/sequences are kept short.

In fact, Gerardi and Gerken (1995) tested this hypothesis by using short (4 measure) monophonic sequences with a constant rhythm and approximately constant mean pitch

height (octave). Gerardi and Gerken’s results indicated that ascending sequences were rated as significantly more happy than descending sequences for college aged participants, but not for 5 or 8 year olds. Thus, Gerardi and Gerken showed that a significant relationship between melodic contour and affect can be demonstrated when short simple sequences of music are used. Unfortunately, the assessment of affect was limited to happy-sad.

Most research in this area has focused on the influence of ascending versus descending sequences with a limited set of affect terms. However, there are more possible melodic contours in music than just ascending or descending. For instance, Huron (1996) found in his analysis of the different types of contours that the melodic arch (in both its regular and inverted form) occurred equally as often as ascending and descending contours. In addition, there are more dimensions to affect than happy-sad.

The current study extends the study of the relationship between contour and affect by using more varieties of contours and more affects. Ascending/descending, arch and more complex, musically valid, 8-note contours were designed and then modeled with polynomial equations of the form $y = a_0 + a_1x + a_2x^2 + a_3x^3 + a_4x^4$. In this, y represents pitch height, x time, and the coefficients (a_0, a_1, a_2, a_3, a_4) capture different aspects of the shape of the contour. For reasons of space, only $a_0, a_1,$ and a_2 are discussed in this work. Listener ratings of affect on ten 3-point affect scales were then compared to these coefficients.

2. METHOD

2.1 Participants

Two groups of fifty participants participated in this study. Both groups were exposed to the same 16 sequences, but different affect scales. Participants (25 male) had a mean age of 19.2 years, and all reported some musical experience, with the average participant reporting having played about 3 instruments (counting voice), with an average of 5.4 years on their most preferred instrument. The groups did not differ demographically.

2.2 Procedure & Stimuli

Each group rated a set of sixteen 8-note sequences on six affect scales. The set of 16 sequences was designed to be contained within the two octaves above and below middle C (C4), with an equal number of sequences above

and below C4. All sequences began and ended on C, were monophonic, were equi-temporal, and were played at a constant tempo. Some sequences were designed to be linear (ascending or descending), some were arches, and some had more complex melodic contours.

Participants rated every possible affect scale / musical sequence combination twice, for a 16 (sequence) x 6 (affect scale) x 2 (times) design. The list of affect scales for each group is presented in Table 1. Note that both groups were exposed the scales “contentment-joy” and “hesitation-confidence”.

3. RESULTS

The regression coefficients were calculated for each of the sixteen sequences, and then correlated to the mean responses provided by the participants. Table 1 shows the correlations for each of the polynomial coefficients (a_0 , a_1 , a_2) to each affect scale.

Table 1. Correlation between Pitch Height Coefficient and Responses (across all musical sequences) for Groups 1 & 2.

Affect Scales	a_0	a_1	a_2
1 contentment-joy	.688***	.042 ns	-.115***
hesitation-confidence	.471***	.019 ns	-.109***
pensiveness-playfulness	.680***	.070*	-.100***
delicacy-strength	-.345***	.031 ns	.050 ns
irritation-calmness	-.511***	-.063 ns	.030 ns
excitement-boredom	-.700***	-.067 ns	.094***
2 contentment-joy	.672***	.092**	-.114***
hesitation-confidence	.403***	.068 ns	-.130***
passivity-aggression	.091*	.132***	.003 ns
questioning-answering	-.019 ns	-.134***	-.076*
surprise-expectation	-.543***	-.120***	.108**
energy-tranquility	-.617***	-.121**	.086*

Notes: ¹ a_0 captures information about pitch height, and a positive coefficient means that the second affect is associated with higher pitches. ² a_1 captures information about the linear ascending or descending nature of the sequence, and a positive coefficient means that second affect is associated with a positive slope. ³ a_2 captures information about the arch and a positive coefficient means that an inverted arch is associated with the second affect term. ⁴shaded cells indicate repeated affect scales.

These correlations were approximately the same for both Groups 1 and 2. Both pitch height (a_0) and melodic arch (a_2) correlated to affect scales contentment-joy and hesitation-

confidence. However, for ascending/descending (a_1) music, Group 2 rated ascending sequences as conveying joy, but Group 1 did not.

These correlations further indicated that higher pitch / octave (a_0) was associated more with ratings of joy, confidence, playfulness, delicacy, irritation, excitement, aggression, surprise and energy. Ascending sequences (a_1) were associated with ratings of playfulness, joy (for Group 2), aggression, questioning, surprise and energy. A melodic arch that rises than falls (a_2) was associated with ratings of joy, confidence, playfulness, exciting, answering, surprise, and energy.

4. DISCUSSION

The current results replicated the results of previous research (e.g. Gerardi & Gerken, 1995) by indicating that ascending sequences were ascribed more positive ratings (i.e. joy) than descending sequences. The current study additionally considered the role of the melodic arch and indicated that not only do listeners ascribe consistent affect ratings to arches, but they may do so more readily for arches than they do for ascending / descending sequences. In this design, however, pitch height (octave) not melodic contour appeared to be the most emotional salient feature of music (more significant responses for a_0). This occurred despite the fact that all sequences were contained between two octaves.

Future research should consider the role of melodic arches in studies of affect.

REFERENCES

Gerardi, G. M., & Gerken, L. (1995). The development of affective responses to modality and melodic contour. *Music Perception*, 12(3), 279-290.

Hevner, K. (1935). The affective character of the major and minor modes in music. *American Journal of Psychology*, 47, 103-118.

Hevner, K. (1936a). The affective value of pitch and tempo in music. *American Journal of Psychology*, 50, 621-630.

Hevner, K. (1936b). Experimental studies of the elements of expression in music. *American Journal of Psychology*, 48, 246-268.

Huron, D. (1996). The melodic arch in western folksongs. *Computing in Musicology*, 10, 3-23.

Schubert, E. (2004). Modeling perceived emotion with continuous musical features. *Music Perception*, 21(4), 561-586.

AUTHOR NOTES

This work was conducted while Joshua Salmon was a Master’s student at Dalhousie University, under the supervision of Dr. Bradley Frankland.

AN INITIAL EXPLORATION OF PARALLELISM IN MUSIC: EQUI-TEMPORAL THREE-TONE DIATONIC SEQUENCES

B. W. Frankland

Dept. of Psychology, Dalhousie University, Halifax, Nova Scotia, Canada, B3H 4J1 brad.frankland@dal.ca

1. INTRODUCTION

The perception of parallelism in music is considered crucial to the understanding and expression of affect in music (cf. Lerdahl and Jackendoff, 1983, p. 51-521). Yet there seem to be no quantitative models of the perception of parallelism in music. Simplistically, the perception of parallelism in two sequences can be divided into pitch-pattern parallelism (parallelism based on the pitch-height of the contour) and time-pattern parallelism (e.g., parallelism based on the timing of events such as onsets, offsets, and durations).

This work tested several models of pitch-pattern parallelism in short, three-note, musically relevant, sequences. To assess parallelism, one can focus on the corresponding changes between adjacent notes (i.e., the intervals), or one can focus on the actual pitches. Both can be rationalized, and both were explored. However, only the interval-based pitch-pattern parallelism is presented herein for reasons of space.

To quantify parallelism, sequences were encoded as intervals and then two sequences were compared interval-by-interval. The sum those comparisons over all intervals is a measure of parallelism. For the comparison, there are several approaches, each having pros and cons, but only most intuitive are cited herein. One can sum the differences between intervals (DifInt), the absolute value of differences between intervals (MADInt), or the root-mean-square of the differences between intervals (RMSInt). The second and third are analogous to the mean absolute deviation and the standard deviation commonly used in statistics. One can also sum the differences between the absolute values of the intervals (DifAInt), which is subtly different from the MADInt. The measures DifInt and DifAInt are arbitrarily affected by the order of computation (i.e., which of two sequences is called A and which is called B). To eliminate those order effects, one can take the absolute value of those measures creating ADifInt and ADifAInt.

A simpler model examines only the Up/Down pattern of the contour. Each interval is coded as increasing (1), unchanging (0) or decreasing (-1). Analogous to the above, one can sum of the differences in the Up/Down pattern (UD), the absolute value of the differences in the Up/Down pattern (MADUD), or the root-mean-square of the differences in the Up/Down Pattern (RMSUD). In addition,

to remove order effects, one can take the absolute value of UD creating AUD.

Each of these models (and many not mentioned) was tested against the empirical assessment of parallelism in a total of 324 pairs of three-note equi-temporal sequences. Equi-temporal sequences of notes were used to avoid time-pattern parallelism.

2. METHOD

2.1 Participants

Sixty participants (40 females) with a mean age of 22.28 ± 7.31 years (range: 17 to 50), with the equivalent of an average of 13.76 ± 15.04 years of instruction at one hour per week (many studied more than one hour per week). All participants were recruited from the university community, primarily the Departments of Psychology and Music. Royal Conservatory of Music (RCM) or equivalent grades ranged from 0 to Grade 10 with mean and standard deviation 2.18 ± 3.46 . One had a degree in music. Most (38) had no formal RCM grade. Participants were quasi-randomly assigned to one of three groups ($n = 20$ per group). Groups did not differ on age, musical experience, sex or handedness.

2.2 Apparati and Stimuli

Participants were presented with pairs of three-note sequences, selected from a set of 18 sequences. All notes of all sequences were confined to the diatonic notes of the key of C within the octave C_4 to C_5 (referenced to $A_4 = 440$ Hz), referred to as c, d, e, f, g, a, b, C. The 18 sequences were ccc, cec, Ceg, feg, bga, agb, ceg, CgC, egc, def, fef, dfe, Cge, cge, geC, fff, aba, dfe. The full set of all 18x18 pairs of sequences was tested, including both orders of each pair (A then B, and B then A).

Sequences were created using the acoustic piano of the internal MIDI driver (instrument 0, mode 0) of a Creative Labs Sound Blaster 16 in an IBM compatible computer. Each pair of sequences (e.g., each trial) was presented binaurally through Sony headphones connected directly to the audio output of the Sound Blaster. All notes were 240 ms (approximately 250 mm). Each trial consisted of the first sequence (720 ms), followed by a 1500 ms pause, then the second sequence (720 ms), and then a 4000 ms response window. Responses were only collected during the response

window. Following the response, there was a 1500 ms inter-trial time. The same computer presented instructions on screen (throughout the experiment) and recorded responses.

2.1 Procedure

While seated comfortably in a Industrial Acoustics sound-attenuating room, each participant completed a single eight-stage experiment. The test session required about 1 hour, including the collection of background information and debriefing.

Stages 1, 3, 5, and 7 assessed the internal representation of tonality of the participant using a modified probe-tone task (cf. Frankland & Cohen, 2004), with Stage 1 as practice. These are not discussed further.

Stages 2, 4, 6, and 8 assessed the perception of parallelism, with Stage 2 as practice. Each of Stages 4, 6, and 8 presented a 6x6 grid of pairs of sequences (i.e., 36 pairs of sequences, or 36 trials). In each trial, participants heard two three-note sequences and rated the degree of parallelism using a 3-point scale. No definition of parallelism was provided. Across three stages, each participant provided ratings for 108 pairs of sequences. Hence, three groups (randomly assigned) were required to complete the entire 18x18 (324 pairs of sequences) grid. Within each stage, there were actually two blocks of trials with the same 36 trials in each block. However, there was no discernable break between blocks. Trials were presented in a unique random order for each block, and for each participant.

3. RESULTS

Preliminary analyses indicated no effect of missing values, and not interactions involving block. Hence, the two blocks were averaged. Cluster analyses indicated that, within each stage, all participants rated the pairs of sequences in much the same manner (i.e., there were minimal effects of training or experience with music). To collapse data across groups, the data of each participant was converted to deviations from the mean of that participant. Mathematically, this is equivalent to removing the subjects and groups (nested within subjects) terms of a mixed ANOVA (cf. Cohen & Cohen, 1983, p. 428-435).

The first analysis examined ratings as a function of pair of sequences using an ANOVA. Not surprisingly, there was a significant effect of pair ($F(323,6154) = 11.45, p < .0005$), but the important statistic is the effect size, η^2 , of .375. The ANOVA captures any and all differences due to the IV (pairs). This implies that, at best, a model of parallelism can only hope to explain 37.5% of the variance. Each model was tested in a regression analysis, using rating as the DV and quantified parallelism as the IV. To capture potential non-linearities in responding, all regression analyses used a fourth-order polynomial fit. The results are presented in Table 1, which shows the increase in explained variance (R^2

and ΔR^2) due to the hierarchical inclusion of each term of the power series.

Table 1: The Analysis of the 10 Interval-Based Models of Parallelism

Model	Linear R^2	Quad ΔR^2	Cubic ΔR^2	Quart ΔR^2	All R^2
DifInt	.000	.004	.000	.006	.011
MADInt	.043	.067	.032	.010	.151
RMSInt	.044	.069	.030	.010	.152
DifAInt	.001	.067	.001	.003	.072
ADifInt	.015	.017	.008	.002	.043
ADifAInt	.088	.004	.001	.014	.115
UD	.001	.007	.000	.010	.138
MADUD	.074	.109	--- ¹	--- ¹	.183
RMSUD	.079	.101	.041	--- ¹	.220
AUD	.014	.004	--- ¹	--- ¹	.017

Note: ¹Term could not be computed.

4. DISCUSSION

Generally, results indicated that participants could provide reliable within- and between-estimates of the perception of parallelism in three-note sequences, despite the lack of an a priori definition of parallelism. However, differences in sequences only explained 37.5% of the total variance in responses. Furthermore, the best models could explain only explain 22.0%, or only 58.7% of those systematic differences.

Other models not discussed, some based on intervals and many more based on the actual pitches (rather than the intervals) fared about the same. Various combinations of various models managed to achieve a more impressive 30.0% of the variance, but this is still only 80.0% of the available systematic variance. Hence, the implication is that other models of parallelism are needed, or that the perception of parallelism may depend on factors that are not truly about the pitch contour (e.g., issues of tonality). This work continues with more models and longer sequences. It is also currently being extended to time-pattern parallelism.

REFERENCES

- Cohen, J. & Cohen, P. (1983). *Applied Multiple Regression/Correlation Analysis for the Behavioural Sciences*. Hillsdale, NJ: Lawrence Erlbaum Associates, Publishers.
- Frankland, B. W. & Cohen, A.J. (2004). Parsing of melody: Quantification and testing of the local grouping rules of Lerdahl and Jackendoff's *A Generative Theory of Tonal Music*. *Music Perception*, 21, 501-545.
- Lerdahl, F. & Jackendoff, R. (1983). *A Generative Theory of Tonal Music*. Cambridge, MA: MIT Press.

CAN SILENCE AFFECT PERCEPTION? DURATION AND FREQUENCY OF OCCURRENCE IN PERCEIVED PITCH STRUCTURE

Michael E. Lantz¹, and Lola L. Cuddy²

¹Dept. of Psychology, University of Prince Edward Island, Charlottetown, P.E.I., C1A 4P3 e-mail: mlantz@upei.ca

²Dept. of Psychology, Queen's University, Kingston, Ontario, K7L 3N6

1. INTRODUCTION

Walsh's (2003) theory of magnitude states that attributes of events such as duration and frequency of occurrence act upon a single mechanism that in turn increments a magnitude accumulator. However, Lantz and Cuddy (1998) found that, within a sequence of tones, longer tones were judged more salient than shorter but more frequent tones. The finding suggests that the duration of an event has perceptual priority over the frequency of occurrence of the event, and brings into question Walsh's (2003) theory of magnitude. Duration should not increment a magnitude accumulator more than frequency of occurrence.

In the current study, we further investigated the nature of duration. A possibility is that a longer duration allows rehearsal, essentially increasing the frequency of occurrence of the event through self-generated repetitions (Johnson, Taylor, & Kaye, 1977). If such is the case, it should not matter whether the event continues throughout the full duration or whether a shorter duration is followed by a period of silence equalling the full duration.

Duration and frequency of occurrence are both elemental in music. In our study, we manipulated the duration and frequency of occurrence of tones, as well as the silence between tones, to understand how they affect the perceived organization or pitch structure of tone sequences.

Listening to a melody establishes a pitch structure or a "sense of key" so that we can easily tell when a tone does not fit, or sounds "sour". In order to measure perceived pitch structure, we used the probe-tone technique (Krumhansl & Shepard, 1979). A sequence of tones is played to the listener, followed by a probe tone, one of the 12 chromatic divisions of the octave. The listener rates how well the probe tone fits the sequence just heard. The sequence is then repeated, followed by a different probe tone until all 12 chromatic tones have been presented and rated. The resulting probe-tone profile of 12 ratings is then examined for evidence of perceived pitch structure. Key-defining sequences yield a hierarchically structured profile that matches Western music-theoretic proposals concerning the relative salience and function of tones within a key (Krumhansl & Kessler, 1982). Nonkey-defining sequences

yield a perceived pitch structure organized according to the surface properties within the sequence, such as the duration (Lantz & Cuddy, 1998) or frequency of occurrence (Oram & Cuddy, 1995).

We asked whether a silence following a tone could affect the perception of pitch structure of a tone sequence. In the current study, three types of sequences were created—an original sequence in which there were shorter but more frequent tones, and two modifications of the original sequence. In one modification, the long tones were shortened and followed by silence so that the duration of the tone plus silence equaled the duration of the long tone in the original. In the other modification, long tones were shortened and followed immediately by the next tone (i.e., no intervening silence). Long tones were expected to receive higher probe-tone ratings than short tones, as in Lantz and Cuddy (1998). More frequent tones were expected to receive higher ratings than less frequent tones, as in Oram and Cuddy (1995). The outcome of particular interest was whether a tone followed by silence would be rated as highly or higher than the more frequent tones.

2. METHOD

2.1 Participants

Twenty-four listeners from an Introductory Psychology class took part for course credit. Half the listeners had achieved at least Royal Conservatory of Music (Toronto) grade VIII music training or equivalent. The rest of the listeners had much less music training, no more than they had received in grade or high school music classes.

2.2 Sequence Construction and Apparatus

Sequences were generated from six-tone tonesets. Each toneset contained the tones of two major triads from maximally distant keys so that tonesets did not correspond to any key of the Western tonal system. Three sequence conditions were created from the tonesets. In Condition 1, the tones of one major triad (Triad Du) were longer than the other tones (2000 ms vs. 125 ms), whereas the tones of the other major triad (Triad Fr) were shorter but occurred more often (12 occurrences vs. 3 occurrences). In Condition 2, the first sequence was modified so that long Triad Du tones were shortened to the 125 ms duration of Triad Fr tones and immediately followed by silence such that the tone plus

silence equaled the duration of the long tones in Condition 1. In Condition 3, the original sequence was again modified such that long tones were shortened and followed immediately by the next tone (i.e., no intervening silence).

Sequences were Musical Instrument Digital Interface (MIDI) files. Presentation of sequences and collection of responses were controlled by a Zenith Z-200 computer. All tones were pure tones in the range C4 to B4 generated by a Yamaha TX802 FM tone generator. Sequences were delivered to the listener through Sennheiser 480 headphones in a sound-attenuated chamber.

2.3 Procedure

Listeners were tested individually with the probe-tone technique. Each of the three sequences was heard 14 times in succession. The first two trials were practice with the probe tone selected randomly. The 12 experimental trials were each followed by one of the 12 chromatic tones in random order. Listeners rated how well each probe tone 'fit' with the sequence on a scale of '1 – fits very poorly' to '7 – fits very well'. Listeners then filled in a form about their music training.

3. RESULTS AND DISCUSSION

Ratings from each listener for each condition were ordered according to (1) the three tones of Triad Du, (2) the three tones of Triad Fr, and (3) the six tones not in the tonal set. A 12 x 3 x 2 (Probe Tone X Condition X Group) mixed factorial ANOVA with orthogonal contrasts was conducted. The contrasts of concern compared ratings for Triad Du to ratings for Triad Fr. Overall, there was no difference in ratings for Triad Du and Triad Fr, $F(2, 22) = 0.28, p > .60$. However, there was a significant interaction across conditions that can be seen in Figure 1, $F(2, 22) = 9.49, p = .006$. The long tones of Triad Du received the highest ratings in Condition 1, and the more frequent tones of Triad Fr received the highest ratings when Triad Du had no duration bias in Condition 3. As expected, duration had priority over frequency of occurrence, although frequency of occurrence had an effect on perception when duration was removed as a cue to pitch structure. Of more interest is that a short tone followed by silence had an effect on the ratings of Triad Du in Condition 2. If silence had no effect on perceived pitch structure, then ratings for Triad Fr should have been higher than ratings of Triad Du. However, neither group rated Triad Fr higher than Triad Du. The musically trained group rated Triad Du higher than Triad Fr, just as they had when the tone had been played throughout the full duration. The musically untrained group rated Triad Du just as highly as Triad Fr.

Silence clearly had an effect on perceived pitch structure, with an increase in ratings for Triad Du for the short duration followed by silence compared to ratings for Triad Du tones of the same duration but without subsequent

silence. Those with music training perceived the tones with silence to be just as important as the long tones of Condition 1. The musically untrained group perceived the tones with silence to be just as important as the more frequent tones in Condition 2.

The improved ratings of a tone with silence may be due to rehearsal (Johnson et al., 1977), echoic memory, or to placement at the end of a phrase, with the silence indicating a phrase boundary. In any case, the results are problematic for Walsh's (2003) theory of magnitude. Any accumulator must increment the magnitude of tones even in the absence of the sounding of a tone.

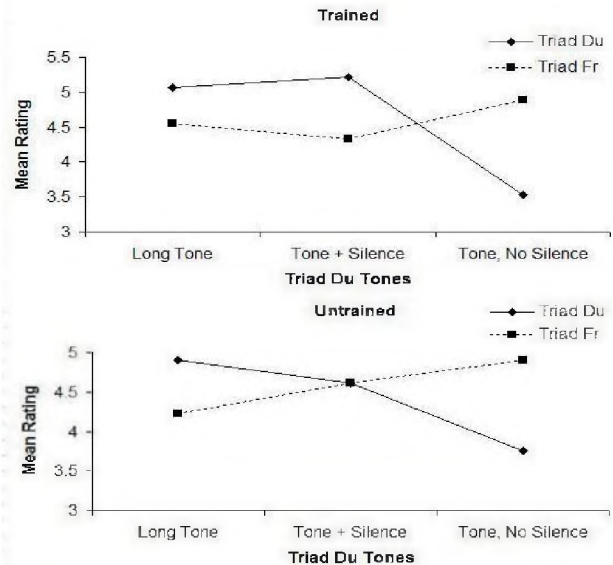


Fig. 1. Mean ratings for Triad Du and Triad Fr across the three conditions: Triad Du tones played for a long duration, a short duration followed by a silence, and a short duration without subsequent silence. The two panels show ratings from musically trained listeners (top) and musically untrained listeners (bottom).

REFERENCES

- Johnson, M.K., Taylor, T.H., & Kaye, C. (1977). Fact and fantasy: The effects of internally generated events on the apparent frequency of externally generated events. *Memory & Cognition*, 5, 116-122.
- Krumhansl, C.L., & Kessler, E.J. (1982). Tracing the dynamic changes in perceived tonal organization in a spatial representation of musical keys. *Psychological Review*, 89, 334-368.
- Krumhansl, C.L., & Shepard, R.N. (1979). Quantification of the hierarchy of tonal function within a diatonic context. *Journal of Experimental Psychology: Human Perception and Performance*, 5, 579-594.
- Lantz, M.E., & Cuddy, L.L. (1998). Total and relative duration as cues to surface structure in music. *Canadian Acoustics*, 26, 56-57.
- Walsh, V. (2003). A theory of magnitude: Common cortical metrics of time, space and quantity. *Trends in Cognitive Sciences*, 7, 335-338.

This study was supported by a research grant to the second author from the Natural Sciences and Engineering Council of Canada.

THE ROLE OF MUSIC, SOUND EFFECTS & SPEECH ON ABSORPTION IN A FILM: THE CONGRUENCE-ASSOCIATIONIST MODEL OF MEDIA COGNITION

Annabel J. Cohen, Kelti MacMillan, & Robert Drew

University of Prince Edward Island, 550 University Ave., Charlottetown, PE, Canada, C1A 4P3

acohen@upei.ca, kamacmillan@upei.ca, rdrew@upei.ca

1. INTRODUCTION

Feature films aim to engage an audience in a story. In the present paper, we refer to such engagement as *absorption*. We are interested in the contribution of soundtracks to absorption. They typically consist of speech, sound effects and music. Unlike speech and sound effects, music plays no part in the story as music per se. Without this rationale, how does music contribute to audience engagement? Should it not instead distract the audience? The Congruence-Associationist Model (C-A M; cf., Boltz, 2004; Cohen, 2001, 2005) provides an answer.

C-A M assumes that the audience's goal is to create a meaningful story from the material of the film: two visual (scenes and text) and three audio (music, effects, and speech) channels (see Fig. 1). At lower levels of analysis, information in these distinct channels is analyzed for meanings and structures. Some information leaks upward to long-term memory which then provides inferences about the narrative. The best match between top-down inferences and bottom-up analysed information results in the conscious *working narrative*—the experience of the film as the audience knows it. In C-A M, the brain can exploit that part of musical information has value for the story (e.g., emotional meaning) while ignoring the rest (e.g., the acoustical properties of the musical sounds). The principle of Association aggregates meanings from the five channels. Thus emotional meaning of music can provide context for a neutral visual scene. The principle of Congruence accounts for impact of shared structural features across channels, e.g., shared rhythm of music and visual motion could draw attention to the agency of the visual motion.

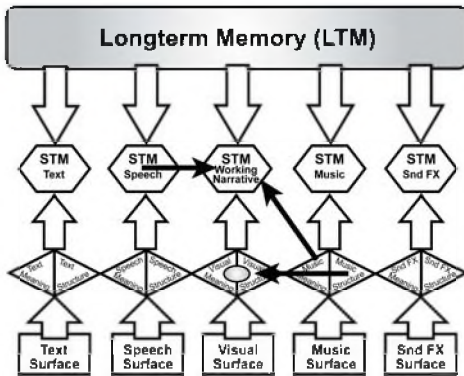


Fig. 1. Congruence-Associationist Model of Media Cognition (C-A M; from Cohen, 2005, p. 30)

Our laboratory has been exploring the role of music on absorption in a film. We have shown that the presence as opposed to absence of music in a film clip can lead to higher self-ratings of absorption in the clip (Cohen, MacMillan, & Drew, 2005). The present study extends this enquiry by comparing absorption as a function of three different soundtracks (only sound effects, only speech, and only music) for the same visual clip. Three soundtracks were created to make sense with the film so as to determine whether the music track, as compared to the speech and sound effects tracks, promoted audience absorption.

2. METHOD

2.1 Stimuli

Video information consisted of two 1-minute clips from DVD's of *Witness* (P. Weir, 1985) and the *Day of the Jackal* (F. Zinneman, 1973). The original soundtrack for the *Witness* (George Delerue) contained only music. The original soundtrack for *Jackal* contained speech and sound effects. For *Witness*, two additional soundtracks were created; one containing only realistic sound effects typical of the police-office setting (sirens, typing etc.), the other containing speech of the characters on the screen (a boy and several older people). For *Jackal*, three new soundtracks were created: a music track from music found elsewhere in the film (Maurice Jarre); a speech track of possible dialogue associated with the actors in the scene (an older criminal, a female victim, and a military officer); and a sound effects track matching the outdoor and apartment scenes (crowds, crutches on pavement, running water, ticking clock, etc). The tracks were created using Avid and Digidesign non-linear editing facilities, Foley techniques for the sound effects as well as digital sound libraries. In addition to these independent soundtracks, two combination soundtrack conditions were created for each of the video clips. One combined the two realistic sets of sounds (sound effects and speech) and the other combined all three soundtrack types. The combinations entailed some boosting and attenuation of various tracks in order to avoid masking of the speech by the music, for example. For each of the 5 soundtrack conditions, two DVD's were created: one which presented the *Witness* clip first and the other which presented the *Jackal* clip first. The main emphasis of the present paper is the soundtracks representing only one domain, music, effects, or speech.

2.2 Participants

There were 60 adults primarily from the university population participated in the study (mean age 22.23 years, SD = 5.26, range 18-44; 12 for each soundtrack group).

2.3 Procedure

Participants were tested alone or in groups of up to three. They were told that they would be presented with a short clip of a presentation and that they would be asked to rate on a 7-point scale their *absorption* in the presentation, the *realism* of the presentation, and the *professional quality* of the presentation. Prior to each of the two clips, they were asked to read the synopsis of the story that took the reader to the beginning of the clip. After rating absorption, realism, and quality, they were asked to rate their certainty that certain events would occur following the clip. Biographical information and some other questions about media were then completed.

3. RESULTS.

The study aimed to determine whether music led to audience absorption in a manner comparable to that of sound effects or speech. It is this questions that we focus on. Judgments of realism and quality provide measures of control, to assure that absorption judgments are not simply based on a sense of general professionalism of the production rather than on the specific mode of the soundtrack.

The mean Absorption, Realism, and Quality ratings for the only- music, speech, and sound effects conditions for each of the two film clips are shown in Table 1. The highest level of absorption is found under the condition with music for the film *Witness*. The lowest is for *Jackal* with speech.

Table 1. Mean Rating as a function of Film (<i>Jackal/Witness</i>) & Soundtrack type: Sound Effects (FX), Speech (Spc) and Music (Mus) [<i>max se.</i> = .44]						
	<i>Day of the Jackal</i>			<i>Witness</i>		
	FX	Spc	Mus	FX	Spc	Mus
Absorption	4.7	3.5	4.4	4.0	4.7	5.5
Realism	3.1	3.6	4.0	4.7	4.5	4.6
Quality	3.9	3.6	4.6	4.8	5.1	5.2

The absorption, realism and quality ratings were entered into an ANOVA with 2 within-subject factors of rating type (Absorption, Realism, and Quality) and film (*Witness/ Jackal*) and 1 between-subject factor of Soundtrack Condition. Separate analyses were also carried out for Absorption, Realism, and Quality. In the overall analysis, there was a significant interaction of Rating type (Absorption/ Realism/Quality), Soundtrack Condition (FX,

Speech, Music) and Film, $F(4,66) = 3.59; p < .01$, with significant linear and quadratic effects. The only other significant effect in the analysis was that of Film, with *Witness* leading to higher ratings overall than *Jackal*. Thus, the film soundtrack type influenced the judgments of absorption, realism and quality for a particular film in different ways. In separate analysis of absorption, there was a significant interaction of film and soundtrack type, $F(2,33) = 3.9; p < .03$. For the analyses of realism and quality, this interaction was not significant. Mean quality and realism were statistically higher for *Witness* than *Jackal*.

4. DISCUSSION

The degree of self-assessed absorption in the clips depended on whether the soundtrack was composed of sound effects, speech, or music, even when the professional quality of these three soundtracks was deemed statistically equal. Because the effect was observed under a highly controlled and unnatural situation of viewing a clip for only 1 minute, the results suggest that the effects of music on absorption are efficient and that music alone may at times hold a privileged path to absorption while watching a film, even without a basis in the narrative for the music as music per se. In cases where music adds to audience absorption, it is likely that music is contributing essential information, such as emotional information, to the story-telling. Such an account is consistent with the Congruence-Associationist Model (Cohen, 2001, 2005).

5. REFERENCES

- Boltz, M. (2004). The cognitive processing of film and musical soundtracks. *Memory & Cognition*, 32, 1194-1205.
- Cohen, A. J. (2001). Music as a source of emotion in film. In P. Juslin & J. Sloboda (Eds.) *Music and Emotion* (pp. 249-272). Oxford: Oxford University Press.
- Cohen, A. J. (2005). How music influences the interpretation of film and video: Approaches from experimental psychology. In R. A. Kendall & R. W. Savage (Eds.). *Perspectives in Systematic Musicology. Selected Reports in Ethnomusicology*, 12, 15-36.
- Cohen, A. J., Macmillan, K.A. & Drew, R. (2005). Music influences absorption in motion pictures: Interactions with Genre. Poster presented at Music & Neurosciences II, Leipzig.

6. ACKNOWLEDGEMENTS

The work is supported by a grant from the Social Sciences and Humanities Research Council of Canada (SSHRC) and made use of equipment provided by the Canada Foundation for Innovation (CFI) and Canadian Heritage under the Arts-Netlantic Project and the Institute for Interdisciplinary Research in Culture, Multimedia, Technology & Cognition Project (CMTC).

ERROR BOUNDS, UNCERTAINTIES AND CONFIDENCE LIMITS OF OUTDOOR SOUND PROPAGATION

Nicholas Sylvestre-Williams^{1,2} and Ramani Ramakrishnan³

¹Dept. of Mechanical Engineering, Ryerson University, 350 Victoria St., Ontario, Canada, M5B 2K3 nsylvest@ryerson.ca

²Pinchin Environmental, Mississauga, Ontario

³Dept. of Architectural Science, Ryerson University, 350 Victoria St., Ontario, Canada, M5B 2K3 rramakri@ryerson.ca

1. INTRODUCTION

The evaluation of noise levels from sources in the atmosphere has been wrought with difficulties. Embleton in a tutorial paper highlights the complex nature of outdoor sound propagation [1]. The noise prediction models have varied from complex procedures as shown by Schmoer and White [2] to a very simple engineering method being adopted by an International Standard [3].

Part 2 of ISO 9613 [Reference 3] specifies a method for calculating the attenuation of outdoor sound propagation. While the standard discusses the accuracy and limitations of the method, it only provides a general uncertainty in the final sound level calculation. The uncertainty provided is based solely on the source-receiver height and distance separation. However, other environmental factors play important roles during sound level calculations. For instance, the normal range of temperatures varies from -5°C to +40°C for outdoor sound measurements. The standard does not provide adequate error analysis to account for such varying outdoor factors.

The present investigation focuses on the determination of uncertainties of the predicted noise levels associated with the standard environmental variables encountered while taking measurements such as temperature, wind speeds, and relative humidity. Measurements will be compared to the predicted sound level calculated via the ISO 9613 standards, using the software program CADNA/A [4], and an associated error for the changing variables will be developed. Preliminary results of the measurement program will be presented, with the intention of quantifying the uncertainties at a later date.

2. ISO 9613-2

ISO 9613-2 specifies an engineering method for calculating the attenuation of sound outdoors in order to predict the downwind sound pressure level from a variety of noise sources. The attenuation from specific physical effects include geometric divergence (A_{div}), atmospheric absorption (A_{atm}), ground effect (A_{gr}), barriers (A_{bar}) and effects of foliage, industry, houses etc. (A_{misc}). The primary factor in attenuation is A_{div} , with A_{atm} and A_{gr} also playing a part. For the purposes of this paper, A_{bar} and A_{misc} were not included in the testing.

A_{atm} , the attenuation due to atmospheric absorption, is dependent on environmental factors. Note #8 and #9 of ISO

9613-2 does address the dependence of atmospheric attenuation on the environmental variables and the need to use “average” values, however it does not address the range.

The method also includes a correction factor to calculate the long-term average A-weighted sound level, where the long-term implies months or years. However, local regulatory agencies require measurements over a 48-hour period [5]. The variation in environmental conditions can be severe over such short periods and the regulatory authorities usually require that the evaluations is conducted under calm weather conditions.

The variability in measured and/or predicted noise levels with variation in environmental conditions is a parameter of utmost importance and is the aim of the current investigation.

3. CADNA A

CadnaA for Windows is a program for noise and air pollution prediction and efficient for expert purposes [4]. It is capable of calculation noise attenuation according to the ISO 9613-2 methods.

Cadna/A allows the user to enter meteorological information for the Pasquill-Gifford stability class, wind speed and direction. This information is taken into account when calculating the noise attenuation.

4. METHOD

The investigation included both predictions of far-field noise levels from known sources of sound as well as measurements of noise levels.

The sound power of the source was determined from near-field sound intensity measurements. The sound power levels were then used in CadnaA in order to predict sound level as per ISO 9613 part 2. A statistical comparison of the actual measurements vs. the predicted levels was carried out, taking into account the recorded environmental variables.

Testing was done in a large, open, flat, grassy field, away from any major noise sources (roads, airplanes etc.) The ambient noise at the field did not exceed 40 dBA at any time. The loud speaker was set-up at a height of 2.0 meters above the ground. A continuous “pink-noise” source was fed to the speaker to generate a sound, with an L_p of 100 dBA at 1 meter.

The far-field microphone was set-up at distances of 100 and 300 meters from the speaker, at a height of 1.5 meters above the ground. The sound level meter was set-up to record the L_{eq} 1/1-octave spectrum from 31.5Hz to 8 KHz in dB. Measurements were repeated upwind and downwind of the propagation path.

A control microphone was set-up in front of the loud speaker, at a distance of 1 meter from the speaker face. The noise was recorded for the duration of the test to ensure any changes in the noise output were taken into account.

The environmental recording equipment (thermometer, vane anemometer, hygrometer) were all set up next to the far-field microphone. The air temperature and humidity was recorded ever 1 minute. The wind speed was measured once every 5 minutes, with the data captured being the average speed of the preceding 30 seconds.

5. RESULTS

Figure 1 shows the comparison of the predicted noise level from Cadna/A vs. the measured noise at 1 meter, in dBA.

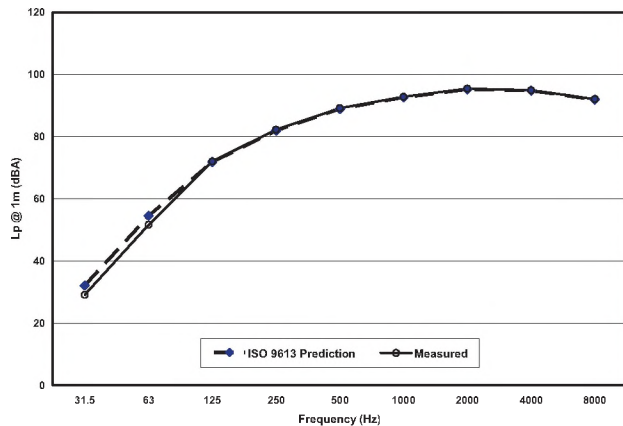


Fig. 1. Pink Noise generated from Speaker, measured at 1 m.

Results from the testing show a good correlation when the distance is 100 meters as shown in figure 2 below. For the purpose of this paper, any measured levels below the ambient background levels were not reported.

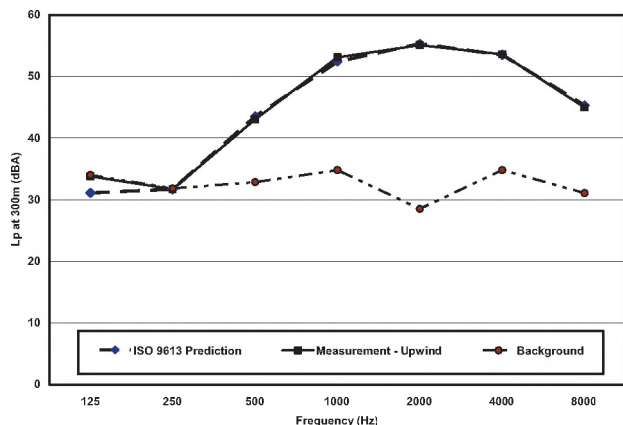


Fig. 2. Predicted vs. Measured values – Pink Noise at 100 m.

For a distance of 300 meters, there are discrepancies different environment variables with the measured values and the predicted values. Figure 3 shows a comparison of the measured and predicted values at a distance of 300 meters.

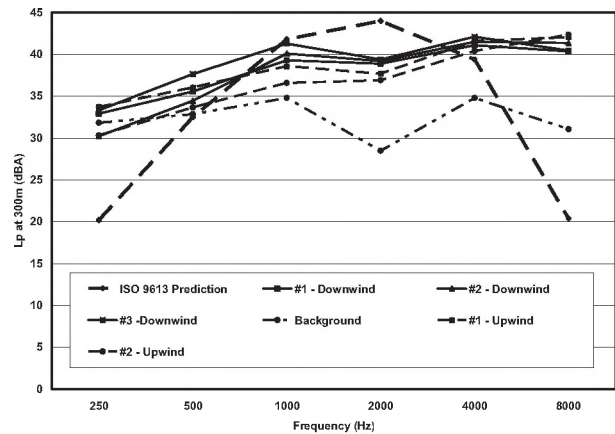


Fig. 3. Predicted vs. Measured values – Pink Noise at 300 m.

6. DISCUSSION

It is clear from the data that the ISO 9613-2 calculations show a high degree of accuracy in predictions of attenuation for shorter distances. At greater distances, there are deviations between the predicted and the measured data.

A detailed explanation of the types of waves that propagate outdoors has not been given, and neither has the detailed factors affecting outdoor noise propagation; however it is clear that one needs to carefully consider them when predicting noise attenuation over large distances.

It is the intention to carry out tests at larger distances (>1km) as well as for different environmental conditions in order to further understand the limits of the current ISO 9613-2 calculation methods.

REFERENCES

1. Embleton, Tony F. (1996). Tutorial on Sound Propagation Outdoors. *J. Acoust. Soc. Am.*, 100, 31-48.
2. Schomer, P. D. and White, M.J (2006). "A Statistical Description of Sound propagation: A Comparison of elevated and near-ground sources. *Noise Control Eng. J.* 54 157-168.
3. International Standards Organization, Geneva (1996) Acoustic - Attenuation of sound during propagation outdoors. Part 2: General method of calculations. ISO 9613-2:1996(E).
4. DataKustik GmbH. (2005). *Cadna Manual*
5. Ministry of the Environment (1978) Model Municipal Noise Control By-Law, Final Report, Ontario MOE, Ontario, Canada

PRELIMINARY ACOUSTIC PERFORMANCE INVESTIGATION OF CONCENTRIC-TUBE PERFORATED MUFFLER DESIGN

Jun Zuo¹, Colin Novak¹, Helen Ule¹, Ramani Ramakrishnan², Robert Gaspar¹

1. University of Windsor, Dept. of Mechanical, Automotive and Materials Eng, 401 Sunset Ave.; Windsor, ON
2. Ryerson University, Department of Architectural Science, 350 Victoria St.; Toronto, ON

INTRODUCTION

It has been demonstrated through simulation and experimental techniques that perforated tube mufflers have better acoustic attenuation properties than simple expansion chamber mufflers. Such perforated tube elements are widely used in resonators and mufflers to attenuate exhaust system noise.

A systematic aeroacoustical analysis of perforated-elements by Sullivan and Crocker was applied in a mathematical model for the prediction of transmission loss of concentric-tube resonators [1]. The analysis, however, was limited to simple cases with constant impedance of the perforation along the tube, an appropriate mode number (plane waves), and a rigid end boundary condition. In addition, the results were for a zero mean flow in the cavity and hence the acoustic performance of cross-flow element was not be predicted. A later model by Sullivan used a segmentation method, which does not suffer the above limitations [2, 3]. In this method the perforated element is physically treated as a branch and a solid pipe in between for each segment. A separated transfer matrix can be derived in each segment. The negative aspect of this method is the slow convergence of the solution if variation in the impedance of the perforation (nonlinear model) is considered. A decoupling approach was further developed and used to simulate the transmission loss of various perforated designs [4].

The impedance of the perforated mufflers used in the transmission loss evaluation can be found through theoretical derivation, or from experiments on a sample. In this paper two impedance models based on the theoretical and empirical results are compared using a one dimensional segmentation method to explore the differences in predicted transmission loss (TL) of a concentric-tube perforated muffler with zero mean flow. The results are also compared with those from a Ricardo Wave simulation. The present study shows the usefulness of using a simple theoretical model to predict acoustic performance of a perforated muffler during the preliminary design and analysis phase.

THEORY OF SEGMENT MODEL

In the segmentation method developed by Sullivan, the perforated tube shown in Fig.1 (a) is physically divided into numerous segments shown in Fig.1 (b) [2, 3]. The physical simplification includes the effect of perforation in each segment which is considered as a branch with a solid tube connecting the branches of each adjoining segment. The assumed simulation conditions are at room temperature without flow.

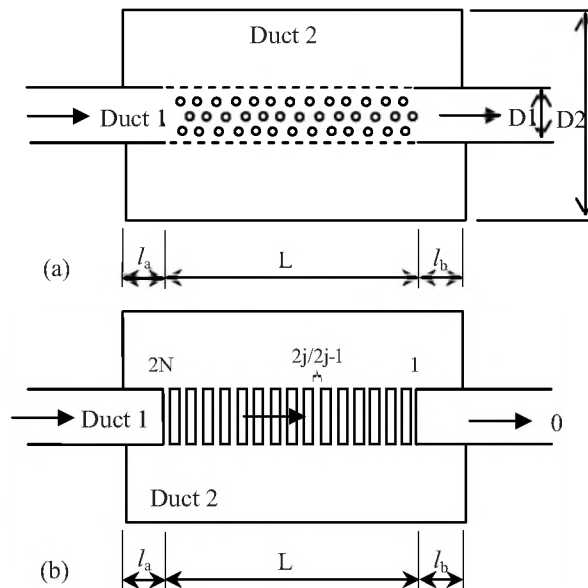


Figure 1. (a) Configuration of concentric-tube perforated muffler (b) Simplification of (a) in segmentation method

The equations for determining the acoustic pressures and mass velocities at the branches are derived from the equations of mass continuity and energy continuity. The equations between each branch assume that the wave travels as plane wave between-branches in ducts 1 and 2. Applying boundary conditions, the transmission loss is simply related to transfer matrix parameters as [See References 1 and 2],

$$TL = 20 \log_{10} \left(\frac{1}{2} |T'_{1,1} + T'_{1,2} + T'_{2,1} + T'_{2,2}| \right) \quad (1)$$

MODELLING AND SIMULATION

The impedance of the perforation can be approximately derived from radial momentum continuity are given by [5]:

$$\zeta = 8 \frac{kl^*}{S^2} + j \frac{4kl^*}{3}, \quad S < 1 \quad (2)$$

$$\zeta = 2^{1/2} \frac{kl^*}{S} + jkl^*, \quad S > 10 \quad (3)$$

The perforate impedance in the absence of mean flow and low sound pressure level of the source reported by Sullivan is given by [2, 3]:

$$\zeta = 6 \times 10^{-3} + jk(l + 1.5r_0) \quad (4)$$

The transmission loss of a concentric-tube perforated resonator is calculated based on the above two impedance models. The dimensions of the resonator are: $L=66.7$, $l_a=l_b=6.4$, $D_1=49.3$, $D_2=101.6$ (all in mm). The duct 1 of wall thickness 0.81 mm was drilled uniformly with 2.49 mm diameter holes with a porosity of 3.7%. Figure 2 shows the prediction of transmission loss at a temperature of 22°C and experimental data of Sullivan [3]. The agreement between the two models and the empirical results in the first peak region is quite good. The large discrepancy is in the second peak region of high frequencies. The second peaks of both predictions are around 2920 Hz, whereas Sullivan's experimental data shows the peak to be around 2750 Hz.

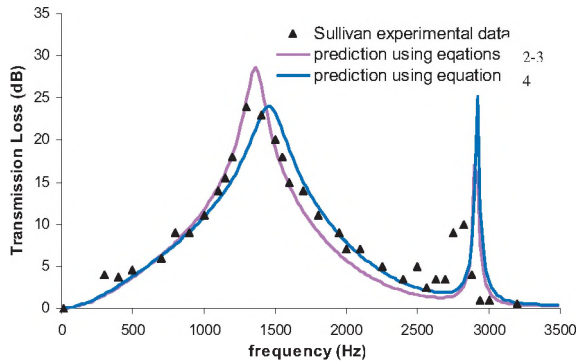


Figure 2. Comparison of transmission loss with two different perforate impedance models

A numerical prediction of a nonlinear perforated impedance model was also performed using Ricardo WAVE, a computer-aided engineering code which analyzes the dynamics of the pressure waves, mass flows, and energy losses in ducts. As a one dimensional simulation tool, WAVE has the capability of simulating the transmission loss of a concentric-tube muffler based on geometric and operating parameters as inputs.

Acoustic nonlinear impedance of orifices has been observed and investigated by many researchers. Once the sound pressure level (SPL) is greater than 130 dB and the velocity amplitude in the orifice is more than 10 m/s, a strong nonlinear resistance has been found. Figure 3 shows the transmission loss of a concentric-tube muffler simulated by Ricardo WAVE. Simulation results indicate acoustic nonlinearity exists when the SPL is less than 130 dB. The fundamental difference lies in the two peak regions shown.

The transmission loss calculated by Wave with a 90 dB sound source is compared with Sullivan's experimental data and segment modeling using linear perforate impedance models. The results are shown in Figure 4. It is noted that the three calculated curves are very similar to the measured results except at the second peak.

SUMMARY AND CONCLUSIONS

A one dimensional segment model is compared with Ricardo WAVE, a commercial software modeling package. For a small size (and relatively short) concentric-tube muffler configuration with a 3.7% perforation rate, all

simulation results agree very well with the experimental data. For a large size muffler configuration with a 10% perforation rate, large discrepancy in prediction of transmission loss is found between the WAVE and the linear segment model. Further investigation is ongoing.

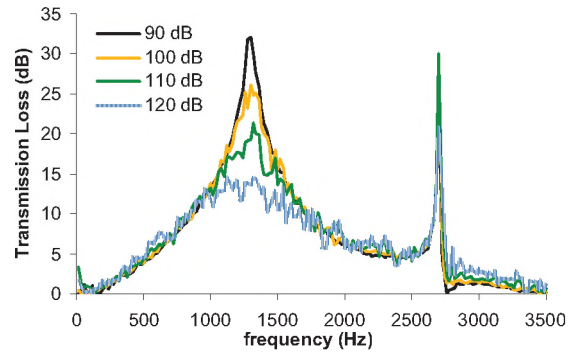


Figure 3. Comparison of transmission loss with varying SPL of sound source using a WAVE simulation

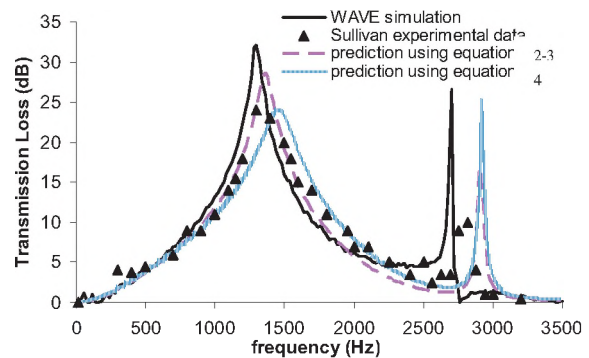


Figure 4. Comparison of muffler performance prediction by WAVE simulation, segment modeling and Sullivan experimental data

REFERENCES

1. Sullivan J. W. and Crocker M.J. (1978). Analysis of Concentric-tube resonators having Unpartitioned cavities. *J. Acoust. Soc. Am.* 64, 207-215.
2. Sullivan J. W. (1979). A Method for Modeling Perforated Tube Muffler Components. I. Theory. *J. Acoust. Soc. Am.* 66, 772-778.
3. Sullivan J. W. (1979). A Method for Modeling Perforated Tube Muffler Components. II. Applications. *J. Acoust. Soc. Am.* 66, 779-788.
4. Jayaraman, K and Kit Yam (1981) Decoupling Approach to Modeling Perforated Tube Muffler Components. *J. of the Acoust. Soc. Am.* 69 390-396.
5. Sivian, L.J. (1935) Acoustic Impedance of Small Orifices. *J. Acous. Soc. Am.* 7 94-101.

EXPERIMENTAL EVALUATION OF AUTOMOTIVE CABIN NOISE USING PSYCHOACOUSTIC ANALYSIS TECHNIQUES

Neb Radic¹, Colin Novak, and Helen Ule

Dept. of Mechanical, Automotive and Materials Engineering, University of Windsor, 401 Sunset Ave.; Windsor, Ontario, Canada, N9B 3P4 ¹Corresponding author: radic@uwindsor.ca

1. INTRODUCTION

In recent years, the automotive industry has invested significant time and money in research and development associated with the reduction of vehicle noise pollution. Much of this attention has been devoted to the areas of the Noise, Vibration and Psychoacoustics as how they relate to the automotive interior. This has been in answer to consumer demands for more comfortable vehicles. This is particularly important with today's increased use of cellular phones, entertainment multimedia systems and interactive voice controls.

Psychoacoustics, or quality of sound, is very important aspect in the development of a product if it is to portray a sense of quality. There are many different psychoacoustic metrics that are used today. Some of the more common metrics include: Loudness, Sharpness, Roughness and Fluctuation Strength. Some of the lesser known ones would be: Brightness, Pitch Strength, Impulsiveness, Rhythm, Speech Interference Level (SIL) amongst others.

2. SOUND QUALITY METRICS

As already stated, many sound quality metrics exist; however, care must be taken in their application. Each metric has a specific use and applicability dependant on the source of noise. In addition to the traditional FFT analysis the psychoacoustic metrics considered in this investigation include: Zwicker Loudness, Fluctuation Strength and Roughness. These will be considered in the evaluation of automotive cabin noise.

Zwicker Loudness is one of the most widely used psychoacoustic metrics and is standardized in ISO 532B. This metric takes into account the critical band spectrum of the human hearing. Tonal components as well as the masking properties of the sound are also considered [1]. Loudness is expressed in units of "Sones" rather than dB and Loudness level in "Phons". A relationship exists between sound pressure level and Phons where a pure tone of 1000 Hz having an SPL of 40dB equals 40 Phons. This point is taken to be "loudness unity". From here, it can be seen that 1 Sone equals 40 Phons. The most significant benefit of using Sones instead of Phons as the unit of Loudness is the fact that this perception of level can be expressed in a linear matter [2].

Modulation Metrics such as **Fluctuation Strength** and **Roughness** measure modulation between specific frequencies. Hearing sensation that describes modulation of sound in the frequency range between about 0.5 Hz to 20 Hz is referred to as Fluctuation Strength. "*The unit of measure for FS is vacil, with 1 vacil arbitrarily defined as the FS associated with a 60 dB SPL, 1 kHz tone 100% amplitude-modulated at 4 Hz*" [3]. Alternatively, sound modulations that occur within the range of 20-300 Hz are characterized as Roughness. "*The reference value for roughness of 1 "asper" is defined as that generated by a 60dB 1 kHz tone which is 100% amplitude modulated by a 70 Hz tone*" [4].

3. PROCEDURE

For this investigation, acoustic pressure measurements are taken inside the vehicle cabin both at the driver's ears location using conventional microphones as well as at the passenger's ears position using a binaural head. The purpose of the binaural head was to acquire the acoustic data in a manner representative of what a human passenger would perceive. The intent of this study is to relate the results of the psychoacoustic analysis of the vehicle cabin noise to the operation of the vehicle.

In order to simulate a real life scenario, as well as to conduct the tests in a safe manner, an automotive test track of 500 meter length was used. Testing was done using the operating conditions of both a self propelled and towed vehicle. The speed of the towed and self propelled vehicle was maintained during all periods of acquisition at 50 km/hr.

4. RESULTS

At the tested road speed, it is observed that the engine noise contributed little to the overall loudness (Fig. 1) within vehicle's cabin since the "driving curve" is only marginally greater than the "towing curve" (mean 16.92 sones compared to mean 16.51 sones). Given this, it is surmised that, under the test conditions, that the predominant source of noise measured was due mostly to the road-tire-suspension interactions. Although not presented in this paper a sharpness analysis of any high frequency content indicated that wind noise was also negligible.

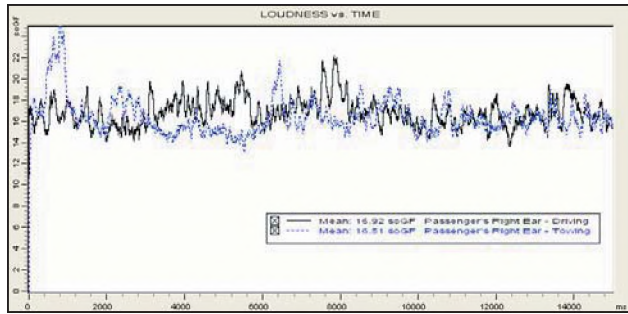


Fig. 1: Results of Loudness vs. Time (measurements taken at passenger's ear using binaural head for both driving and towing cases.

Inspection of the graph representing Roughness (Fig. 2) indicates the presence of two “strange” peaks that occur at the beginning of the measurement for the case of the towed vehicle and at the end for the driving case. These peaks were due to the presence of a series of small “wash board” speed bumps in the test track which resulted in high modulation levels for a very short period of time. There are present at only one end of the test track. Since the towed testing was done in one direction and the driving in the other, this phenomenon is shown at opposite sides of the results, i.e. one at the beginning and the other at the end of measurement. The towed vehicle showed higher levels indicating that the presence of engine noise contributed to the masking of the modulated signal from the road noise.

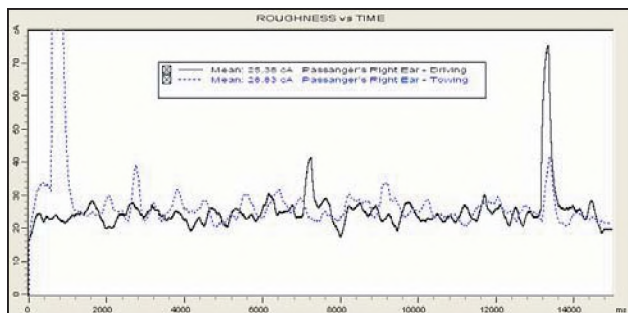


Fig. 2: Results of Roughness vs. Time (measurements taken at passenger's ear using binaural head for both driving and towing cases.

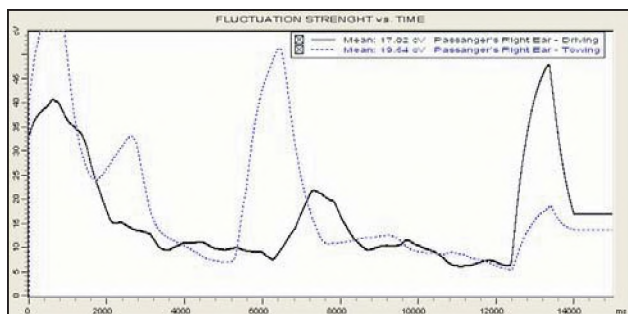


Fig. 3: Results of Fluctuation Strength vs. Time (measurements taken at passenger's ear using binaural head for both conditions.

Similar observations are made with Fluctuation Strength (Fig. 3) where due to a lack of any more lower frequency modulation, the curves are relatively smoother.

While little additional information is provided by the FFT spectrogram (Fig. 4), confirmation of some of the previous observations is given. Specifically, the predominant frequency of the measured noise is in the low spectrum, under 100 Hz. This again is indicative of the road-tire-suspension mechanism being the primary noise contributors. The lack of the high frequency signal again indicates the absence of any aeroacoustic noise generation.

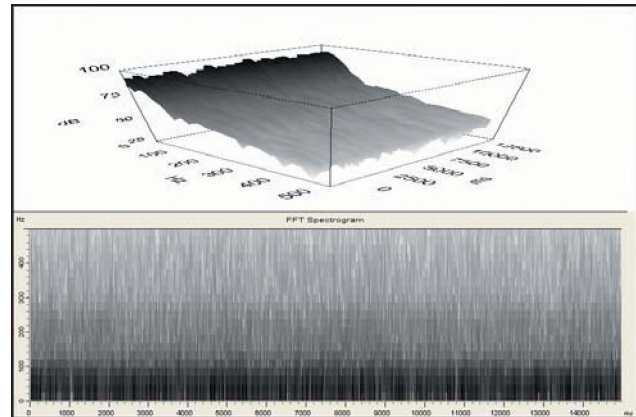


Fig. 4: FFT Spectrogram (measurements taken at passenger's ear using binaural head driving at 50 km/h).

5. CONCLUSION

From the results discussed above, it is observed that predominate noise contribution within the vehicle cabin is the result of road - tire- suspension interactions. Future studies of this vehicle will focus on relating vibration measurements taken of this vehicle's suspension and relating any realized Transfer Path Analysis to the resulting cabin noise from a psychoacoustic perspective.

REFERENCES

- [1] Hojbjerg, K. (1991). *Measuring the Loudness of Door Slams* Bruel & Kjaer, Denmark. SAE Technical Paper: 911090
- [2] Genult, K., Glerlich, W., H. *Investigation of the Correlation between Objective Noise Measurement and Subjective Classification*. Aachen, Germany. SAE Technical Paper: 891154
- [3] Blommer, M. and Otto, N. *A New Method for Calculating Fluctuation Strength in Electric Motors*. SAE Technical Paper: 2001-01-1588
- [4] Feng, J., B. and Otto, N. *Synthesis of Powertrain Sounds for Investigations in Roughness*. SAE Technical Paper: 931333

THE USE OF ENVIRONMENTAL NOISE STANDARDS AND GUIDELINES IN CANADA

Bill Gastmeier

HGC Engineering (Howe Gastmeier Chapnik Limited), 2000 Argenta Road, Plaza 1, Suite 203, Mississauga, Ontario, Canada, L5N 1P7, bgastmeier@hgcengineering.com

1. INTRODUCTION

This paper presents a summary of the environmental noise standards and guidelines currently in use in Canada. The Canadian Standards Association (CSA) currently administers a number of standards dealing directly with environmental noise and there is ongoing activity to endorse or adopt standards prepared by other organizations for use in the Canadian Context. Input was received from members of the Environmental Noise Subcommittee of the Z107 Technical Committee of the CSA illustrating how the various standards are guidelines presently used. Suggestions for future standards activities are provided.

2. ENVIRONMENTAL NOISE STANDARDS CURRENTLY IN USE IN CANADA

The environmental noise standards currently administered by the CSA include the following:

1. **Z107.53-M1982 (R1994)** Procedure for Performing a Survey of Sound Due to Industrial, Institutional, or Commercial Activities. (To be replaced by ISO1996 below)
2. **CAN/CSA – ISO 1996-1**, Description, Measurement and Assessment of Environmental Noise. Part 1: Basic Quantities and Assessment Procedures
3. **CAN/CSA – ISO 1996-2**, Description, Measurement and Assessment of Environmental Noise. Part 2: Acquisition of Data Pertinent to Land Use
4. **CAN/CSA – ISO 1996-3**, Description, Measurement and Assessment of Environmental Noise. Part 3: Application to Noise Limits
5. **CAN3-Z107.54-M85 (R1993)** Procedure for Measurement of Sound and Vibration Due to Blasting Operations.
6. **CAN/CSA-Z107.55-M86** Recommended Practice for the Prediction of Sound Levels Received at a Distance from an Industrial Plant.
7. **CAN/CSA-Z107.9-00:** Standard for Certification of Noise Barriers.
8. **ISO 9613-1:** Attenuation of Sound during Propagation Outdoors – Part 1: Calculation of the Absorption of Sound by the Atmosphere
9. **ISO 9613-2:** Attenuation of Sound during Propagation Outdoors – Part 1: General Method of Calculation
10. **ISO 4872:** Acoustics - Measurement of Airborne Noise Emitted by Construction Equipment Intended for Outdoor Use – Method for Determining Compliance with Noise Limits.
11. **ISO 6393**, Acoustics - Measurement of Airborne Noise Emitted by Earth-Moving Machinery – Method for Determining Compliance with Limits for Exterior Noise Stationary Test Condition
12. **ISO 6394**, Acoustics-Measurement of Airborne Noise Emitted by Earth-Moving Machinery Operators Position-Stationary Test Condition
13. **ISO 6395**, Acoustics-Measurement of Airborne Noise Emitted by Earth-Moving Machinery Dynamic Test Conditions
14. **SAE J919**, Sound Measurement-Earthmoving Machinery – Operator Position
15. **SAE J1096**, Measurement of Exterior Sound Levels for Heavy Trucks
16. **ISO 2922**, Measurement of Noise Emitted by Vessels on Inland Waterways and Harbours
17. **ISO 5130**, Measurement of Noise Emitted by Stationary Road Vehicles – Survey Method
18. **ISO 7188**, Measurement of Noise Emitted by Passenger Cars under Conditions Representative of Urban Driving
19. **ISO 14509**, Measurement of Airborne Sound Emitted by Powered Recreational Craft

Input from a number of committee members resulted in the following list of standards and guidelines in common use in addition to the above. This is not meant to be a comprehensive list.

20. **ANSI B113.8, (ISO 6190)**, Measurement of sound pressure levels of gas turbine installations for evaluating environmental noise – Survey method
21. **IEEE 656**: IEEE standard for the measurement of audible noise from overhead transmission lines.
22. **ANSI S12.9-1988**, Part 1 and 3: Quantities and procedures for description and measurement of environmental sound
23. **ANSI S12.18-1994**: Procedures for outdoor measurement of sound pressure level
24. **SAE J1075**: Sound measurement – Construction sites
25. **IEEE C57.12.90-1993**, Sound level Testing for Establishing Acoustic performance ratings for Transformers
26. **IEC 61400-1**, Sound level measurement and acoustic performance verification of Wind Turbines
27. **CONCAWE Report 4-81** Noise Modeling
28. **ISO 2631-1, 2,3** – Evaluation of Human Exposure to Whole Body Vibration
29. **ISO 8297**, Determination of Sound Power Levels of multisource industrial plants for evaluation of sound pressure levels in the environment.

Many standards addressing methods of measuring source emission levels and measurement equipment standards were also referenced by the subcommittee members, but these are more appropriate to other technical subcommittees of the Z107 Technical Committee.

In addition, the following guidelines are also in common use in the area of environmental noise assessment.

30. Guidelines for the measurement of audible noise emitted by Hydro-Québec plants"
31. Guidelines for the management of noise emitted by Hydro-Québec construction sites
32. Alberta Energy and Utilities Board (EUB) Interim Directive on Noise (ID99-8).
33. Ontario Guideline D1- Land Use Compatibility
34. Ontario Guideline D6 – Compatibility Between Industrial Facilities and Sensitive Land Uses
35. Guidelines for the evaluation of power transformers and shunt reactors sound power levels"
36. Ontario MOE Noise Pollution Control (NPC) Guidelines
37. Ontario MOE Guideline LU-131, Noise Control in Land Use Planning
38. Ontario MOE 4739e, Interpretation for applying MOE technical publications to wind turbine generators

3. DISCUSSION

The large number of standards referenced above illustrates how the field of environmental noise has increased in importance in recent years.

This exercise has revealed that there are a number of standards in common use in Canada which have not yet been officially adopted by the CSA. Future activities of the Environmental Noise Subcommittee would include reviewing those standards and, if appropriate, putting them forward for adoption. The CSA encourages the use of these standards by environmental professionals, industry and regulators across the country to increase and harmonize their application.

These standards and guidelines are routinely applied in obtaining regulatory approvals for industrial, energy production and power generation facilities. They are used in support of license applications for mines, pits, quarries, landfill sites and recycling facilities. In the area of municipal planning and land development they can be applied through the entire planning process from determining initial land use compatibility to site plan approvals.

Regulators and approval authorities are encouraged to use these standards to develop policies and guidelines related to environmental noise in their respective jurisdictions.

ACKNOWLEDGEMENTS

The following individuals (firms) provided input concerning the standards currently in use. Tim Kelsall (Hatch Associates), Vince Gambino (Aercooustics Engineering Limited), Steven Bilawchuk (ACI Acoustical Consultants Inc.) Jason Tsang (RWDI), Blaise Gosselin (Hydro Quebec).

AUTHOR NOTES

To date, the committee has representation and input from members in BC, Alberta, Ontario and Quebec, but none from Manitoba, Saskatchewan, the Maritimes or the north. Noise control equipment and instrumentation suppliers, regulatory agencies, transportation, power generation, gas transmission and consultants are represented.

Please contact the author for a listing of the committee members or if you are interested in participating.

AUTOMATIC CLASSIFICATION OF IMPULSIVE-SOURCE ACTIVE SONAR ECHOES USING PERCEPTUAL SIGNAL FEATURES FROM MUSICAL ACOUSTICS

Victor W. Young, Paul C. Hines, and Sean Pecknold

Defence R&D Canada – Atlantic, 9 Grove St., Box 1012, Dartmouth, NS, B2Y 3Z7 victor.young@drdc-rddc.gc.ca

1. INTRODUCTION

False alarm returns from naturally occurring objects in the environment often plague active sonar systems. These types of echoes are known collectively as clutter.

Typically a human operator is responsible for discriminating between echoes from true targets and echoes from clutter objects using visual displays, such as time-frequency sonograms. There have also been attempts to create automatic classifiers based upon purely statistical signal features. Both of these conventional techniques for active sonar classification ignore a potentially valuable tool: the human auditory system.

There is mounting experimental evidence to suggest that human listeners can aurally discriminate between target and clutter echoes¹. This paper investigates the possibility of using cues known to be perceptually relevant in the human auditory system as signal features in an automatic classifier.

Drawing an analogy between active sonar echoes and percussive musical timbre, this paper examines signal features that have been identified as underlying the perception of timbre. These perceptual signal features are used to automatically classify impulsive-source active sonar echoes recorded on a towed-array.

The purpose of this paper is to demonstrate that active sonar echoes can be successfully classified using perceptual signal features, and not to suggest that this technique is superior to human-operator classification using visual displays or to automatic classification with statistical signal features. Indeed, the optimum classification technique probably involves a combination of all three approaches.

2. EXPERIMENTAL DATA

The experimental data consists of 98 target echoes from two different objects and 100 clutter echoes from 28 different objects. The two target objects are an oil rig and the tanker ship that attends it. The 28 clutter objects are naturally occurring seafloor structures.

The data were collected during a sea trial on the Malta Plateau using signals underwater sound (SUS) charges and a

towed-array. A total of nine SUS charges were deployed during the experiment. Each SUS charge contained 0.82 kg of TNT and was set to detonate at a depth of 87.0 m. The towed-array consisted of 96 omni-directional elements sampled at a rate of 4096 Hz, and it was towed at a speed of 10 knots and a depth of 40 m. Average water depth in the area was about 100 m.

The towed-array data were beamformed to obtain a total of 81 horizontal beams. Each beam was spectrally whitened using a Butterworth filter and then normalized to eliminate reverberation using a two-pass mean technique². Then an energy threshold was applied and samples that exceeded the threshold were taken to be detections. To eliminate signal-to-noise ratio (SNR) as a possible target-clutter discrimination cue, care was taken to balance the target and clutter SNR distributions so that the distribution of SNR values within the target class was very nearly identical to the distribution of SNR values within the clutter class.

3. PERCEPTUAL SIGNAL FEATURES

Musical timbre is defined as “that attribute of auditory sensation in terms of which a subject can judge that two sounds similarly presented and having the same loudness and pitch are dissimilar”³. There have been many musical acoustics studies that investigate the signal features that underlie the perception of timbre⁴. This paper will apply several perceptual signal features identified in those studies to the problem of active sonar classification.

Perceptual signal features considered in this paper include: duration, sub-band attack and decay time, sub-band synchronicity, spectral character of the pre-attack noise, and the peak value, centroid, and roughness of the perceived loudness spectrum. Because these features are inherently perceptual, they must be measured using a model of the human auditory system. The auditory model employed in this paper consists of two main components: an auditory filter bank⁵, which breaks the sonar echoes down into sub-bands, and a loudness model⁶, which converts the output of the filter bank into a perceived loudness spectrum.

Time-frequency features – like sub-band attack and decay time and sub-band synchronicity – are measured at the output of the filter bank (*i.e.*, prior to applying the loudness model). Purely spectral features – like the peak value,

centroid, and roughness of the loudness spectrum – are measured at the output of the loudness model. To eliminate total loudness (*i.e.*, the integral across the perceived loudness spectrum) as a target-clutter discrimination cue, each echo is scaled to have the same total loudness.

Many of the features considered in this paper are multi-valued in that they consist of multiple values for each echo. For example, consider the feature sub-band attack time: for a single echo there are sub-band attack time values for each channel of the filter bank, but the analysis which follows requires single-valued features. Conversion of a single multi-valued feature into multiple single-valued features is achieved using summary statistics. Sub-band attack time is thus converted into three single-valued features: minimum, mean, and maximum sub-band attack time. In this way a total of 58 single-valued features are constructed.

Each of the 58 perceptual features is normalized so that, over all 210 returns, the mean feature value is 0 and the standard deviation is 1. This normalization process ensures that each feature is weighted equally in the analysis that follows.

4. PRINCIPAL COMPONENT ANALYSIS

Principal component analysis (PCA) is a statistical technique for projecting a multi-dimensional feature-space defined by M possibly correlated signal features down onto a multi-dimensional feature-space defined by N uncorrelated signal features, where $N \leq M$. PCA is applied by first obtaining the eigenvectors of the correlation matrix defined by the M original features. The eigenvectors are sorted according to the magnitudes of their corresponding eigenvalues and the first N eigenvectors are then used to define a transformation matrix, which projects points (*i.e.*, echoes) in the old M -dimensional feature-space down onto the new N -dimensional feature-space.

The following section presents $N=2$ PCA results for several different M values. The M features included in the PCA are those which, when considered in isolation, have the least overlap between the target and clutter classes.

5. AUTOMATIC CLASSIFICATION

The full data set (consisting of 210 echoes described by $N=2$ PCA features) is split into two sub-sets, which are used to train and test a Gaussian-based automatic classifier. During the training phase, separate target and clutter Gaussian probability density functions (PDF) are defined using sample mean and covariance matrices estimated from the echoes in the training sub-set. During the testing phase, each echo in the testing sub-set is classified as either target or clutter based upon its relative position on these two PDFs. The error rate (*i.e.*, the fraction of misclassified echoes in the testing sub-set) is then calculated

and used as a metric to quantify the success of the classification process.

Automatic classification using this technique is carried out twice for the $M=5 / N=2$ PCA results: the first time training on echoes from the tanker ship and 14 of the 28 clutter objects then testing on echoes from the oil rig and the other 14 clutter objects (scheme A), and the second time reversing the training-testing echoes (scheme B). Results for training-testing scheme A are presented in the Figure 1. Automatic classifier results for other M values are presented in Table 1.

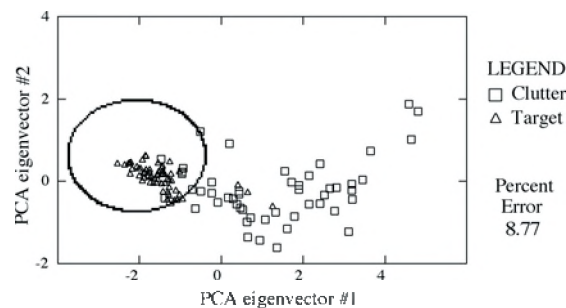


Fig. 1. $M=5/N=2$ automatic classifier results for scheme A; the ellipse represents the decision surface

Table 1. $N=2$ automatic classifier error rates

M	2	5	58
Scheme A	12.28%	8.77%	7.89%
Scheme B	9.52%	13.10%	14.29%

6. DISCUSSION

Results presented in this paper demonstrate that perceptual features can be used to successfully classify impulsive-source active sonar echoes: using perceptual features with a Gaussian classifier, error rates less than 10% can be achieved. However, care must be taken when selecting features for inclusion in the analysis since in many situations fewer features (*i.e.*, smaller M) yield better results. Moreover, A-B comparison suggests that the “best” choice of features for any classification task depends on the data used for training. Future plans include applying the perceptual feature automatic classifier to echoes from real submarines and to coherent-source active sonar data.

REFERENCES

1. N. Allen et al., *151st Meeting Acoust. Soc. Am.* (Providence, RI, 2006), pp. 3395.
2. W. A. Struzinski and E. D. Lowe, *J. Acoust. Soc. Am.* **76** (6), 1738 (1984).
3. W. A. Yost, *Fundamentals of Hearing*, 4th ed. (Elsevier, Toronto, 2000).
4. J. M. Grey and J. W. Gordon, *J. Acoust. Soc. Am.* **63** (5), 1493 (1978).
5. M. Slaney, *An Efficient Implementation of the Patterson-Holdsworth Auditory Filter Bank* (Apple Comp. Inc. TR35, 1993)
6. J. E. Appel, *Loudness Models for Rehabilitative Audiology* (Ph.D. dissertation, U. of Oldenburg, Germany, 2002).

GEOACOUSTIC INVERSION IN A RANGE-DEPENDENT ENVIRONMENT UNDER THE ASSUMPTION OF RANGE-INDEPENDENCE

Michael G. Morley, Stan E. Dosso, and N. Ross Chapman

School of Earth and Ocean Sciences, University of Victoria, Victoria, B.C., Canada, V8W 3P6

1. INTRODUCTION

A significant amount of research has been devoted to estimating the geoacoustic properties of the seabed by matched-field inversion (MFI) in recent years. The assumption of range independence reduces the number of parameters in the problem and significantly improves the computational efficiency of MFI; however, neglecting spatial variability in the properties of the real environment degrades the accuracy in modelling the acoustic field. This may lead to large theory errors and produce unacceptable inversion results. The aim of this paper is to investigate the effect that ignoring random variability of individual model parameters has on the accuracy of the inversion results for a simple, shallow-water model. In Ref. 1 the authors investigated how well a range-independent inversion could recover average values for the parameters of a range-dependent environment. Their results suggested that ignoring range dependence leads to large biases in the recovered parameters but their conclusions were based mostly on single frequency inversions for a hard-bottom environment. This study re-examines the issue addressed in Ref. 1; however, a much faster forward model is used making it practicable to use multiple frequencies in the inversion – a more common practice in the ocean acoustics community. The study is extended to consider a soft-bottom environment as well. The degree of random, range-dependent variability in water depth and seabed sound speed that can be tolerated is examined by inverting synthetic data sets generated from many unique, random realizations of the environment. Comparisons are made between inversion results using single and multiple frequencies for the two environments. The results indicate that the biases in the recovered parameters are much smaller than previously suggested, although in some cases significant biases can occur.

2. METHOD

The general form of the geoacoustic model considered in this study consisted of an 80 m deep ocean of sound speed 1460 m/s over a semi-infinite sediment layer. Two different sediment regimes were considered: a hard-bottom case similar to the one in Ref. 1 with sound speed 1677 m/s, density 2.06 g/cm³, and attenuation 0.436 dB/λ, and a soft-bottom case with sound speed 1500 m/s, density 1.5 g/cm³, and attenuation 0.2 dB/λ. The experimental geometry consisted of a source at 35 m depth and 4 km

away from a 70 m long vertical array with hydrophones spaced at 1 m intervals from 5 m to 75 m in the water column. For each case in the study, one hundred unique realizations of a range-dependent environment were generated by adding scaled random perturbations to either the sediment sound speed or water depth at regular intervals so as to achieve a desired mean and variance [1]. Data for each realization were generated at 50 Hz intervals over the 100-800 Hz band using a range-dependent, parabolic equation acoustic propagation model. Several data sets were generated for different degrees of range dependence ranked by the standard deviation of the random fluctuations in sound speed, σ_{cp} , or water depth, σ_H . Spatially white, Gaussian noise was added and an inversion was performed for each data set using the adaptive simplex simulated annealing (ASSA) hybrid inversion algorithm [2] with a normal mode acoustic propagation model. The inversions solved for the water depth, sound speed, density and attenuation parameters assuming the environment was range independent. Separate inversions were performed using a single frequency of 100 Hz and for all 15 frequencies within the band.

3. RESULTS

The distributions of the best-fit model parameters from all of the inversions are used as an indicator of how well the range-dependent environment can be approximated by a range-independent model. These distributions are described by the standard deviation about the true mean parameter value, the standard deviation about the distribution mean, and the bias of the distribution. Figure 1 shows a plot of these values for multiple and single frequency inversions at 100 Hz for the case of variable sound speed in a hard bottom. The multiple frequency inversion results from all the data sets in this case are distributed tightly about the true mean model values even when there is considerable deviation in sound speed in the bottom. The single frequency inversion results are broadly distributed with large biases. This indicates that in this environment significant fluctuations of sound speed in the seabed can be effectively averaged over by including multiple frequencies in the inversion.

For the soft-bottom case shown in Fig. 2 the inversion results are more dependent on each realization of the range-dependent environment. Beyond $\sigma_{cp} = 20$ m/s the

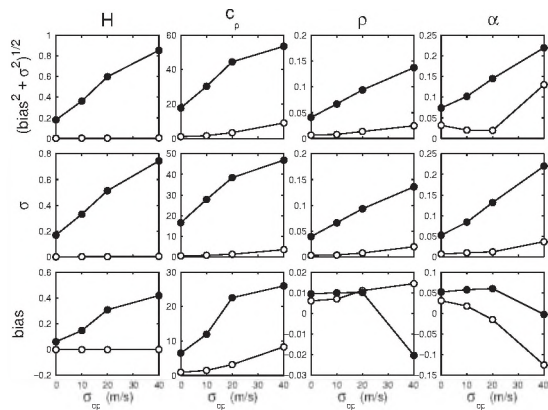


Fig. 1. Summary of the distributions of results for variable sound speed in the hard bottom model. Multiple frequency (open circles) and single frequency results at 100 Hz (closed circles) are shown.

distributions of the best-fit model parameters are wider with larger biases than for the hard-bottom case; however, reasonable average sound speed and water depth values are still found.

When the range-dependent water depth data were inverted the results are highly sensitive to the particular realization of the environment for the hard bottom but not for the soft bottom. A summary of the distributions of best-fit model parameters are shown in Fig. 3 for the hard bottom. A significant improvement is observed when using multiple frequencies in the inversion; however, beyond $\sigma_H = 0.25$ m the biases and standard deviations of the distributions of the geoacoustic parameters become significant. For the soft-bottom case in Fig. 4 the biases and standard deviations remain quite small even when there are significant random fluctuations in the water depth.

There is significant improvement in the consistency of the inversion results when multiple frequencies are used.

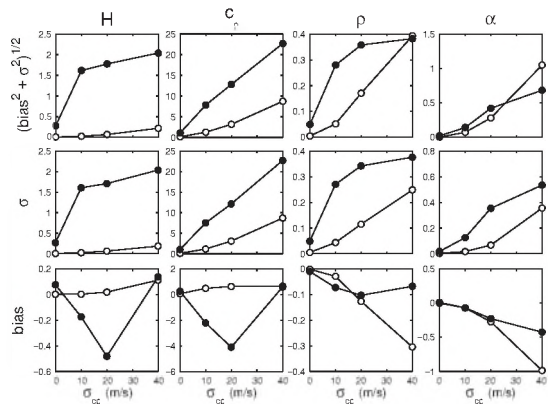


Fig. 2. Summary of the distributions of results for variable sound speed in the soft bottom model.

Inversions performed for the hard-bottom environment are sensitive to fluctuations in water depth but relatively insensitive to changes in sound speed. The opposite is true for the soft bottom. These sensitivities result in biased values for sound speed, density and attenuation. In the range-dependent data the fluctuations in seabed sound speed or water depth increase the amount of acoustic energy loss. To account for this loss in the range-independent approximation the inversion results are biased toward smaller average values for sound speed and density and larger values for attenuation.

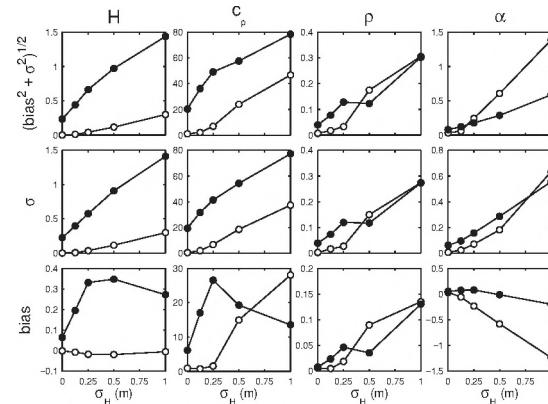


Fig. 3. Summary of the distributions of results for variable water depth for the hard bottom model.

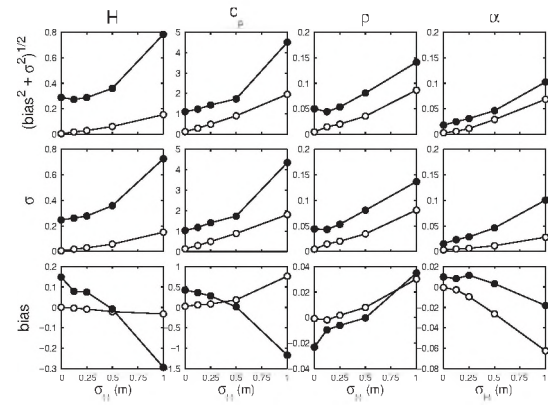


Fig. 4. Summary of the distributions of results for variable water depth for the soft bottom model.

REFERENCES

- [1] Lapinski, A. -L. S., Chapman, D. M. F. "The effects of ignored seabed variability in geoacoustic inversion," *J. Acoust. Soc. Am.*, **117**(6), 3524-3538 (2005).
- [2] Dosso, S. E., Wilmut, M. J., and Lapinski, A. -L. S. "An adaptive-hybrid algorithm for geoacoustic inversion", *IEEE J. Oceanic Eng.*, **26**, 324-336 (2001).

ACKNOWLEDGEMENTS

The authors would like to thank Anna-Liesia Lapinski and Dave Chapman of DRDC-Atlantic for providing some of the computer codes used in this work.

QUANTIFYING OCEAN ACOUSTIC ENVIRONMENTAL SENSITIVITY

Stan E. Dosso¹, Diana F. McCammon², Peter M. Giles³, Sean Pecknold⁴, and Paul C. Hines⁴

¹School of Earth and Ocean Sciences, University of Victoria, Victoria, B.C. Canada, V8W 3P6

²McCammon Acoustical Consulting, 475 Baseline Rd, Waterville, NS Canada, B0P 1P0

³General Dynamics Canada, 11 Thornhill Dr., Dartmouth, NS Canada, B3B 1R9

⁴Defence Research and Development Canada–Atlantic, Dartmouth, NS Canada, B2Y 3Z7

1. INTRODUCTION

This paper defines and examines linear, linearized, and nonlinear measures of environmental sensitivity for ocean acoustic propagation that account for realistic uncertainties in various environmental parameters (water-column sound-speed profile and seabed geoacoustic properties). Simple interpretations of sensitivity are typically based on the implicit assumption of a linear relationship between parameter sensitivity and parameter uncertainty. This assumption is examined by comparing the three sensitivity measures over a range of parameter uncertainties about the actual assumed environmental uncertainty. Sensitivity range and depth dependencies are illustrated for realistic geoacoustic uncertainties and oceanographic variability of the sound-speed profile.

2. THEORY

The interpretation of sensitivity is well defined for linear problems, which provide a basis for addressing nonlinear problems such as ocean acoustic propagation. For a linear problem, the change in datum d_i due a change δm_j to the j th environmental model parameter m_j is

$$\delta d_i^j = d_i(m_j + \delta m_j) - d_i(m_j) = \frac{\partial d_i}{\partial m_j} \delta m_j. \quad (1)$$

Equation (1) indicates how uncertainties transfer from parameters to data for a linear problem: If the uncertainty for parameter m_j is Gaussian distributed with standard deviation σ_j , then the corresponding uncertainty for datum d_i is also Gaussian with standard deviation $\partial d_i / \partial m_j \sigma_j$; i.e., sensitivities scale directly with parameter uncertainties. A linear sensitivity measure that is independent of data/parameter scales and units is defined

$$S_{ij} = \frac{|\delta d_i(\delta m_j = \sigma_j)|}{|d_i|}. \quad (2)$$

Equation (2) represents the ratio of the standard deviation of the i th datum to its expected value and is equivalent to the coefficient of variation, a quantity commonly used for comparing the variability of potentially disparate quantities.

The above concepts can be extended to weakly nonlinear problems. Expanding the data functional for a parameter perturbation about the background model and neglecting second-order terms leads to an approximate local linear relationship between data and parameter perturbations which can be used in a linearized sensitivity measure; for improved accuracy, a two-sided average can be defined

$$S_{ij} = \frac{1}{2} \left[\frac{|d_i(m_j + \delta\sigma_j) - d_i(m_j)|}{|d_j|} + \frac{|d_i(m_j - \delta\sigma_j) - d_i(m_j)|}{|d_j|} \right] \quad (3)$$

To address nonlinearity explicitly, the full data uncertainty distribution can be sampled using a Monte Carlo approach to draw random model perturbations δm_j from a Gaussian distribution with zero mean and standard deviation σ_j , and computing the corresponding data perturbation for each sample. A nonlinear sensitivity measure is based on the root-mean-square average perturbation

$$S_{ij} = \frac{\left[\left\langle \left[d_i(m_j + \delta m_j) - d_i(m_j) \right]^2 \right\rangle \right]^{1/2}}{|d_i|} \quad (4)$$

For a linear problem, the linear, linearized, and nonlinear sensitivity measures are identical. Due to the highly variable nature of propagating acoustic fields, data sensitivities must be spatially averaged, as indicated in the following section, to obtain a stable, representative sensitivity measure [1].

The linearity of parameter sensitivities can be examined by comparing the linear, linearized, and nonlinear sensitivity measures over a range of parameter standard deviations σ_j about the actual environmental uncertainty.

3. EXAMPLES

This section provides examples of the sensitivity analysis outlined above. The environmental parameters and uncertainties are based on the Malta Plateau, a well-studied region of the Mediterranean Sea. The environmental model, illustrated in Fig. 1, is comprised of a 131-m water column

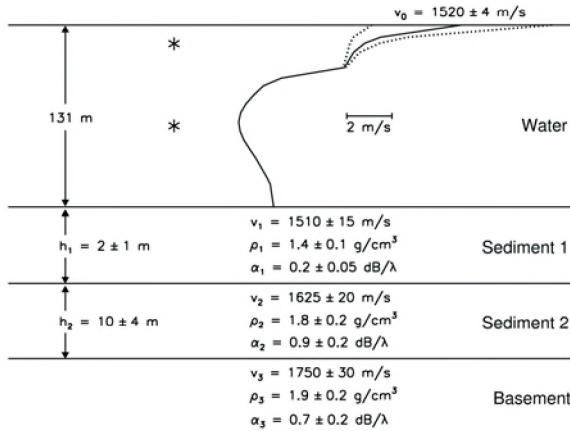


Fig. 1. Malta Plateau environment, including assumed values and standard deviations for environmental parameters. Asterisks indicate source depths.

over a three-layer seabed. The ocean sound-speed profile (SSP) includes a strong negative gradient in the near-surface waters and a weak sound channel with its axis near mid-water depth. The three seabed layers are characterized by sound speeds v_1 , v_2 , v_3 , densities ρ_1 , ρ_2 , ρ_3 , and attenuation coefficients α_1 , α_2 , α_3 . The upper two sediment layers are of thicknesses h_1 and h_2 (the basement layer is semi-infinite). Geoacoustic and SSP parameters values and uncertainties representative of the Malta Plateau region are given in Fig. 1. The SSP uncertainty is taken to represent oceanographic variability due to surface heating/cooling and wind mixing, with the effects decaying exponentially with depth over the top 30 m, as shown in Fig. 1. This variability is represented by the standard deviation of the surface sound speed v_0 .

Fig. 2 shows the three sensitivity measures for all environmental parameters averaged over 0–30 m receiver depth and 0–20 km range for source depths of 15 and 65 m. Sensitivities for the different parameters vary over almost six orders of magnitude, with the most sensitive parameters being those of the upper seabed layer and SSP, followed by the second and then third seabed layers. The sensitivity results for the two source depths in Fig. 4 are generally similar, with the largest difference for the SSP parameter v_0 . In all cases the linearized estimate provides a better approximation to the true nonlinear sensitivity measure.

Figure 3 illustrates the three sensitivities for selected parameters as a function of range and depth, with the parameter standard deviation fixed at the assumed environmental uncertainties for the Malta Plateau region (Fig. 1). For the three geoacoustic parameters v_1 , v_2 , and h_1 , the source is at 65-m depth near the sound-channel axis, while for the SSP parameter v_0 , the source is at 15-m depth within the variable near-surface layer. The sensitivity to the second sediment layer sound speed v_2 includes high values at short ranges, as steep propagation paths (which attenuate with range) interact significantly with the deeper layer. The

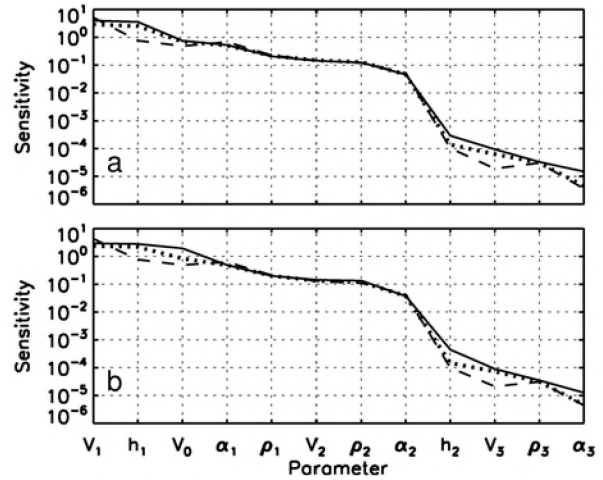


Fig. 2. Parameter sensitivities averaged over receiver depths of 0–30 m for source depths of (a) 65 m and (b) 15 m. Nonlinear, linearized, and linear sensitivity measures are indicated by solid, dotted, and dashed lines, respectively.

highest sensitivity for the SSP parameter v_0 is confined to depths over which the SSP varies. The agreement of the linearized and linear sensitivities with the nonlinear sensitivity in Fig. 3 is good for parameter v_1 and excellent for v_2 , with generally better agreement for the linearized measure. The linearized sensitivity is in reasonable agreement with the nonlinear sensitivity for parameter h_1 , but in poor agreement for v_0 . The linear sensitivity differs substantially from the nonlinear sensitivity for h_1 and v_0 .

REFERENCES

- [1] R. T. Kessel, "A mode-based measure of field sensitivity to geoacoustic parameters in weakly range-dependent environments," *J. Acoust. Soc. Am.*, **105**, 122–129 (1999).

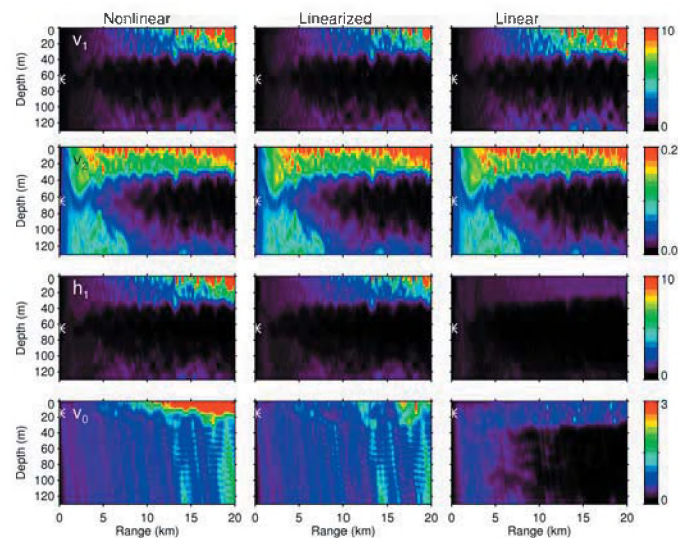


Fig. 3. Sensitivity sections for parameters v_1 , v_2 , h_1 , and v_0 (rows) and nonlinear, linearized, and linear sensitivity measures (columns). Source depth indicated by asterisks.

ACOUSTIC SOURCE LOCALIZATION WITH ENVIRONMENTAL UNCERTAINTY

Stan E. Dosso and Michael J. Wilmut

School of Earth and Ocean Sciences, University of Victoria, Victoria, B.C. Canada, V8W 3P6

1. INTRODUCTION

This paper applies a nonlinear Bayesian formulation to study uncertainty in ocean acoustic source localization due to uncertainty in the knowledge of ocean environmental properties (water-column sound-speed profile and seabed geoacoustic parameters). Localization uncertainty is quantified in terms of probability ambiguity surfaces (PAS), which consist of joint marginal probability distributions for source range and depth integrated over uncertain environmental parameters. The integration is carried out using Metropolis Gibbs' sampling for environmental parameters and two-dimensional heat-bath Gibbs' sampling for source range and depth to provide efficient sampling over complicated source search spaces with many isolated local maxima [1]. The approach is illustrated for acoustic data recorded on a hydrophone array in a shallow-water environment in the Mediterranean Sea where previous geoacoustic studies have been carried out [2]. Localization uncertainty is considered as a function of the level of uncertainty in the prior information for environmental properties.

2. EXPERIMENT

The PROSIM shallow-water geoacoustic experiment was carried out by the NATO Undersea Research Centre in the Mediterranean Sea off the west coast of Italy near Elba Island [2]. The experiment consisted of recording acoustic signals from a transducer towed at approximately 10-m depth along a track with nearly range-independent bathymetry (water depth: 132 m). The source emitted a 0.5-s linear frequency-modulated signal over the band 300–800 Hz every ~ 0.25 km along the track. The signals were received at a bottom-moored vertical line array (VLA) of 48 hydrophones which spanned from 26–120-m depth with 2-m sensor spacing. The water-column sound-speed profile (SSP) measured during the experiment consisted of a weakly downward-refracting gradient that varied from about 1520 to 1510 m/s.

The environment and source parameters that comprise the model for Bayesian focalization are illustrated in Fig. 1. The acoustic source is at depth z and range r from the VLA in water of depth D . The SSP is represented by four sound-speed parameters c_1 – c_4 at depths of 0, 10, 50, and D m. The geoacoustic parameters include the thickness h of an upper sediment layer with sound speed c_s , density ρ_s , and

attenuation α_s , overlying a semi-infinite basement with sound speed c_b , density ρ_b , and attenuation α_b .

Geoacoustic inversion was applied previously to the PROSIM data for a source range of approximately 3.95 km, employing 11 frequencies at 50-Hz intervals over the 300–800-Hz source band [2]. The signal-to-noise ratio (SNR) for the data was approximately 30 dB, although the effective signal-to-noise ratio (ESNR), which also accounts for theory error, varied from about 7 to 0 dB over the band. The prior information for the geoacoustic parameters consisted of uniform distributions over wide parameter bounds representing essentially no knowledge of seabed properties. The geoacoustic inversion results from [2] are given as marginal probability distributions in Fig. 2.

3. RESULTS

This section considers the dependence of source localization uncertainty distributions on the prior information (uncertainties) of environmental parameters. Fig. 3 compares PASs computed for measured data at source ranges of approximately 3.1, 4.2, 5.3, and 6.3 km, with four different states of environmental information consisting of uniform prior distributions with: wide prior bounds for both geoacoustic and SSP parameters (top row of Fig. 3); wide bounds for geoacoustic parameters and narrow bounds for SSP parameters (second row); narrow bounds for geoacoustic parameters and wide bounds for SSP parameters (third row); and narrow bounds for both geoacoustic and SSP parameters (bottom row). The wide geoacoustic bounds are identical with the prior bounds used

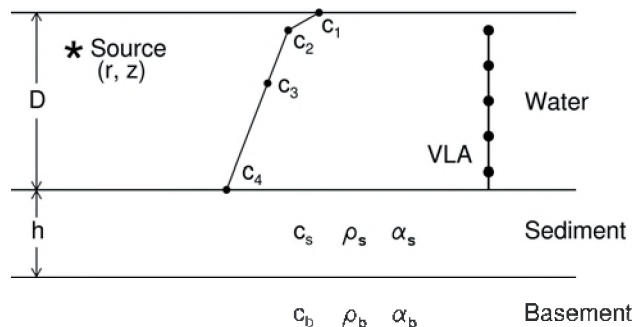


Fig. 1. Schematic diagram of experiment configuration and environmental parameters (defined in text).

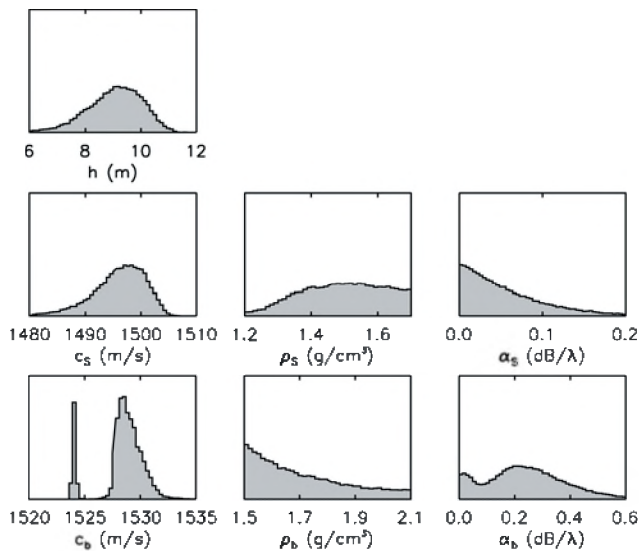


Fig. 2. Marginal probability distributions from geoacoustic inversion.

in the earlier geoacoustic inversion [2], and represent essentially no knowledge of the seabed properties. The narrow geoacoustic bounds are taken to be the 95% credibility interval from the geoacoustic inversion results shown in Fig. 2, and represent the typical state of seabed information available for localization from a previous geoacoustic inversion survey in a given region. The wide and narrow SSP bounds consist of intervals 10 m/s and 2 m/s wide, respectively, with the measured sound-speed values at or near the centre of the interval.

The acoustic data used in the Bayesian focalization consist of the complex pressure recorded at a single frequency of

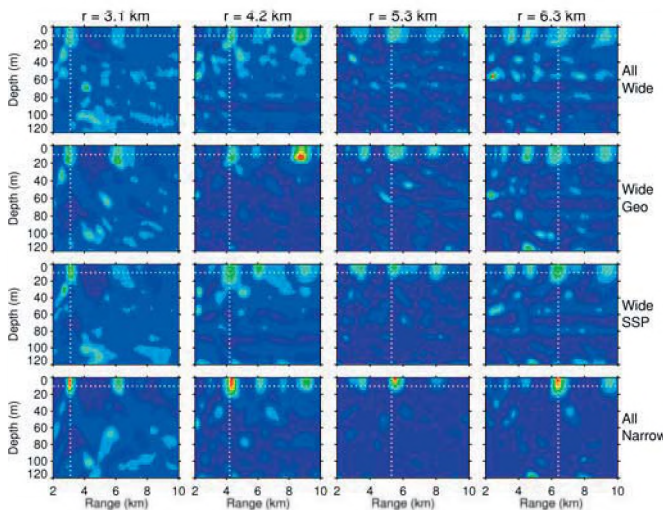


Fig. 3. PASs for various source ranges (indicated by column labels) and levels of prior information (row labels), including combinations of narrow and wide bounds for geoacoustic and SSP parameters. Dotted lines indicate the true source depth and range.

300 Hz, with random Gaussian-distributed errors added to the measured data to reduce the SNR to -3 dB. In addition to the additive Gaussian errors, the data uncertainties also include theory error resulting from the limitations of the model parameterization and numerical propagation model.

Figure 3 shows that a region of elevated probability is associated with the true source location in all cases. However, localization results are poor for the two cases involving wide geoacoustic parameter bounds. Localization is improved for the case of narrow geoacoustic and wide SSP bounds, although the true location is not unambiguous. Finally, for narrow geoacoustic and SSP bounds, Bayesian focalization provides good localization with small uncertainties for all four source ranges.

It is important to note that the good localization results obtained for the narrow environmental bounds do not indicate that any and all environmental models within these bounds suffice for localization. Rather, the Bayesian focalization samples parameter combinations within the prior that are consistent with the acoustic data. To illustrate this point, Fig. 4 compares the PAS for the source at 4.3-km range computed via integration over narrow environmental bounds to PASs computed for three cases in which geoacoustic and SSP parameters were drawn at random from the narrow bounds and held fixed. Each of the fixed-environment cases yield poor localization results.

REFERENCES

- [1] S. E. Dosso, "Environmental uncertainty in ocean acoustic inversion," *Inverse Problems*, **19**, 419–431 (2003).
- [2] S. E. Dosso, P. L. Nielsen, and M. J. Wilmut, "Data error covariance in matched-field geoaoustic inversion," *J. Acoust. Soc. Am.*, **119**, 208–219 (2006).

ACKNOWLEDGEMENTS

We thank Peter Nielsen of the NATO Undersea Research Centre for providing the PROSIM acoustic data.

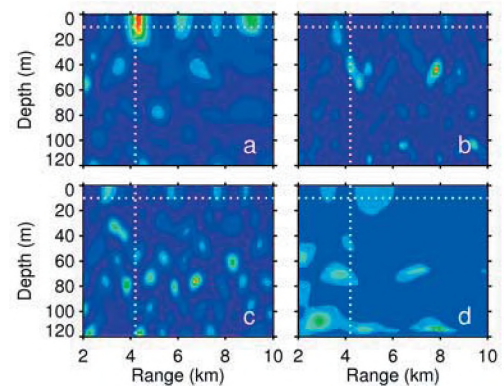


Fig. 4. (a) PAS for source at 4.2-km range from Bayesian focalization over narrow prior uncertainty bounds. (b)–(d) PASs for fixed environmental parameters drawn at random from narrow uncertainty bounds.

SOUND PRESSURE AND PARTICLE VELOCITY MEASUREMENTS FROM MARINE PILE DRIVING WITH BUBBLE CURTAIN MITIGATION

Alex MacGillivray and Roberto Racca

JASCO Research Ltd., #2101-4464 Markham St., Victoria BC, Canada, V8Z 7X8
alex@jasco.com, rob@jasco.com

1. INTRODUCTION

In October 2005, JASCO Research Ltd (JASCO) performed measurements of underwater acoustic pressure and acoustic particle velocity near marine pile driving work at Washington State Ferries' Eagle Harbor maintenance facility, located on Bainbridge Island in Washington State. Ten steel piles, all 30 inches in diameter, were installed at the construction site in 10 metre deep water. Bubble curtain mitigation was employed by the construction contractor to reduce underwater sound levels generated by the pile driving. The goal of this study was to determine the effectiveness of the bubble curtain at reducing acoustic particle velocity levels as well as sound pressure levels, since injuries to the hearing organs of fish may be more directly related to particle motion than to pressure (Hastings and Popper, 2005).

2. THEORY

Acoustic particle velocity can be measured using the pressure gradient method, as described for example by Fahy (1977). Euler's linearized momentum equation can be used to show that the acoustic particle velocity is related to the time integral of the acoustic pressure gradient:

$$\mathbf{v} = -\int \nabla p / \rho_0 dt \quad (1)$$

where \mathbf{v} is the vector particle velocity, ρ_0 is the fluid density and p is the acoustic pressure. Experimentally, the pressure gradient may be measured from the differential pressure between two closely spaced hydrophones:

$$\frac{\partial p}{\partial x} = -\rho_0 \frac{\partial v_x}{\partial t} \approx \frac{p(x+h/2) - p(x-h/2)}{h} \quad (2)$$

where p is acoustic pressure, v_x is the component of velocity along a single axis and h is the hydrophone spacing. The finite difference approximation of Equation 2 depends on the condition that hydrophone separation h be small relative to the acoustic wavelength; consequently there is an upper frequency limit for the practical application of this formula. It may be demonstrated that the amplitude error, in decibels, due to this finite-difference approximation is less than the quantity:

$$\epsilon = 20 \log_{10} \left(\frac{k_x h}{2 \sin(k_x h / 2)} \right) \quad (3)$$

where $k_x = 2\pi f/c$ is the acoustic wavenumber, f is the frequency of sound and c is the speed of sound in water.

3. METHODS

Apparatus

Acoustic particle velocity from pile driving was measured by the pressure gradient method using a custom

built, multi-component hydroacoustic sensor designed by JASCO. The pressure gradient sensor was composed of a pyramidal frame supporting four Reson TC4043 hydrophones and a JASCO AIM attitude/depth sensor. The hydrophones were cross-calibrated before and after the field measurements using a swept reference signal (from 100 Hz to 2 kHz) from an underwater loudspeaker. A schematic diagram of the pressure gradient measurement system is shown in Figure 1.

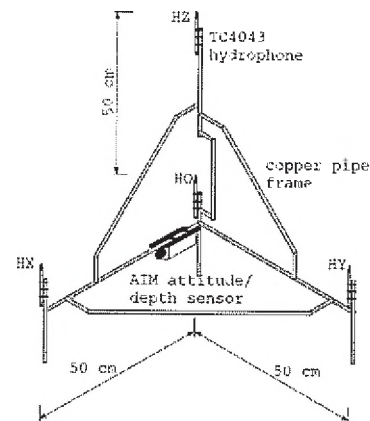


Fig. 1. Schematic diagram of the pressure gradient sensor shown in isometric projection. Four Reson TC4043 hydrophones are located at the positions indicated HO (origin) HX (X-axis) HY (Y-axis) and HZ (Z-axis). The AIM attitude/depth sensor is oriented in the X-direction. The axial hydrophones HX, HY and HZ are all located 50 cm from the origin hydrophone HO.

Pressure signals from the four hydrophones were sampled at 25 kHz per channel, with 16-bit resolution, using a laptop PC based digital acquisition system. Custom software, written using the data analysis language IDL (Research Systems, Inc.), was used to compute three acoustic particle velocity traces from the time integral of the pressure gradient between the hydrophones, according to Equation 2.

The differential pressure traces were low-pass filtered at 1330 Hz to limit errors in the differential pressure calculation caused by aliasing of higher frequencies — 1330 Hz corresponds to the 3 dB error point in the finite difference approximation according to Equation 3. The traces were also high-pass filtered at 15 Hz to remove cumulative integration errors in the particle velocity calculation. High-pass filtering is required because the integral operator in Equation 1 effectively multiplies the power spectrum of the differential pressure by the inverse of frequency, causing preferential amplification of low frequency noise.

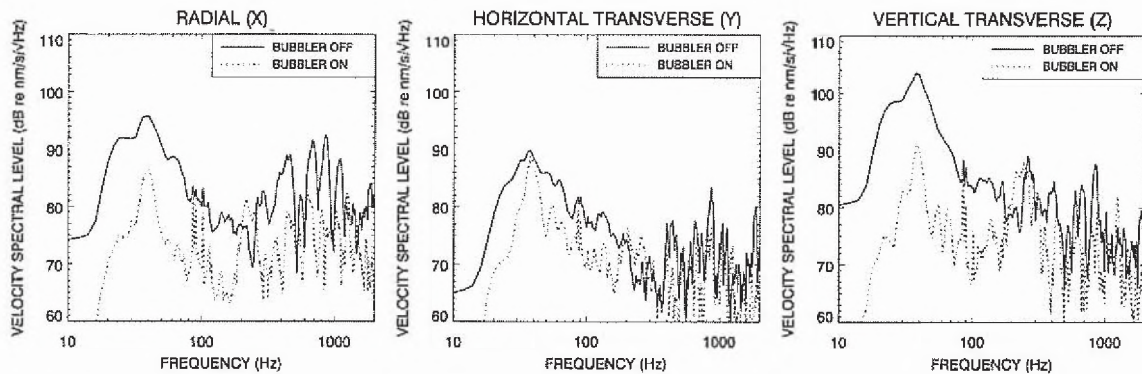


Fig. 2. Average X, Y and Z velocity spectral levels for inactive bubble curtain (solid line) and active bubble curtain (dotted line). The velocity sensor was oriented with the X-axis towards direction of the pile-driving and the Z-axis pointing vertically.

Measurements

Measurements were obtained during the installation of eight cylindrical steel piles next to a pier at the ferries maintenance facility. The outside diameter of the piles was 30 in. and the wall thickness was 1 in.; the length ranged from 75 ft. to 80 ft. and the weight per unit length was 311 lbs/foot. A Delmag 62 single-action diesel impact hammer with a 14,600 lbs hammer piston was used to drive the piles into the substrate. The bubble curtain apparatus consisted of a 1 in. thick cylindrical PVC sleeve, 44 ft. long and 47 in. outside diameter, that was lowered over each pile before hammering. Air was injected through two internally mounted aerating tubes, one located at the base of the sleeve and the other 10 ft. above the base. An air compressor supplied the aerating tubes at a rate of 300-350 CFM (cubic feet per minute).

The nominal water depth at the site was 10 meters and the acoustic sensor was deployed mid water column at a depth of 5 meters. Sound pressure and particle velocity waveforms were measured at horizontal ranges from 9 to 19 meters from the pile driving. For some of the measurements the air curtain apparatus was purposely left inactive (sleeve in position but with no air supply) to allow comparative measurements to be taken.

4. RESULTS

Figure 2 shows average X, Y and Z velocity spectral levels for hammering of a single pile with the bubble curtain active (12 strikes) and inactive (15 strikes) respectively. Above 100 Hz, maximum velocity spectral levels were observed on the radial (X-axis) velocity trace, which was oriented towards the direction of the pile driving. Below 100 Hz, maximum velocity spectral levels were observed on the vertical (Z-axis) trace; this was due to the low frequency vertical particle displacement caused by the downward movement of the pile upon impact of the pile driving hammer.

Table 1. Average acoustic particle velocity and sound pressure levels measured at 10 metres range.

Level	Curtain ON	Curtain OFF
Peak velocity	129.1 dB//nm/s	140.5 dB//nm/s
RMS velocity	117.3 dB//nm/s	129.4 dB//nm/s
Pulse length	141.9 ms	61.7 ms
Peak pressure	194.4 dB//μPa	204.2 dB//μPa
RMS pressure	183.3 dB//μPa	192.6 dB//μPa
Pulse length	49.3 ms	38.1 ms

Table 1 shows the average peak and 90% RMS particle velocity and sound pressure levels measured from hammering of a single pile at 10 metres range. Average measurements from hammering of three different piles at different ranges showed that the active bubble curtain reduced peak velocity levels by 11.4 dB and 90% RMS velocity levels by 12.1 dB. Similarly, the active bubble curtain reduced peak pressure levels by 9.1 dB and 90% RMS pressure levels by 8.6 dB. Thus the bubble curtain proved effective in mitigating both sound pressure and particle velocity levels generated by the pile driving.

REFERENCES

- Fahy, F. J. (1977). Measurement of acoustic intensity using the cross-spectral density of two microphone signals. *J. Acoust. Soc. Am.* 62, pp. 1057-1059.
- Hastings, M. C. and Popper, A. N. (2005). Effects of sound on fish. California Department of Transportation Contract 43A0139 Task Order, 1.

ACKNOWLEDGEMENTS

This study was sponsored by the Washington State Department of Transportation. In particular, the authors would like to acknowledge the cooperation and support of Jim Laughlin of Washington State Department of Transportation and Ellie Ziegler of Washington State Ferries.

AN ACOUSTICAL STUDY OF IPOD OUTPUT: EFFECTS OF HEADSETS AND CONTROL SETTINGS

Desiree Pereira, Shaun Sharma and Kathy Pichora-Fuller

University of Toronto at Mississauga, Department of Psychology, 3359 Mississauga Rd N, Mississauga, Ontario L5L 1C6

1. INTRODUCTION

Exposure to noise for long periods of time can cause damage to hearing (Fligor, 2006). Recently, the possible risk of noise-induced hearing loss for young adult wearers of portable audio devices has been questioned. Companies have launched numerous new devices and headsets to maximize the quality of sound in portable audio devices with mass storage capability, the most notorious being the Apple iPod. Apart from the specifications and control features of the device itself, its compatibility with different headphones will also alter the sound output. Three factors that differentiate one set of headphones from another are sensitivity, impedance, and frequency response. The purpose of this study is to evaluate several headsets through physical measurements and to decide if the resultant sound levels could be potentially hazardous to hearing health. We compared acoustical output measurements for samples of two genres of music played at four volume settings and different equalizer settings for three different headsets.

2. METHOD

Equipment

A Bruel & Kjaer Sound Quality Head and Torso Simulator (OSKAR dummy head) type 4128-C-001 with binaural microphones was used to measure the sound intensity on an A-weighted scale (dBA). All measurements made with OSKAR were recorded using Bruel & Kjaer's Pulse Labshop version 9.0.0.352.

A 30-GB Apple iPod Video MP3 player (MA146LL/A) was used to present the sound through different headsets to OSKAR's ears. A rectangular piece of paper divided into four equal segments was positioned below the iPod's visually displayed volume meter and used to code the volume setting as falling into one of four different ranges: 0-25, 25-50, 50-75 or 75-100%.

The output was measured for three different styles of headsets coupled to the iPod, one sold with the iPod by Apple and two alternatives sold by other companies. The brands of headsets tested and their corresponding specifications are as follows:

1. 30-GB iPod Video Earphones with a frequency range of 100Hz - 20kHz, sensitivity of -90 ± -3 dB, impedance of $32 \Omega \pm -15\%$ and maximum power input of 10mW.
2. Mirai Earphones (MI-SL-730BV-Black) with a frequency range of 20Hz - 20kHz, sensitivity of $113\text{dB} \pm 3\text{dB}$,

impedance of 32Ω and maximum power input of 60 mW.

3. Panasonic Earphones (RP-HV288) with a frequency range of 10Hz - 25kHz, sensitivity of 104 dB/mW, impedance of 16Ω and maximum power input of 50 mW.

Stimulus Material

Two 30-second sound clips were used for the tests; one from the Hip Hop genre the other from Electronica. These two particular kinds of music were chosen because of their current popularity with young adult listeners. Hip Hop songs are known for their strong percussions, thus most of their energy is concentrated in the low-frequency range between 1 and 4 kHz. In contrast, a typical Electronica song features synthetically produced sounds spanning a frequency range from 1 to 12 kHz.

Procedure

The evaluation of the iPod with the three different headsets took place in an IAC double-walled sound-attenuating booth. OSKAR was positioned on a small desk in a fixed location within this booth. There are 23 different equalizer settings options on the iPod and each of them was coded with numbers from 0 through 22. The sound intensity in dBA was recorded at 25, 50, 75, and 100% volume settings for each of the 23 equalizer settings.

The standard iPod earphones were the first to be assessed. After positioning the earphones in OSKAR's conchas, a 30-second Hip Hop sound clip was presented to OSKAR. The initial equalizer setting and volume were adjusted to 0=default and 25%, respectively. The average dBA level was recorded over the 30-second duration of the clip. The measurements were obtained in the same way for the three other volume levels at the default equalizer setting. We then tested the next equalizer setting at each of the four volume levels until all 23 equalizers had been tested using the Hip Hop song. The entire process was repeated with the Electronica test stimulus.

We calculated the average difference in dBA between Hip Hop and Electronica for each condition. The largest and smallest differences at each volume level were used to determine which equalizer settings made the most difference (see Results section). Based on these findings, two equalizer options were selected for further testing with the other two headphones. Specifically, Mirai and Panasonic earphones were tested at the equalizer settings 10=jazz and 13=lounge across the four different volume levels.

3. RESULTS

For the iPod earphones, we took the average dBA measurements of both ears and plotted them against the 23 equalizer settings at the four different volume levels.

Not surprisingly, dBA levels increased with volume. For Hip Hop, the average sound level (\pm SD) increased from volume 1 through 4 in the following manner: 52.5(\pm 5.3), 61.9(\pm 8.2), 77.9(\pm 5.7) and 93.7(\pm 5.7) dBA (see Figure 1).

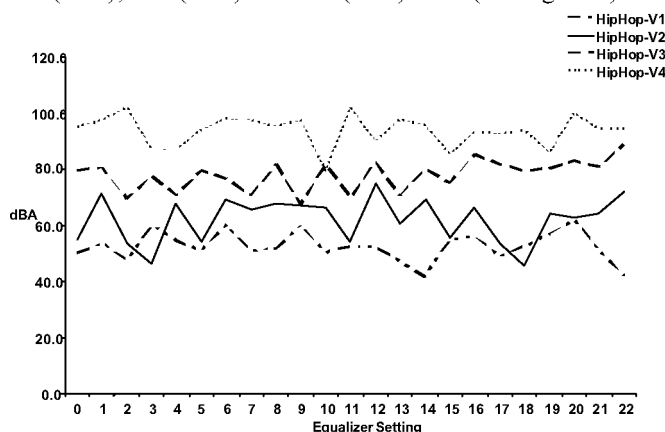


Figure 1. Average of left and right-ear dBA outputs for iPod earphones with the Hip Hop music at four volume settings and 23 equalizer settings.

Interestingly, the average dBA output was greater for Electronica than for Hip Hop for volume levels 1 through 4 respectively: 53.6(\pm 3.2), 68.4(\pm 4.2), 84.3(\pm 3.3), 96.7(\pm 3.6) dBA. The output depended on equalizer and volume settings; however, the variability was greater for Hip Hop.

At each volume and equalizer setting, the difference due to genre was calculated by subtracting the dBA outputs (Hip Hop - Electronica). For example, at volume 4, the largest negative difference was -19 dBA (equalizer 13, “lounge”) and the largest positive difference was +8.3 dBA (equalizer 10, “jazz”). Thus, it seemed interesting to examine these two settings more closely. Accordingly, we tested the Mirai and Panasonic earphones at the default setting and with the equalizer set at 10=jazz and 13=lounge.

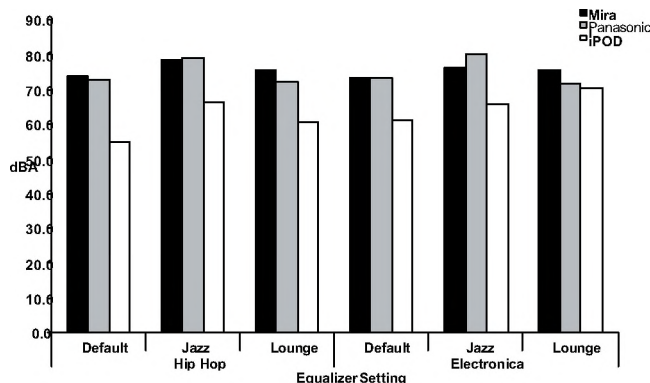


Figure 4. Left and right-ear average dBA outputs for three earphones at 50% volume with default, jazz and lounge equalizer settings for Electronica and Hip Hop.

All tests with the Mirai and Panasonic earphones were conducted at a 50% volume setting because that was assumed to be a typical user setting.

As seen in Figure 2, the dBA output from the Mirai and Panasonic earphones were comparable for each equalizer setting across the two test stimuli; the largest difference between them was 4.1 dB in the jazz setting for Electronica. They always yielded dBA output levels between 70 and 80 dBA. Furthermore, the outputs were consistently greater than the outputs from iPod earphones. At the default and lounge settings, a clear trend was seen with the Mirais louder than the Panasonics which were both louder than the iPods. This trend, however, was not maintained at the jazz setting where the Panasonics were slightly louder than the Mirais, but with both again being louder than the iPods.

4. DISCUSSION AND CONCLUSIONS

This acoustical study has investigated the level of sound output from different kinds of headsets and how output depends on factors such as equalizer and volume control settings. We found that the genre of music influences the level of sound output by any given headset. For instance, the Electronica sample was found to be consistently louder than Hip Hop at each volume setting using the iPod earphones. Furthermore, variability due to equalizer setting and headphone was noted and interacted to some degree with type of music and volume setting; e.g., at volume 4, there was a difference of 27.3 dB between the sound output in the jazz setting and the sound output in the lounge setting. This indicates that a simple change in equalizer setting at any given volume level can dramatically influence the output.

These physical measurements can be used to estimate the risk to human hearing. Of course, increasing the volume setting results in increasing dBA output. The alternative headsets such as the Mirai and Panasonic were consistently found to emit more hazardous sound levels than the standard iPod headset. It is commonly accepted that 85 dBA for a period of 8 hours is the maximum level of safe exposure (NIOSH). With every 3 dB increase, the duration for safe exposure is halved. Relating this information to our study, at 100% volume, regardless of type of music or equalizer settings, the sound intensity levels exceed 85 dBA. If a 3 dB increase reduces the duration of safe exposure by half, then the 27.3 dB change from one equalizer to the next could be potentially dangerous if listeners do not exercise caution.

REFERENCES

- Bruel & Kjaer. “Product data sound quality head and torso simulator-types 4100 and 4100D.” Accessed at <http://www.bksv.com/pdf/Bp1436.pdf>; April 1, 2006.
- Fligor, B.J. (2006). “Portable” music and its risk to hearing health. *The Hearing Review*, 13(3), 68-72.
- National Institute for Occupational Safety and Health (NIOSH). “Common Hearing Loss and Prevention Terms”. Accessed at <http://www.cdc.gov/niosh/hpterms.html>; April 19, 2006.

RELATING USE OF PORTABLE AUDIO DEVICES TO AUDIOMETRIC THRESHOLDS IN UNIVERSITY STUDENTS

Brenda Garrido, Andrew Gross and Kathy Pichora-Fuller

University of Toronto at Mississauga, Department of Psychology, 3359 Mississauga Rd N, Mississauga, Ontario L5L 1C6

1. INTRODUCTION

Hearing loss in adults has been largely associated with the process of aging, whereas noise and noise-induced trauma were believed to be primarily an industrial health problem. Accordingly, most people have not considered recreational and leisure activities to pose a threat to hearing (but see Health & Welfare Canada, 1988).

Researchers, however, have known for quite some time that noisy leisure activities may pose a real danger to people's hearing if the ears are not adequately protected. In fact, many common household items have been a source of concern because of the high level of noise they produce. For example, in the past, noise associated with the ring of the cordless telephone was the subject of a great deal of concern. Similarly, the vacuum cleaner, the hair dryer and even the household electric knife have been thought to pose a risk to hearing (Health & Welfare Canada, 1988). Despite efforts to educate the public about these effects, it seems that most people are resistant to the idea, and that young adults are the most difficult people to convince about the dangers of excessive exposure to non-industrial noise.

The hearing health of young adults is a concern now more than ever because of the introduction of portable audio devices with mass storage that enables a listener to hear a larger selection of music. The enhanced selection options are presumed to entice listeners to wear the devices for much longer durations compared to earlier technologies. The increasing popularity of these devices has prompted the media to draw attention to the question of whether the extended use of these devices is creating hearing problems, particularly in youth (e.g., Hawaleshka, 2005). Although much research has been done (Fearn & Hanson, 1989), more data are needed to establish a definitive connection between the use of current portable audio devices and hearing loss.

The present experiment is part of a larger study attempting to determine whether or not there is a connection between the use of portable audio devices and early warning signs of hearing loss. We focus on comparing the hearing health of individuals and relating it to the frequency and manner of their use of portable audio devices. The participants' experience with portable audio devices was

determined by questionnaire in the first part of the study and a subset of the participants who completed the questionnaire returned to have their hearing thresholds measured.

2. METHOD

Participants

The participants were primarily individuals from the first year Psychology class at the University of Toronto who received course credit for their participation. However, a few other students volunteered to participate in this study without compensation because of their interest in the topic. Participants were those who had completed a questionnaire for a larger study on the use of portable audio devices and had agreed to continue participation in the broader study. In total, the subject pool consisted of 45 university students.

Procedure

Each individual completed a hearing test lasting less than 30 minutes. Thresholds were tested for pure-tones of .25, .5, 1, 1.5, 2, 3, 4, 6, 8, 10, and 14 kHz. Participants sat in a sound-attenuating double-walled IAC booth. Standard test frequencies were delivered to Telephonics TDH-50P HB7 headphones from a Grason-Stadler GSI-61 audiometer. High-frequency testing (above 8 kHz) was conducted using a special option on the audiometer and Sennheiser HAD 200 headphones. Using a standard ascending procedure, the test tone was presented starting at a level of 30 dB HL, and decreased by 10 dB until the participant no longer responded and then the level of the tone was increased by 5 dB until a response was made. This bracketing procedure was repeated to determine the level at which the participant correctly detected each frequency 50% of the time. The ear to which the stimulus was presented was that which the participant believed to be of lesser ability or if both ears were believed to be equally good then the left ear was tested

Clinically normal results for hearing thresholds are considered to be between 0-25 dB HL (Mencher, 1997). Following the recommendation of Mencher, if the thresholds of any participant exceeded 20 dB HL at 3 kHz or 30 dB HL at 4 kHz, and if the person wished to have a diagnostic hearing test then a referral to an audiologist

would have been made; however, no participant met the criteria that would have triggered a referral

3. RESULTS

The distribution of hearing thresholds (dB HL) measured at each of the test frequencies presented is shown in Figure 1. All 45 students had thresholds less than 10 dB HL at 1, 1.5, and 4 kHz. For all other frequencies, except 6 kHz, at least $\frac{3}{4}$ of the students had thresholds of 5 to 10 dB HL, well within the normal range. Outliers with thresholds falling outside of the range considered to be clinically normal were observed at 30 dB HL for .25 kHz, and at 40 dB HL for 14 kHz.

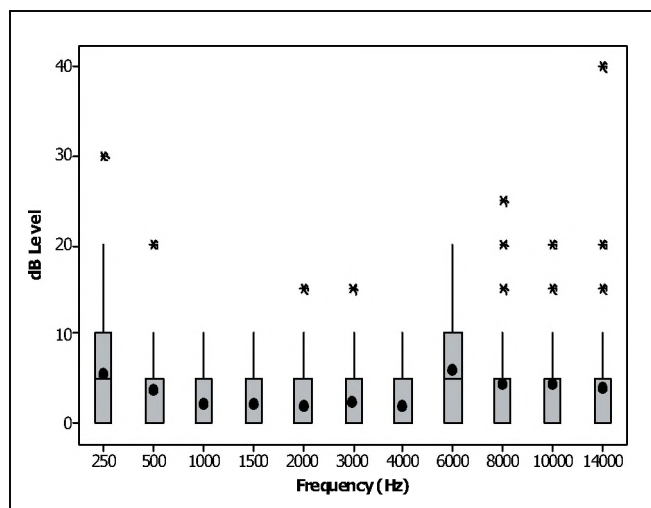


Figure 1. Box and whisker plots showing the mean dB HL threshold (black dots), median (centres of box), inter-quartile ranges (box ends), and minimum and maximum (ends of whisker lines) thresholds of hearing (dB HL) at each pure-tone frequency tested. Outliers are indicated by *.

4. DISCUSSION

The results obtained from the current study indicate that there is no evidence of clinically significant hearing loss in the group of 45 students tested, with the exception of two participants, one of who had a threshold of 30 dB HL at .25 kHz and one who had a threshold of 40 dB HL at 14 kHz. Importantly, all students had thresholds no worse than 10 dB HL at 4 kHz where the first signs of noise-induced hearing loss are expected to be observed. Moreover, the high thresholds of two participants at the extreme frequencies cannot be attributed to noise exposure.

The result of the present study cannot be extended to the general population of young adults for a number of reasons. It is important to consider that the sample was comprised of self-selected university students whose lifestyle may differ from that of the general population of

their peers. For example, university students may be more likely to have had little industrial work experience, whereas peers without post-secondary education are more likely to be working, many in jobs with high levels of noise exposure, such as in factory or construction workplaces. It is also possible that the university students, especially those who self-selected for the study, may be more health-conscious than their peers and they may take fewer health risks, including engaging in noisy hobbies. A third likely difference is that because of the financial and time demands on them, university students may have less opportunity than their peers to engage in noisy hobbies.

6. CONCLUSIONS

In light of the present audiometric results, it is not possible to conclude that noise-induced hearing loss is widespread amongst university students, either as a result of the use of portable listening devices or from any other cause. It may simply be too early to discern whether noise-induced damage has begun in young adults who listen to portable audio devices such as today's iPod. This should not, however, discount the fact that sound presented to the auditory system at a level of 85 dB A for 40 hours per week over an extended period of time has been documented to be enough to result in permanent noise-induced hearing loss, and is mandated against by occupational safety regulations (Mencher, 1997). Although young adults may not show signs of such loss yet, this should not suggest that prolonged exposure to portable audio devices at these levels will not result in future hearing loss. Furthermore, even if an effect had been found in our study, it would be difficult to establish that portable audio devices were the primary culprit. Longitudinal studies will be needed to shed more light on this important question. Future research should focus on isolating the direct effect of portable audio devices on hearing from the effects of environmental noise exposure in a larger sample and also to relate audiometric measures to long-term patterns and conditions of usage of these devices.

REFERENCES

- Health & Welfare Canada, Health Services Directorate Task Force. (1988). *Acquired Hearing in Impairment in the Adult*. Health and Welfare Canada: Ottawa.
- Fearn, R.W., & Hanson, D.R. (1989). Hearing level of young Subjects exposed to amplified music. *Journal of Sound Vibration*, 128 (3), 509-512
- Hawaleshka, D. (Dec 01, 2005). Turn it down! Now hear this: Auditory experts are warning that the iPod Nation may soon become the deaf generation, Macleans.ca http://www.macleans.ca/topstories/technology/article.jsp?content=20051205_116945_116945.
- Mencher, G., Gerber, S., & McCombe, A. (1997). *Audiology and Auditory Dysfunction*. Allyn & Bacon.

A SURVEY OF THE USE OF PORTABLE AUDIO DEVICES BY UNIVERSITY STUDENTS

Shazia Ahmed, Matthew King, Timothy W. Morrish, Ewelina Zaszewska, and Kathy Pichora-Fuller

University of Toronto at Mississauga, Department of Psychology, 3359 Mississauga Rd N, Mississauga, Ontario L5L 1C6

1. INTRODUCTION

As our environment becomes more complicated, people are continuously bombarded with noise that is potentially detrimental to hearing health. Portable audio devices are increasingly popular among today's adolescents and young adults. Many fear that the use of these devices has become excessive and dangerous to hearing health. It is widely held that constant exposure to noise in recreational activities could affect hearing health (Williams, 2005; Chung, 2005). In particular, a recent telephone-based survey found that high school students are most likely to listen to their audio devices for longer periods at higher settings compare to adults. Furthermore, these students are much more likely to report experiencing symptoms of hearing loss, including turning up the volume of the TV, tinnitus, and difficulty understanding speech (Zogby, 2006). In most previous studies on the use of audio devices, factors that resurfaced were the low level of awareness of the risk to hearing health, and the low level of concern about hearing health, at least in the case of those who were not educated about hearing loss (Williams, 2005; Chung, 2005; Zogby 2006).

The current study is part of a larger study which aims to determine the relationship between the sustained use of portable audio devices and hearing health in university students. This part of the study focuses on the administration of a survey, with the goal of determining how portable audio devices are used by university students, how their use interacts with other sources of noise exposure, and whether their patterns of use raise concerns for hearing health. An additional goal of the project was to increase awareness about noise-induced hearing loss by providing an information session to those who completed the survey.

2. METHOD

2.1 Participants

There were 150 participants in the study, 126 of whom were undergraduate students who received a credit towards their Psychology 100 course at the University of Toronto at Mississauga. The rest were other undergraduate students who volunteered to complete the study with no monetary compensation. All participants provided informed consent. Participants from Psychology 100 were recruited using the course website and they were tested in groups in a computer lab at the university that was reserved for the study. The survey took less than 30 minutes to complete and it was followed by an information session. All participants were

young adults: 71.3% of the participants were in the 18-20 year age range; 56.7% were male and 43.3% female.

2.2 The Survey

A 124-item online survey was designed to probe items that would provide information on users of portable audio devices in the university student population. Items were designed to investigate a number of topics, including: demographic characteristics, transportation usage patterns, work environments, hearing history, family hearing history, recreational activities (including noisy hobbies, frequency of attendance at bars, concerts and sporting events), as well as questions on the use of portable devices.

Other parts of the project were conducted to examine audiometric thresholds in users and non-users of portable audio devices as well as to obtain acoustical measurements to quantify how listeners use a typical device in different noise environments. To satisfy the overall purposes of the larger study, a number of items in the survey were created to enable correlations between the findings. Among others, these items related to the participants' subjective estimations of the volume levels that they set on their own devices, and subjective perceptions of their hearing abilities. Thus, the survey was intended to aid in establishing trends relating hearing loss to excessive use of portable audio devices.

2.3 The Information Session

Following the completion of the online survey, participants received a 15-minute information session presented in PowerPoint. The goal of this information session was to educate those involved with the study about hearing health and hearing loss. During the session the participants were also debriefed regarding the hypotheses and goals of the study, and they were able to ask the researchers additional questions about hearing and their participation in the study.

3. RESULTS

Most (82.7%) of the participants owned a portable audio device. On average, 46% of the participants reported using their portable audio device for 5 to 7 days per week, for the average duration of 2 hours per listening session. However, there were 35 students that reported listening to their devices as frequently as seven days a week, and seven students listened to their devices for as long as 4 to 8 hours

in a typical single session. As for the volume, the mean level at which the students set their devices was 60% on a scale from 0 to 100% with 100% being the maximum volume. However, there were 21 individuals who reported setting the sound level in the 80-100% range. This initial evidence suggests that the majority of students use their devices frequently, but in safe volume ranges; however, there is a minority of university students who may use their portable audio devices excessively and at dangerous volumes. Gender differences were observed (see Figure 1). More females than males reported setting the volume in the 25-50% range. Curiously, more males than females preferred the highest ranges, but of those who preferred the lowest volume, more were males.

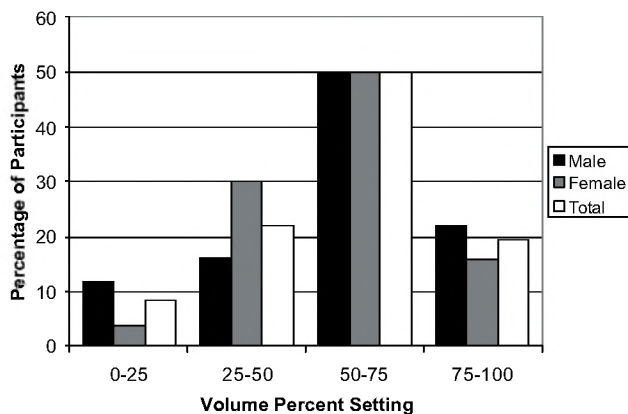


Figure 1. Percentage of male and female users of portable audio devices and their volume preferences; volume divided into quadrants.

Self-reports on hearing health indicated that 31% of the students thought their hearing was worse than five years ago. Also, 13% believed they had a hearing loss and 13% believed it was noise related. Importantly, these reports on hearing health did not differ between the users and non-users of portable audio devices. In other words, there was no indication that more users than non-users of portable audio devices reported hearing concerns. In addition, close to 90% of students did not wear ear protection, even though over half enjoyed listening to loud music.

Comparing the present results those by Zogby (2006) who conducted a survey on high school students and adults, we found a number of commonalities even though there was on average a 3 year age difference between our sample and Zogby's high school sample. About a third (30%) of the university sample reported turning up the TV volume more than they used to (compared to 27% of high school students). Tinnitus was experienced by 17% of high school students in the Zogby (2006) study. In the present survey, although few university students reported having persistent ringing in the ears, all but 30% had experienced it after exposure to a loud sound.

4. DISCUSSION

Our data show that the majority of university students own a portable audio device. This may mean that noise-induced hearing loss may be a larger concern now than ever before, if the use of portable audio devices is excessive and /or if it is combined with exposure to other noise sources. However, the majority of respondents reported setting their devices in the middle volume ranges, and only a minority of students reported their work/volunteer places to be loud.

Cause for concern is raised by the finding that a third of the participants felt that their hearing had worsened in the past five years, and only 12% of participants used hearing protection compared to the 31% who felt that their hearing was deteriorating. Thus, our data suggests that although most students tend not to expose themselves to excessive noise (recreational noise, noise at work, or music noise while listening to portable audio devices), at the same time they do not recognize the possibility of losing their hearing and the importance of protecting it from noise. Also, they may simply be not aware that exposure to loud music can result in hearing loss. This assumption was also stated by Chung Roches, Des Meunier, and Eavey (2005) who conducted an online survey on views on health issues including hearing loss in adolescents and young adults. They concluded that some types of education may be crucial to motivating young people to change their listening habits. Moreover, in the study by Zogby (2006), the respondents indicated that school classes, teen magazines, and TV programs may be effective means for educating young people about hearing. Thus, it seems that, with such widespread use of portable audio devices among young adults, increasing awareness about hearing and early noise-induced hearing loss is essential, and boosting young people's motivation to protect their hearing may likely protect this generation from widespread hearing problems in years to come.

5. REFERENCES

- Chung, J. H., Roches, C. M., Des Meunier, J., Eavey, R. D. (2005). Evaluation of noise-induced hearing loss in young people using a web-based survey technique. *Pediatrics*, 115(4), 861- 867.
- Williams, W. (2005). Noise exposure levels from personal stereo use. *International Journal of Audiology*, 44(4). 231-236.
- Zogby, J. (Zogby International). (2006). *Survey of Teens and Adults about the Use of Personal Electronic Devices and Head Phones*. American Speech-Language-Hearing Association.

AN ACOUSTICAL STUDY OF IPOD USE BY UNIVERSITY STUDENTS IN QUIET AND NOISY SITUATIONS

Sina Fallah and Kathy Pichora-Fuller

University of Toronto at Mississauga, Department of Psychology, 3359 Mississauga Rd N, Mississauga, Ontario L5L 1C6

1. INTRODUCTION

Exposure to loud noises in high doses can cause permanent damage to the cochlea and central auditory pathways resulting in noise-induced hearing loss (NIHL) (Fabiani, Mattioni, Saponara, & Cordier, 1998). Even though people may realize that excessive noise is dangerous, most do not have knowledge of what levels of sound are hazardous and so it is immensely important for professionals to educate the public about noise-induced hearing loss (Clark, & Bohne, 1999). Furthermore, even if people are informed about hazardous levels in terms of numerical decibel levels descriptions, they may not be able to relate decibel levels to their everyday experience. Therefore it is important to relate everyday auditory experience to the numerical quantification of noise.

The current experiment is part of a larger study and focuses on the acoustical measurement of iPod outputs, measured at user settings. By measuring the typical outputs at user settings, we attempted to determine what actual decibel levels young people choose while listening to their devices, how much they change the volume settings depending on the ambient noise, and in consequence, whether typical use of these portable audio devices may pose an actual risk to hearing health.

2. METHOD

Listeners adjusted an iPod to their preferred listening level for two samples of music in five background conditions.

Participants

Twenty four university students volunteered for this study. All were between 18 and 25 years of age and had hearing thresholds below 20 dB HL from 0.25 to 14 kHz. Most students earned 1 course credit in Psychology 100 for their participation in the study and a few volunteered without compensation because of their interest in the topic. Informed consent was obtained from all participants.

Stimuli

Two samples of music were used. Each sample was representative of a particular genre, either Hip-Hop or Electronica. These genres were chosen because they are very popular with undergraduate students. A typical 30-second segment of each song was presented in each condition and was used to calculate the dBA level output at each user's preferred settings. The Hip-Hop segment had more low-frequency content, whereas the Electronica segment had more high-frequency content.

Each sample of music was tested in five background conditions: quiet, multi-talker babble at 50 and 70 dB SPL, and traffic noise at 50 and 70 dB SPL. The levels of the background noise were chosen to typify mildly and moderately adverse conditions that might be encountered in everyday situations.

Equipment

All testing was conducted in an IAC double-walled sound-attenuating booth. The background noise was delivered over two loud speakers, positioned at 45° on either side of the listener. The delivery of sound was controlled using a TDT System III. Music was presented to all listeners from the same black 30-GB iPod Video, with standard earbuds. At the beginning of each condition, the equalizer settings were set to the default position. At the beginning of each session, a calibration test was done in which the output was measured with volume set to maximum and the equalizer to the default position. The output from the iPod was measured by placing the ear-buds in the ears of a Bruel and Kjaer dummy head model Type 4128 C001, fitted with microphones and a Zwislocki coupler in both ears. The output to the ears of the dummy head was measured using a Bruel and Kjaer PULSE Sound Analyzer 9.0, Labshop.

Procedures

Participants completed the experiment in one of four orders. In two orders, Electronica was tested first and Hip-Hop second, and the types of music were reversed in the other two orders. Within each music type, half of the time traffic noise was tested first and multi-talker babble was

tested second, and the types of background noise were reversed otherwise.

Participants sat on a chair located centrally in the sound booth facing the back wall with the loud speakers located in the back left and right corners of the room. The participant was instructed that he or she would listen to a set of ten music clips, five from the genre of Electronica and five from Hip-Hop. For each clip, the experimenter asked the participant to listen and adjust the iPod to his or her preferred listening level for the particular listening environment (quiet, babble, or traffic noise). No hints about how to adjust the device were given but the experimenter did show the participants how to adjust the iPod volume and equalizer controls.

After the participants were satisfied with their adjustment in each condition, the experimenter noted the volume setting on the screen of the device with reference to a pre-marked scale from 0 (minimum) to 4 (maximum). The earbuds were then placed in the ears of the Bruel and Kjaer dummy head and the 30-second clip was analyzed using the PULSE Sound Analyzer to determine the average output level in dB(A) for each ear at the user's preferred settings.

3. RESULTS

On average, listeners adjusted the iPod to 67.6 dBA, but their preferred listening level depended on ear, and the type of music and background noise (see Figure 1).

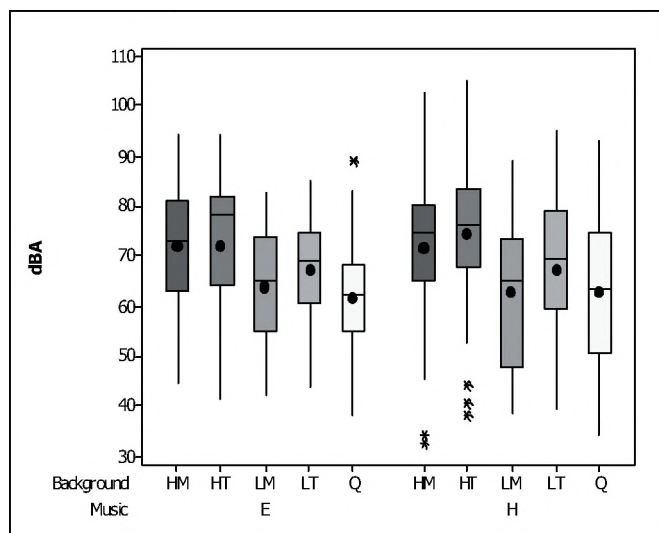


Figure 1. Box and whisker plots showing the means (black dots), medians (centres of box), inter-quartile ranges (box ends), and minimum and maximum values (ends of whisker lines) for dBA outputs measured when the iPod was adjusted by listeners to their preferred settings for Electronica (E) and Hip-Hop (H) music under five background conditions (HM = high-level multi-talker babble, HT = high-level traffic noise, LM = low-level multi-talker babble, LT = low-level traffic noise, Q = quiet). Results for the two ears are averaged. Outliers are indicated by *.

Output was lowest when there was no background noise (62.1 dBA) or when there was a low level of multi-talker babble (63.4 dBA). Output was greater when there was a low level of traffic noise (67.2 dBA). Output was greatest when there was high level noise, with little difference between multi-talker babble noise (71.7 dBA) and traffic noise (73.3 dBA). Curiously, mean output was 2.7 dB greater for the right than for the left ear.

These descriptions were confirmed by an Analysis of Variance with three between-subjects factors: Ear (right or left), Music (Hip-hop or Electronica), and Background (quiet, low-level multi-talker babble, high-level multi-talker babble, low-level traffic noise, high-level traffic noise). There were significant main effects of ear $F(1, 23) = 35.2, p < .01$, and background, $F(4,92) = 21.3, p < .01$. A Student-Newman-Keuls test of multiple comparisons confirmed that there was no significant difference between the outputs preferred in the quiet and low-level babble, but that the outputs in these conditions were significantly lower than in low-level traffic noise, and that the outputs in the high-level noise conditions were significantly greater ($p = .05$).

4. DISCUSSION

It has been suggested that the maximum output of an iPod can reach 115 dBA (e.g., Spencer, 2006); however, the present study found that most university students preferred to listen to the iPod at a lower output level that would not be considered to be hazardous even if worn for 8 hours per day. Not surprisingly, the preferred output increased when the background noise was higher. Importantly, there was a large range of preferred outputs. The maximum output level that any individual listened to was 105 dBA which could pose a risk if listening time were not limited. In fact, over a third of the participants ($n=9$) selected a volume setting in at least one condition that exceeded 85 dBA, a level of noise that would trigger intervention in an industrial setting assuming an 8-hour daily exposure time. Health education should target individuals who are at risk so that they learn how to use their portable audio devices more safely. Such education should stress that listening in quieter environments and for limited durations will minimize risk.

ACKNOWLEDGMENTS

We wish to thank Sun Xiaoming for technical assistance.

REFERENCES

- Clarke, W. W., & Bohne, B. A. (1999). Effects of noise on hearing. *J of the American Medical Association.*, 281(17), 1658-1659.
- Fabiani, M.; Mattioni, A, Saponara, M., & Cordier, A. (1998). *Scandinavian Audiology*, 27(Suppl 48), 147-153.
- Spencer, J. (2006). Behind the Music: iPods and Hearing Loss. *The Wall Street Journal Online*, http://online.wsj.com/public/article/SB113685799723842312dZrxb_eZm44vfy74topaLm4evP8_20070110.html?mod=tff_main_tff_top.

831 sound level meter/real time analyzer

- Consulting engineers
- Environmental noise monitoring
- Highway & plant perimeter noise
- Aircraft noise
- General Surveys
- Community noise



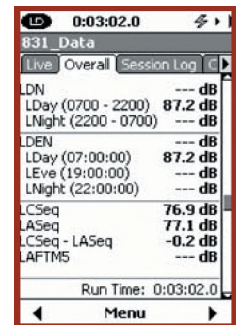
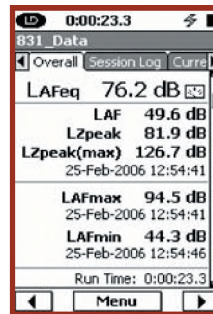
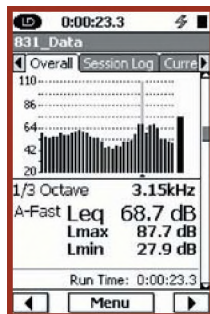
FEATURES

- Class 1/Type 1 sound level meter
- Small size with large display. Ergonomic
- User friendly operator interface
- 120MB standard memory expandable up to 2GB
- Single measurement range from 20 to 140 dB SPL
- Up to 16 hours of battery life
- Provided with utility software for instrument set-up and data download
- Field upgradeable
- AUX port for connection to USB mass storage & cellular modems



MEASUREMENT CAPABILITIES

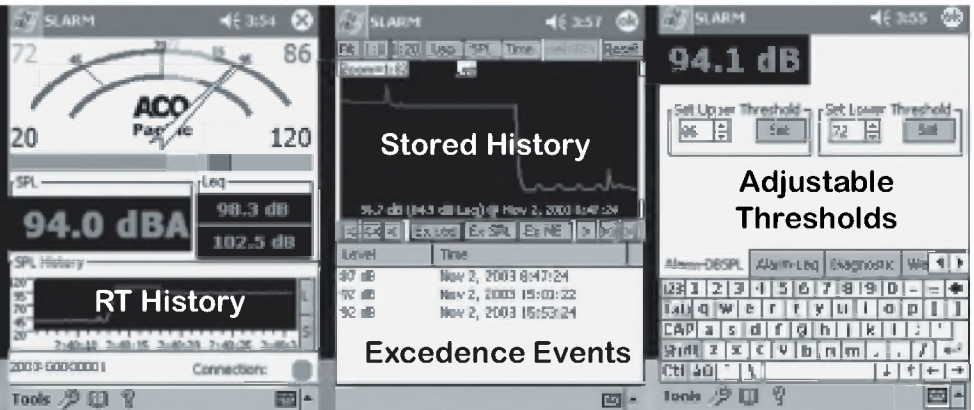
- Real time 1/1 & 1/3 octave frequency analysis
- Simultaneous display of several noise measurements—ANY DATA (Leq, Lmax, Spectra, etc)
- Automatic logging of user selectable noise measurements (Leq, Lmax, Spectra, etc...)
- Exceedance logging with user selectable trigger levels
- Audio and voice recording with replay



Noise Pollution

The SLARM™ Solution

PDA & Laptop
Displays
Wired
Wireless



The SLARM™ developed in response to increased emphasis on hearing conservation and comfort in the community and workplace incorporates ACOustAlert™ and ACOustAlarm™ technology. Making the SLARM™ a powerful and versatile sound monitoring/alarm system.

Typical Applications Include:

Community

- ◆ Amphitheatres
- ◆ Outdoor Events
- ◆ Nightclubs/Discos
- ◆ Churches
- ◆ Classrooms

Industrial

- ◆ Machine/Plant Noise
- ◆ Fault Detection
- ◆ Marshalling Yards
- ◆ Construction Sites
- ◆ Product Testing

FEATURES

- ✓ Wired and Wireless (opt)
- ✓ USB, Serial, and LAN(opt) Connectivity
- ✓ Remote Displays and Programming
- ✓ SPL, Leq, Thresholds, Alert and Alarm Filters (A,C,Z), Thresholds, Calibration
- ✓ Multiple Profiles (opt)
- ✓ 100 dB Display Range:
- ✓ 20-120 dBSPL and 40-140 dBSPL
- ✓ Real-time Clock/Calendar
- ✓ Internal Storage: 10+days @1/sec
- ✓ Remote Storage of 1/8 second events
- ✓ 7052S Type 1.5™ Titanium Measurement Mic



2604 Read Ave., Belmont, CA 94002 Tel: 650-595-8588 FAX: 650-591-2891
www.acopacific.com acopac@acopacific.com

ACOustics Begins With ACO™

LOCALIZATION OF RIGHT WHALES USING MATCHED CORRELATION PROCESSING

Gordon R. Ebbeson and Francine Desharnais

DRDC Atlantic, PO Box 1012, 9 Grove St., Dartmouth, NS, Canada, B2Y 3Z7, gordon.ebbeson@drdc-rddc.gc.ca

1. INTRODUCTION

In August of 2005, researchers at DRDC Atlantic deployed a horizontal hydrophone array on the seafloor in the Bay of Fundy, Canada, in order to record and analyse the vocalizations and “gunshot” type sounds from North Atlantic right whales (*Eubalaena Glacialis*). The purpose of the experiment was to investigate various methods of marine mammal localization. The right whale gunshots are spectrally similar to the signature of an imploded light bulb. In this paper, we demonstrate the use of Matched Correlation Processing (MCP) to localize the position of a light-bulb signature [1]. We then apply the MCP technique to the right whale data.

2. MATCHED CORRELATION PROCESSING

For many years, model-based Matched Field Processing (MFP) techniques have been researched with the goal of improving the capability of passive sonar systems for localizing quiet underwater sources [2]. Recently, researchers at DRDC Atlantic have been investigating MCP as a faster alternative to MFP. In this method, the cross-correlations for a broadband source as measured with a pair of hydrophones in a horizontal array are matched with those generated with a correlation model for many candidate ranges and depths along a candidate bearing. These matches are carried out with a number of hydrophone pairs to form many range-depth ambiguity surfaces. The maximum on the average of these surfaces is assumed to yield the best estimate of the source position. By carrying out this procedure over a number of candidate bearings, a full 3D search for the source location is achieved.

3. THE EXPERIMENTS

Figure 1 shows the MCP setup for an experiment that was carried out in St. Margaret’s Bay, Nova Scotia,

during the fall of 2005. A three-sensor horizontal array (red curve) with an aperture of 125 m was deployed on the sea bottom in 68 m of water and the hydrophones were localized using an Array Element Localization (AEL) procedure [3]. A light bulb was imploded at a depth of 41.5 m, 232 m from hydrophone 1 along a bearing of 189°T (black dot) and the resulting signature was recorded on the array.

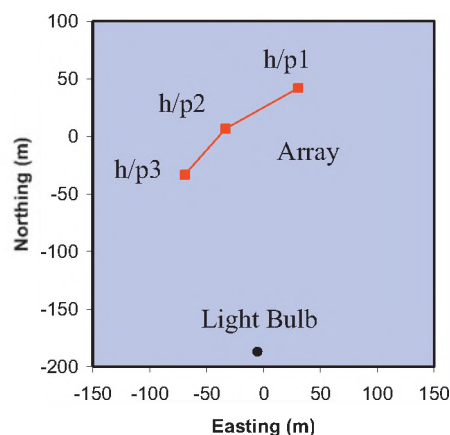


Fig. 1 The light bulb localization setup in St. Margaret’s Bay.

The MCP algorithm was used to localize the position of the light bulb. The search was carried out over ranges from 0 to 600 m in steps of 5 m, over depths of 0 to 65 m in steps of 5 m, and over 360° of bearing in steps of 5°. That search resulted in a correlation peak of 0.6725 along a bearing of 190°T. The range-depth ambiguity surface corresponding to that bearing is shown in Fig. 2. The peak is very sharp and, as indicated by the white cross hairs, is located at a range of 235 m and a depth of 40 m. The errors in this MCP localization are smaller than the steps sizes used in the search. Thirteen other light bulbs with a variety of ranges and bearing were also successfully localized.

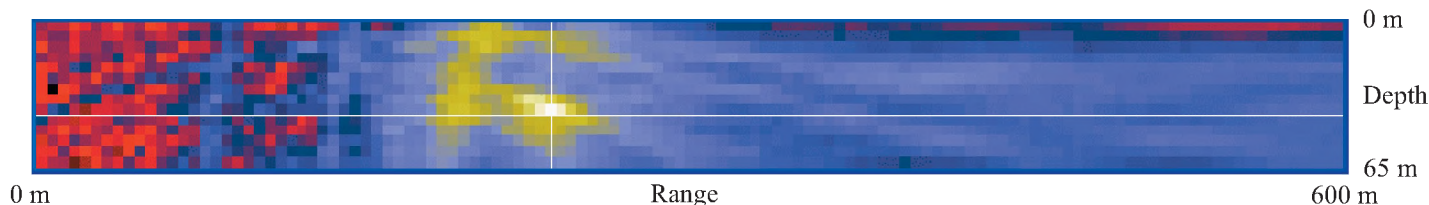


Fig. 2 The ambiguity surface at 190°T in St. Margaret’s Bay. The white cross hairs show the estimated position of the light bulb.

As shown in Fig. 3, a similar experiment was carried out in the Bay of Fundy, Nova Scotia, during the right whale localization trials of 2005. In this case, the array aperture was shorter at 28.9 m, the bottom depth was deeper at 101 m and the light bulb was imploded at a depth of 40.2 m, 215 m from hydrophone 1 along a bearing of 222°T.

The ambiguity surface that contains the maximum correlation is shown in Fig. 4. Although the MCP algorithm accurately localized the light bulb at a bearing of 225°T, the localization of the range and depth is extremely poor. This was due to the low reflection coefficient of the bottom at this site. The MCP algorithm requires good bottom-bounce arrivals to find the range and depth. Similar results were found for the other nineteen light bulbs.

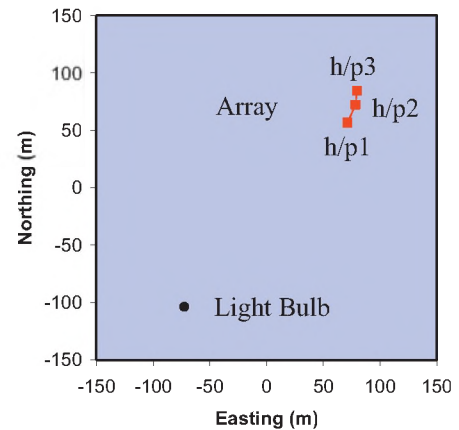


Fig. 3 The light bulb localization setup in the Bay of Fundy.

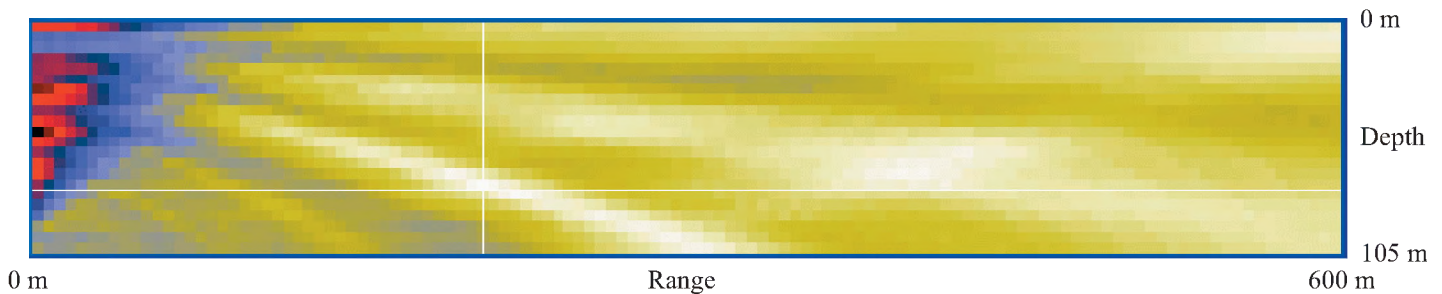


Fig. 4 The ambiguity surface at 225°T. The white cross hairs are at a range and depth of 205 m and 75 m, respectively.

Although it was clear that the range and depth of the right whales could not be estimated with the MCP algorithm in the Bay of Fundy environment, an attempt was made to track the whales in bearing. The results are shown in the bearing vs. time plot of Fig. 5. The algorithm successfully localized the right whales to bearings between 143 and 170°T over a one-hour time period. Because the variation of the bearing with time was small, it was concluded the whales were well outside the 600-m range of the MCP system. In fact, these localized bearings are in the general direction of an area some 10 to 15 km away that is known historically to have the highest concentration of right whales at this time of year.

4. DISCUSSION

The concept of a MCP localization system for right whales was presented. Using light bulbs as simulated right whale gunshots, the technique was shown to work extremely well out to a range of about six water depths in an environment that has sufficient bottom reflections. Even over softer sea beds with little or no reflections, it was demonstrated that the right whales could still be tracked in bearing.

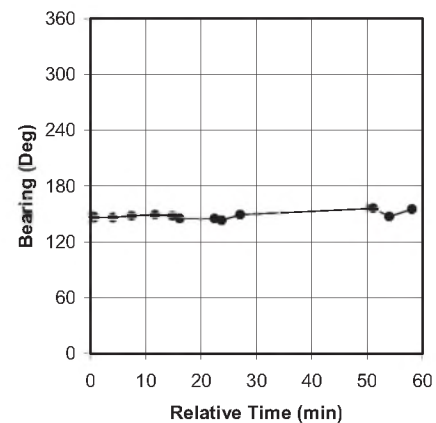


Fig. 5. Estimated whale bearings in the Bay of Fundy.

REFERENCES

- [1] Matthews, M.R., Ebbeson, G.R., Heard, G.J., and Desharnais, F. (2005) "Broadband Target Localization in Very Shallow Water," DRDC Atlantic TM 2004-178.
- [2] Tolstoy, A. (1993) *Matched Field Processing in Underwater Acoustics*, World Scientific, Singapore.
- [3] Dosso, S.E., *et al.* (1998) "Array element localization for horizontal arrays via Occam's inversion," *J. Acoust. Soc. Am.* **104** (2), 846–859.

UTILITY OF ACOUSTIC LOCATION TECHNOLOGY FOR STUDYING AVIAN DAWN CHORUSES: SOCIAL DYNAMICS OF MALE BLACK-CAPPED CHICKADEES

Jennifer Foote¹, Daniel Mennill², and Laurene Ratcliffe¹

¹Dept. of Biology, Queen's University, Ontario, Canada, K7L 3N6 footej@biology.queensu.ca; ratcliff@biology.queensu.ca

²Dept. of Biological Sciences, University of Windsor, Ontario, Canada, N9B 3P4 dmennill@uwindsor.ca

1. INTRODUCTION

Beginning before sunrise, males of many songbird species participate in a distinct chorus characterized by high song rates and simultaneous singing by all males. Despite widespread occurrence, the function of chorusing is not well understood. Adjustment of social relationships among territorial neighbours by interactive communication has been proposed to be the most likely function of chorusing (Staicer et al. 1996). The social dynamics hypothesis predicts that social relationships among males will be reflected in their dawn chorusing interactions.

Recently developed acoustic location systems (ALS or microphone arrays) can be used to locate singers in space and time and monitor the content of vocal interactions of multiple individuals (McGregor et al. 1996). Prior to ALSs, it was difficult to record multiple individuals in the field and as a result, the social dynamics hypothesis has remained largely untested. We used a 16 microphone ALS to simultaneously record dawn choruses in four areas up to 160,000m². Because a considerable amount of song and background noise occurs during the dawn chorus, we tested whether black-capped chickadee (*Poecile atricapillus*) choruses could be reconstructed from multi-channel ALS recordings. If choruses are successfully reconstructed then acoustic location can be used to examine content and function of male dawn choruses.

2. METHOD

2.1 Field Methods

We monitored an individually colour-marked population of black-capped chickadees at Queen's University Biology Station near Chaffey's Locks, Ontario (44°34'N, 76°19'W) from January – June 2005. We tabulated pairwise dominance interactions at feeding stations in order to determine each bird's position in its winter flock hierarchy as described by Otter et al. (1993).

Once birds began defending individual territories in early spring we monitored territory boundaries and nesting stages of pairs. From 3-8 May we recorded the dawn chorus in four different regions of continuous chickadee habitat using a 16 microphone ALS. Microphones were placed ≥ 50 m apart throughout male territories where topography and

vegetation were suitable and were connected to a central computer using 2200m of cable. A multi-channel data acquisition card was used to digitize microphone input. While recording, three observers walked through the recorded area describing male positions and identifications. GPS coordinates of microphones and nests were taken using a Trimble GPS system.

2.2 Recording Analysis and Localization

We used Syrinx PC (John Burt, Seattle, Washington) to browse the 16 channel recordings. Using the time and frequency cursors we selected all songs of all males recorded during the chorus. We then used MATLAB (Mathworks Inc, Natick, MA) to localize every 20th song of each male. When a song was overlapped by song of another chickadee or species, the previous/next closest non-overlapped song was located instead. As black-capped chickadees do not move often at dawn (Otter and Ratcliffe 1993) this sampling effort is sufficient to determine all male positions during the chorus. When males made large movements, additional locations were estimated to determine the path of movement. For a detailed description of the MATLAB cross-correlation and location estimate components of the localization process, as well as accuracy of this system, see Mennill et al. (2006). The end of each dawn chorus was defined as the point when the second last male stopped singing and only one male remained.

3. RESULTS

The four arrays recorded complete dawn choruses for 26 males (Table 1). One male was on the edge of two arrays and was recorded twice.

Table 1. Duration and content of 4 chickadee dawn choruses recorded in array configurations 1-4 in 2005

Array	1	2	3	4
Date	3 May	4 May	7 May	8 May
Duration (min)	41	51	54	50
# of males	6	5	10	6
# of songs	2723	2893	4859	2821
# of localizations	177	189	324	223

All songs could be assigned to a territorial male based on location; locations matched those described while recording. Therefore, the time and location of each song in the dawn chorus of these males was successfully extracted from the multi-channel recordings. Chorus end time varied from 41-54 minutes after the first song of the morning. Fig. 1 shows the dawn chorus positions of 2 neighbouring males during the first 30 minutes after the chorus began.

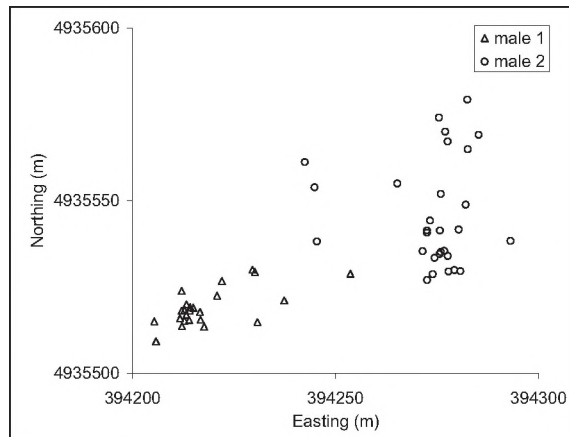


Fig. 1. Positions of 2 males in a 100m X 100m area during the first 30 minutes of the dawn chorus. Male locations are represented by symbols.

4. DISCUSSION

We used acoustic location to simultaneously record 5-10 male chickadees during each dawn chorus. Despite the quantity of sound recorded during dawn choruses, songs of males could be successfully localized to known male singing areas. This technology will be particularly useful for determining if male songbirds are: 1) involved in intra-sexual countersinging interactions at dawn as predicted by the social dynamics hypothesis; or 2) singing individually, for example, for mate advertisement purposes (Staicer et al. 1996), as inferred from close proximity to female nests (Otter et al. 1993). Acoustic location systems are unique because they allow analysis of real-time dawn chorusing interactions, which were previously difficult to study. Using ALS, Burt and Vehrencamp (2005) found that in a tropical species (*Thryothorus pleurostictus*), males song-type match at dawn. We predict that temperate passerines interact in similar ways during the dawn chorus.

Black-capped chickadees present an ideal species with which to investigate the social dynamics hypothesis as they have been well-studied with respect to winter flock and dominance behaviours. Both daytime singing interactions and individual dawn choruses have also been characterized. Once breeding territories are established, pairs are frequently involved in boundary disputes (Smith 1991). Thus status-related signalling differences are probably detectable in naturally occurring vocal-interactions of territory holders.

Black-capped chickadees can vary the frequency at which they sing their single song type continuously within an 860 Hz range (Horn et al. 1992). Frequency matching is used in daytime interaction (Mennill and Ratcliffe 2004) and would, therefore, be a good interaction measure to look for during the dawn chorus. From our ALS recordings we will determine if males interact at dawn using frequency matching and whether interactions reflect male social dynamics. Now that chorus songs have been localized and males have been identified, the frequency of all songs recorded can be measured using SYRINX. Because the ALS records time of each song, songs of neighbouring male can be compared to determine if they frequency match and how frequently matching occurs. We hope that this analysis will contribute to a greater understanding of the function of avian dawn choruses.

REFERENCES

- Burt, J.M. and Vehrencamp, S.L. (2005). Dawn chorus as an interactive communication network. In *Animal Communication Networks*, ed. P. McGregor. Cambridge, Cambridge University Press, pp. 320-343.
- Horn, A.G., Leonard, M.L., Ratcliffe, L., Shackleton, S.A. and Weisman, R.G. (1992). Frequency variation in songs of black-capped chickadees (*Parus atricapillus*). *Auk*, 109, 847-852.
- McGregor, P.K. and Dabelsteen, T. (1996). Communication networks. In *Ecology and Evolution of Acoustic Communication in Birds*, ed. D.E. Kroodsma and E.H. Miller. Ithaca, NY, Cornell University Press, pp. 409-425.
- Mennill, D.J., Burt, J.M., Fristrup, K.M. and Vehrencamp, S.L. (2006). Accuracy of an acoustic location system for monitoring the position of duetting tropical songbirds. *Journal of the Acoustical Society of America*, in press.
- Mennill, D.J. and Ratcliffe, L.M. (2004). Overlapping and matching in the song contests of black-capped chickadees. *Animal Behaviour*, 67, 441-450.
- Otter, K. and Ratcliffe, L. (1993). Changes in singing behavior of male black-capped chickadees (*Parus atricapillus*) following mate removal. *Behavioral Ecology and Sociobiology*, 33, 409-414.
- Smith, S.M. (1991). *The Black-capped Chickadee: Behavioral Ecology and Natural History*. Ithaca, Cornell University Press.
- Staicer, C.A., Spector, D.A. and Horn, A.G. (1996). The dawn chorus and other diel patterns in acoustic signaling. In *Ecology and Evolution of Acoustic Communication in Birds*, ed. D.E. Kroodsma and E.H. Miller. Ithaca, Cornell University Press, pp. 426-453.

ACKNOWLEDGEMENTS

We thank L. Reed, R. Bull, D. Potvin, A. McKellar, M. Stapleton, J. Baldock and S. Doucet for field assistance; Queen's University Biology Station for logistical support; the Curtis, Lundell, Toohey, Warren, Weatherhead-Metz and Zink families for access to property. Funding was provided by the American Museum of Natural History, the American Ornithologists' Union, the Society of Canadian Ornithologists, and from the Natural Sciences and Engineering Research Council of Canada (NSERC) and Canadian Foundation for Innovation (CFI).

DESIGN AND TESTING OF A THERMOACOUSTIC SYSTEM FOR THERMAL MANAGEMENT

Masoud Akhavanbazar¹, M. H. Kamran Siddiqui², and Rama B. Bhat³

¹mas_akhavan@yahoo.com, ²siddiqui@encs.concordia.ca, ³rbhat@encs.concordia.ca

Dept of Mechanical and Industrial Engineering, Concordia University, Montreal, Quebec, Canada

1. INTRODUCTION

The thermoacoustic phenomenon was known more than a century ago, but the principle was not exploited in a significant way until two decades ago when Greg Swift and his research group at the Los Alamos National Laboratory developed different types of thermoacoustic refrigerators and heat engines [1]. Even after two decades of research by his group and a few other groups across North America and Europe, the development of such devices is still at preliminary stages. Garret et al. [2] developed a spacecraft cryocooler, using resonant intense sound waves in pressurized inert gases in a resonator to pump heat. This cryocooler was used in the space shuttle Discovery. Tijani et al. [3] were able to obtain temperature as low as -65°C in their device. Using this device, they studied the effect of some thermoacoustic parameters, such as the Prandtl number and the spacing of stack plates. Bailliet et al. [4] measured the acoustic power in the resonator of a thermoacoustic refrigerator using Laser Doppler Anemometry (LDA) along with sound pressure level measurements with microphones. They observed good agreement between the experimental and theoretical results. A thermoacoustic engine was used by Jin et al. [5] to drive a thermoacoustic refrigerator. The device established an impressive temperature difference of approximately 120 K across the stack.

Although efficiencies of existing thermoacoustic refrigerators are lower than their conventional counterparts, efficiency comparable to vapor-compression refrigerators have been predicted theoretically [6]. The thermoacoustic devices have many advantages over conventional refrigerators. No environmentally hazardous refrigerants are required in thermoacoustic devices. They use air or other inert gases and thus, they do not have any harmful effect on the environment. In addition, these devices are simple in design and have no moving parts. Thus, they are more reliable and have low fabrication cost.

In the present paper, a simple thermoacoustic device is designed and tested to study the thermal gradient established at the two ends of its stack. The results are presented and discussed.

2. THERMOACOUSTIC PHENOMENON

A thermoacoustic device consists of an acoustic resonator (tube) containing a working fluid, that can be air

or an inert gas. The resonator is driven by an exciter such as a speaker or an electrodynamic exciter to generate a standing acoustic wave inside the resonator. The length of the acoustic resonator is typically set equal to half the wavelength of the standing acoustic wave [6]. A stack of thin parallel plates are installed towards one end inside the resonator. The gas parcels inside the resonator experience displacement and temperature oscillations along with the pressure variations. When such oscillations in the gas occur close to a solid surface, such as a stack of closely spaced parallel plates, heat can be transferred to or from the surface. The gas parcels transfer heat from the end of the stack that is close to the pressure node to the other end of the stack, creating a temperature gradient across the two ends of the stack. Swift [6] gives detailed explanation of the thermoacoustic process. If heat exchangers are attached at both ends of the stack then the heat is transferred from the fluid of the cold-end heat exchanger to the stack and by the thermoacoustic process, this heat is delivered to the hot-end of the stack from where it is transferred to the fluid of the hot-end heat exchanger. Thus, the heat is pumped from a cold medium to a hot medium and the device works as a refrigerator.

3. FABRICATION OF THE DEVICE AND EXPERIMENTAL SETUP

A simple thermoacoustic device was designed, fabricated and tested in the laboratory [7]. An acrylic tube of length 0.385 m corresponding to half the wavelength of the acoustic wave at 450 Hz was used as the resonator tube. The internal diameter of the tube was 6.3 cm and wall thickness was 6 mm. A schematic of the device is shown in Fig. 1. A 15 watt, 8 Ω , electrodynamic-type loudspeaker was used as the acoustic driver. The loudspeaker was driven by a function generator at a frequency of 450 Hz. A power amplifier was used to provide the required acoustic power to excite the working fluid inside the resonator.

Air at the atmospheric pressure was used as a working fluid. The optimum length of the stack and the spacing between the stack plates was determined through a theoretical analysis [7]. The length of the stack was set equal to 3 cm. The stack was made of 0.13 mm thick Mylar sheet. Fishing line spacers (0.36 mm thick) glued onto the surface of the sheet provided the spacing between the sheets. The Mylar sheet was wound around a 4 mm PVC-rod to obtain a spiral

stack [3]. Thermocouples were used to simultaneously measure the temperature at both ends of the stack. The accuracy of the thermocouple was ± 0.1 °C.

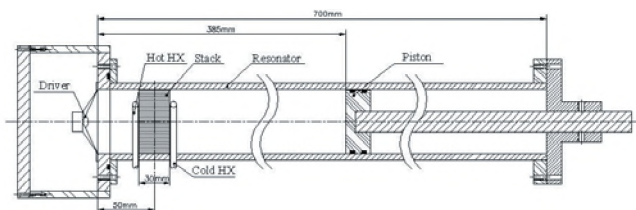


Fig. 1: Schematic of the fabricated thermoacoustic refrigerator.

4. RESULTS

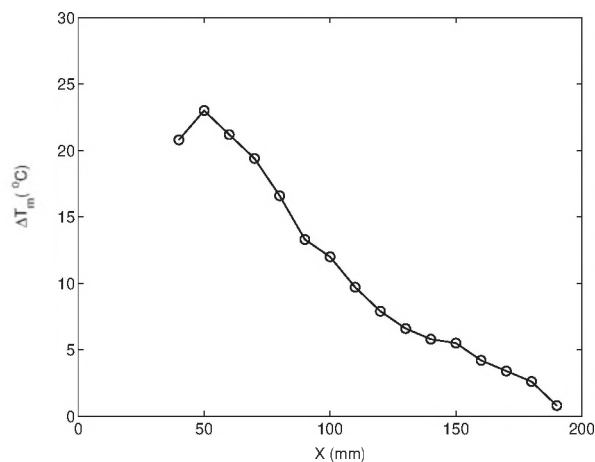
The position of the stack inside the resonator is crucial for the optimum performance of the thermoacoustic refrigerator. The position of stack (X_s) inside the resonator tube was changed from 40 mm to 190 mm from the driver-end of the resonator, with 10 mm increments. The temperature difference across both sides of the stack, ΔT_m , was measured at each stack position. The data was sampled for 350 s at each stack position at a sampling rate of 100 Hz. The values of ΔT_m are plotted in Fig. 2, against the stack position. The plot shows that the temperature difference across the stack is minimum (approximately 1 °C) when the stack was placed at the center of the resonator (i.e. at 190 mm from the resonator end). As the stack was shifted towards the pressure antinode, ΔT_m increased from 1 °C to 23 °C up to $X_s = 5$ cm. As the stack was shifted further towards the pressure antinode (i.e. $X_s < 5$ cm), a decrease in ΔT_m is observed. Thus, the results indicate that the optimal stack position of the stack is 5 cm. The optimum position of the stack obtained experimentally is in agreement with that predicted theoretically [7].

REFERENCES

1. Swift, G.W. (1995) Thermoacoustic engines and refrigerators. *Physics Today*, 48 (7), 22-28.
2. Garrett, S.L., Adef, J.A., and Hofler, T.J. (1993) Thermoacoustic refrigerator for space applications. *J. Thermophysics Heat Transfer*, 7 (4), 595-599.
3. Tijani, M.E.H., Zeegers, J.C.H., and De Waele, A.T.A.M. (2002) Construction and performance of a thermoacoustic refrigerator. *Cryogenics*, 42 (1), 59-65.
4. Bailliet, H., Lotton, P., Bruneau, M., Gusev, V., Valiere, J.C., and Gazengel, B. (2000) Acoustic Power Flow Measurement in a thermoacoustic resonator by means of Laser Doppler Anemometry (L.D.A.) and microphonic measurement. *J. Applied Acoustics*, 60, 1-11.

5. Jin, T., Chen, G.B., Wang, B.R., and Zhang, S.Y. (2003) Application of Thermoacoustic Effect to Refrigeration. *Review of Scientific Instruments*, 74 (1), 677-679.
6. Swift G. W. (2002) *Thermoacoustics. The Acoustical Society of America*, Melville, NY.
7. Akhavanbazz, M. (2004) Design, Analysis, Testing and Development of a Thermoacoustic System for Refrigerator Applications. M.A.Sc. thesis, Department of Mechanical and Industrial Engineering, Concordia University, Montreal, Canada.

Fig. 2: Temperature difference across the stack (ΔT_m) versus the mid-stack position. The mid-stack position is measured from the speaker-end of the resonator.



ACKNOWLEDGEMENTS

This research was funded by the grants from the Natural Sciences and Engineering Research Council of Canada to Kamran Siddiqui and Rama Bhat.

REVIEW OF COMPUTATIONAL AEROACOUSTICS FOR APPLICATION IN ELECTRONICS COOLER NOISE

Jeff Defoe¹ and Colin Novak

Dept. of Mechanical, Automotive and Materials Engineering, University of Windsor, 401 Sunset Ave.; Windsor, Ontario, Canada, N9B 3P4 ¹Corresponding author: defoe2@uwindsor.ca

1. INTRODUCTION

The acoustic performance of heat sink and fan combination cooling systems is important for computer manufacturers, in addition to thermal performance. These systems are usually tested experimentally, which can be very costly and time-consuming. In many applications, computational fluid dynamics (CFD) has replaced or supplemented experimental methods in order to shorten design and testing times and to reduce costs. In order to use CFD for acoustics, very detailed simulations are required because of the differences in scales between the flow and acoustic phenomena. Only recently has computational aeroacoustics (CAA) begun to penetrate into design strategies in applications, like electronics cooling, where acoustic performance matters. Numerical simulation of the flow inside and around heat sinks and fans can lead to a prediction of the emitted noise while they are still in the design phase. Research in determining the required level of detail in modeling the flow is ongoing.

2. COMPUTATIONAL AEROACOUSTICS

Computational aeroacoustics encompasses all numerical methods where the purpose is to predict the noise emissions from a simulated flow. There are four main methods: direct, acoustic analogy, vortex/boundary element methods (BEM), and broadband methods [1, 2, 3, 4].

Direct CAA is theoretically the best way to predict flow-based acoustic phenomena numerically, but is also the most costly and difficult to use. This method does not use any models; the idea is to simulate both bulk flow and acoustic phenomena everywhere from the source to the receiver. This is very computationally expensive due to the large differences in scales between acoustic and flow phenomena [1]. Computational resources are the most significant limitation to the use of direct CAA [1]. Extremely fine meshes and time steps are necessary, and the resolutions required are proportional to the highest frequency to be simulated. Given this, direct CAA is typically used only for low-frequency sound prediction [5]. A CFD solver such as Fluent [6] can be used to obtain the acoustic data. Despite the high cost of direct CAA, some studies [7] have been

undertaken which use it for higher frequency phenomena.

Less computationally demanding alternatives to direct CAA are acoustic analogy methods [1]. These are typically based on Lighthill's theory [8, 9]. These methods work only when the propagation of the noise is towards free space [1]. Also, it is critical that the acoustic wave propagation does not influence the flow [8], as acoustic analogy methods separate the production and propagation of noise. The latter is analytically predicted using the wave equation [10]. Two prominent formulations of the theory are Kirchhoff's and Ffowcs-Williams and Hawkings' (FW-H) [11, 12, 13]. The Kirchhoff formulation is based on the wave equation and thus must be used only in linear regions of the flow [13]. The FW-H formulation also accounts for aerodynamic noise generated by moving surfaces [14]. Extensions of this method allow the surfaces to be arbitrary. Another method available is to compute the flow field solution and source terms using CFD and then export that data to an external program, such as SysNoise or ACTRAN/LA [1, 15]. ACTRAN/LA overcomes the free-space limitation, but is also more computationally demanding [15].

The boundary element method (BEM) offers low computational cost at the expense of some detail in the information provided. This method does not use a computational grid [3], but instead uses vortex-surface calculations to determine tonal noise.

Broadband methods offer the lowest computational effort of any CAA method [1]. These are the only methods which can use a steady CFD solution in order to determine noise levels. The disadvantage of broadband methods is that only the overall sound power level of a source can be predicted, and not with great accuracy [1]. This can be useful for quickly comparing several designs in order to determine the quietest of several alternatives [6].

3. COMPUTER COOLING SOLUTIONS

Axial fans are commonly used to increase the airflow and thus the heat transfer over heat sinks within computer cases. They are relatively quiet and inexpensive. Rotating blades cause tonal dipole noise, while turbulent intake and wakes cause broadband quadrupole noise [3].

Rotor-stator interactions can also cause dipole sound [10].

Recently, radial fans have begun appearing in computer cooling applications. They have higher air-moving potential, but this comes at the expense of greater noise emissions. Tonal noise can be more dominant with radial fans than it is for axial fans [16]. Some full 3D, unsteady CFD studies of radial fans have been performed [17].

The core of the vast majority of heat-dissipation systems in computers is the heat sink. Most CFD of heat sink flows has focused on thermal performance [18, 19]. Noise predictions are also important for these flows, however, as the channel exits create jets which are sources of quadrupole noise. Few studies exist that have attempted to use CFD for noise predictions from heat sink flows.

4. PREDICTION METHODS

In [16], the vortex surface or boundary element method is used to predict the noise generation of a centrifugal fan. This prediction method gives only the tonal components of the noise [16]. This method is also used in [3], where both axial and radial fans are considered. The direct CAA method was used to predict the acoustic emissions of a shrouded fan in [7].

In the modeling of heat sinks, thermal performance has been the focus rather than acoustics. The level of detail required in modeling in order to obtain accurate thermal predictions is examined in [18], but the results do not apply to acoustic predictions, which require greater levels of detail than flow predictions. Another study [19] goes even further and uses a porous block modeling techniques for heat sinks, which is completely inappropriate for noise prediction.

5. CONCLUSIONS REGARDING FUTURE RESEARCH

If the overall acoustic performance of fan and heat sink cooling solutions is to be predicted accurately, the simulations must be combined so that both components are present, in order to capture interaction effects. Acoustic analogy methods seem to be the best compromise of accuracy and computational cost. Very detailed source simulations in the fan and heat sink region coupled with the use of analogy methods could result in excellent simulation results with a reasonable computational effort.

REFERENCES

1. *Fluent 6.2 User's Guide* (Chapter 21), Fluent Inc., January 11, 2005.
2. Lewy, S., "Overview on Fan Noise Prediction," *Kolloquium für Fluid- und Thermodynamik*, June 20, 2002.
3. Lee, D.-J., Jeon, W.-H. and Chung, K.-H., "Development and Application of Fan Noise Prediction Method to Axial and Centrifugal Fan," *Proceedings of ASME FEDSM'02*, Montreal, July 2002.
4. Powell, A., "Theory of Vortex Sound," *Journal of the Acoustical Society of America*, Vol. 26, No. 1, 177-195, January 1964.
5. An, C.-F., "Survey of CFD Studies on Automotive Buffeting," *13th Annual Conference of the CFD Society of Canada*, St. John's, NL, August 1, 2005, 223-230.
6. "Fluent 6.2: The World's Best CFD Code Just Got Faster!," <http://www.fluent.com/software/flent/fluent62.htm>, February 2, 2006.
7. Park, J., "A Sound Method for Fan Modeling," *Fluent News*, Summer 2005.
8. Lighthill, M. J., "On Sound Generated Aerodynamically, I: General Theory," *Proc. of the Royal Soc. of London, Series A, Mathematical and Physical Sciences*, Vol. 211, No. 1107 (Mar. 20, 1952), pp. 564-587.
9. Lighthill, M. J., "On Sound Generated Aerodynamically, II: Turbulence as a Source of Sound," *Proc. of the Royal Soc. of London, Series A, Mathematical and Physical Sciences*, Vol. 222, No. 1148 (Feb. 23, 1954), pp. 1-32.
10. Maaloum, A., Kouidri, S., Rey, R., "Aeroacoustic performance evaluation of axial flow fans based on the unsteady pressure field on the blade surface," *Applied Acoustics* 65 (2004) pp. 367-384.
11. Pilon, A. R. and Lyrantzis, A. S., "Integral Methods for Computational Aeroacoustics," *AIAA paper 97-0020*, January 1997 (AIAA Meeting Papers – AIAA, Aerospace Sciences Meeting & Exhibit, 35th, Reno, NV, Jan. 6-9, 1997).
12. Lyrantzis, A. S., "Surface integral methods in computational aeroacoustics – From the (CFD) near-field to the (Acoustic) far-field," *Aeroacoustics*, vol. 2, num. 2, 2003, pp. 95-128.
13. Brentner, K. S. and Farassat, F., "An Analytical Comparison of the Acoustic Analogy and Kirchhoff Formulations for Moving Surfaces," *American Helicopter Society 53rd Annual Forum*, Virginia Beach, Virginia, April 29 – May 1, 1997.
14. Ffowcs Williams, J. and Hawkings, D., "Sound Generation by Turbulence and Surfaces in Arbitrary Motion," *Phil. Transactions of the Royal Society of London, Series A, Mathematical and Physical Sciences*, Vol. 264, No. 1151 (May 8, 1969), pp. 321-342.
15. Caro, S. et. al, "Identification of the Appropriate Parameters for Accurate CAA," *11th AIAA/CEAS Aeroacoustics Conference*, May 2005, Monterey, CA.
16. Jeon, W.-H., "A Numerical Study on the Effects of Design Parameters on the Performance and Noise of a Centrifugal Fan," *Journal of Sound and Vibration*, Vol. 265 221-230, 2003.
17. Velarde-Suarez, S. et. al, "Numerical Prediction of the Aerodynamic Tonal Noise in a Centrifugal Fan," *Proceedings of ASME FEDSM'02*, Montreal, July 2002.
18. Linton, R. and Agonafer, D., "Coarse and Detailed CFD Modeling of a Finned Heat Sink," *1994 InterSociety Conference on Thermal Phenomena*, IEEE, 156-161.
19. Narasimhan, S., Bar-Cohen, A. and Nair, R., "Flow and Pressure Field Characteristics in the Porous Block Compact Modeling of Parallel Plate Heat Sinks," *IEEE Transactions on Components and Packaging Technologies*, Vol. 26, No. 1 147-157, March 2003.

GRAPHICS PROCESSING UNIT COOLING SOLUTIONS: ACOUSTIC CHARACTERISTICS

Matt Nantais¹, Colin Novak, Jeff Defoe

Department of Mechanical, Automotive and Materials Engineering, University of Windsor, 401 Sunset Ave.; Windsor, Ontario, Canada, N9B 3P4. ¹Corresponding author: matt.nantais@gmail.com

1. INTRODUCTION

The utilization of the graphics processing unit (GPU) has evolved from supporting interactive games and complex engineering design applications in personal computers to console gaming and home entertainment systems. The functions of a GPU require a great deal of processing power and a major setback of the advancement of this technology is the production of greater amounts of heat. This is a trend that will continue in the foreseeable future. Currently, GPU cards are produced with dedicated active cooling solutions in order to alleviate this concern. These consist of a metal heat sink with an attached fan that represents a new source of noise within the computer. This research involved testing three commercially available GPUs for their acoustic emission characteristics. It will be shown how the acoustic characteristics of the overall system change as a result of changing the GPU.

2. EXPERIMENTAL SETUP

All tests were performed using identical configurations of the software and system hardware. The hardware used for this project consisted of the following components.

Table 1: Hardware Components

CPU	AMD Athlon 64 X2 3800+ Dual Core S939
Motherboard	ASUS A8R-MVP ATX
HDD	Western Digital Caviar SE16 250 GB SATA2 7200 RPM 16 MB
Memory	OCZ Performance PC3200 2GB DDR400
Power Supply	OCZ PowerStream 520W
Optical Drive	Pioneer DVR-111D DVD+DL
Additional Cooling	Generic 120mm Rear Case Fan

All three cards were operated under the conditions of a graphics benchmarking program called 3DMark 2005. The tests were performed in a semi-anechoic environment. The computer case was positioned on the hard floor in the centre of a ten point measurement hemisphere. Measurements were made at each of the ten microphone

locations in accordance with the International Standards ISO 3745:2003 [1] for performing measurements in a hemi-anechoic room, and ISO 7779 [2] for performing measurements of airborne noise emitted by information and technology equipment. For each case, the system was allowed to run until thermal stability occurred. Then data was acquired using analysis software made by 01dB called dB-RTA. Acoustic metrics including loudness were measured.

3. EXPERIMENTS PERFORMED

The screen resolution was 1280x1024 pixels. Three experiments were performed: GPU in-system running 3DMark 2005; GPU in-system running Microsoft Windows OS.; and GPU stand-alone running at 12 volts DC. Acquiring data at all ten microphone locations around the computer compensated directionality characteristics associated with the noise source. Frequency spectrum data was also acquired. In this work, the results from the measurements taken for each GPU tested are analysed and compared.

4. RESULTS AND DISCUSSION

Table 2 shows the revolutions per minute of the cooling fans for each of the GPUs. These results were obtained using a photo tachometer and reflective tape adhered to one particular fan blade.

Table 2: RPM Data

	Fan 1	Fan 2	Fan 3
3V	1595	1325	N/A
4V	2705	1845	1765
5V	3550	2270	2265
6V	4190	2632	2735
7V	4685	2950	3175
8V	5100	3270	3585
9V	5455	3500	3960
10V	5780	3735	4035
11V	6070	3930	4370
12V	6320	4105	4680

Table 3: Fan Characteristics

	Fan 1	Fan 2	Fan 3
Type of Fan	Axial	Axial	Radial
Number of Blades	13	13	29

Some observations may be made based on this RPM data. Fan 1 has a significantly greater angular velocity compared to fan 2 at similar voltage levels. Both fans have 13 blades, however, fan 2 is larger in diameter. These results may be due to the presence of similar electric motors in both cooling solutions. It is expected that the acoustic emissions from fan 2 will be more acceptable than those from fan 1. Fan 3 is designed to produce a much greater air flow rate than the other fans. It is a much heavier fan than the others and thus its electric motor cannot overcome the momentum of the fan with the starting voltage of 3V. Initially, the rpm values of fan 3 are less than that of fan 2. At 6V however, the rpm values surpass those of fan 2. The values never exceed those for fan 1.

For the measurements taken, all ten microphone signals are kept as data and not combined to derive any overall sound quality metrics. Although it may be useful to combine the data some time in the future, there is no reason to do so now. It should be noted that microphone 1 is located at the back of the computer case and so it should be expected that the most useful GPU cooling fan information would be detected there. One of the most useful pieces of information that may be gathered from these measurements is sound pressure level versus frequency spectrum data. For microphone 1, the prominent frequency and loudness data is given in the following table.

Table 4: Prominent Frequency and Loudness Data

Fan Number and Test	Prominent Frequency (Hz)	Loudness (sones)
Fan 1 – 3DMark 2005	1374	5.77
Fan 1 – Windows	1374	4.22
Fan 1 – Stand - Alone	1374	3.41
Fan 2 – 3DMark 2005	433, 866	3.39
Fan 2 – Windows	433, 866	3.19
Fan 2 – Stand - Alone	866	3.70
Fan 3 – 3DMark 2005	1456, 1542	4.23
Fan 3 – Windows	433, 866, 1542	3.25
Fan 3 – Stand - Alone	687, 1029, 1374	7.12

The results for fan 1 make logical sense as the blade passing frequency of the fan at 12V is nearly equal to 1374 Hz. Similarly, for fan 2, the blade passing frequency is approximately equal to 866 Hz. The appearance of the 433 Hz prominent tone is unknown and somewhat peculiar as it is exactly half of the blade passing frequency. The results for fan 3 are very different from the other two. There are several prominent frequencies in the spectrum which may be the result of the flow of air exiting from the cooling fan duct. The primary difference between this fan and the first two is how it is designed to cool the GPU, and how it

removes the warm air. In the case of fans 1 and 2, warm air remains in the computer case where it circulates with the air being drawn in by the front case fan. Fan 3 however brings in air from within the case, cools the GPU, and then blows the warm air out through the rear of the case. This style of cooling solution acts as like an exhaust for the computer case, ensuring that warm air is not re-circulated in the interior of the case. The frequency results may simply be a result of unusual aeroacoustic interactions of the jet of air at the back of the case. Further testing and analysis is needed to explain the source of the unusual prominent frequencies in fan 3.

In the previous table, loudness results were shown. Loudness is a psychoacoustic metric developed by Zwicker and Fastl which aims to quantify how loud a sound is perceived to be in comparison to a standard sound [3]. Thus, the higher the value of loudness, the more undesirable a sound is. Its calculation is described in the International Standard ISO 532B [4].

As may be seen in each of the three cases, the loudness value is less when the system is idle as opposed to when the software application is running. This is intuitive since the cooling fan does not need to remove as much excess heat. In the case of fan 1, the loudness for the stand-alone test is less than for the in-system tests. This makes sense because the fan is operating at its 12V speed. It is clear however that fan 3 is not operating at its 12V speed during the in-system tests performed as its loudness has a much higher value during the stand-alone test.

CONCLUSIONS

These results show that it is not merely the size or cooling requirements of the fan that determines the loudness of a corresponding sound. The fans' rotational velocity as well as the design of the entire cooling solution are important variables also. If the complexity of the cooling solution increases, so does the inherent noise generation mechanism.

REFERENCES

1. ISO 3745, "Acoustics – Determination of sound power levels of noise sources using sound pressure – Precision methods for anechoic and hemi-anechoic rooms," International Standards Organization (ISO), 2003.
2. ISO 7779, "Measurement of Airborne Noise Emitted by Information Technology and Telecommunications Equipment," ISO, 1999.
3. Zwicker, E. and Fastl, H., *Psychoacoustics: Facts and Models* (2nd Ed.), 1999, Berlin, Germany : Springer.
4. ISO 532B, "Acoustics – Method for calculating loudness level," ISO, 1975.

THE EFFECT OF VARYING HEAT SINK FIN DISTANCES FROM COOLING FAN BLADE TIP ON NOISE EMISSIONS

Helen Ule, Colin Novak, Robert Gaspar

Dept. of Mechanical, Automotive and Materials Engineering, University of Windsor, 401 Sunset Ave.; Windsor, Ontario

INTRODUCTION

The challenge to deliver performance improvements in computer graphic cards has surpassed the ability of finned, passive, cooling devices to dissipate the heat generated by next generation graphics processing units (GPU). The dissipation rates required by these latest GPU designs can only be delivered by more complicated thermal management systems which often require forced air cooling of finned heat sinks. The concurrent challenge to the industry is to provide this cooling while minimizing the noise generated by these cooling fans. One of the fundamental mechanisms for the generation of fan noise is the dynamic force fluctuations on the fan blade and how these fluctuations interact with fixed irregularities such as adjacent cooling fins. This study investigates the effect on the acoustic emissions resulting from the variation of the distance between the fan blade tips and the heat sink fins.

COOLING FAN NOISE

The generation of cooling fan noise is usually attributed to two fundamental source mechanisms. Both of these are sources of dynamic force variations between the surface of the fan blade and the immediate surrounding air.

The first of these is random generated noise produced at the fan inlet. If the inlet flow is turbulent, a force results which is dependant on the influence of the lifting force to the angle of attack. Acoustic models which predict the generated sound power of this force can be readily found in aeroacoustic literature. The resulting amplitude of this random noise generation is directly dependant on the level of inlet turbulence. As such, the inlet path must be kept as unobstructed as possible to minimize the creation of any turbulence.

The second source of noise generation is caused by spatially fixed irregularities which can produce a wake in either the inlet or outlet flow. In the case of computer cooling solutions, these irregularities can be the result of either the presence of heat sink fins or an improperly designed shroud. The resulting dynamic forces can contribute to strong tones which are usually found at the blade passage frequency.

To lessen the impact of these mechanisms of noise generation, one can either modify the blades of the fan or lessen the impact of the irregularities on the flow. For this study, the affect of the distance between the fan blade tips and the heat sink fins has on the acoustic emissions is experimentally investigated.

NOISE MEASUREMENTS

For this investigation, the emitted sound pressure level (SPL) at a distance of 0.5 metres as well as the radiated sound power level was determined. While A-weighted SPL is the traditional analytical approach and serves well to quantify the amplitude of acoustic emissions, it offers no insight to the perceived quality of the sound produced by the graphic card cooling fans. Given this, the acoustic product evaluation of computer graphic card cooling noise should include sound quality or psychoacoustic analysis. Therefore, in order to truly determine the full acoustic impact that an active cooling solution will have on the end user, the measurement of the applicable psychoacoustic metrics is warranted.

For this investigation, measurements of loudness will be presented. While somewhat similar to the A-weighting scale discussed above, loudness is a more detailed representation of how loud a source is perceived. It also includes compensation for the effect of temporal processing and audiological masking effects of sounds across the frequency range. Also determined in this study is prominent tone (PR). This psychoacoustic metric gives an objective measure of the prominence of a tonal component of a measured sound. The prominent tone is defined as the ratio of the power of the critical (frequency) band centred on the tone under investigation to the mean power of the two adjacent critical bands. For this investigation, only the presence of prominence will be indicated.

In order to investigate the affect of varying distance between the 53 mm diameter fan and the sink fins, a movable fin design was devised. This fin module, which was radiused to the contour of the impeller, was designed to be positioned at six different distances from the tip of the fan blades. The distances used were 1mm, 4mm, 7mm, 10mm, 13mm and 16mm. The fan was operated at each of the six distances at three different speeds.

RESULTS AND DISCUSSION

Figure 1 illustrates the measured sound pressure level results of each fan-fin distance for each of the three measured speeds. An obvious pattern exists for each of the speeds. The sound pressure level is greatest for the 1mm and 4mm spacing between the fan tip and cooling fin. However, after the spacing is increased to 7 mm, the sound pressure level exhibits a rapid decline where it remains somewhat constant for subsequent spacings of 7mm, 10mm and 13mm for this fan. For the 16mm distance between the fan and fin

another rapid decline in sound pressure level is realized. Inspection of Figures 2 and 3 for sound power level and Loudness respectively show very similar trends in the measured data.

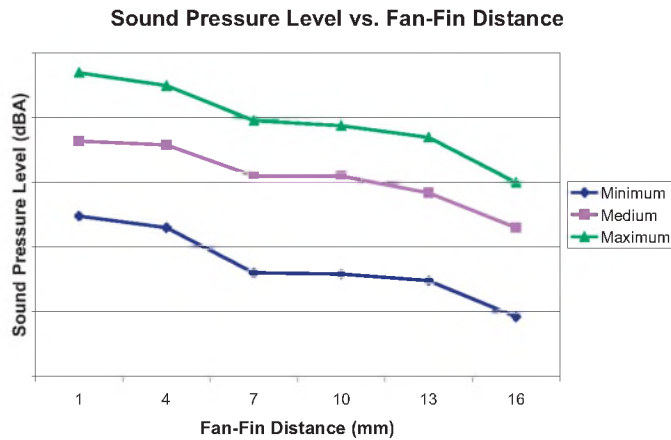


Figure 1: Graph of Measured Sound Pressure Level versus Distance from Fan tip to Cooling Fin for 3 Fan Speeds

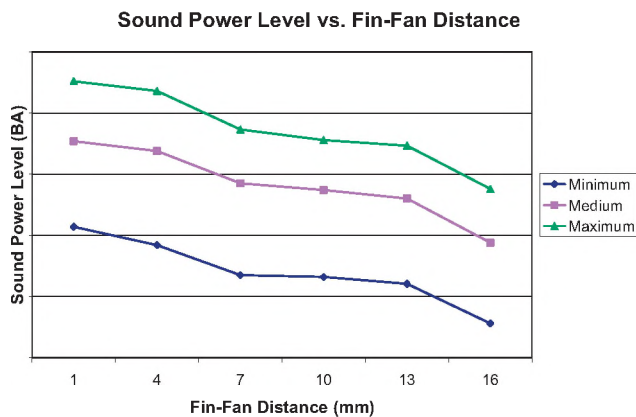


Figure 2: Graph of Calculated Sound Power Level versus Distance from Fan tip to Cooling Fin for 3 Fan Speeds

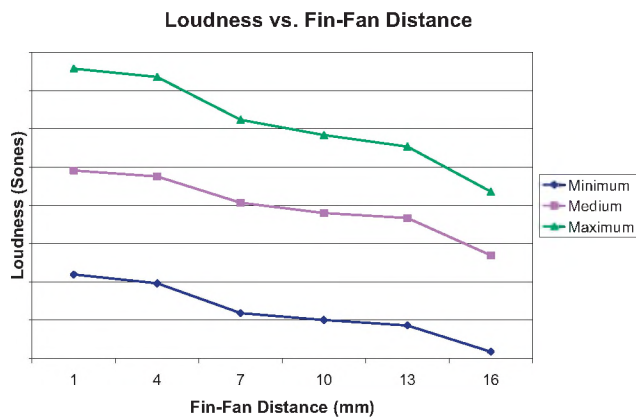


Figure 3: Graph of Calculated Loudness versus Distance from Fan tip to Cooling Fin for 3 Fan Speeds

For very close clearance spacing between the blade tip and cooling fin, it appears that a prominent mechanism of noise generation is present. Due to flow straightening affects of the long fins, it is safe to assume that the flow at the immediate exit would not be highly turbulent. The noise generation would then be surmised to be the result of the presence of the spatially fixed irregularities in the very close proximity of the blade tips. This is reinforced by the presence of prominent tones at the two closest distances as is shown in Table 1. It should also be noted that the type of noise generation demonstrated here can at times also be controlled by other means including redesign of the fan blade curvature or cross sectional profile. The latter of these two is more effective for larger diameter fans.

Table 1: Presence of Prominent Tone (Yes/No)

Distance (mm)	Minimum	Medium	Maximum
1	Yes	Yes	Yes
4	Yes	Yes	Yes
7	No	Yes	No
10	No	Yes	Yes
13	No	No	No
16	No	No	No

For the distances of 7 mm, 10 mm and 13 mm, an obvious reduction in noise emission is observed. Further, it is seen that the changes in noise level caused by the change in spacing are not very different from each other. It is suggested that the noise is created by a combination of both noise generation mechanisms. Inspection of Table 1 demonstrates a continued presence of prominent tones at the 7 mm and 10 mm distances. Therefore, the interaction of the cooling fins with the dynamic forces at the blade tips is still present. It should also be noted that, as the distance is increased, the flow straightening affect of the cooling fins is lessened. In other words, there is an increase in noise generation due to an increasing level of turbulence. Once the cooling fins have been located at a distance of 15 mm from the fan, another drop in acoustic emissions is realized.

SUMMARY AND CONCLUSIONS

Through the use of acoustic measurement and analysis techniques, it has been demonstrated that the generation and presence of acoustic emissions is the result of the two mechanisms of noise generation discussed. From the presented results, it has been shown that a fine balancing act is necessary to minimize the noise emissions caused by these two mechanisms. While it is obvious that a decrease in sound level is realized with increasing distance between the cooling fins and fan blades, a definitive decision of optimum distance can not be made in the absence of consideration of the required thermal performance of the heat removal system. Instead, careful design of the fan rotor and shroud used for flow directionality shroud be given great design importance.

COMPARITIVE STUDY OF NOISE AND VIBRATION MEASUREMENTS OF COMPUTER COOLING FANS

Colin Novak, Helen Ule, Robert Gaspar

Dept. of Mechanical, Automotive and Materials Engineering, University of Windsor, 401 Sunset Ave.; Windsor, Ontario, Canada, N9B 3P4, novak1@uwindsor.ca

INTRODUCTION

Due to consumer demands in the computer industry, video processor chips have become more powerful with a resulting requirement to dissipate ever increasing amounts of heat. As such, the performance requirements of cooling fans have been increasingly taxed to deliver higher flow rates. To accomplish this, large fans of various designs are used at relatively high rotational speeds. This, however, often results in structural resonance due to dynamic imbalances of the fan rotor. With larger fans are larger fan housings which often have higher acoustic radiation efficiencies resulting in a 'speaker effect' which can amplify the fan vibration into audible noise. This study investigates the relationship between measured vibration levels of several cooling fan heat sink designs to experimentally determine acoustic emission levels. Specifically, an attempt to correlate the realized acceleration levels to both sound power and sound pressure levels was sought. It was found that a correlation of overall noise and vibration levels was possible. Further, an even more obvious comparison was realized with the examination of one third octave frequency spectra of the two metrics. A discussion of vibration reduction measures is also included.

VIBRO-ACOUSTICS

The structure of a computer heat sink shroud can be modelled to represent a pulsating structure which displaces air from one side while drawing it in on the other. This is referred to as an acoustical dipole. The force required to move the shroud is related to the mass of the shroud itself as well as the added mass due to the reaction with the air. The sound radiation is representative of the force that is required to accelerate the added mass of the air.

Two mechanisms of excitation exist which can result in vibro-acoustic radiation. One is simple mechanical excitation from the movement of the fan. Sources can include the motor which can input mechanical energy into the system as can also the effects of a bad bearing or an unbalanced fan. The later is amongst the most common source of mechanical energy input. The second mechanism is the result of turbulence created by the passage of the fan blades that cause the air flow. When turbulence impinges on a body, a force is also exerted by the fluctuating components of the flow on the body and vice versa. This reaction force can also produce sound in the air.

VIBRATION MEASUREMENTS

For this investigation, vibration measurements of four fan sink designs were taken using a very small accelerometer placed at five locations on the heat-sink shroud at various operating speeds. A very low mass accelerometer is essential so as to not mass load the measured structure and by doing so, change it's mechanical properties. For this investigation, a sensor with a mass of 0.5 grams was used.

Using this procedure, un-weighted acceleration values (m/s^2) were recorded and further converted to un-weighted acceleration levels using the following equation with a reference value of $1.0e-5 m/s^2$.

$$L_a (dB) = 20 \times \log_{10}(a/1.0e-5)$$

Also presented are the 1/3 octave band data for the measured vibrations across the frequency range of 0 to 1000 Hz.

NOISE MEASUREMENTS

In addition to the vibration measurements, acoustic emissions of the computer cooling applications were also measured under the same operating conditions. To quantify the acoustic emissions of the fans, the emitted A-weighted sound pressure level at a distance of 0.5 meters was measured. All acoustic measurements were conducted in a semi-anechoic room and in accordance to the standards of ECMA-74, ISO 7779 and ISO 3744.

RESULTS AND DISCUSSION

Figures 1, 2 and 3 illustrate the frequency spectra of the vibration acceleration, noise levels and vibration level for each of the four designs operating at the maximum speed.

Inspection of the vibration frequency spectra clearly show the locations of the fundamental and corresponding harmonics for each design. The reason for the non-corresponding locations for most of these peaks is that the maximum speed for each design operates at different RPMs. There are, however, harmonic similarities between the third and fourth designs which are in fact also operate similarly. Design 3 though does exhibit greater harmonic energy at the lower frequencies and design 4 at the higher frequencies. This is more clearly illustrated in the graph of acceleration versus frequency given in Figure 3.

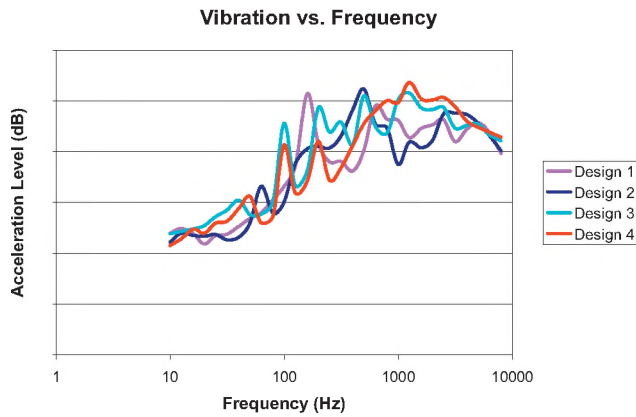


Figure 1: Graph of Frequency spectrum of Measured Vibration Level for Four Fan Designs

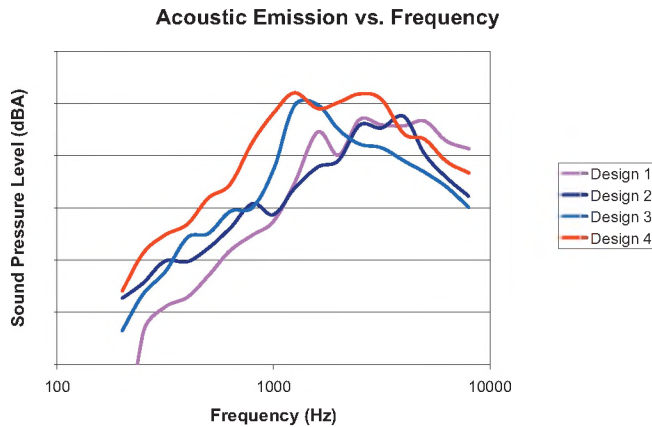


Figure 2: Graph of Frequency spectrum of Measured Acoustic Emission for Four Fan Designs

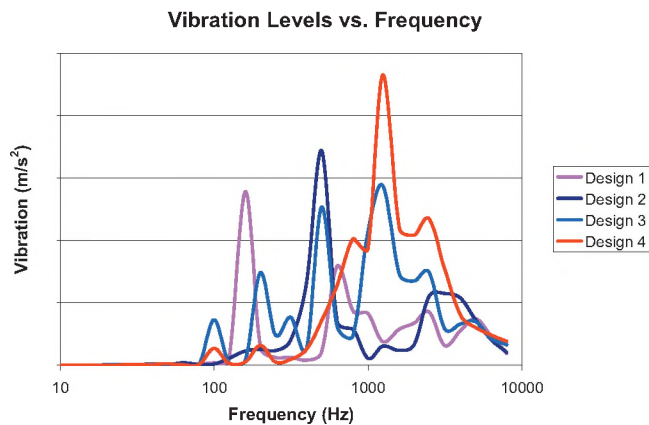


Figure 3: Graph of Frequency vs. Acceleration for Four Fan Designs

Inspection of the acoustic frequency plots in Figure 2 demonstrate much less defined responses with a clear lacking of predominate harmonics. This is indicative of the additional acoustic energy that is present in these measurements that can not be detected with a vibration sensor. Specifically, this spectra also includes the affect of flow noise mechanisms which would ‘fill in the gaps’ present in the vibration spectra and thus making meaningful correlation between the two difficult.

CONCLUSIONS

Several mechanisms for the generation of acoustic emissions exist which plague the designers of active cooling systems for state of the art video graphic cards. The fundamental noise generation is the result of aeroacoustic noise derived from the flow through the cooling system. The secondary noise source is structure borne noise from shell vibration. This vibration can be the result of either mechanical sources such as an unbalanced fan or flow induced from the presence of turbulent flow.

Four cooling designs were experimentally investigated for both noise and vibration. While useful information was derived from all of the measurement methods, a direct correlation between the noise and vibration data was difficult to obtain. This is due to the fact that the vibration measurements can predict the noise contribution from the vibrating sources only. The noise measurement data showed the resulting noise from not only the vibrating sources, but also from any aeroacoustic generated noise. It should also be remembered that it is these flow induced noise sources that contribute most to the overall noise levels.

The vibration results did give some insight into some of the design properties. It was found that the designs which incorporated aluminum shrouds produced the greatest overall vibration levels when compared to the plastic directional shrouds.

In order to reduce the affects of vibration induced noise, several design criteria should be followed. Fans should be well balanced and of good mechanical design to avoid the creation of resonance into the structure. Air directional shrouds should be small as possible to minimize the acoustic radiation efficiency and made of materials that exhibit good damping properties. Care should also be taken to ensure that all locations of mounting are also appropriately isolated. This eliminates the transference of any mechanical energy to or from the computer chassis where it can be further amplified.

AUTOMATED DETECTION OF WHITE WHALE (*DELPHINAPTERUS LEUCAS*) VOCALIZATIONS IN ST. LAWRENCE ESTUARY AND OCCURRENCE PATTERN

Bédard, Catherine¹ and Yvan Simard^{1,2}

¹Institut des sciences de la mer, Université du Québec à Rimouski, 310 allée des ursulines, Québec, Canada, G5L 3A1

²Institut Maurice-Lamontagne, 850 route de la mer, Mont-Joli, Québec, Canada, G5H 3Z4

1 INTRODUCTION

White whales (*Delphinapterus leucas*) are odontocete cetaceans that have a circumpolar distribution. The size of the St. Lawrence estuary population is currently estimated to 600-1000 animals and has been classed as threatened by COSEWIC¹ since 2004 (MPO, 2005). Detailed behavioural and habitat information on this white whale population is needed for improving their protection.

Conventional behavioural observations are usually made by visual observations from ships, airplanes or land observatories. The performance of these visual methods depends on many factors such as weather conditions, water transparency and ambient light intensity (Costa, 1993). Recent advances in passive acoustical monitoring techniques are being used for studying behaviour and habitat of vocalizing marine mammals. Such an approach can be used for monitoring several individuals in continue over long periods, independently of weather and light conditions, and without disturbing marine mammal's behaviour or affecting their environmental conditions (Erbe, 2000).

White whales are well known for their high degree of acoustic activity. Beluga's repertoire can be divided into three main categories : whistles, pulsed tones and clicks (Sjare and Smith, 1986; Faucher, 1988). All white whale vocalizations are very variable in time and frequency, and it is difficult to stereotype each of them for automatic detection.

Here, an automated method using a sequence of signal processing algorithms was developed to detect white whale calls, except clicks, under the loud shipping noise of the St. Lawrence estuary.

2 METHOD

Continuous recordings were collected from 5 to 11 September 2003 using a coastal hydrophone at a depth of 130 m in front of Cap-de-bon-Désir in Saguenay—St. Lawrence Marine Park (Québec, Canada). Records were bandpassed in the 0.5-5 kHz band, where the majority of the white whale's calls are emitted. White whales were simultaneously observed in daytime from a Belvedere at the study site.

Shipping noise was first removed using an adaptive spectral subtraction algorithm (Martin, 1994), which uses minimum statistics to identify the noise spectrum before subtracting it from the recordings. The remaining masking periods, due to close ships, were identified and considered as missing values in further processing. Then a threshold was applied to transform the spectrogram into a binary image on which residual noise was cleaned using two specific image filters. Each positive pixel of this final binary image was considered as a detection of a white whale's vocalization. The false detection rate was statistically estimated from visual validation of 3 % of the total recording period.

A vocalization rate index for each 30 minutes was estimated by the ratio (%) of detections over the total number of pixels on the binary image. Autocorrelation of the occurrence pattern, presence of circadian rhythms, and cross-correlations with wind speed, tide level and current velocity during the same period were analysed.

Finally, the main frequency band used by white whales on these recordings was determined.

3 RESULTS

The false detection rate due to residual noise was estimated to $7 \pm 4\%$. The vocalizations occurred during a short period (~ 1 s) and more than 80% of the silent periods lasted less than 10 s. The frequency band of the vocalizations was relatively stable over the seven days of sampling, but the vocalization rate was variable from day to day (Fig. 1). Call detections was higher on 5 and 11 September. The main frequency band used by white whales in these recordings was between 1.1 to 3.5 kHz.

Autocorrelation did not show any periodicity in the occurrence pattern. Daytime and nighttime calling during this short period did not show differences supporting any clear circadian rhythm. Low significant cross-correlations ($r = -0.2$, delay = 0.5 h) were computed between vocalization rate and wind speed, indicating that more detections occurred 0.5 hour after a low wind period. Low significant cross-correlations ($r < 0.3$) were also computed with tide level and along-channel current velocities, indicating that detection calls seemed to be higher 2.5-3.5 hours after high tide at the study site.

¹ COSEWIC : Committee on the Status of Endangered Wildlife in Canada

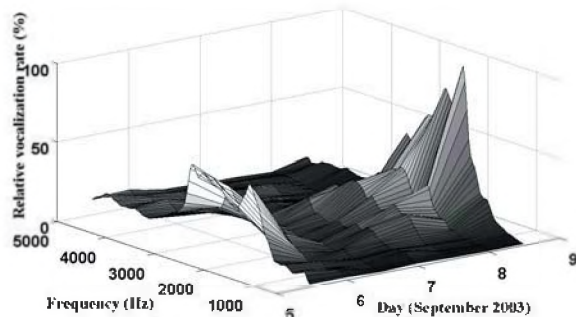


Fig. 1. White whale relative vocalization rate by frequency band [0,5-5] kHz from 5 to 11 September 2003; 0 = 2003-09-05 00 :00 :00 (HAE).

4 DISCUSSION

4.1 Automatic detection method

An automated detection method of white whale vocalizations was developed and tested on a 7-day sampling period. It allowed analysing their occurrence pattern over a continuous time-series for the first time.

This method can detect all the diverse white whale whistles and pulsed tones emerging in the signal after noise filtration. The detection was not based on stereotyped calls, which would be difficult for the loquacious beluga. Detections were associated to white whale calls because they largely dominate in this environment, from manually analyzed recordings and the land-based observations during the sampling period in the study area.

The performance of the method under the loud shipping noise of this environment was computed by the false detection rate estimated at 7 ± 4 %. The vocalization rate intensity of these false detections was however very low compared to that of the detected calls. Therefore the false detections did not strongly influence the call occurrence pattern.

This automated detection method could be worthwhile for analyzing long recordings using an objective and systematic approach, which would be difficult to do manually by an observer. On the other hand, a lot of parameters used in this method were manually adjusted according to regional noise context. It would be interesting to have them automatically adjusted for recordings from other environments.

4.2 Occurrence pattern

Although circadian rhythms in vocal behaviours have been shown for many marine mammals species (Au *et al.*, 2000; Stafford *et al.*, 2005; Ichikawa *et al.*, 2006), no apparent circadian rhythm was observed in this white whale call occurrence pattern.

The meaning of the low significant cross-correlation computed between the vocalizations rate and wind speed is unclear. White whales could have been less abundant in the area during strong wind periods, or they could then have been silent.

Significant cross-correlations between vocalization rate and tide level or current velocities indicated that high level of detection occurred a few hours after the flood upwelling period at the study site (Lavoie *et al.*, 2000). This observation could be due to the presence of concentrated capelin preys at this moment (Simard *et al.*, 2002). However, the correlation coefficients were low and white whale vocal detections were slightly influenced by these factors. A longer recording period and more investigation of the complex dynamics in this area of the St. Lawrence estuary are needed to understand the meaning of all these correlations.

4.3 Dominant frequency band

The main frequency band used by white whales in these recordings was slightly lower than that estimated by Lesage *et al.* (1999) about 65 km upstream (2.6-4.4 kHz). This could result from the sex segregation of the beluga in the Estuary during summer, whereas juveniles and adult white whales (females) are observed upstream, while males are found in our recording region (Michaud, 1993).

REFERENCES

- Au, W., J. Mobley, W. Burgess, M. Lammers & P. Nachtigalla. (2000). Seasonal and diurnal trends of chorusing humpback whales wintering in waters off Western Maui. *Mar. Mam. Sci.*, 16 (3), 530-544.
- Costa, D. (1993). The secret life of marine mammals : novel tools for studying their behavior and biology at sea. *Oceanography*, 6 (3), 120-128.
- Erbe, C. (2000). Census of marine mammals. New technologies for observing marine life. SCOR, W.G.118, Sidney, B.C. (Ca.), 9-11 Nov. (<http://pulson.seos.uvic.ca/meeting/scor2000/erbe/erbe.html>).
- Faucher, A. (1998). The vocal repertoire of the St. Lawrence estuary population of beluga whale (*Delphinapterus leucas*) and its behavioral, social and environmental contexts. MSc Thesis, Dalhousie University, Halifax. 102 p.
- Ichikawa, K., C. Tsutsumi & A. Nobuaki. (2006). Dugong (*Dugong dugon*) vocalization patterns recorded by automatic underwater sound monitoring systems. *J Acoust. Soc. Am.*, 119 (6), 3726-3733.
- Lavoie, D., Y. Simard & F. Saucier. (2000). Aggregation and dispersion of krill at channel heads and shelf edges : the dynamics in the Saguenay—St. Lawrence Marine Park. *Can. J. Fish. Aquat. Sci.* 57, 1853–1869.
- Lesage, V., M. Kingsley & B. Sjare. (1999). The effect of vessel noise on the vocal behavior of belugas in the St. Lawrence river estuary, Canada. *Mar. Mam. Sci.*, 15 (1), 65-84.
- Martin, R. (1994). Spectral subtraction based on minimum statistics. *Proc. Eur. Signal Processing Conf.*, 1182-1185.
- Michaud, R. 1993. Distribution estivale du béluga du Saint-Laurent ; synthèse 1986 à 1992. *Rapp. Tech. Can. Sci. Halieut. Aquat.* 1906. 23 p.
- MPO, (2005). Évaluation du potentiel de rétablissement des populations de bélugas de la baie Cumberland, de la baie d'Ungava, de l'est de la baie d'Hudson et du Saint-Laurent (*Delphinapterus leucas*). *Secr. can. de consult. sci. du MPO, Avis sci.* 2005/036.
- Simard, Y., D. Lavoie & F. Saucier. (2002). Channel head dynamics : capelin (*Mallotus villosus*) aggregation in the tidally driven upwelling system of the Saguenay-St. Lawrence Marine Park's whale feeding ground. *Can. J. Fish. Aquat. Sci.*, 59, 197-210.
- Sjare, B. & T. Smith. (1986). The vocal repertoire of white whale, *Delphinapterus leucas*, summering in Cunningham Inlet, Northwest Territories. *Can. J. Zool.*, 64, 407-415.
- Stafford, K., S. Moore & C. Fox. (2005). Diel variation in blue whale calls recorded in the eastern tropical Pacific. *Animal behaviour*, 69, 951-958.

THE EFFECT OF LOCALIZED SOUND LEAKS ON THE SPEECH PRIVACY OF CLOSED ROOMS

Bradford N. Gover and John S. Bradley

Institute for Research in Construction, National Research Council, 1200 Montreal Rd., Ottawa, Ontario K1A 0R6
brad.gover@nrc-cnrc.gc.ca

1. INTRODUCTION

Speech privacy is related to how difficult it is for a listener to hear or understand speech. For a closed room, conversations occurring within are to be private from listeners outside the room, in the adjoining spaces. The degree of audibility or intelligibility of the speech at the listening positions will depend on the sound insulation provided by the building. Near a localized area of reduced sound insulation (i.e., a sound leak), the speech sounds could be much more audible or intelligible. This paper reports results on the detectability and severity of several sound leaks intentionally introduced into a test wall.

2. SPEECH PRIVACY MEASUREMENT

At a listening position outside of a closed room, the speech privacy can be rated according to a new measurement procedure [1]. A uniform sound field is established inside the closed room using multiple source positions and a white noise test signal. The one-third-octave band levels within the room $L_S(f)$ (room-averaged) and at each spot listening position outside the room $L_R(f)$ are measured. These are used to determine the band level differences $LD(f) = L_S(f) - L_R(f)$. These level differences are an objective measure of the architectural sound insulation to each listening position. They are used to calculate the *Speech Privacy Index, SPI*, according to

$$SPI = \frac{1}{16} \sum_{f=160\text{Hz}}^{5\text{kHz}} [S(f) - LD(f) - N(f)] \quad (1)$$

where in each one-third-octave band centred at frequency f , $S(f)$ is the average speech level in the closed room, and $N(f)$ is the background noise level at the listening position. The *SPI* has been shown to be well correlated with responses of listeners in intelligibility tests [2]. The point at which 50% of listeners were able to understand at least one word from the test sentences is referred to as the *threshold of intelligibility*, and corresponds to an *SPI* value of -16 dB.

3. TEST WALL MEASUREMENTS

A test wall sample (2.44-by-3.66 m) was constructed between two reverberation rooms. The wall consisted of 2 layers of 16 mm drywall mounted on both sides of 90-by-33 mm lightweight steel studs (406 mm on centre). The cavities of the stud spaces were filled with 90

mm mineral fibre batts. From this base configuration, a 3.8 cm diameter sealed pipe was inserted through a 5.4 cm diameter hole in the wall, as shown in Fig. 1(a). The pipe was not touching the drywall, and the absorptive batts were not removed from the wall. After the wall was repaired, two standard 5-by-8 cm (6.5 cm deep) duplex electrical boxes were installed back-to-back, as shown in Fig. 1(b). The absorptive batts were not removed from the wall; the boxes compressed it between them.

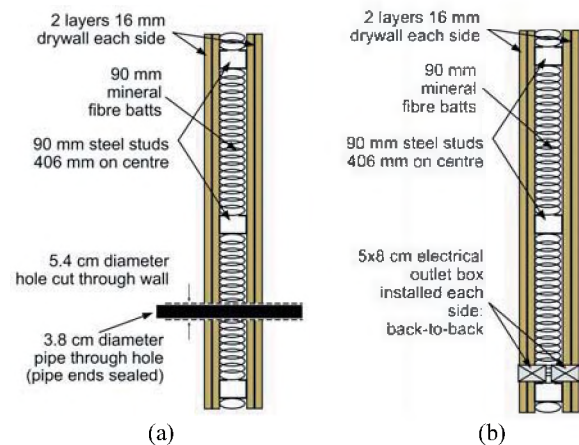


Fig. 1. Wall configurations: (a) sealed pipe passed through wall, (b) back-to-back electrical boxes.

For each wall configuration: 1.) A conventional ATSM E90 test was conducted to measure the transmission loss versus frequency, and determine the STC; and 2.) The speech privacy measurement procedure was used to obtain $LD(f)$ at each of 63 (a grid of 7-by-9, spaced 0.45-by-0.38 m) receiving positions 0.25 m from the test wall. At each position, *SPI* was calculated from Eq. (1) assuming a speech level of 65.7 dBA with a spectrum corresponding to a “Raised” effort, and a noise level of 31.5 dBA with a -5 dB/octave “neutral” spectrum [3], typical of HVAC noise.

The transmission loss versus frequency is shown in Fig. 2 for the base case of no intentional leaks (solid line with no markers, STC 56), the pipe through the wall (dashed line, STC 56), and for the back-to-back electrical boxes (solid line with square markers, STC 55). The pipe through the wall had a very small effect on the transmission loss, and no effect on the STC. The back-to-back electrical boxes caused a noticeable reduction of the transmission loss between 400 and 1600 Hz, but only resulted in a one point change of STC.

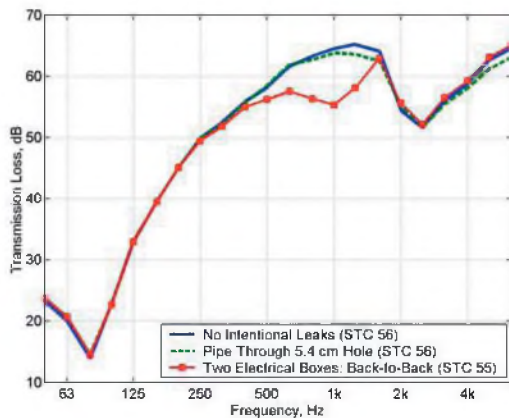


Fig. 2. Transmission loss versus frequency for: no intentional leaks (solid curve), pipe through wall (dashed curve), and back-to-back electrical boxes (solid curve with square markers).

The results of the new speech privacy measurement are shown in Fig. 3(a) for the base case of no intentional leaks. The grayscale plot indicates the value of *SPI* at locations 0.25 m from the wall. There are no features indicating any weak spots. The range (difference of maximum and minimum) of values was 1.2 dB, with a standard deviation of 0.3 dB. At all locations, *SPI* was less than -16 dB, indicating conditions below the threshold of intelligibility.

In Fig. 3(b) are the results for the case of the pipe through the wall. The range of values was 2.0 dB, with a standard deviation of 0.4 dB. At most locations, *SPI* was below -16 dB, except near the penetration. Only in the vicinity of the pipe were conditions above the threshold of intelligibility. The location of the maximum *SPI* accurately indicates the location of the defect (indicated by the black square).

In Fig. 3(c) are the results for the case of back-to-back electrical boxes. The range of values was 2.5 dB, with a standard deviation of 0.4 dB. At almost all locations, *SPI* was greater than -16 dB, corresponding to conditions above the threshold of intelligibility. The maximum value of *SPI* occurred at the location of the defect (indicated by the black square). The back-to-back electrical boxes degraded the speech privacy conditions near the wall at almost all locations, not just in their immediate vicinity.

4. CONCLUSIONS

The new speech privacy measurement procedure is capable of identifying the presence, location, and severity of localized sound leaks in a test wall. The results accurately indicate reduced speech privacy, depending on the severity of the penetration, even if the conventional transmission loss test does not reveal any problems.

REFERENCES

[1] J.S. Bradley and B.N. Gover, "Designing and Assessing the Architectural Speech Security of Meeting Rooms and Offices," IRC Research Report 187 (2006). <http://irc.nrc-cnrc.gc.ca/ircpubs/>

[2] B.N. Gover and J.S. Bradley, "Measures for assessing architectural speech security (privacy) of closed offices and meeting rooms," *J. Acoust. Soc. Am.*, **116**, 3480–3490 (2004).

[3] J.S. Bradley and B.N. Gover, "Speech and Noise Levels Associated with Meeting Rooms," IRC Research Report 170 (March 2004). <http://irc.nrc-cnrc.gc.ca/ircpubs/>

ACKNOWLEDGEMENTS

This work was jointly funded by Public Works and Government Services Canada (PWGSC), the Royal Canadian Mounted Police (RCMP), and the National Research Council (NRC).

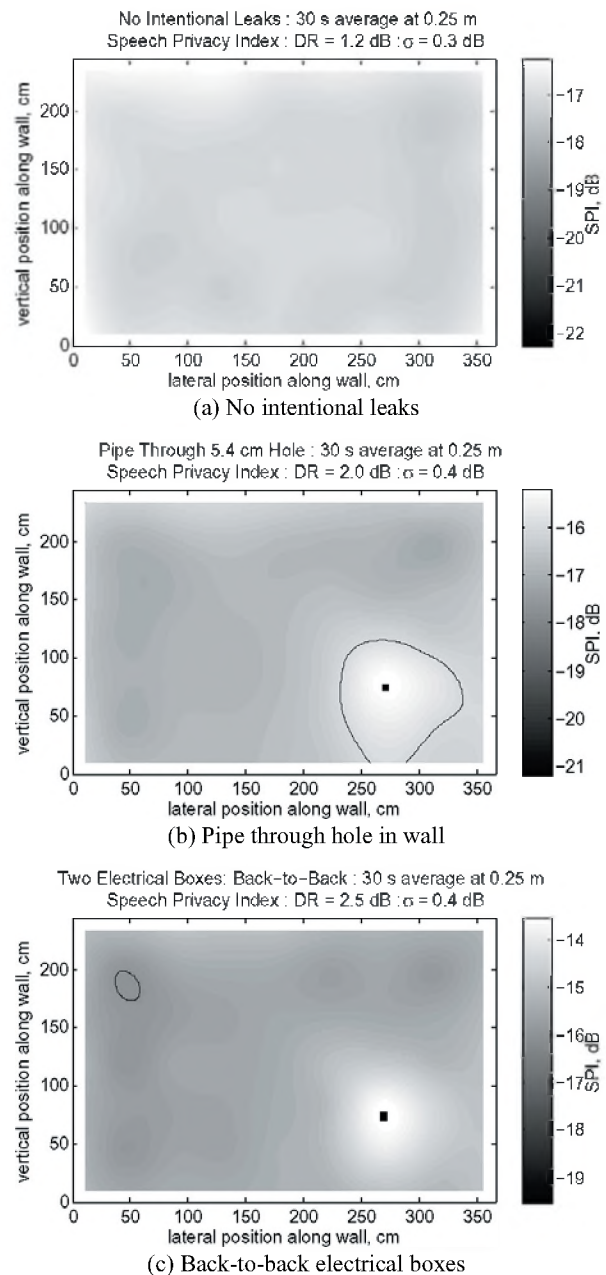


Fig. 3. *SPI* at 0.25 m from the wall, calculated for 65.7 dBA speech and 31.5 dBA noise. The contour is for -16 dB, which corresponds to the threshold of intelligibility. All plots self-normalized so that lightest grey corresponds to peak *SPI*.

DEVELOPING A GUIDE FOR FLANKING SOUND TRANSMISSION IN WOOD FRAMED CONSTRUCTION

J. David Quirt, Trevor R.T. Nightingale, Frances King

Inst. for Research in Construction, National Research Council, Ottawa, K1A 0R6, Canada

1. INTRODUCTION

This paper reports results from continuing studies of sound transmission between adjacent units in wood-framed multi-dwelling buildings. First, the paper presents some recent extensions of our multi-year experimental study, which has assessed how common construction details affect structure-borne (flanking) transmission between adjacent rooms, for a broad range of wall and floor constructions. Previous reports have focused on the wall and floor surfaces connected at the wall/floor junction - especially the floor surface, which is often the dominant problem. This paper includes a number of other paths that may collectively become significant when more obvious paths are controlled.

Estimates of the apparent sound isolation (in terms of Apparent STC) were obtained by summing the energy transmitted directly through the separating wall or floor assembly with that for all the flanking paths involving wall, floor, or ceiling surfaces abutting the separating assembly. These estimates provide the basis for a simplified design guide¹ to predict sound isolation in typical wood-framed row housing or apartment buildings. This paper presents a subset for airborne sources and horizontal transmission.

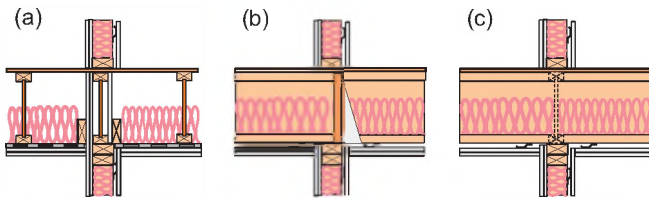


Figure 1: Construction details of the 3 wall/floor systems. Joists were oriented (a) parallel to the wall, (b) perpendicular to the wall, and (c) with joists continuous across the wall, perpendicular to it.

Results in this paper apply to wood-framed constructions, with the wall and floor assemblies shown in Figure 1, or variants on them. Construction specifications and architectural drawings are given in detail elsewhere. References to the pertinent technical standards, and procedures to determine the “**Direct** Sound Transmission Loss” (due to transmission through just the separating wall or floor assembly between two rooms) or the “**Apparent** Sound Transmission Loss” (either for individual paths involving specific surfaces in the two rooms, or the overall transmission for sound energy via all paths) are also given in Reference 2.

2. RESULTS AND DISCUSSION

As discussed in previous papers, sound isolation between two adjacent units in a wood-framed building typically involves significant transmission via several paths. Figure 2 compares direct sound transmission through the separating wall between two side-by-side apartments vs. the flanking transmission via the floor surfaces for the wall and floor assemblies illustrated in Figure 1. In this case, most of the sound is transmitted via the floors. There are other paths – such as via the ceiling or the abutting side walls – but they transmit much less than these dominant paths.

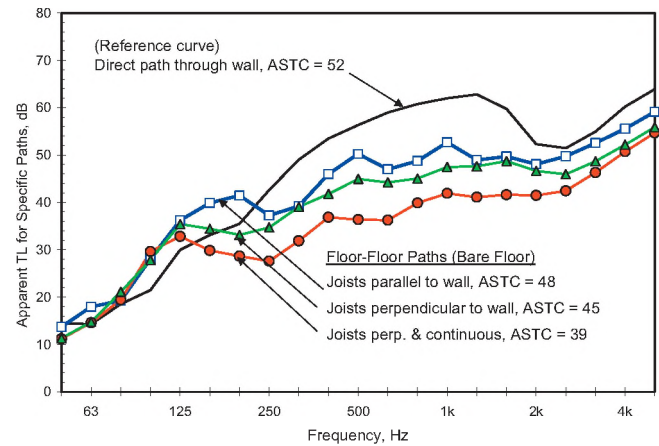


Figure 2: Apparent sound transmission loss (TL) via specific paths with bare OSB subfloor and basic separating wall, as in Figure 1.

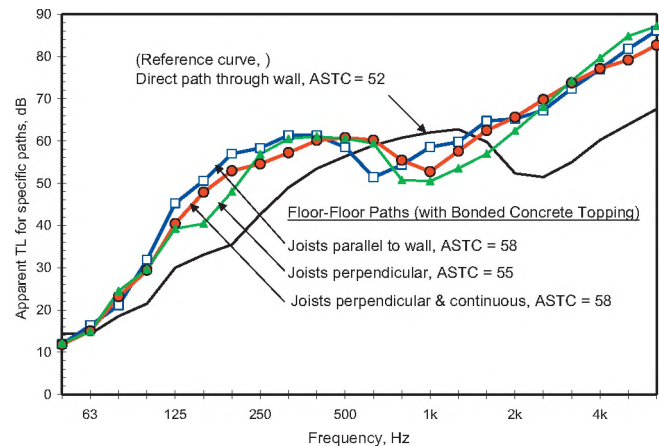


Figure 3: Apparent TL via specific paths with the same basic separating wall, and concrete topping over the OSB subfloor.

As shown in Figure 3, adding a topping over the subfloor increases the transmission loss of this path; other toppings would provide somewhat different improvements. This would increase the overall Apparent STC. In this case, other (weaker) paths become more significant; two obvious paths of concern involve the ceiling or the abutting walls.

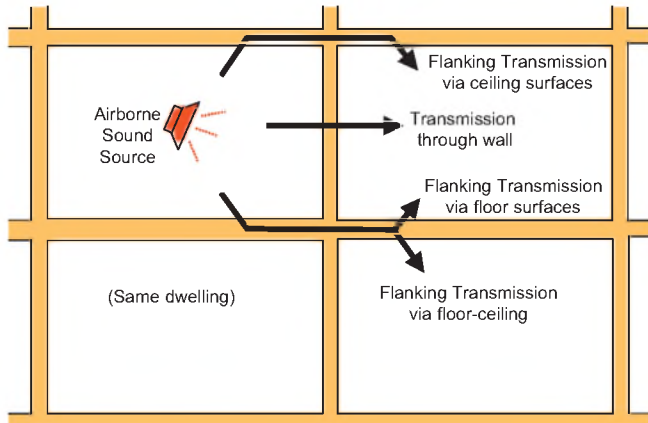


Figure 4: Transmission paths between adjacent units; the walls parallel to the plane of this figure (side walls) also transmit sound.

Figure 4 indicates some of the typical transmission paths between adjacent units. In apartments, the gypsum board ceiling is normally mounted on resilient channels (to give isolation from the apartment above), which reduces flanking transmission via this path to insignificance. But in row housing (where transmission between stories within a dwelling unit is not a concern) the ceiling would be fastened directly to the joists; then this flanking path also becomes significant (ASTC 52, as shown in Figure 5). Flanking via an abutting side wall transmits less sound (~ASTC 61 for one wall in the case tested) but this could also limit overall performance if the separating wall and the floor were improved, and would drop to ASTC 58 if there were two such walls. All paths should be considered for good design.

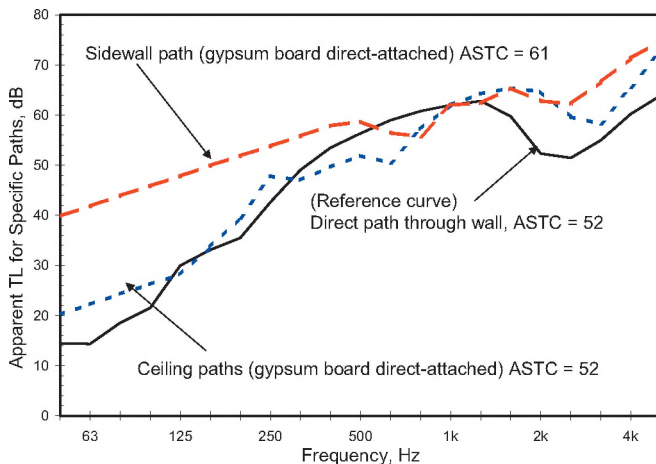


Figure 5: Estimates for flanking paths not via wall/floor junction.

In the Guide¹, tables present the combined effect of all paths for typical variants. The tables presented below are for the

case with joists perpendicular to separating walls - case (b) in Figure 1. Apparent STC in a given building will not exactly match these values, but the trends should apply.

Separating wall	Basic Wall (STC 52)		Better Wall (STC 57)	
	Direct or resilient		Direct	Resilient
Sidewall gypsum board			Direct	Resilient
Floor Surface	(Apparent-STC)			
No topping (basic)	43	43	43	43
19 mm OSB stapled to subfloor	48	50	50	50
25 mm gypsum concrete bonded to subfloor	49	51	52	52
38 mm gypsum concrete + resilient mat on subfloor	51	53	55	55

Table above is for “apartment design” (ceilings on resilient channels); that below is for “row house” (direct-attached).

Separating wall	Basic Wall (STC 52)		Better Wall (STC 57)	
	Direct or resilient		Direct	Resilient
Sidewall gypsum board			Direct	Resilient
Floor Surface	(Apparent-STC)			
No topping (basic subfloor)	42	43	43	43
19 mm OSB stapled to subfloor	47	48	49	49
25 mm gypsum concrete bonded to subfloor	48	49	50	50
38 mm gypsum concrete + resilient mat on subfloor	49	51	52	52

In all cases, the overall Apparent STC is lower than that for the separating wall – in some cases much lower. By altering design details to balance transmission via specific paths a cost-effective yet satisfactory design can be chosen.

3. SUMMARY AND REFERENCES

This paper provides a very terse overview of how experimental characterization of the direct and flanking sound transmission paths in wood-framed construction can lead to a manageable set of path transmission terms to represent the effect of specific design tradeoffs. By combining the energy transmitted via all paths it is possible to arrive at estimates of the Apparent STC for a range of constructions.

We wish to acknowledge the support of our industry partners: CMHC, Forintek Canada, Marriott International, Owens Corning, Trus Joist, and USG.

- 1 Quirt, J.D. Nightingale, T.R.T. King, F. Guide for Sound Insulation in Wood Frame Construction, **RR219**, IRC, NRC Canada, (2006)
- 2 Nightingale, T.R.T. Quirt, J.D., King F., Halliwell, R.E. Flanking Transmission in Multifamily Dwellings: Phase IV, **RR218**, NRC Canada, (2006).
(Note that the reports are available on the IRC website at <http://irc.nrc-cmrc.gc.ca/ircpubs/>.)

ON ESTIMATING SOUND POWER FROM A FEW SINGLE POINT MEASUREMENTS

Werner Richarz, Ph.D. P.Eng., FASA

Pinchin Environmental, 5749 Coopers Ave., Mississauga, ON, L4Z 1R5 wricharz@pinchin.com

1. Introduction

Even under controlled conditions the measurement of sound power emitted by a stationary source can present difficulties. In the field, these are often augmented by constraints that preclude measuring at a sufficiently large number of points. This note describes the nature of a sound field generated by a broad-band source located above a reflecting surface and discusses some of the implications regarding the estimation of sound power levels from a small number of field measurements.

2. Mathematical Model

A simple source radiating into an unbounded space, induces a spherically symmetric acoustic field about the centroid of the source: $p(r,t) = A/r g(t-r/c)$. In the far-field the flux of acoustic energy $\langle p^2 \rangle / \rho c$, when integrated over a sphere of radius r , recovers the sound power W . A^2 takes the value $\rho c W / 4\pi$ if $\langle g^2 \rangle = 1$. A reflecting plane h_s meters below the source confines all the acoustic energy to the 'upper half space'. This is equivalent to the field of a source and a 'mirror image' of identical strength (figure 1)

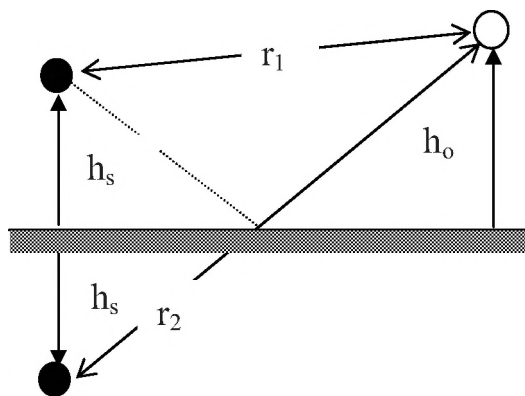


Figure 1. Simple source above a reflecting plane

The mean-square sound pressure is composed of three terms, two of which are contributions from the direct and reflected waves. The third term describes the interaction of the two wave fields:

$$\langle p^2(r) \rangle = A^2 [1/r_1^2 + 1/r_2^2 + 2 R_{gg}((r_2 - r_1)/c) / (r_1 r_2)] \quad [1]$$

The differential time delay in the argument of $R_{gg}(\tau)$ plays an important role, even though it frequently ignored. Many field measurements are performed with 1/3 octave band analyzers. The autocorrelation function of the

band-pass filtered signal can be approximated without a priori knowledge of the power spectral density (PSD) of the function $g(t)$, provided that there are no pure tones and that the PSD is smooth. The band-limited PSD is modeled with a series of unit steps $H(f)$:

$$\Phi_{gg}(f) = \Phi_o \{H(f+f_2) - H(f-f_2) - [H(f+f_1) - H(f-f_1)]\} \quad [2]$$

This idealized process differs little from real band-limited systems. It is well known that the power spectral density $\Phi_{gg}(f)$ and the autocorrelation $R_{gg}(\tau)$ are Fourier Transform pairs. The latter resembling a 'cosine burst' centered at $\tau = 0$:

$$R_{gg}(\tau) = \cos[\pi(f_2 + f_1)\tau] \frac{\sin \pi(f_2 - f_1)\tau}{\pi(f_2 - f_1)\tau} \quad [3]$$

For a 1/3 octave filter the 'corner frequencies' are defined by in terms of the centre frequency f_o : $f_2 = \alpha f_o$, $f_1 = f_o / \alpha$, where $\alpha = 2^{(1/6)}$. The typical response time-scale is $T \sim (f_2 - f_1)^{-1}$.

The broad-band nature of the noise does not preclude wave interference. Figure 2 illustrates the distribution of mean square pressure in the 500 Hz 1/3 octave band for a source 0.5 m above the reflecting plane.

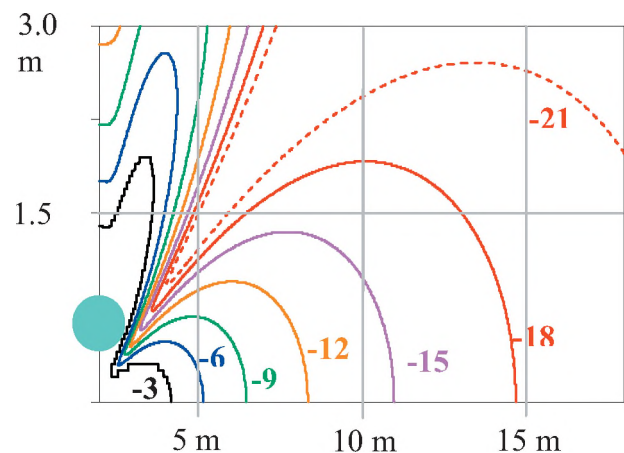


Figure 2 Isobars (in -3dB increments) for the 500 Hz 1/3 octave band levels from a 'broad-band source' located 0.5 m above reflecting plane

The sound field is rather more complex than the hemispherical spreading described by the ubiquitous formula:

$$\langle p^2(r) \rangle = 2A^2/r_1^2 \text{ or : SPL} = L_w - 10 \log(2\pi r_1) \quad [4]$$

3. Estimating Sound Power

It is common practise to ‘estimate’ sound power levels of sources by one or two ‘spot-checks’. The ratio of the estimated sound power [based on eq. 4] and the true sound power is

$$W_{est}/W_{act} = \{0.5[1+r_1^2/r_2^2] + (r_1/r_2)R_{gg}[(r_2-r_1)/c]\} \quad [5]$$

Whenever the auto-correlation function is negative, the estimated power is smaller than the actual power. Figure 3 illustrates this for a source height of 0.5 m and an observer height of 1.5 m. The 1/3 octave predictions have been converted to octave levels: changing the bandwidth does not eliminate the effect.

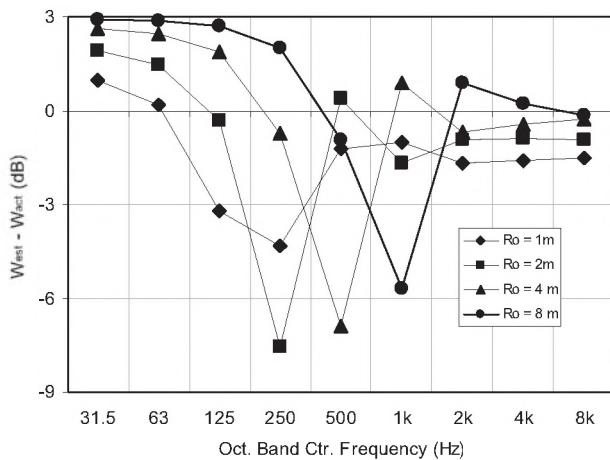


Figure 3 Deviation in sound power estimate (in octave bands) for a simple ‘broad-band’ source (500 Hz octave band), Ro =distance from the source

At low frequencies the sound power levels are over-estimated. This is because the relative phases of direct and reflected waves differ only by a small fraction of a wavelength. At high frequencies the relative error is small. For moderate source heights the worst-case errors occur in the mid-frequency range.

4. Estimating Sound Power using Measurements conforming to ISO 3744

When more measurement locations are included, one might expect these errors to diminish. The ISO 3744 standard prescribes measurements at selected field points. The hemispherical scheme, based on 10 field points is discussed here. It is found that the sound power estimates based on such measurements exhibit bias errors. These deviations arise irrespective of other ‘random errors’.

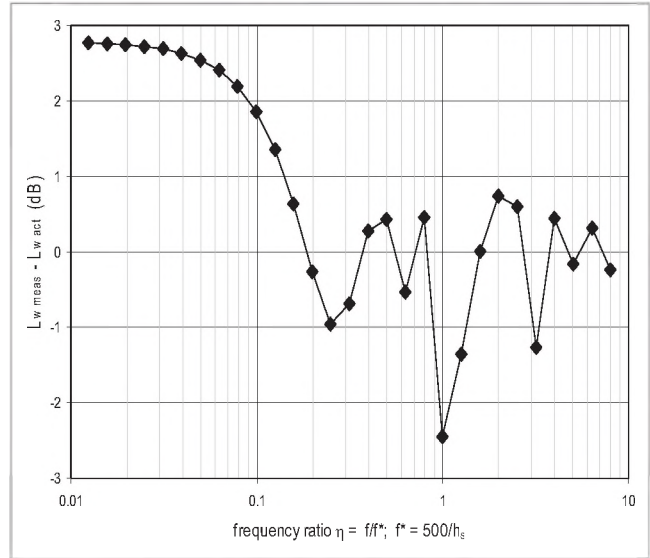


Figure 4 Bias errors for 1/3 octave sound power levels ‘measured’ according to ISO 3744

Whenever the radius of the (virtual) measurement surface is greater than $4h_s$, the bias error is self-similar in f/f^* ; $f^*=500/h_s$. Low frequencies have a positive bias: sound power levels are over-estimated. The bias is small for mid and high frequencies, with some bands showing bias errors of the order of 2 to 3 dB.

5. Summary

Certain features of sound pressure measurements over reflective ground have been examined for compact sources radiating ‘broad-band’ noise. The formalism uses the method of images and treats the measurement by 1/3 octave band filters in a realistic manner. Even though the sources are assumed to radiate broadband noise, wave effects cannot be ignored. The common 3 dB correction for hemispherical spreading leads to errors that are of the order of 6 dB at mid-frequencies (125 Hz to 1 kHz). Fortunately, these bias errors tend not impact estimates of A weighted sound power levels.

6. References

- Beranek, L.L.; Noise and Vibration Control, McGraw Hill, 1971
- Anon. Acoustics-Determination Of Sound Power Levels Of Noise Sources Using Sound Pressure—Engineering Method In An Essentially Free Field Over A Reflecting Plane ISO-3744:1994(E)

THE EFFECT OF ANCILLARY VOLUME ON SOUND TRANSMISSION MEASUREMENTS USING ASTM STANDARD TEST METHOD E336

Frances King, Trevor R.T. Nightingale

Institute for Research in Construction, National Research Council, Ottawa, Ontario, Canada K1A 0R6

1. INTRODUCTION

The ASTM Standard E336-05 provides methods to assess the airborne sound isolation between a source and receiving room. In certain field situations, the determination of what constitutes the source or receiving room and its volume may not be obvious. An example is a living room (principal volume) connected to a kitchen (ancillary volume) through an opening in the wall separating the two, and the party wall under test is a surface of the living room (principal volume). Some judgment may be required to define the volume and where the sound field of the "room" should be measured. The Standard requires that the ancillary volume be disregarded if the average sound pressure level in the ancillary volume is 6 or more decibels below the average level in the principal portion of the source or receiving room to which it is coupled at all measurement frequencies. Otherwise, the ancillary volume shall be included as part of the measurement space. This paper investigates the suitability of this criterion.

2. MEASUREMENTS AND RESULTS

The basic premise was the Apparent Transmission Loss (ATL) should be invariant of the coupled ancillary volume. Thus, the appropriate measurement procedure is the one that best approximates the (reference) ATL measured when there was no coupled ancillary volume. To evaluate this and arrive at the recommended measurement procedure, different field scenarios were simulated using the four-room Flanking Transmission Facility at the NRC/IRC. (See sketches of Figures 1-3). The volume of the rooms ranged from about 35 to 50 m³. In Figures 1-3 the ATL was computed for both directions between room pairs AC and BD using sound field measurements of the principal volume only. The wall between C and D (lower horizontally separated rooms) was systematically opened up from 0%, 8%, 17%, 36% to 100% to increase the coupling to the ancillary volume. Absorption was added to one of the lower rooms to simulate heavy furnishings.

Ancillary Volume Coupled to Source Room has only minimal effect on the ATL and this is largely independent of the size of the opening between the source and ancillary volumes. Although Figure 1 shows the case with an absorptive source room (worst case), similar results were observed when either ancillary or principal source volume

was highly absorptive (reverberation time, RT, ~ 0.4 s) or when both were not (RT > 1.0 s).

Ancillary Volume Coupled to Receiving Room will result in an overestimation of the ATL if receive room measurements are made only in the principal volume. The results shown in Figure 2 are typical of when both receive and coupled ancillary volumes are not highly absorptive. By comparing Figures 2 and 3, one can see the overestimation is greater when the principal volume is highly absorptive. It should be noted that effect is considerably less when the ancillary volume is highly absorptive relative to the receive room principal volume. For all cases considered the overestimation increased with opening size.

3. DISCUSSION AND CONCLUSIONS

The practical approach is to select the direction of measurement such that the ancillary volume, if present, is coupled to the source room. However, when the receive room is coupled to the ancillary volume a criterion is required to minimize the effect of an ancillary volume.

Figures 4 and 5 show when there is an ancillary volume coupled to the receive room, the difference in the ATL with and without (reference) an ancillary volume, is a function of two parameters. First is space-average level difference between the principal and ancillary volumes. Second is whether sound field measurements include the ancillary volume. There is a data point for each one-third octave in the range 125-4kHz. The figures show that there is practically no ATL overestimation for two conditions, 1.) small level difference between the coupled volumes and the sound field averaged over both and the combined volume is used in calculations, 2.) large level difference between the coupled volumes and the sound field in principal volume is used in the calculations. For intermediate conditions, the overestimation is appreciable and should be minimized. For the room volumes and reverberation times considered here, the regression lines suggest, when the difference in space average level between the principal and ancillary volumes is greater than about 4 dB estimates of ATL should be obtained using sound field measurements restricted to the principal volume. However, when difference is less than 4 dB both principal and ancillary volumes must be used.

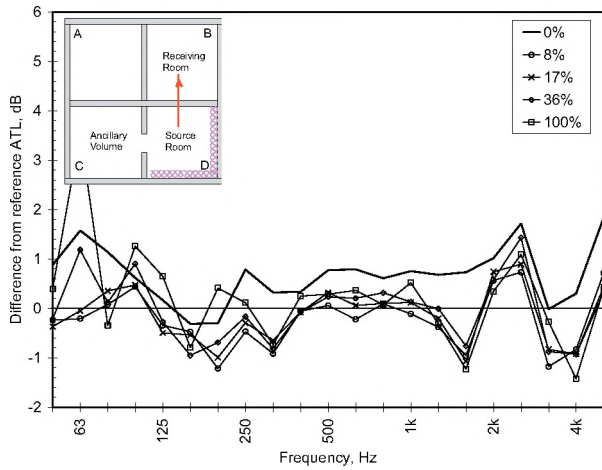


Figure 1: Effect of an ancillary volume and percent opening when coupled to a heavily furnished source room

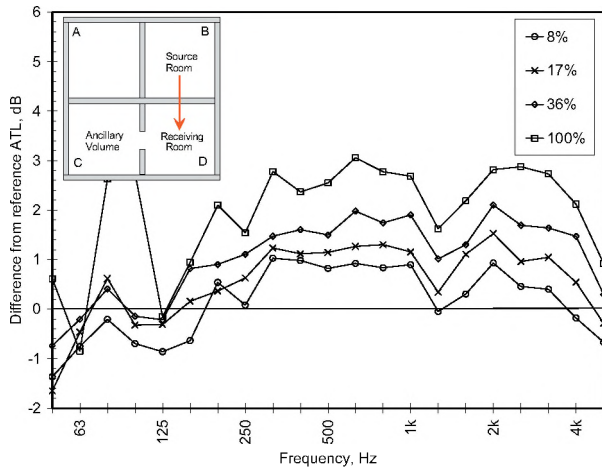


Figure 2: Effect of an ancillary volume and percent opening when coupled to a receive room.

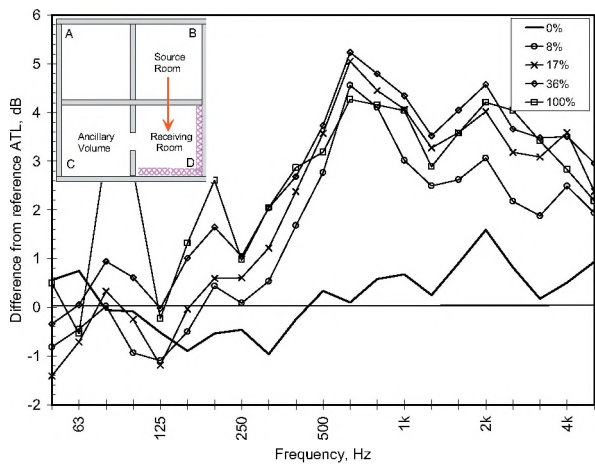


Figure 3: Effect of an ancillary volume and percent opening when coupled to a highly absorptive receive room.

In both cases, the room volume used in the calculation is consistent with the space where the sound fields were measured. Since there is a tendency to overestimate the ATL, an alternate procedure would be to compute the ATL twice – first using measurements made in the principal volume, and second using measurements in the combined volumes – and take the lower of the two values. For rooms typical of most apartments (volume 35-50 m³ and reverberation times 0.4 – 1.0 s), this small systematic study has shown the E336 criterion is not optimal, but is close.

The authors wish to thank Don MacMillan and Brian Fitzpatrick for their help in this study.

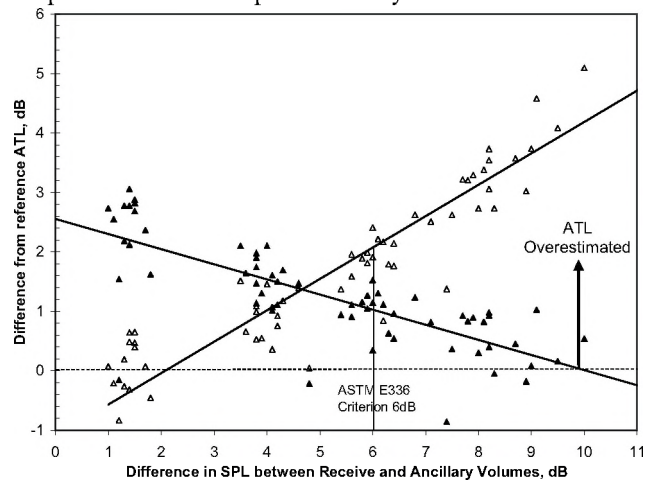


Figure 4: ATL errors when an ancillary volume is coupled to receiving room. Open symbols are estimates obtained from measurements in both the ancillary and receive volumes. Closed symbols are estimates obtained from measurements in the principal receive volume. There is a data point for each one-third octave band in the range 125 – 4kHz.

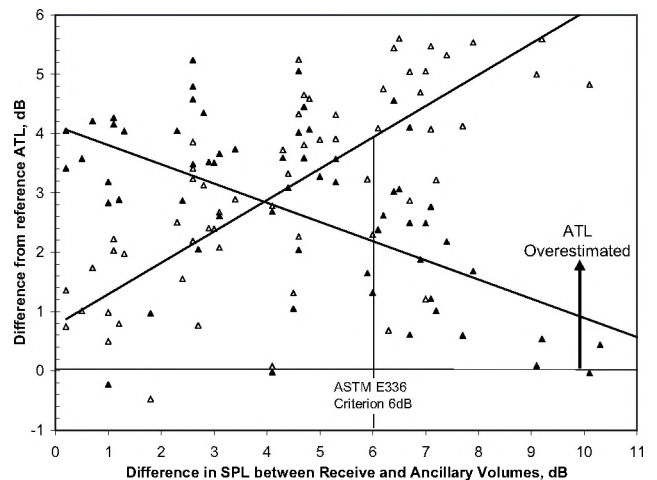


Figure 5: ATL errors when an ancillary volume is coupled to a heavily furnished receiving room. Open symbols are estimates obtained from measurements in both the ancillary and receive volumes. Closed symbols are estimates obtained from measurements in the principal receive volume. There is a data point for each one third octave band in the range 125 – 4k Hz.

A CROSS-LANGUAGE VOWEL NORMALISATION PROCEDURE

Geoffrey Stewart Morrison and Terrance M. Nearey

Department of Linguistics, University of Alberta, Edmonton, AB, T6G 2E7

1. INTRODUCTION

Vowel classification models trained on production data typically have higher correlation with human listeners' perception when the acoustic properties of the production data are normalised prior to training and testing. Vowel normalisation procedures seek to remove inter-speaker variance due to factors such as vocal tract size, which human listeners discount when identifying vowels. Extrinsic normalisation makes use of information from a representative sample of a speaker's vowel inventory. For example, Nearey's log-mean normalisation [1] applies Equation 1:

$$N_{kivs} = G_{kivs} - \bar{G}_s \quad (1)$$

where N_{kivs} is the normalised value of G_{kivs} which is the k -th formant frequency (in log-Hertz) of instance t of vowel category v produced by speaker s ; and \bar{G}_s , the within-speaker normalisation factor, is the mean of all the speakers' vowel productions:

$$\bar{G}_s = \frac{1}{(V \cdot T \cdot K)} \cdot \sum_{v=1}^V \sum_{t=1}^T \sum_{k=1}^K G_{kivs} \quad (2)$$

Normalised vowel formant values are therefore represented as a displacement from a reference value \bar{G}_s . This normalisation is valid under the assumptions that the set of vowels used to calculate \bar{G}_s have the same pattern for all speakers, but that vocal-tract size differences may shift the pattern along a track in the F1–F2 space (constant ratio hypothesis / constant log-interval hypothesis). The first assumption can reasonably be expected to be fulfilled when all the speakers share the same language and dialect, but is clearly violated across languages or dialects when they have different numbers of vowels in their inventories, or different skews in the distribution of the same number of vowels, see [2].

This paper presents and tests a variation of log-mean normalisation which may be applied in cross-language and cross-dialect experiments.

2. NORMALISATION PROCEDURE

Imagine an ideal bilingual who is indistinguishable from a monolingual speaker of language A when speaking language A, and indistinguishable from a monolingual speaker of language B when speaking language B. The ideal bilingual

would likely have different \bar{G}_s for language A than for language B, hereafter \bar{G}_A and \bar{G}_B . Since vowels from both languages are produced by the same speaker, differences between \bar{G}_A and \bar{G}_B would not be due to differences in vocal tract size. However, \bar{G}_A and \bar{G}_B would differ as a result of cross-language differences in inventory size and skew. Formant values for vowels from language A would be normalised as displacements around \bar{G}_A , and vowels from language B as displacements around \bar{G}_B . Displacements around the reference value for one language can be translated to displacements around the reference value for the other language by adding or subtracting the difference between \bar{G}_A and \bar{G}_B , a cross-language normalisation factor.

Over sufficiently large and balanced samples of speakers from each language, it is reasonable to expect that the mean vocal-tract length (and any other factors underlying formant scale differences) are approximately equal. If so, then rather than relying on mythical ideal bilinguals, the cross-language normalisation factor, \bar{G}_L , can be calculated as the difference between the mean reference values from samples of L1 speakers from each language.

$$\bar{G}_L = \bar{G}_A - \bar{G}_B \quad (3)$$

$$\bar{G}_A = \frac{1}{S_A} \cdot \sum_{s_A=1}^{S_A} \bar{G}_{s_A} \quad \bar{G}_B = \frac{1}{S_B} \cdot \sum_{s_B=1}^{S_B} \bar{G}_{s_B} \quad (4)$$

The procedure for classifying vowels from language B in terms of categories from language A is as follows: First, perform a within-language vowel normalisation for vowel formant data from language A using Equation 5.

$$N_{kivs_A} = G_{kivs_A} - \bar{G}_{s_A} \quad (5)$$

Second, train a model on the normalised data from language A. Third, apply a cross-language normalisation to vowel formant data from language B using Equation 6.

$$N_{kivs_A} = G_{kivs_B} - \bar{G}_{s_B} - \bar{G}_L \quad (6)$$

Finally, use the model trained on language A to classify the cross-language normalised data from language B.

3. TEST OF PROCEDURE

3.1 Method

The effectiveness of the cross-language normalisation procedure was tested using acoustic data from productions of L1-Spanish non-low front vowels (Sp/i/,Sp/ei/,Sp/e/), and L1-English non-low front vowels (Eng/i/,Eng/ɪ/,Eng/e/,Eng/ɛ/). The data, taken from [3], consisted of 10 productions of each vowel category from 59 L1 speakers of various Spanish dialects (32 females and 27 males) and 49 L1 speakers of Western Canadian English (32 females and 17 males).

Linear discriminant analysis models were trained on the L1-English data using the following acoustic variables: F1 and F2 measured at 25% of the duration of the vowel, $\Delta F1$ and $\Delta F2$ (the formant differences between 25 and 75% of the duration of the vowel), and vowel duration. The models were then used to classify the L1-Spanish data. Three models were trained and tested, one used non-normalised log-Hertz values for both training and testing, a second used within-language-normalised values (Equation 1 applied to training and test data), and the third used cross-language-normalised values (Equation 5 applied to training data, Equation 6 applied to test data). Normalisation was applied to both formant and duration measurements. Because of a difference in the ratio of male to female speakers across the language groups, 10 L1-Spanish males were randomly selected, and their data was excluded from the calculation of \bar{G}_L ; hence, \bar{G}_L was based on a male to female ratio of 17:32 in both languages.

A subset of L1-Spanish vowels (3 instances of each vowel category randomly selected from the productions of each of 28 randomly selected L1-Spanish speakers) were presented to eleven monolingual English listeners for identification (each stimulus was identified once by each listener). The perception experiment also included L1 and L2-English vowels.

The correlations between the listeners' identifications (proportion of responses for each vowel category for each stimulus pooled over listeners, \mathbf{X}) and the classifications from a model (a posteriori probabilities for each vowel category for each stimulus, \mathbf{Y}) were calculated using Equation 7, where v indexes the vowel category, V is the number of vowel categories (4), u indexes the stimulus, and U is the number of stimuli (252); see [4, appendix].

$$r = \frac{(UV \sum_u \sum_v x_{uv} y_{uv}) - (\sum_u \sum_v x_{uv} \cdot \sum_u \sum_v y_{uv})}{\sqrt{((UV \sum_u \sum_v x_{uv}^2 - (\sum_u \sum_v x_{uv})^2) \cdot (UV \sum_u \sum_v y_{uv}^2 - (\sum_u \sum_v y_{uv})^2))}} \quad (7)$$

3.1 Results

The models trained on normalised L1-English vowels had a slightly higher correct-classification rate on the training data than the model trained on non-normalised vowels: 98.7% versus 96.2% in a leave-one-participant-out cross-validation.

For the test data, correlation with the listeners' perception of L1-Spanish vowels was greater for the cross-language-normalised model, $r = .869$, than for the within-language-normalised, $r = .853$, and the non-normalised models, $r = .848$. Pooled confusion matrices are given in Tables 1 and 2.

Table 1. L1-English listeners' identification of L1-Spanish vowels, expressed as proportions pooled across repetitions, speakers, and listeners.

Produced	Perceived			
	Eng /i/	Eng /ɪ/	Eng /e/	Eng /ɛ/
Sp /i/	.951	.036	.009	.004
Sp /ei/	.005	.003	.982	.010
Sp /e/	.004	.275	.473	.248

Table 2. Mean a posteriori probabilities for classification of L1-Spanish vowels by the cross-language normalised model.

Produced	Classified			
	Eng /i/	Eng /ɪ/	Eng /e/	Eng /ɛ/
Sp /i/	.997	.001	.001	
Sp /ei/			1.000	
Sp /e/	.014	.583	.286	.117

4. CONCLUSION

Use of the cross-language vowel normalisation procedure increased the correlation between monolingual English listeners' perception of L1-Spanish vowels and the classification of L1-Spanish vowels by a statistical model trained on L1-English vowel productions.

REFERENCES

- [1] Nearey, T. M. & Assmann, P. F. (in press). "Probabilistic 'sliding-template' models for indirect vowel normalization," in *Experimental Approaches to Phonology*, edited by M. J. Solé, P. S. Beddor, and M. Ohala (Oxford: Oxford University Press).
- [2] Disner, S. F. (1980). "Evaluation of vowel normalization procedures," *J. Acoust. Soc. of Am.*, 67, 253-261.
- [3] Morrison, G. S. (2006). "L1 & L2 production and perception of English and Spanish vowels: A statistical modelling approach," unpublished doctoral dissertation, University of Alberta.
- [4] Nearey, T. M., & Assmann, P. F. (1986). "Modeling the role of vowel inherent spectral change in vowel identification," *J. Acoust. Soc. of Am.*, 80, 1297-1308.

This work was supported by SSHRC.

CONVERSATIONAL SPEECH INTENSITY UNDER DIFFERENT NOISE CONDITIONS IN HYPOPHONIA AND PARKINSON'S DISEASE

Scott Adams¹, Allyson Dykstra², Kayla Abrams¹, Jennifer Winnell¹, Mary Jenkins³, Mandar Jog³

¹School of Communication Sciences & Disorders, University of Western Ontario, London, Ontario, Canada, N6G 1H1

²Doctoral Program in Rehabilitation Sciences, University of Western Ontario, London, Ontario, Canada, N6G 1H1

³Department of Clinical Neurological Sciences, University of Western Ontario, London, Ontario, Canada, N6G 1H1

1. INTRODUCTION

Low speech intensity or hypophonia is one of the most common speech symptoms in Parkinson's disease (PD). Subjects with hypophonia, often report that their conversational speech is dramatically influenced by the intensity of the surrounding background noise. In general, PD subjects report that the louder the background noise is the more difficult it is for them to communicate. Interestingly, this relationship between conversational speech intensity and background noise level has received limited attention in previous studies of PD. A preliminary report, by Adams and Lang (1992), found that 90dB SLP of white noise produced a marked increase in speech intensity in 10 PD subjects. In contrast, Ho et al. (1999), found that pink noise, presented at 10-30dB above threshold, produced minimal or no increase in speech intensity in a group of 12 PDs. More recently, Adams et al. (2005) found a systematic increase in speech intensity across increases in background noise (positive Lombard effect) during sentence reading in a group of 10 subjects with PD. This study also noted that, PD subjects showed a Lombard relationship that was parallel to control subjects. These inconsistencies may be related to a number of factors such as, the severity of hypophonia, the type background noise, the noise levels, the speech tasks, the intensity measures, and the methods of stimulus presentation. Defining the relationship between speech intensity and background noise has important implications for the understanding, assessment and treatment of hypophonia in PD. The purpose of the present study was to examine the effects of 3 types of background noise on conversational speech intensity in individuals with hypophonia and Parkinson's disease.

2. METHOD

This study included 23 idiopathic PD subjects with hypophonia and 15 age-equivalent controls. All subjects with PD were reported by a Neurologist (MJ) to demonstrate reduced speech intensity or hypophonia. All subjects with PD were stabilized on their anti-parkinsonian medication and were tested at approximately 1 hour after taking their regularly scheduled anti-parkinsonian medication. Normal and PD subjects passed a 40 dB hearing screening.

All subjects were tested in an audiometric booth. During all conditions, subjects sat in a chair facing the experimenter. A loudspeaker was placed 150 centimeters in front of the subjects. Subjects wore a headset microphone (AKG-C420) positioned a constant 15 cm distance from the mouth. The experimenter presented the background noise through the loudspeaker, adjusting the dB level of the noise via a diagnostic audiometer (GSI 61). The speech of each subject was recorded using a digital audio tape recorder (Tascam DA-01). Subjects were engaged in approximately 2 minutes of conversation for each of the 15 noise conditions (total conversation time = 30 minutes). Three types of background noise were examined. These included multi-talker noise (Audiotech - 4 talker noise), music (A taste of soul; 101Strings Orchestra), and pink noise. For each of these 3 noise types, 5 intensity levels (50, 55, 60, 65, 70 dB) were randomly presented.

The subjects' recorded test sentences were digitized using Kay Elemetrics' Visipitch program. The average intensity (dB) for each conversational utterance (minimum length = 6 words) was determined using the Visipitch intensity analysis routine. The average of at least 6 conversational utterances determined the conversational speech intensity for each noise condition. Three separate two-factor (noise level, group) repeated measures ANOVAs were used to examine the effects of each noise type on speech intensity. A series of planned comparisons (t-tests) were used to compare the 3 noise types.

3. RESULTS

The effects of each of the 3 noise types (multi-talker, music, pink) on the conversational speech intensity of the PD and control groups are shown in Figure 1. For each of the 3 noise types, both PDs and controls showed a significant increase in conversational speech intensity across increases in the level of background noise ($p=.0001$). Thus, the PD and control subjects showed a significant positive Lombard effect for each noise type. In addition, PD subjects were significantly lower (3-5 dB) than controls across all noise types and noise levels ($p<.005$).

For each of the noise types examined, the group x noise level interaction was not significant (multi-talker $p=.22$; music $p=.42$; pink $p=.82$). These interaction results

suggest that the PD subjects have a Lombard relationship that is essentially parallel to the controls. This parallel relationship is illustrated by the regression lines in Figure 1.

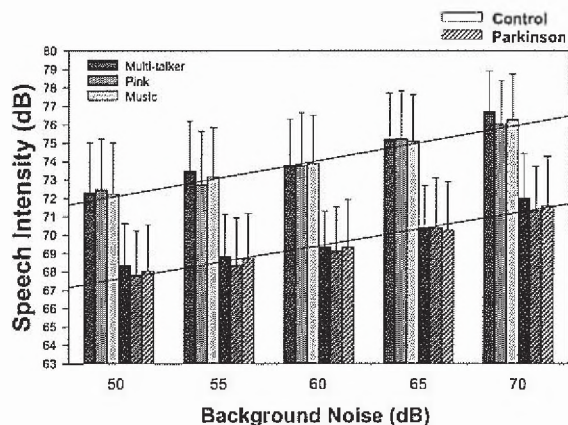


Figure 1. Average conversational speech intensity obtained from Parkinson disease and control subjects during multi-talker noise, pink noise and music presented at 5 levels (50, 55, 60, 65, 70 dB). Corresponding regression lines are shown for each group.

The comparisons of the noise types at each noise level revealed very few significant differences. For the PD subjects, there was only one significant comparison. During the 70dB multi-talker noise the PDs used a conversational speech intensity that was 0.66dB higher than during the 70dB pink noise ($p=.02$). The control subjects, also had a significantly higher speech intensity (0.69dB) during the 70dB multi-talker noise than during the 70dB pink noise ($p=.002$). The controls also had a significantly higher speech intensity (0.74dB) during the 55dB multi-talker noise than during the 55dB pink noise ($p=.034$). Thus, only 3 of the 30 statistical comparisons of noise types were significant. In all three cases, these involved the multi-talker noise being associated with a higher speech intensity than the comparable pink noise.

4. DISCUSSION

The results of this study suggest that PD subjects show a systematic increase in speech intensity across increases in background noise. These findings are consistent with two previous reports on the 'Lombard effect' in PD (Adams & Lang, 1992; Adams et al., 2005). These previous reports involved the use of white noise and multi-talker noise during sentence reading. The present study extends this 'Lombard effect' in PD to conversational speech as well as pink noise and background music. Thus, the 'Lombard effect' in PD appears to be fairly consistent across speech tasks and noise conditions. The present study also showed that the positive relationship between speech intensity and background noise is approximately parallel to that of controls. Interestingly, despite this positive Lombard

relationship, the PD subjects' speech intensity was consistently below that of the controls for each of the noise levels examined. Thus, relative to controls, the PD subjects showed a parallel but reduced speech versus noise intensity relationship. This suggests that individuals with PD may show a normal pattern of speech intensity regulation but with an "overall gain reduction". These results may have important implications for the development of assistive devices and new treatment procedures for hypophonia in PD.

REFERENCES

- Adams, S.G. & Lang, A.E. (1992). Can the Lombard effect be used to improve low voice intensity in Parkinson's disease? *European Journal of Disorders of Communication*, 27, 121-127.
- Adams, S.G., Haralabous, O., Dykstra, A., Abrams, K., & Jog, M. (2005). Effects of multi-talker background noise on the intensity of spoken sentences in Parkinson's disease. *Canadian Acoustics*, 33, 94-95, 2005.
- Ho, A., Bradshaw, J., Iansek, R., & Alfredson, R. (1999). Speech volume regulation in Parkinson's disease: Effects of implicit cues and explicit instructions. *Neuropsychologia*, 37, 1453-1460.

ACKNOWLEDGEMENTS

This research was funded by a grant from the University of Western Ontario's Academic Development Fund that was awarded to the first author.

DIRECTIVITY PATTERNS FOR A SHORT LINE ARRAY OF BARREL-STAVE FLEXTENSIONAL TRANSDUCERS

Dennis F. Jones

Defence R&D Canada – Atlantic, P.O. Box 1012, Dartmouth, NS, Canada B2Y 3Z7

dennis.jones@drdc-rddc.gc.ca

1. INTRODUCTION

Barrel-stave flextensional transducers are compact underwater sound sources that were developed over the past two decades at DRDC Atlantic [1, 2]. Several designs were built for a variety of applications including horizontal line arrays, active sonobuoys, acoustic communications systems, and broadband transmitters.

For security applications such as underwater alarm systems and diver warning systems, short arrays with directional radiation patterns in the audible frequency band may be attractive. The barrel-stave flextensional transducer shown in Fig. 1 is ideal for these applications owing to its small size. In this work, the directivity patterns of a short barrel-stave transducer line array are presented.

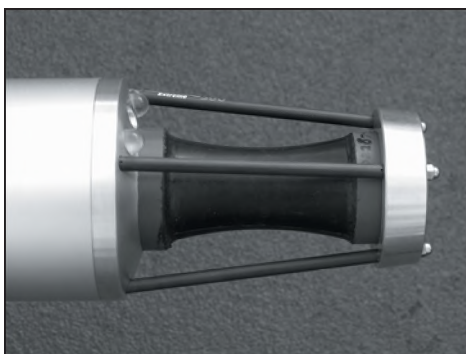


Fig. 1. A barrel-stave flextensional transducer integrated into an expendable submarine communications buoy.

2. TRANSDUCER PERFORMANCE

Four barrel-stave flextensional transducers driven by piezoceramic stacks were built at DRDC Atlantic for a short line array. Each transducer had an outside diameter of 5.7 cm, length of 12.7 cm, and mass of 1.1 kg.

The performance parameters, measured at the DRDC Atlantic Acoustic Calibration Barge on Bedford Basin near Halifax, are listed in Table 1. The fundamental flexural resonance frequency, transmitting voltage response (TVR) at resonance, and mechanical quality factor (Q) at resonance were well matched. At the flexural resonance, the transducer is omnidirectional since it is small compared to a wavelength. The pattern at 2.0 kHz is shown in Fig. 2.

Table 1. Transducer performance parameters.

Transducer	Frequency (Hz)	TVR ^a (dB//1μPa-m/V)	Q ^a
Element 1	1550	126.7	3.5
Element 2	1540	126.6	3.5
Element 3	1540	126.8	3.6
Element 4	1540	126.9	3.5

^aValues determined at the resonance frequency.

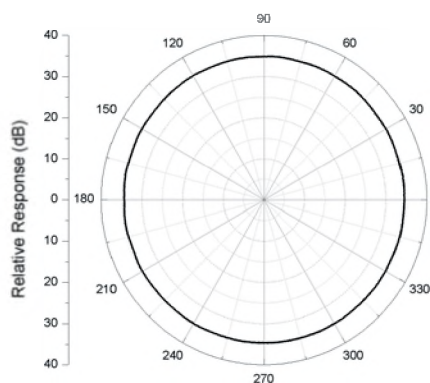


Fig. 2. At 2.0 kHz the barrel-stave transducer is omnidirectional. The transducer's longitudinal axis lies along the 90°-270° axis.

3. ARRAY DIRECTIVITY PATTERNS

The four-element line array shown in Fig. 3 was constructed and tested at the NAVSEA Seneca Lake Sonar Test Facility near Dresden in upstate New York. The length of the array was 1.3 m with a 40 cm inter-element spacing. Four amplifiers were used to drive the array, one for each transducer. A four-channel Wavetek 650 Synthesizer was used to apply phase and time delays. The directivity patterns were measured using a rotating station at a water depth of 30.5 m. At this depth, the sound speed was 1418 m/s as determined using a Falmouth Scientific 2" Micro CTD.

The radiation pattern shown in Fig. 4 was produced by driving the two center array elements 180° out of phase. At 1640 Hz the spacing between the elements was 0.47λ. This dipole-like pattern had a beamwidth of 94° and a sound pressure level 8 dB higher than that of a single element.

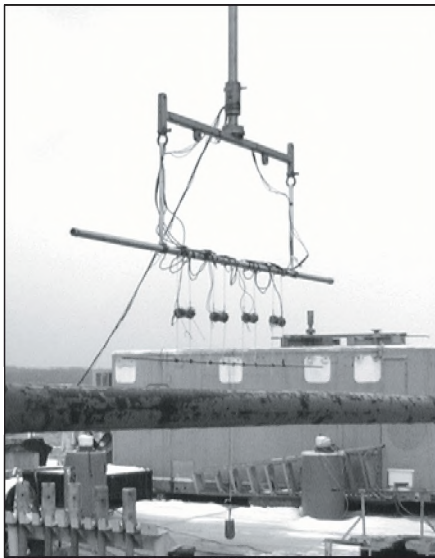


Fig. 3. The four-element line array of barrel-stave transducers at the Seneca Lake Sonar Test Facility.

Cardioid patterns were produced using the same two center elements. By driving the two elements 96° out of phase at 800 Hz, the cardioid in Fig 5 was realized. Note that the inter-element spacing was 0.23λ at this frequency. The beamwidth was 166° , front-to-back ratio was 46 dB and the sound pressure level was 6 dB higher than that of a single element. By switching the relative phase to -96° , the cardioid direction changed to 270° with a front-to-back ratio of 53 dB.

When all four elements were driven in phase at 1640 Hz, the measured radiation pattern was the solid curve in Fig. 6. The inter-element spacing was 0.47λ and the beamwidth of the main lobes on the 0° - 180° axis was 29° . The four side lobes are not fully developed. At frequency f , the main lobes were steered to angle θ_0 by applying phase shift ϕ according to

$$\phi = 0.102 f \sin \theta_0.$$

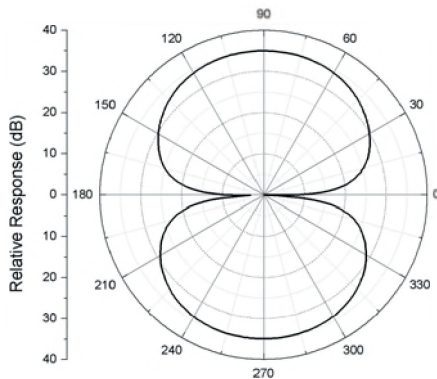


Fig. 4. Two elements driven 180° out of phase at 1640 Hz with a 0.47λ spacing. The array is collinear with the 90° - 270° axis.

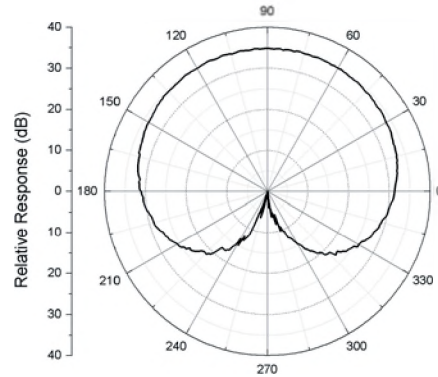


Fig. 5. Two elements driven 96° out of phase at 800 Hz with a 0.23λ spacing. The array is collinear with the 90° - 270° axis.

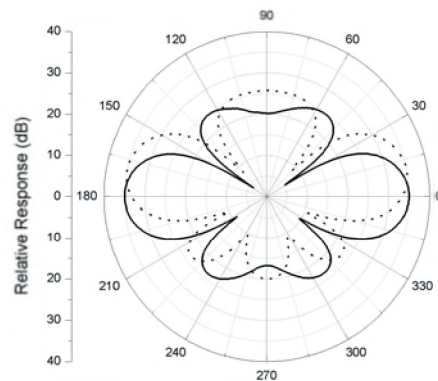


Fig. 6. Four elements driven in phase (solid) and 30° out of phase (dotted) at 1640 Hz with a 0.47λ spacing. The array is collinear with the 90° - 270° axis.

Thus, by applying a phase shift of 30° , the main lobes were steered 10.3° as shown by the dotted curve in Fig. 6. Note that the same steering angle can be achieved using a time delay of $50\mu\text{s}$.

4. CONCLUSIONS

In this work it was shown that a 1.3 m long line array of four barrel-stave flextensional transducers could produce a variety of radiation patterns. An omnidirectional pattern could be created by exciting a single element. Cardioid and dipole-like patterns resulted from driving two elements out of phase. When all four elements were driven, the main lobes were steered using phase shifts or time delays.

REFERENCES

- [1] Jones, D.F. (1989). Low-frequency flextensional projectors. Proceedings of the Annual Meeting of the Canadian Acoustical Association, Edited by A.J. Cohen, 18-23.
- [2] Jones, D.F. and Lindberg, J.F. (1995). Recent transduction developments in Canada and the United States. Proceedings of the Institute of Acoustics, 17(3), 15-33.

UNDERWATER COMMUNICATIONS TESTING OF THE MULTI-MODE PIPE PROJECTOR

Richard Fleming¹, Donald Mosher¹, Joe Hood², Sean Spears¹, and Charles Reithmeier¹

¹DRDC Atlantic, PO Box 1012, Dartmouth, Nova Scotia, CANADA, B2Y 3Z7

²Akoostix Inc., 10 Akerley Blvd., Suite 12, Dartmouth, Nova Scotia, B3B 1J4 formerly of MacDonald, Dettwiler and Associates Ltd., 1000 Windmill Rd., Suite 60, Dartmouth, Nova Scotia, CANADA, B3B 1L7

1. INTRODUCTION

A method for providing undersea navigation was sought in order to provide autonomous undersea vehicles with absolute navigation data while submerged. Floating buoys based on the earlier LAND buoy were developed at DRDC Atlantic to permit transmission of real-time GPS NMEA embedded acoustic signals via underwater sonar transducers.

An experiment, carried out in February 2006 as part of CFAV Quest cruise Q294 in the Gulf of Mexico, was conducted to evaluate the accuracy, range and robustness of the GPS encoding and transmission system. This was also an opportunity to test the multi-mode pipe projector (MMPP) as an underwater communications source. For the purposes of this paper, range and decoding success will be discussed.

1.1 GPS (LAND) Buoy

The floating GPS retransmission buoy was developed using the casing of the earlier Lagrangian (Ambient Noise) drifter (LAND) buoy. The buoy's casing is composed of a water-tight aluminum cylinder with removable end bulkheads and an expanded polystyrene floatation collar.

These buoy are equipped with a GPS receiver and antenna from which time-stamped NMEA-formatted data is stripped. This data is fed to a PC-style microprocessor for translation into a hyperbolic frequency modulated (HFM) coded audio signal with 200 Hz bandwidth. Each of the three constructed buoys had its center frequency set for a particular projector. The audio signal is amplified by a 400-watt commercial car audio unit. A matching inductor in series with the sonar projector keeps the power factor above 0.8. Each buoy is powered with 5-12 VDC deep cycle batteries.

Two MMPP's and one barrel-stave projector were selected as transmitting elements. Each transducer was tethered to its GPS buoy with a strength member and conducting cables to operate at a depth of 30 m.

1.2. Multi-Mode Pipe Projector

The Multi-Mode Pipe Projector is a wideband, inexpensive, and depth insensitive sonar projector that has been under development at Defence Research and Development Canada (DRDC) -Atlantic over the past 3 years.



Figure 1. 30X40 MMPP.

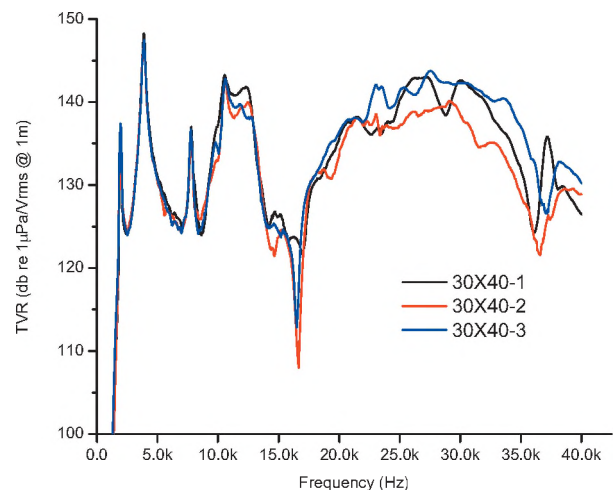


Figure 2. 30X40 MMPP slot-direction transmitting voltage response.

The MMPP's wide bandwidth is achieved through juxtaposition of resonant mode frequencies by optimization of various projector dimensions and materials. The low frequency modes are generated by cavity and flexural modes of the cup-shaped endcaps while high frequencies are generated from drive motor breathing modes.

The 30X40 version of the MMPP has a useable band from 1.8 to 34 kHz from its slot-fire direction. This projector (see Figure 1) is 0.232 m long, 0.119 m in diameter and has a mass of 3.4 kg in air. For this trial the first and second resonance frequencies centered at 1950 Hz and 3850 Hz (see Figure 2) for 30X40 MMPP's were selected. As well, a barrel-stave projector was employed at its 1500 Hz first resonance.

2. EXPERIMENT DESCRIPTION

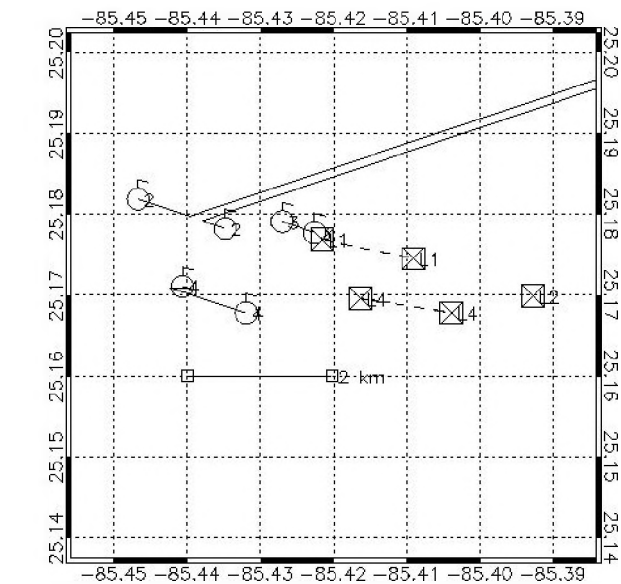
The three transducer-equipped GPS buoys were deployed at a test site off the west coast of Florida in the Gulf of Mexico (see Fig. 3). The GPS buoys were assigned labels L1, L2 and L4 which corresponded to the barrel-stave projector at 1500 Hz, MMPP at 1950 Hz and MMPP at 3850 Hz respectively. Source levels were kept low so that acoustic emissions did not exceed the maxima stated in the cruise plan. GPS NMEA data was encoded on HFM sweeps at a rate of 8 symbols per second. A group of type SSQ-53F(GPS) sonobuoys were laid out to receive the GPS encoded acoustic signal and subsequently retransmit the data via RF link to CFAV Quest. The GPS coordinates of the type 53F buoys were also tracked for later comparison

3. RESULTS

GPS Buoy labeled L2 provided no usable GPS decodes likely due to its 3km distance from the sonobuoys. The signals were received with high enough signal to noise ratio, but the time variance between symbol arrivals was too high to be decoded consistently enough to produce usable data. Ignoring L2, 70% clear and another 26% highly usable transmissions were decoded. With L2, useable decoded transmissions decreased to 47% and 18% respectively.

4. DISCUSSION

Preliminary results in this and related experiments during Q294 indicate that the MMPP is a good candidate for use in underwater communications. MMPP performance was minimally impacted by multi-path distortion at ranges of less than 2 km given the geometry of this experiment and water conditions. Further analysis of the data is planned to assess acoustic GPS positioning accuracy using this method of acoustic GPS data transmission.



of computed position to actual position.

Fig 3. L1, L2 and L4 Acoustic GPS buoys (square icons) transmitting to a field of 53F sonobuoys (circle icons).

EFFECT OF CARDIOID AND LIMAÇON DIRECTIONAL SENSORS ON TOWED ARRAY REVERBERATION RESPONSE

Dale D. Ellis

DRDC Atlantic, P.O. Box 1012, Dartmouth, N.S., Canada, B2Y 3Z7. Email: dale.ellis@drdc-rddc.gc.ca

1. INTRODUCTION

Reverberation is often the limiting factor affecting the performance of active sonar systems, so receivers with directional beam patterns are used to improve the echo-to-reverberation ratio. Towed horizontal line arrays are often used, but the axial symmetry of their beam pattern gives rise to what is often called “left-right” ambiguity. Elements with directional response can be used to reduce the ambiguity; e.g., the DRDC Atlantic DASM array [Therriault *et al.*, 2006] where the omni-directional elements are augmented with crossed dipole pairs allowing cardioid or limaçon beam patterns to be formed. In this paper, we investigate some of the effects on reverberation response.

2. BEAM PATTERNS

When a receiver beam pattern has azimuthal dependence, the effective beam pattern approach is a useful technique for efficiently computing monostatic reverberation in a range-independent environment [Ellis, 1991]. The effective beam pattern response B^* at vertical angle θ is simply the 3-D beam pattern $B_{\beta_0}(\beta)$ averaged over all azimuth angles ϕ :

$$B_{\beta_0}^*(\theta) = (2\pi)^{-1} \int_0^{2\pi} [B_{\beta_0}(\theta, \phi)] d\phi,$$

where β_0 is the towed array beam steering angle, $\cos \beta = \cos \theta \cos \phi$, and all angles are measured from forward endfire of the array. The beam patterns for linear arrays with point elements and various weightings are well known; when the elements have identical directional responses $D(\beta)$

and the same weightings, the usual line array beam response is simply multiplied by $D(\beta)$.

An omnidirectional element and a horizontal dipole, equally weighted, will produce a broadside cardioid response of

$$D(\beta) = [(1 + \sin \beta)/2]^2.$$

By weighting the omni by $\sin \beta_0$, the general limaçon formula can steer a null in the centre of the ambiguous beam [Franklin, 1984]

$$D(\beta) = [(\sin \beta_0 + \sin \beta)/(2 \sin \beta_0)]^2,$$

where the denominator normalizes to unit response at horizontal in the beam steering direction.

Fig. 1 shows polar plots of the various responses in the horizontal plane, for a ~ 15 -wavelength array. In the left plot the linear array has equal response (blue solid) at 60° and 300° ; when multiplied by the broadside cardioid (green dash-dot line), the combined response (red dashed line) has a much reduced response at 300° , which is only obvious on a dB plot (middle). In the right plot, the linear array has equal response (blue solid) at 30° and 330° , the normalized limaçon response (green dash-dot line) has a null at 330° and the multiplied response (red dashed line) has a single lobe at 30° . Even on a dB plot (not illustrated), the limaçon shows no ambiguous beam.

Fig. 2 shows some effective beam patterns for the broadside beams and beams 60° off broadside, for a ~ 44 -wavelength array. Note at broadside that the cardioid (or limaçon) directionality reduces the response at vertical incidence by

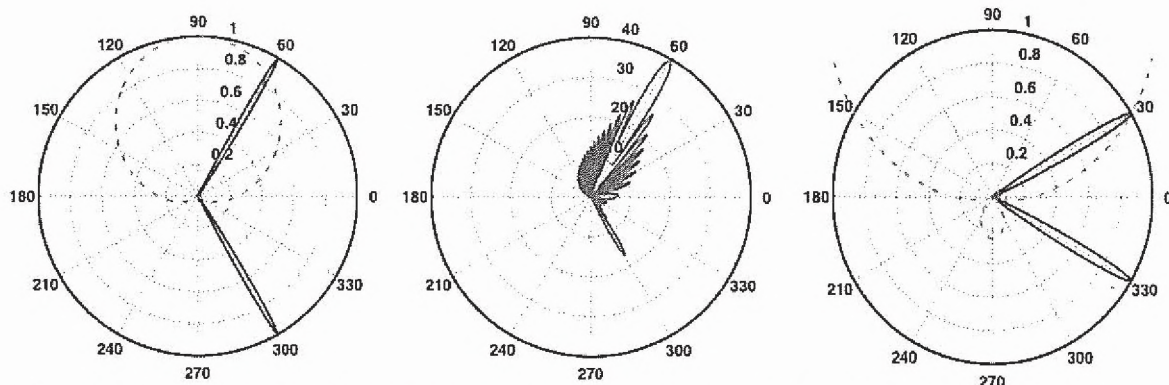


Fig. 1. Polar plots: (left) including cardioid response; (middle) normalized response as a dB plot; (right) including limaçon response.

6 dB, and elsewhere by about 3 dB, producing a much “flatter” effective beam pattern as a function of grazing angle. For off-broadside beams the limaçon response produces a slightly lower and flatter response between the “cusps”.

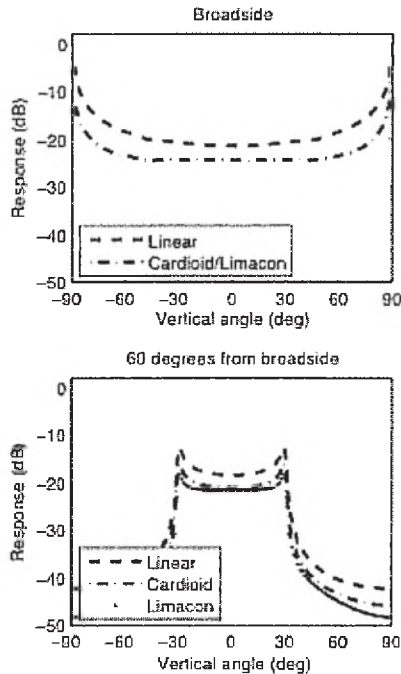


Fig. 2. Effective beam patterns for a 44λ array: (upper) broadside; (lower) 60° from broadside.

3. REVERBERATION CALCULATIONS

A normal mode reverberation model with beam patterns [Ellis, 1993, 1995] was used for the calculations. A typical “Pekeris” environment was used: water of depth 100 m, and sound speed 1500 m/s, over a homogeneous bottom halfspace of sound speed 1800 m/s, relative density 2.0, and attenuation 0.36 dB/wavelength. The bottom scattering was Lambert’s rule, with a -27 dB strength. A 1.4 kHz CW pulse for a duration of 0.1 s and 10 dB source level was used. The receiving array had 96 elements (omni-dipole pairs) spaced at 0.5 m (~ 44 wavelengths), with uniform weighting along the array.

Figure 3 shows reverberation predictions using the effective beam patterns of Fig. 2. The horizontal array reduces the reverberation by about 20 dB compared to an omni, and the cardioid response reduces it by about another 3 dB. Even at 60° from broadside, the limaçon produces only a marginal additional reduction in reverberation.

4. DISCUSSION

Previous calculations have illustrated results for horizontal line arrays with omni-directional elements. In this

paper, calculations are presented for towed array beam patterns with cardioid or limaçon directional sensors replacing the omni-directional elements. As one would expect, the cardioid sensors reduce the reverberation by about 3 dB, and suppress the ambiguous beam, particularly near broadside. The limaçon sensors, even with the null steered in the direction of the ambiguous beam, provide only a marginal improvement in the predicted reverberation. They, however, reduce the ambiguous beam much more effectively than the cardioid, and so are very useful for target detection [Theriatul *et al.*, 2006].

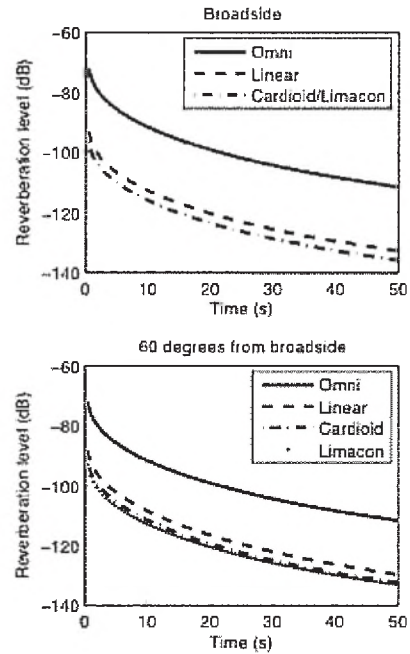


Fig. 3. Reverberation predictions: (upper) omni and broadside beams; (lower) omni and beams 60° from broadside.

REFERENCES

- Ellis, D. D. (1991). Effective vertical beam patterns for ocean reverberation calculations. *IEEE J. Ocean. Eng.*, **16**, 208-211.
- Ellis, D. D. (1993). Shallow water reverberation: normal-mode model predictions compared with bistatic towed-array measurements. *IEEE J. Ocean. Eng.*, **18**, 474-482.
- Ellis, D. D. (1995). A shallow-water normal-mode model reverberation model. *J. Acoust. Soc. Am.*, **97**, 2804-2814.
- Franklin, J.B. (1984). Informal communication. DREA, Dartmouth, NS, Canada.
- Theriatul, J. A., J. Hood, D. G. Hazen, O. Beslin (2006). Performance comparison of arrays of directional versus omnidirectional sensors using BASE '04 data. *Proc. 8th ECUA*, Carvoeiro, Portugal, 603-608.

ACKNOWLEDGEMENTS

Useful discussions were held with Jim Theriatul, John Preston, and Sean Pecknold. This work was supported in part by the US Office of Naval Research, and hospitality at the Applied Research Laboratory at Penn State University.

SPHERICAL MICROPHONE ARRAYS FOR ANALYSIS OF SOUND FIELDS IN BUILDINGS

Bradford N. Gover

Institute for Research in Construction, National Research Council, 1200 Montreal Rd., Ottawa, Ontario K1A 0R6
brad.gover@nrc-cnrc.gc.ca

1. INTRODUCTION

In evaluating room acoustics, sound transmission through walls and floors, or other building acoustics problems, a directional sound detector can potentially be of great value. Beamforming microphone arrays have become increasingly practical and affordable in recent years, and can make flexible and highly directional detectors. This paper describes two recently developed arrays, and application to some building acoustics problems.

2. ARRAY DESIGN ALGORITHM

For a given geometrical arrangement of sensors (omnidirectional microphones), any number of beamformers can be implemented to realize a variety of beampatterns. A simple approach is to “delay and sum” the element signals, with no magnitude scaling. A more powerful approach is to “filter and sum” to implement a frequency-dependent magnitude and phase weighting for each sensor signal. For a given set of sensor weights $\mathbf{w}(\omega)$, the *array gain* $G(\omega)$ at frequency ω is given by

$$G(\omega) = \frac{\mathbf{w}^H \mathbf{R}_{SS} \mathbf{w}}{\mathbf{w}^H \mathbf{R}_{NN} \mathbf{w}}, \quad (1)$$

where \mathbf{R}_{SS} is the signal correlation matrix, determined by the steering direction, and \mathbf{R}_{NN} is the noise correlation matrix, determined by the noise at the sensors. One robust beamformer design seeks to maximize G , subject to constraints on the white noise gain [1]. The white noise gain is given by Eq. (1) for the case $\mathbf{R}_{NN} = \mathbf{I}$, and is a measure of the ability of the beamformer to tolerate uncorrelated noise.

In the current work, an estimate of the sensor magnitude and phase mismatch is used to construct a noise constraint [2]. The signal and noise correlation matrices in Eq. (1) are replaced with the expected matrices, incorporating the mismatch, and the sensor weights \mathbf{w} that maximize G are determined for a range of frequencies. This procedure specifies, in the frequency domain, the filter weights \mathbf{w} .

3. ARRAYS

Two types of arrays have been designed and constructed. Shown in Fig. 1(a) is a 16 cm diameter “open” or “free field” array, in which 32 omnidirectional electret microphones (6 mm diameter) lie on the surface of a (notional) sphere. This array has been discussed in Ref. [3]. The geometry is that of a “pentakis dodecahedron”, related to the familiar 32-faced soccer ball. Fig. 1(b) shows the array gain versus frequency assuming a 0.1 dB sensitivity mismatch among microphones (solid curve). Shown for comparison are: the maximum gain possible assuming no sensor mismatch (dash-dot curve), and the gain for a delay and sum beamformer (dashed curve). Fig. 1(c) shows the white noise gain for all three beamformer designs. The higher the white noise gain, the better the ability to tolerate noise. Fig. 2 shows comparable results for a newly-constructed 10 cm diameter rigid array, in which 32 omnidirectional electret microphones (6 mm diameter) are flush mounted in the surface of a hollow aluminum sphere. The scattering of sound by the sphere is taken into consideration in the beamformer design. The rigid sphere increases the apparent separation of the microphones, and also serves to smooth the white noise gain.

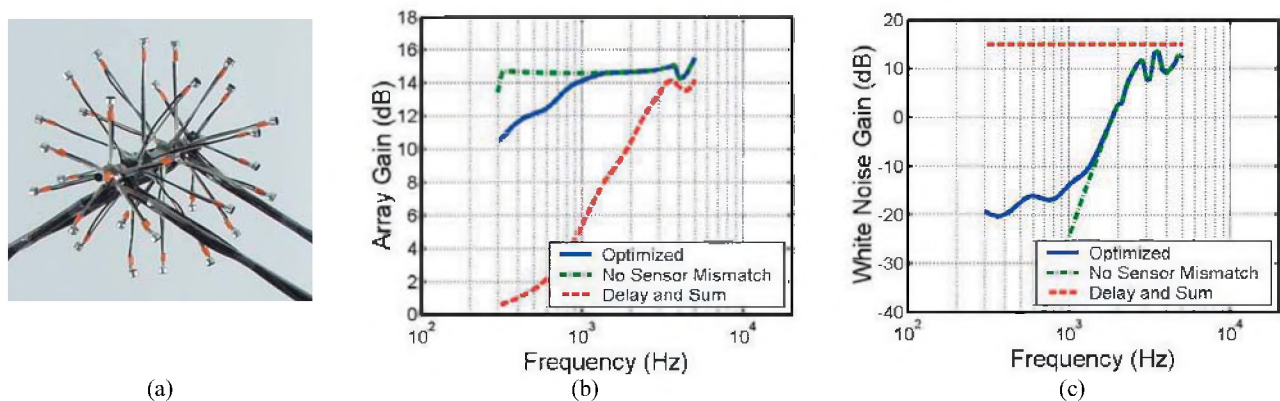


Fig. 1: 16 cm diameter “free field” array: (a) Photograph, (b) array gain and (c) white noise gain for: optimal design assuming 0.1 dB sensor mismatch (solid curve), no sensor mismatch (dash-dot curve), and delay and sum (dashed curve).

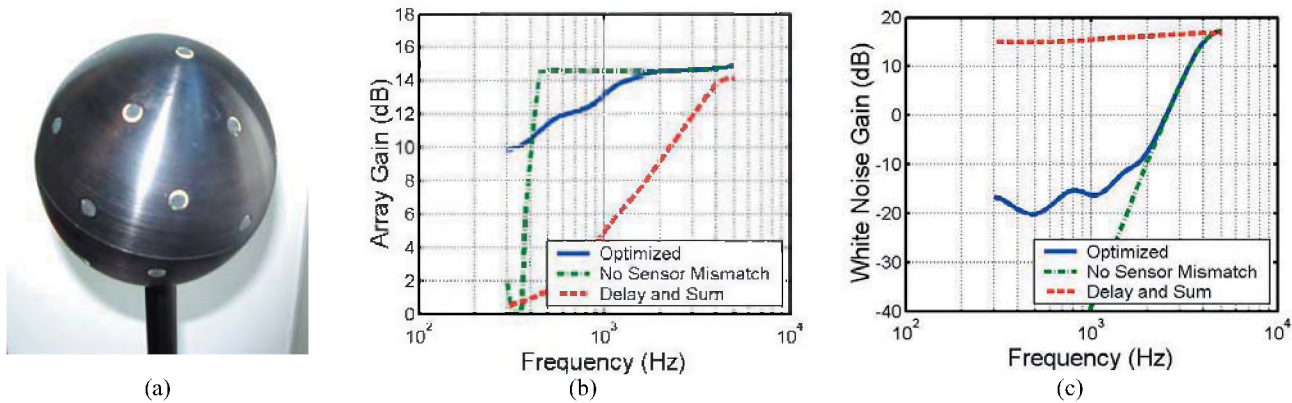


Fig. 2: 10 cm diameter rigid array: (a) Photograph, (b) array gain and (c) white noise gain for: optimal design assuming 0.1 dB sensor mismatch (solid curve), no sensor mismatch (dash-dot curve), and delay and sum (dashed curve).

It can be seen for both arrays that the optimal design “trades off” some robustness to noise for increased gain, or alternately, “trades off” some of the maximum theoretical gain for increased robustness to noise. For both arrays there is a frequency range of about 1.7 octaves over which the array gain is flat, and greater than 14 dB or so. The beam pattern in this range (not shown) has a main lobe beamwidth of about 28 degrees.

4. APPLICATIONS

4.1. Analysis of sound fields in rooms

Shown in Fig. 3 are results from Ref. [4] using a free field array to measure sound arriving at a point in a lecture theatre. The room is shown in (a), and the omnidirectional impulse response at one of the array elements is shown in (b). In panels (c)–(e), the radius of the surface in a given direction indicates the level arriving from that direction. Panel (c) shows the levels arriving at the array position over the entire time record, allowing analysis of the isotropy of the sound field. Panels (d), (e) indicate the directions of incidence of individual arrivals or reflections.

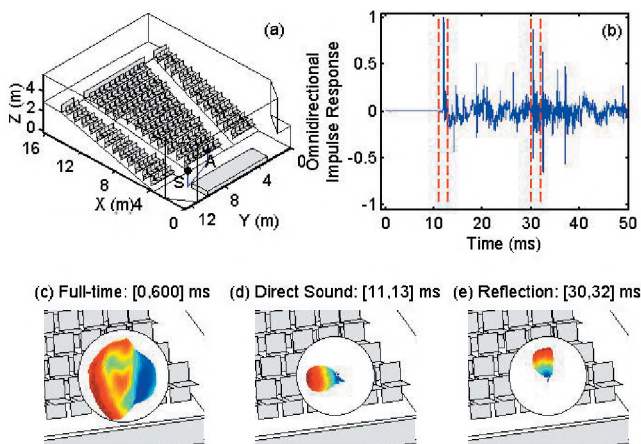


Fig. 3: Measurement in lecture theatre: (a) room, array position (A), and source position (S); (b) omnidirectional impulse response; (c) sound arriving at array position, integrated over entire time record; (d) sound arriving at array between 11–13 ms, corresponding to direct arrival; (e) sound arriving at array between 30–32 ms, corresponding to ceiling reflection.

4.2. Detection of sound leaks in walls

Figure 4 shows results from Ref. [5] indicating the levels arriving at a free field array, projected onto a wall that separated the array from the room containing the sound source. The wall contained a pair of back-to-back electrical boxes, which caused increased levels at the array position, arriving from their direction. The boxes constituted a sound leak in the wall, which was identified by the array.

Two Electrical Boxes: Back-to-Back : Array at 1.05 m
1250 Hz : 1-30 ms : DR = 13.2 dB : $\sigma = 2.6$ dB

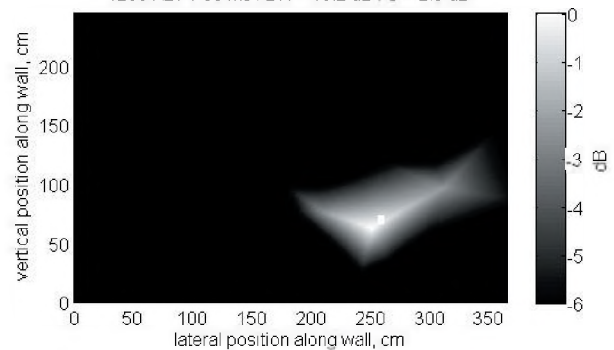


Fig. 4: Levels arriving at array position, projected onto wall that contained back-to-back electrical boxes. Light feature indicates increased sound transmission through the defect.

5. CONCLUSIONS

Beamforming microphone arrays are promising diagnostic tools for the analysis of sound in buildings. The array designs can be highly directional and robust.

REFERENCES

- [1] H. Cox, et al., IEEE Trans. ASSP, **35** 1365–1376, 1987.
- [2] M.R. Stinson and J.G. Ryan, Canadian Patent Application 2292357, filed Dec. 1999. Available from <http://patents1.ic.gc.ca/>
- [3] B.N. Gover, et al., J. Acoust. Soc. Am., **112**, 1980–1991, 2002.
- [4] B.N. Gover, et al., J. Acoust. Soc. Am., **116**, 2138–2148, 2004.
- [5] B.N. Gover and J.S. Bradley, Convention Paper presented at 121st Audio Engineering Society Convention, San Francisco, 2006.

ACKNOWLEDGEMENTS

Portions of this work developed in collaboration with Jim Ryan (Gennum Corporation), and Mike Stinson (NRC). Final assembly of the rigid array was by San Nguyen.

THE EFFECT OF SENTENCE REPETITION ON SPEECH INTELLIGIBILITY IN NOISE

Roxanne Larose, Isabelle Mercille, Christian Giguère, Chantal Laroche, Véronique Vaillancourt

Audiology/SLP Program, University of Ottawa, Ontario, K1H 8M5

1. INTRODUCTION

Good verbal communication is essential to ensure safety in the workplace and active social participation during daily activities. In many situations, however, speech comprehension may be difficult due to hearing problems, the presence of noise or other factors. As a result, listeners must sometimes ask the speaker to repeat what was said in order to understand the complete message. A few early studies indicated that repetition may slightly increase speech intelligibility, primarily for the first repetition [1-3]. However, there is relatively little data available on the exact benefits of this commonly-used strategy for different noise conditions, despite Pollack's early observation that the "*diversity of successive speech and/or noise samples is an important determinant of the improvement in intelligibility with successive presentations*" [4].

The objectives of this research are: (1) to compare the relative benefits of repetition on word intelligibility under continuous and fluctuation noise conditions, and (2) to document the effect of noise conditions on the parameters of the performance-intelligibility (PI) function for sentences spoken once or twice. Intuitively, one can hypothesize that the benefit of repetition on intelligibility may be greater under fluctuating than continuous noise conditions, if independent noise samples are used on the first and second presentations. Under fluctuating noise conditions, the listener may be able to benefit from masking troughs during the repetition to identify speech sounds masked upon the initial presentation. Under continuous noise conditions, speech sounds are uniformly masked across presentations.

2. METHOD

2.1 Subjects

Eighteen French-speaking subjects (10 males, 8 females), aged between 20 and 30 years, participated in the study. Subjects had normal hearing defined by the following criteria: a) air conduction hearing threshold ≤ 15 dBHL between 0.6 and 6 kHz bilaterally; b) normal tympanograms, c) negative otologic history, and (d) score on the Canadian French HINT test [5] within normal.

2.2 Materials

Subjects were presented lists of 20 sentences from the Canadian French HINT test under three different noises selected from the ICRA database [6]: continuous speech-spectrum noise for a male speaker (Noise A), modulated speech-spectrum noise corresponding to a single speaker

(Noise B), and modulated speech-spectrum noise corresponding to a group of 6 persons speaking simultaneously (Noise C). They correspond to ICRA1, ICRA5 and ICRA7 noises respectively. Listening tests were carried out at three different S/N ratios for each of the three noises, for a total of 9 experimental conditions per subject. A different list of sentences was chosen for each condition. Lists were counterbalanced across subjects, noises and S/Ns.

2.3 Procedure

The speech lists were so designed that each of the 20 independent sentences was presented twice. After the first presentation, the subject was requested to repeat or guess what was heard and the experimenter scored the number of words correctly identified. The same recorded sentence was then presented a second time and the subject was again requested to repeat what was heard for scoring purposes. It was thus possible to obtain two scores for each experimental condition: a percent intelligibility on the initial presentation of the 20 sentences and a similar score after the second presentation (i.e. repetition). Independent noise samples were used on the first and second presentation of each sentence. Thus, instantaneous noise masking peaks and troughs were not synchronized with the speech waveform upon successive presentations of the same sentence.

3. ANALYSIS AND RESULTS

A simple means of characterizing the effect of repetition was used to interpret the experimental results. If one assumes that the probability of words correctly recognized on the initial presentation is p , then the probability of incorrect recognition is $q=1-p$. If the spoken communication is repeated in the same conditions, and the probabilities of correct and incorrect word recognition remain the same and are independent of the initial presentation, then the joint probability of incorrect word recognition after the repetition is q^2 , and the probability of correct recognition is $1-q^2 = p + pq$. The term pq represents the benefit of repetition if the assumptions above hold true. A more general model, $p + \alpha pq$, is obtained by introducing a repetition coefficient α to adjust the contribution from the second presentation to the overall probability of correct recognition ($0 \leq \alpha \leq 1/p$). If α is 0, the second presentation does not improve recognition. If $\alpha = 1$, word recognition is independent of presentation. Figure 1 illustrates the percent word recognition after the second presentation as a function of percent recognition during the first presentation for different coefficients α of the repetition model.

The repetition model can also be used to predict the effect of the second presentation on the shape of the performance-intensity (PI) function in different noise conditions (as determined by different repetition coefficients α). This is illustrated in Figure 2. As can be seen, repetition is expected to decrease the SRT and increase the slope of the PI function, and these effects are more important the larger the repetition coefficient α .

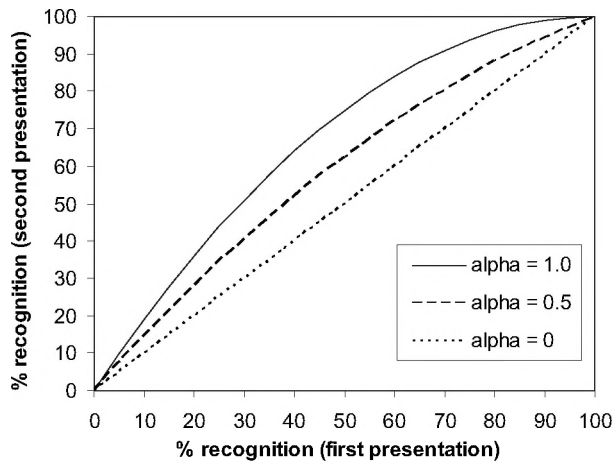


Fig. 1: Repetition effect for different coefficients α (0, 0.5, 1.0) of the repetition model.

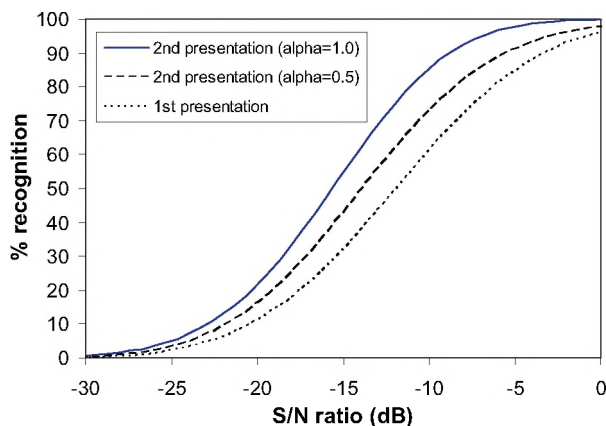


Fig. 2: PI functions for two hypothetical values of the repetition coefficient α in comparison with the PI function for the initial presentation (SRT = -12 dB S/N and slope of 6%/dB).

Table 1 lists the optimal repetition coefficient calculated from an analysis of the experimental data obtained in the three noise conditions used in this study. These coefficients carry the least amount of error between model predictions and the experimental data for each noise. As expected, the continuous speech-spectrum noise (Noise A) exhibits the lowest repetition coefficient α , and the most highly modulated noise (Noise B) exhibits the highest α . In the latter case, the value is very close to 1, indicating statistical independence of the first and second presentations.

The experimental data were also analyzed to extract the SRT and the slope of the PI function in the three noises and two presentation conditions. Table 1 lists the improvement in SRT between the first and second presentations, and the ratio of PI slopes in the three noises conditions. Repetition improves the SRT and increases slightly the slope of the PI function, as expected. The improvement in SRT ranges from 2.0 to 5.4 dB across noises. The PI slope increases by up to 34%. These effects are most pronounced for the most highly modulated noise (Noise B), and least pronounced for the continuous noise (Noise A). Thus, dependence of the repetition effect on noise type is confirmed.

Table 1: Summary of results: repetition coefficient α , difference in SRT between presentations, and ratio of PI slopes (A: continuous noise, B: modulated noise from a single speaker, C: modulated noise from 6 speakers).

Noise	α	SRT ₂ - SRT ₁ (dB)	Slope ₂ /Slope ₁
A	0.65	-2.0	0.98
B	0.98	-5.4	1.34
C	0.89	-3.2	1.11

4. CONCLUSIONS

Results show that the benefit of repeating sentences in noise depends on the temporal structure of the noise for normally-hearing listeners. The larger the temporal fluctuations in the noise, the more benefits in intelligibility can be gained by repetition. The experimentation needs to be replicated for a group of hearing-impaired individuals to determine if the main results generalize to this population.

The findings of this study could be useful in a wider context to develop predictive tools to assess speech communication scenarios under various listening conditions [7].

REFERENCES

- [1] Miller, G.A., Heise, G.A. & Lichten, W. (1951). The intelligibility of speech as a function of the context of the test materials. *J. Exp. Psychol.* 41, 329-335.
- [2] Thwing, E.J. (1956). Effect of repetition on articulation scores for PB words. *J. Acoust. Soc. Am.* 28: 302-303.
- [3] Clark, J.E., Dermody, P. & Palethorpe, S. (1985). Cue enhancement by stimulus repetition: Natural and synthetic speech comparisons. *J. Acoust. Soc. Am.* 78, 458-462.
- [4] Pollack, I. (1959). Message repetition and message reception. *J. Acoust. Soc. Am.* 31, 1509-1515.
- [5] Vaillancourt V., Laroche, C. Mayer C. et al. (2005). Adaptation of the HINT (Hearing In Noise Test) for adult Canadian Francophone populations. *Int. J. Audiology* 44, 358-369.
- [6] Dreschler, W.A., Verschuure, H., Ludvigsen, C. & Westermann, S. (2001). ICRA Noises: Artificial noise signals with speech-like spectral and temporal properties for hearing aid assessment. *Audiology* 40, 148-157
- [7] Laroche, C., Soli, S., Giguère, C. et al. (2003). An Approach to the Development of Hearing Standards for Hearing-Critical jobs. *Noise & Health*, 6(21), 17-37.

The role of formant amplitude in the perception of /i/ and /u/ in normal hearing listeners

Lacey Marshall, Teresa Enright, and Michael Kieffe

School of Human Communication Disorders, Dalhousie University, 5599 Fenwick Street, Halifax, NS, Canada, B3H 1R2

1. INTRODUCTION

It is known that each vowel in English has a unique configuration of formants, and this configuration is thought to help in the discrimination of vowel sounds. It is generally accepted that the three lowest formants are the most important for vowel perception (Rosner & Pickering, 1994). However, it is still debated whether it is formant frequency, spectral shape, or some combination of formant frequency, spectral shape, and formant amplitude that makes the largest contribution to vowel perception.

Although early studies indicated that formant amplitude plays only a minor role in vowel perception (e.g., Miller, 1984), recent research has indicated that formant amplitude may be more important than previously thought (Nabelek et al., 1992). However, effects of formant amplitude as observed in Nabelek et al. (1992) could instead be due to relatively basic psychoacoustic phenomena such as simultaneous masking. Perhaps related to this, Ainsworth and Millar (1972) concluded that listeners' perception of vowels changed when the amplitude of F_2 was decreased, but only when the difference in the amplitudes of F_1 and F_2 was no more than 28 dB.

Aaltonen (1985) performed a series of perception experiments in which the amplitude of F_2 and F_3 was varied in the Finnish vowels /i/ and /y/. It was found that reducing the amplitude of F_2 alone increased the number of /i/ responses, while reducing the amplitude of F_3 alone resulted in more /y/ responses. Aaltonen suggested that the reason for this response pattern was that when the amplitude of F_2 was reduced, F_3 was perceived as F_2 .

Hedrick and Nabelek (2004) used synthetic full-spectrum vowels in a perception experiment in which the amplitude of F_2 was decreased in a nine-step continuum from /u/ to /i/. The results indicate that, for normal hearing listeners, a decrease in the amplitude of F_2 resulted in a greater number of /i/ responses. In studying vowel perception, the use of full-spectrum vowels could be problematic because when F_2 amplitude is low relative to the amplitude of the harmonics between formants, formant peaks simply lose contrast as the peak becomes less sharp. With full-spectrum stimuli, it may be difficult to distinguish if a change in vowel perception is due to a change in the spectral saliency of the peak, or due to higher frequency formants being masked by lower formants.

The purpose of this research is to investigate what role formant amplitude plays in the perception of vowels for speakers of English. Though studies have manipulated either F_2 or F_3 individually, this study varied the amplitude of both F_2 and F_3 in a fully-crossed design. This is done in order to separate out the perceptual effect of spectral tilt, which is a potential confound in synthetic monophthongs (Kieffe & Kluender, 2005).

Because changes in identification could be due to loss of spectral sharpness or simultaneous masking, this study used two sets of stimuli to resolve this problem. Full-spectrum stimuli were synthesized normally while incomplete-spectrum stimuli consisted of harmonics at the centre of the first five formants, as well as one harmonic on either side.

2. METHOD

Figures 1 (a) and (b) show spectra of the /u/ and /i/ endpoints of the full-spectrum continuum, respectively. Likewise, figures 1 (c) and (d) show spectra of the /u/ and /i/ endpoints of the incomplete-spectrum continuum.

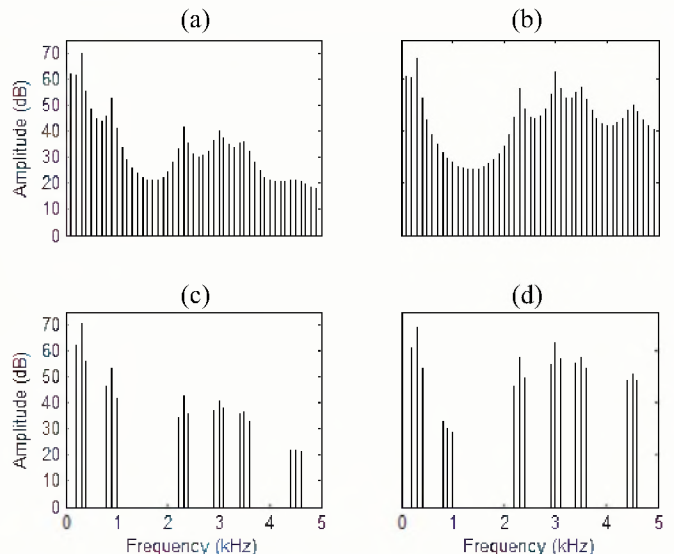


Fig. 1. Spectra of stimuli used in Experiment I.

Eligible participants completed a forced-choice vowel identification task with two sets of stimuli: full-spectrum and incomplete-spectrum. Participants labeled stimuli as either /i/ or /u/. The stimuli varied in amplitude of F_2 and F_3 in a fully-crossed 7x7 design. Each participant identified each stimulus 8 times. Each stimulus in the 7x7 design was pre-

sented randomly following the phrase “you will now hear the vowel...”.

3. RESULTS

The following figures present the number of /i/ responses of 14 participants for the full-spectrum and incomplete-spectrum, respectively. The maximum number of possible responses for each stimulus is 112.

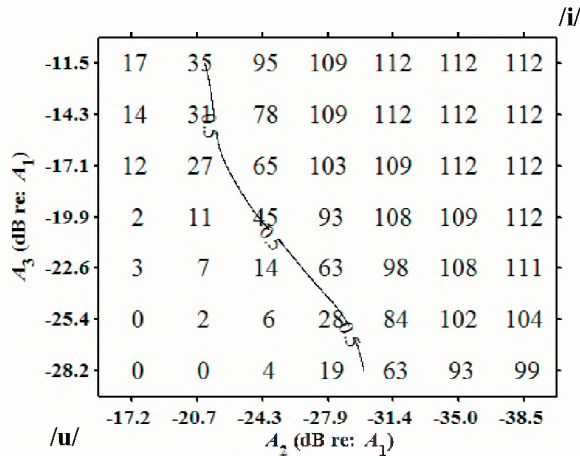


Fig. 2. Number of /i/ responses for the full-spectrum stimuli.

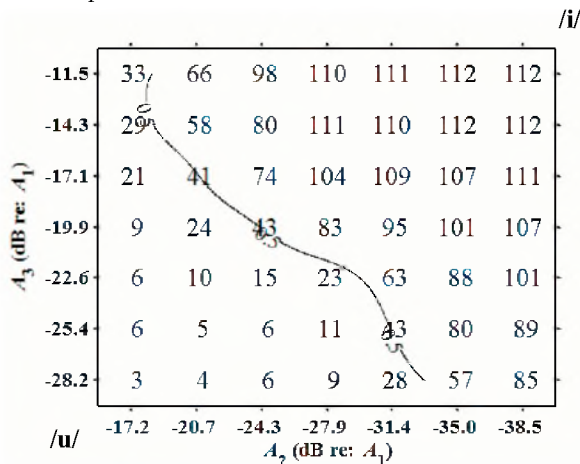


Fig. 3. Number of /i/ responses for the full-spectrum stimuli.

Overall, there were a greater number of /i/ responses in the full-spectrum condition. It is possible that this is a result of reduced spectral contrast. A potential explanation for this is that reduced spectral contrast caused listeners to perceive F_3 as F_2 , and identify the stimulus as /i/.

There were more /u/ responses in the incomplete-spectrum condition. One possibility is that listeners were able to perceive F_2 even at very low amplitudes.

Logistic regression was performed on the responses from each subject (McCullagh & Nelder, 1989). Regression coefficients were then subjected to within-subjects t -test (Davis, 2002). There was a significant difference in coeffi-

cients for F_2 amplitude between the two conditions ($p = .001$). However, there was no significant difference in coefficients for spectral tilt between the two conditions.

4. DISCUSSION

Results from this experiment suggest that several perceptual mechanisms may account for shifts in vowel identification with changes in formant amplitude. First, formant amplitude contributes to the global spectral shape of the vowel, which has been shown to influence vowel perception in synthetic monophthongs (e.g., Kiefe and Klunder, 2005). However, differences in response patterns between the two conditions suggest that spectral contrast in the region of F_2 also contributes to vowel identification. It is likely that simultaneous masking plays a role as well.

Future studies will continue to examine the role of F_2 in vowel perception using a signal detection task. Participants will be presented with stimuli that are identical in formant frequency and amplitude, except that in some pairings the second formant has been removed. Three different pairings will be used: identical, unaltered stimuli; one unaltered stimulus followed by one altered stimulus; one altered stimulus followed by one unaltered stimulus. The stimuli will be separated by 250 ms of silence. Participants will be asked to choose if the stimuli are the same or different.

REFERENCES

- Aaltonen, O. (1985). The effect of relative amplitude levels of F_2 and F_3 on the categorization of synthetic vowels. *Journal of Phonetics*, 13, 1-9.
- Ainsworth, W.A. & Millar, J.B. (1972). The effect of relative formant amplitude on the perceived identity of synthetic vowels. *Language and Speech*, 15, 328-341.
- Davis, C.S. (2002). *Statistical Methods for the Analysis of Repeated Measurements*. New York: Springer.
- Hedrick, M.S. & Nabelek, A.K. (2004). Effect of F_2 intensity on identity of /u/ in degraded listening conditions. *Journal of Speech, Language, and Hearing Research*, 47, 1012-1021.
- Ito, M., Tsuchida, J. & Yano, M. (2001). On the effectiveness of whole spectral shape for vowel perception. *Journal of the Acoustical Society of America*, 110(2), 1141-1149.
- Kiefe, M. & Klunder, K.R. (2005). The relative importance of spectral tilt in monophthongs and diphthongs. *Journal of the Acoustical Society of America*, 117(3) 1395-1404.
- McCullagh, P. & Nelder, J.A. (1989). *Generalized Linear Models*, 2nd ed. London: Chapman & Hall.
- Miller, J.D. (1984). Auditory processing of the acoustic patterns of speech. *Archives of Otolaryngology*, 110, 154-159.
- Nabelek, A.K., Czyzewski, Z., & Krishnan, L.A. (1992). The influence of talker differences on vowel identification by normal hearing and hearing-impaired listeners. *Journal of the Acoustical Society of America*, 92(3), 1228-1246.
- Rosner, B.S. & Pickering, J.B. (1994). *Vowel Perception and Production*. Oxford: Oxford University Press.

HEARING AND COGNITIVE PERFORMANCE IN LOW-FREQUENCY NOISE

Ann M. Nakashima, Sharon M. Abel, Matthew Duncan and David Smith

Defence Research and Development Canada – Toronto, P.O. Box 2000, 1133 Sheppard Ave West,
Toronto, ON, M3M 3B9 E-mail: ann.nakashima@drdc-rddc.gc.ca

1. INTRODUCTION

A recent investigation of noise and whole-body vibration exposure in Canadian Forces armoured vehicles found that the noise during high-speed driving is low-frequency dominant [1]. The crewmembers also indicated in their questionnaire responses that they had difficulty communicating inside the vehicle because of the noise. Low-frequency noise (LFN) may present challenges that are different from those associated with broadband noise because 1) it is difficult to attenuate with conventional hearing protectors, 2) low-frequency sounds mask higher frequency sounds, which may impair the ability to understand speech or detect auditory alarms and 3) it has been shown to cause greater annoyance and disruption in concentration than broadband noise, which may affect cognitive performance [2]. It was thus of interest to study hearing and cognitive performance in low frequency noise. In this study, auditory detection, speech intelligibility and cognition (by means of a cognitive test battery) were investigated in the presence of different noise exposures (quiet, pink noise and recorded armoured vehicle noise). The effects of wearing hearing protection (passive and active noise reduction [ANR]) were also examined.

2. MATERIALS AND METHODS

This study was approved by the Human Research Ethics Committee of DRDC Toronto. In total, 36 subjects (18 males and 18 females), aged 18 to 55 years with hearing thresholds no greater than 25 dB HL at 0.5 kHz, 1 kHz, 2 kHz and 4 kHz were chosen for participation. The subjects were divided into three groups of 12, balanced between age and gender. The first group performed the battery of tests in quiet, the second group in pink noise at 80 dBA and the third group in recorded LAV III noise (light-armoured vehicle) at 80 dBA. The subjects were tested under three listening conditions: unoccluded, wearing a passive earmuff (David Clark H10-13XL, ANR off) and wearing an active earmuff (David Clark H10-13XL, ANR on). The spectra of the pink and vehicle noise are shown in Fig. 1.

Auditory detection was measured using a variation of Békésy tracking [3] at six third octave band frequencies from 0.5 kHz to 8 kHz. Speech understanding was evaluated using the Modified Rhyme Test (MRT) of consonant discrimination [4]. The level at which the target

words were presented was adjusted iteratively such that 60% of the words were correctly recognized.

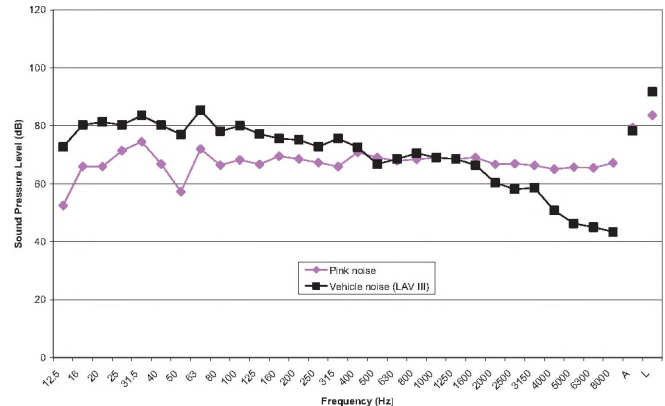


Fig. 1. Spectra of the pink and vehicle (LAV III) background noises.

The cognitive test battery consisted of a subset of tasks that have been used extensively in previous performance studies conducted at DRDC Toronto. The tasks included two subjective questionnaires (relating to mood, motivation and fatigue), a short term memory task, a serial reaction time task, mental addition, detection of repeated numbers and a logical reasoning task. For the questionnaires, subjects responded using a visual analogue scale (VAS) from 1 to 10. Descriptions of the tasks are given in [5].

3. RESULTS

3.1 Detection

The mean detection thresholds in the three backgrounds (quiet, pink noise and vehicle noise) are shown in Fig. 2 for the three ear conditions (unoccluded, ANR off and ANR on). In quiet, mean unoccluded thresholds were less than 20 dB from 0.25 to 2 kHz and 8 kHz. The threshold for 4 kHz was outside the range of the system for all subjects. When the muff was worn with ANR off, significant increases to 36 dB SPL were observed across the frequency region tested. With ANR on, significant increases to 52 dB at 0.25 kHz and 0.5 kHz, and 40 dB at 1 kHz were realized, compared to ANR off ($p < 0.001$). Detection thresholds in pink noise

were fairly consistent at 60 to 70 dB SPL regardless of ear condition or frequency. By comparison, detection thresholds in vehicle noise decreased from 79 dB SPL at 0.25 kHz to 45 dB SPL at 8 kHz. From 0.5-2 kHz, detection thresholds in the pink and vehicle noises, with or without earmuffs worn, were similar at 66 dB SPL.

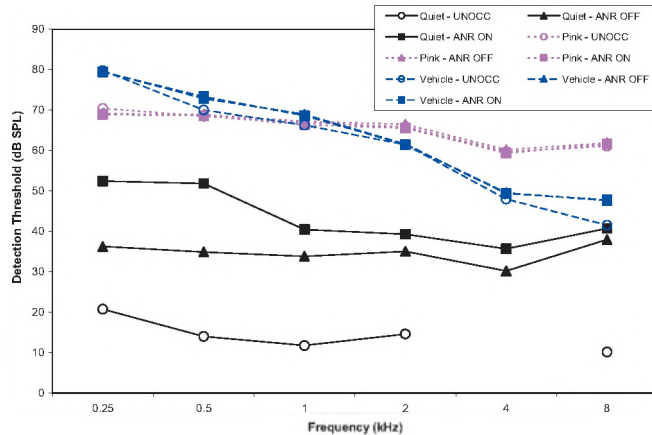


Fig. 2. Detection thresholds in quiet, pink noise and vehicle (LAV III) noise under three ear conditions: unoccluded (UNOCC), muff with ANR off and muff with ANR on.

3.2 Modified Rhyme Test

The mean speech levels required for 60% correct understanding are given in Table 1. An ANOVA applied to these data showed significant effects of group, ear condition and group by ear condition ($p < 0.001$). The required speech levels were significantly higher in both types of noise than in quiet, but there were no differences due to ear condition in the presence of noise (pink or vehicle). The increase in required speech level by 4 dB in pink noise compared to vehicle noise was significant.

Table 1. Speech levels (and standard deviations) required for 60% correct responses on the MRT.

Ear condition	Speech level required for 60% correct (dB SPL)		
	Background noise		
	Quiet	Pink	Vehicle
Unoccluded	41.4 (4.5)	88.8 (3.3)	84.5 (3.0)
ANR off	58.2 (4.7)	87.6 (3.4)	84.4 (2.8)
ANR on	63.6 (3.4)	87.6 (2.5)	84.0 (2.8)

3.3 Cognitive Test Battery

Analysis of the cognitive test battery results is in progress. The subjective questionnaire responses are particularly difficult to interpret because of the wide range of responses given. The preliminary analysis of

performance on the cognitive tasks indicates that both pink and vehicle noise interfere with performance on vigilance tasks (serial reaction time, detection of repeated numbers).

4. DISCUSSION

The preliminary results of this study indicate that the use of the ear muff in pink or vehicle noise did not significantly affect signal detection at any frequency, for both the passive and active modes. This finding was consistent with the MRT results. A small, but significant (4 dB) increase in speech level was required for 60% correct understanding in pink noise compared to vehicle noise. This indicated that the vehicle noise had a weaker masking effect on speech. For the cognitive tests, it appears that the presence of noise affects vigilance, but does not affect performance on short-term memory or reasoning tasks.

5. ACKNOWLEDGEMENTS

The authors would like to thank Lauren Batho and Quan Lam for their assistance in running this study.

REFERENCES

1. Nakashima AM, Borland MJ and Abel SM. (2005). Characterization of noise and vibration exposure in Canadian Forces land vehicles. DRDC Toronto Technical Report 2005-241.
2. Persson Wayne K, Rylander R, Benton S. and Leventhall HG. (1997). Effects on performance and work quality due to low frequency ventilation noise. *J. Sound. Vib.* 205(4),467-474.
3. Brunt MA., (1985). Bekey audiometry and loudness balance testing. In: Katz, J, (ed.) *Handbook of Clinical Audiology*. 3rd ed. (Baltimore: Williams & Wilkins), pp. 273-291.
4. House AS, Williams CE, Hecker MH and Kryter KD. (1965). Articulation-testing methods: Consonantal differentiation with a closed-response set. *J. Acoust. Soc. Am.* 37, 158-166.
5. Abel SM et al. (2004). Hearing and performance during a 70-hr exposure to noise simulating the space station environment. *Aviat. Space and Environ. Med.* 75(9), 764-770.

WAKE ACOUSTIC MEASUREMENTS AROUND A MANEUVERING SHIP

Mark V. Trevorrow¹, Boris Vasiliev¹, and Svein Vagle²

¹Defence R&D Canada Atlantic, 9 Grove St., Dartmouth, N.S., B2Y 3Z7 mark.trevorrow@drdc-rddc.gc.ca

²Institute of Ocean Sciences, 9860 W. Saanich Rd., Sidney, B.C., V8L 4B2 vagues@dfo-mpo.gc.ca

1. INTRODUCTION

Ships are significant source of underwater sound, and their bubbly wakes generate significant disturbances to the near-surface underwater acoustic environment. Wakes are important because medium- to high-frequency acoustic systems, such as active sonars and underwater acoustic telemetry modems, are often operated from moving ships. Additionally, certain types of torpedoes exploit wakes to home in on a ship. The wake bubble properties while a ship is cruising on a straight course are reasonably well known (e.g. Trevorrow et al. 1994). However, ship maneuvers are thought to significantly increased wake depths and bubble densities. Since aggressive maneuvering is key to torpedo evasion, it is important to understand bubbly wake properties under these conditions.

In a collaboration between DRDC Atlantic and the Institute of Ocean Sciences, a set of four Broad-band Underwater Recording Buoys (BURBs) were built, providing a means for recording both underwater radiated noise and man-made acoustic transmissions. These self-contained buoys digitally record two hydrophone channels along with their differential GPS position. These buoys were built upon earlier systems for marine mammal monitoring on the B.C. coast (Vagle et al. 2004). In the case of ship trials with BURBs, GPS receivers on all surface craft provide sufficient information to calculate the ship's radiated source levels and acoustic propagation losses in the wake.

This work describes an initial underwater acoustic measurement trial conducted in April 2005 utilizing the *CCGS Vector* (40 m LOA) in Saanich Inlet, B.C. A variety of straight-line and maneuvering runs past the BURBs were made with the ship. Simultaneously, a separate acoustic source, transmitting 2 - 18 kHz LFM pulses, was utilized to probe the wake. This work focuses on the acoustic propagation measurements.

2. INSTRUMENTATION

The BURB system was composed of a set of four, identical self-contained buoys, each complete with the necessary hydrophones, cables, connectors, batteries, and GPS receivers. A detailed description of the BURBs is given in Trevorrow et al. 2005. Each buoy supported two independent hydrophone channels, each digitized at 40,000 samples per second with 16-bit resolution. Each BURB was

equipped with a differential GPS receiver, providing position and time synchronization data at 1-s intervals. Mechanically, each buoy was constructed around a 20.3 cm diameter by 92 cm long pressure housing, with a 20-cm high by 61-cm diameter foam floatation. The total weight of each buoy (in air) was 47 kg. Connection to the internal computer for configuration and data download was provided through industry-standard VNC protocols over ethernet.

The BURB hydrophones were omni-directional, broad-band (10 Hz to >20 kHz) receivers with an integral 20 dB pre-amplifier. The receiver electronics were designed for a maximum sound pressure level (SPL) of approximately 185 dB re 1 μ Pa. Up to a 55 dB in data-adaptive gain was provided. In these trials the two hydrophones on each BURB were suspended at depths of 5 and 15 m.

For the pulse propagation tests, a Medium-Frequency Multi-Mode Pipe Projector (MF-MMPP, see Fleming 2003) was used to transmit 2 - 18 kHz x 10-ms duration LFM pulses twice per second. Using a portable audio amplifier, the nominal acoustic source level was 180 dB (re 1 μ Pa at 1 m) across this band. The transmit pulse was pre-compensated for the frequency response of the MF-MMPP. This transmitter was deployed at 5 m depth from a small boat, which was allowed to freely drift on the opposite side of the ship wake from the BURBs. Acoustic transmissions were started approximately 2 minutes before the ship run, and continued for approximately 10 minutes after the ship passage. Ship speed during the runs were between 10 and 12 knots. At the same time other small boats conducted CTD casts and HF echo-sounder transects across the wake.

3. RESULTS

Although detailed analysis of the pulse propagation data is still underway, some preliminary results are presented here to show typical features of the field data. The first stage of processing was to match-filter the received time-series, extracting peak power of the LFM pulses. Corrections for spherical spreading loss (absorption is negligible at these frequencies and ranges) were applied. Figures 1 and 2 show comparisons of the received pulse power at the two BURB hydrophones for a straight-line and 180° turning runs. Direct and surface-reflected arrivals were separated by less than 1 ms; bottom-reflected paths arrive more than 100 ms later. In both cases the separation

of the source and BURB was approximately 200 m. There was a negligible near-surface sound-speed gradient during these trials, so refraction effects can be ignored.

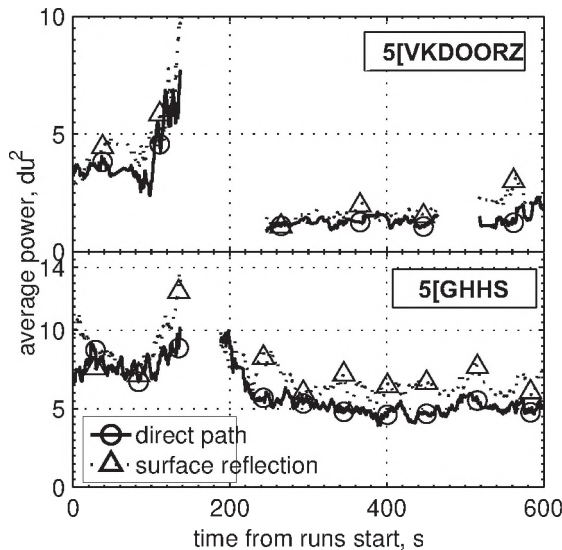


Figure 1. Matched-filter output power vs. time for LFM pulses received at 5 and 15 m depth for a straight-line ship run. Ship crosses line between source and receiver at time = 150 s.

In both cases the received pulse power prior to transit of the ship provided a baseline, which although different between the shallow and deep hydrophones, were similar for the two run types. In both cases there was a significant drop-out of roughly 60 to 100 s duration, coincident with the ship passing by the BURB. Analysis of the pulse signal-to-noise ratio reveals that this drop-out was simply due to the masking effect of the ship radiated noise.

In general the wake effects were more pronounced for the shallow receiver, where both the direct and surface-reflected paths were similar in length and had to traverse the bubbly wake, which extends downwards to approximately 2 ship drafts, or 10 m depth. In both cases the continued reception of pulses after the ship noise drop-out was delayed in the shallow hydrophone relative to the deep hydrophone, due to acoustic masking in the wake. This was particularly evident in the case shown in Fig. 2 with an additional drop-out of at least 3 minutes relative to the deeper hydrophone. In both figures the shallow hydrophone power after ship transit was attenuated by approximately a factor of 2 to 4, an effect clearly attributed to acoustic extinction within the wake.

As expected the masking effects for the deeper hydrophone were less pronounced. In Fig. 1 the direct path power was reduced to about 60% of its baseline state. In Fig. 2 there appeared to be no significant reduction in deep hydrophone power relative to the baseline.

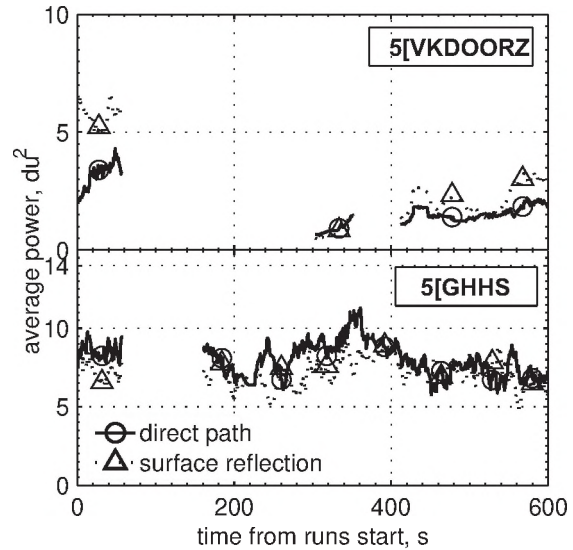


Figure 2. Matched-filter output power vs. time for LFM pulses received at 5 and 15 m depth for a 180° turn ship run. Ship crosses line between source and receiver at time = 90 s.

4. CONCLUSION

Significant acoustic dropouts due to the masking effects of ship radiated noise and the extinction effects from wake micro-bubbles were observed in near-surface pulse propagation, with the effects being more pronounced for shallow (< 5 m deep) acoustic paths. Maneuvering runs generally produced stronger wake acoustic extinction effects. Ongoing work will attempt to reconcile wake extinction losses described above with wake geometry and bubble densities that were measured by accompanying boats.

REFERENCES

- Fleming, R., 2003. High frequency multi-mode pipe projector, DRDC Atlantic TM2003-218.
- Trevorrow, M., S. Vagle, and D. M. Farmer, 1994. Acoustic measurements of micro-bubbles within ship wakes, *J. Acoust. Soc. Am.* **95**(4), 1922-1930.
- Trevorrow, M., S. Vagle, and N. Hall-Patch, 2005. Description and Field Evaluation of the Broad-Band Underwater Recording Buoy System, DRDC Atlantic TM 2005-231.
- Vagle, S., J. Ford, N. Erickson, N. Hall-Patch, and G. Kamitakahara, 2004. Acoustic recording systems for baleen whales and killer whales on the west coast of Canada. *Canadian Acoustics*, **32**(2), 23-32.

ACKNOWLEDGEMENTS

The instrumentation development and field work were supported under the Technology Investment Fund of Defence R&D Canada. Use of the *CCGS Vector* was provided by Fisheries & Oceans Canada.

MODELLING PULSE-TO-PULSE COHERENT DOPPLER SONAR

Len Zedel

Memorial University of Newfoundland, NL, Canada, A1B 3X7, zedel@physics.mun.ca

1. INTRODUCTION

Pulse-to-pulse coherent Doppler sonar can provide current profile information over ranges of order 1 m with sub-cm resolution, see for example (Zedel et al. 2002, Vagle et al. 2005). The analysis of the data is however complicated by the occurrence of range and velocity ambiguities (Brumley et al. 1990). These complications greatly restrict the general use of coherent Doppler to situations where one or both of the ambiguity problems can be constrained. Given the difficulties of working with coherent Doppler, design for any application is critical. A valuable tool in the design process is the ability to accurately model the system before committing to hardware. This paper reports on a computer model that can generate pulse-to-pulse coherent backscatter data. The model is used to simulate data that is compared to calibration data from a 1.7-MHz coherent Doppler sonar.

2. SONAR OPERATION

The phase of acoustic backscatter is determined by the geometric configuration of scatterers relative to the acoustic source and receiver. In coherent sonar, backscatter phase is compared between successive pulses. Coherent motion of the scatterers leads to a deterministic change in phase that is related to the speed of the scatterers. For backscatter geometry, the velocity radial to the transducer is given by

$$V = \frac{\Delta\phi}{\Delta t} \times \frac{C}{4\pi f}, \quad 1$$

where $\Delta\phi$ is the change in phase, Δt is the time between pulse transmissions, C is the speed of sound, and f is the operating frequency of the sonar.

Equation 1 is only valid if the backscatter from successive pulses is coherent. The presence of turbulence (leading to incoherent scatterer motion) and the motion of the scatterers through the acoustic sample volume lead to decorrelation.

3. MODEL DESIGN

In order to simulate coherent sonar operation, it is necessary to accurately reproduce backscatter that retains a coherent component but one that also accurately represents those processes that act to de-correlate the backscatter. The approach taken here is to model individual scatterers as randomly arranged point targets each assigned a velocity

from a prescribed velocity structure. A similar approach has been used in modelling backscatter from blood in medical Doppler applications (see for example Mo et al. 1992). The velocity structure allows for both a deterministic (time dependent) and random component to be included. The point targets are introduced into a (three dimensional) domain that is larger than the region sampled by the sonar (see Figure 1). Targets eventually drift out (down-stream) of the sample domain and are then replaced by new particles introduced on the upstream side: the total number of targets in the domain remains constant.

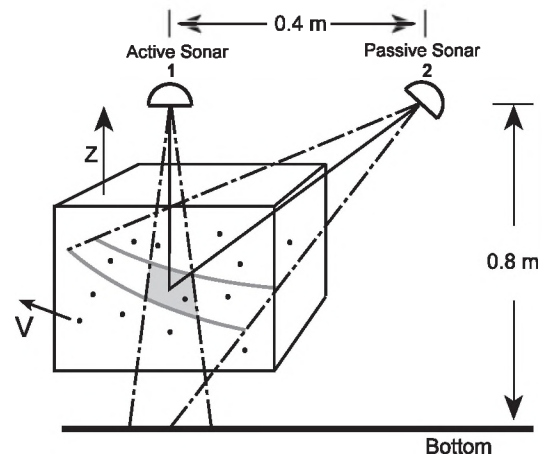


Fig. 1. Model rectangular domain is shown as it might be arranged with a bistatic sonar system. The dot-dash lines indicate sonar beams; point target scatterers are indicated as dots.

The acoustic backscatter is constructed by adding up contributions from each target in the domain accounting for the source-target-receiver geometry and transducer beam-patterns. Each target contributes a return pulse that is an amplitude-scaled replica of the (bandwidth limited) transmit pulse. The total return is given as

$$S(t) = \sum a_i s\left(t - \frac{(r_{si} + r_{ri})}{C}\right), \quad 2$$

where the summation is over all particles in the model domain, a_i is the backscatter amplitude of the i 'th target, $s(t)$ is the transmit pulse template, t is the time since the pulse transmission, r_{si} and r_{ri} are the source-target and target-receiver distances, and C is the speed of sound in water. A

simplification incorporated into Equation 2 is the absence of any time scaling associated with the Doppler shift of the moving particles. The backscatter signal from each scatterer is therefore the same saving a great deal of computation. Coherent Doppler is concerned with the changes between successive acoustic returns so that the absence of a Doppler shift on a single return does not affect the results (see discussion by Bonnefous and Pesque 1986).

Once the backscatter signal is generated, it is processed through simulated analog receiver circuitry and digitised to create the final (simulated) sonar data.

4. MODEL VALIDATION

The reliability of the model was validated both by assessing its performance relative to expected backscatter characteristics and also through comparisons with calibration test data for a 1.7-MHz coherent sonar.

Backscatter Statistics

The statistics of acoustic backscatter are such that phase should be uniformly distributed and amplitude should follow a Rayleigh distribution. Figure 2 shows phase and amplitude statistics for a model realisation accurately reproducing the expected statistics.

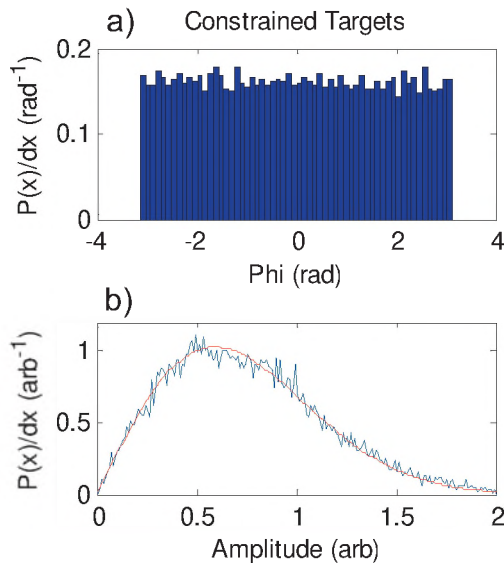


Fig. 2. Model backscatter statistics: a) backscatter phase, and b) backscatter amplitude. The solid (red) line represents a best-fit Rayleigh distribution.

Data Comparison

Calibration data collected with a 1.7-MHz coherent Doppler sonar was available to provide a reference with which to compare model output (Zedel et al. 1994). In coherent Doppler sonar, the quality of velocity estimates is determined by the correlation in backscatter between successive pulses. Aside from system noise and real velocity turbulence at scales below the resolution of the

sonar system, decorrelation is determined by the beam patterns and flow geometry (see Zedel et al. 1994). The model was configured to reproduce the geometry of those calibration tests and the excellent agreement between model and experiment is shown in Figure 3.

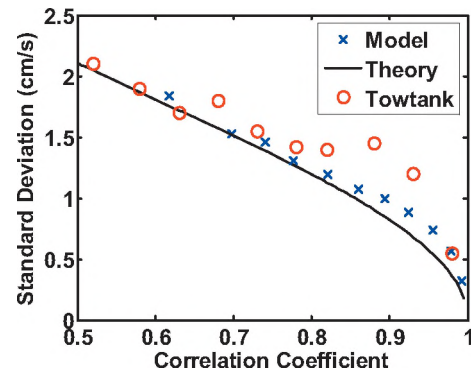


Fig. 3. Comparison of model output, towtank trials and theoretical predictions for the relationship between velocity standard deviation and pulse-to-pulse correlation coefficient.

5. CONCLUSIONS

A model of acoustic backscatter based on point targets that reflect an amplitude scaled copy of the transmit pulse can reproduce volume backscatter that retains the critical characteristics of pulse-to-pulse coherent sonar. This model provides a valuable tool in developing a new generation of coherent Doppler sonar.

REFERENCES

Bonnefous, O., Pesque, P. (1986). Time domain formulation for pulse-Doppler ultrasound and blood velocity estimation by cross correlation. *Ultrasonic Imaging*, 8, 73-85.
 Brumley, B., Cabrera, R., Deines, K., Terray, E. (1990). Performance of a broadband acoustic Doppler current profiler. *Proc. Of the IEEE 4'th Working Conf. on Current Meas.* 283-289.
 Mo L.Y.L., Cobbold R.S.C. (1992). A unified approach to modeling the back-scattered Doppler ultrasound from blood. *IEEE Trans. Biomed. Eng.* 39, 450-461.
 Vagle, S., Chandler, P., Farmer, D.M. (2005). On the dense bubble clouds and near bottom turbulence in the surf zone. *JGR*, 110 (C9).
 Zedel, L., Hay A.E. (2002). A three-component bistatic coherent Doppler velocity profiler: Error sensitivity and system accuracy. *IEEE J. Oceanic. Eng.* 27 (3) 717-725.
 Zedel, L., Hay, A.E., Cabrera, R., Lohrman, A. (1994). Performance of a single-beam pulse-to-pulse coherent Doppler profiler. *J. Atmos. and Ocean. Tech.*, 21, 290-297.

ACKNOWLEDGEMENTS

This work was undertaken while L. Zedel was on sabbatical in St. John's NL at the Institute for Ocean Technology of the National Research Council of Canada and their support is greatly appreciated.

HIGH FREQUENCY BROADBAND ACOUSTIC CHANNEL ESTIMATION ERROR ANALYSIS FOR ST. MARGARET'S BAY DURING THE UNET06 DEMONSTRATIONS.

Paul J. Gendron¹ and Garry J. Heard²

¹ONR Visiting Scientist, Acoustics Div., Naval Research Lab., 4555 Overlook Ave. SW, Washington DC, USA 20024

paul.gendron@drdc-rddc.gc.ca

²Defense Research Development Canada-Atlantic, 9 Grove St., Dartmouth NS, Canada, B3A 3C5

garry.heard@drdc-rddc.gc.ca

1. INTRODUCTION

We are interested in assessing the adversity of a shallow water acoustic channel to coherent communications. The shallow water channel presents a particularly difficult environment for high rate acoustic communications as channel conditions can change dramatically both spatially from site to site and temporally over durations as short as hours. Shallow water coastal environments can range from very calm with relatively coherent acoustic response functions to severely doubly spread environments where multi-path delay is coupled with path dependent Doppler. Doppler spreading is imparted by the temporal dynamics of the water column along with wind driven surface wave motion. Platform motion imparts severe temporal variations for paths that interact with a rough bottom. Each of these processes impact each acoustic path, with its individual launching and arrival angle, differently. The net effect of this delay spread and rapid temporal variation is that communication receivers must model the acoustic channel accurately in order to efficiently decode the sent data. It is the goal of this work to develop a computationally efficient estimator of the channel response function that includes the innovation variance associated with the temporal fluctuations of the channel and apply these to data collected in St. Margaret's Bay during the Unet06 demonstrations.

1.1 Experiment design

During the 2006 Underwater networking experiment (Unet06) DRDC-Atlantic with the Naval Research Laboratory conducted a number of high frequency broadband channel probe experiments designed to characterize the underwater acoustic channels adversity to communications

Figure 1 depicts the experiment layout. The DRDC multimode pipe projector (MMPP) provided a 185 dB // 1 nPa@1m source level at 44 kHz center frequency and was allowed to drift approximately 2 meters from the bottom in 70m of water at ranges between 300 m and 1 km from the NRL ACDS 8-element vertical receiver array. The receiver array was placed approximately mid water column and was sampled at 160 ksp/s. The doubly spread acoustic channel is estimated from the recorded data sets by an augmented Kalman recursion to be described.

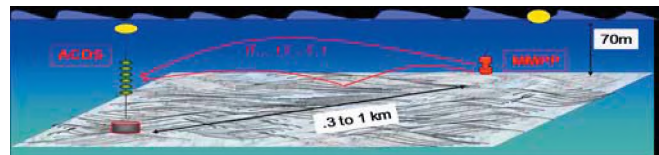


Figure 1, High frequency channel probe experiment. Source is a DRDC multimode pipe projector (MMPP) drifting 2 meters from the bottom. Receiver is an NRL ACDS unit with 2 meters of vertical aperture.

1.2 Model of Acoustic Response Dynamics

The posterior covariance of the acoustic channel is a function of the data and the innovation variance of the Gauss Markov response process. To compute the channel estimate and covariance function this latent innovation variance must be estimated. We augment, by an empirical Bayes approach [1], the Kalman recursion with a point estimate of the innovation variance to improve estimation of the acoustic response function. The underwater acoustic response function h_t is modeled as Gauss-Markov on the interval of observation, that is $h_t | h_{t-D}, q: N_h(Ah_{t-D}, qI_M)$, where $N_x(mS) = |2\pi S|^{-1/2} \exp\{-\frac{1}{2}(x-m)S^{-1}(x-m)\}$ and $x|y: p_x(y)$ denotes the density of x given y . By the form of the innovation covariance we have assumed that the innovation process is uncorrelated and invariant to path delay. The background noise at the k^{th} receive element is assumed to be spatially uncorrelated, stationary, but with temporal covariance S_k . The received data segment at the k^{th} hydrophone, over the t^{th} time interval is $r_{k,t}$, and distributed as $r_{k,t} | h_t, s_t, a_t: N_r(S_t^a h_t, S_k)$. Here S_t^a is the convolution matrix formed from the source signal vector s_t , the t^{th} segment of the source signal, dilated according to $s_a(t) = \sqrt{a(t)} s(a(t))$, where $a(t)$ represents an estimate among all paths and receive elements of the time varying, dilated time index.

1.3. Source signal dilation estimation

The dilation process is dominated by source-receiver platform motion in scenarios where either or both are not rigidly fixed and decoupled from the surface [2,3].

For a fixed receiver array under downward refracting conditions with source drifting near the bottom

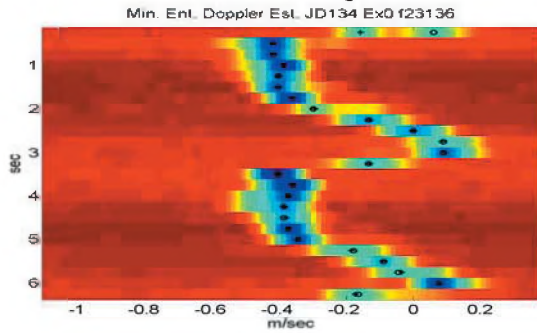


Figure 2: Dilation estimates over signaling packet durations of 6.25 seconds from drifting source. Center frequency is 44 kHz bandwidth is 5 kHz.

source motion is the greatest cause of imparted dilation. Estimates of the dilation process by the method described in [1] are presented in Figure 2. The source held from a cable to a surface vessel imparts a noticeable time varying dilation. The accelerations are over 1m/sec² as depicted.

2. Motivation for estimating parameters of the Gauss-Markov model

Under the Gauss-Markov assumption on the acoustic Green's function with known innovation variance q it follows that $h_t | q, r_{<t} : N(\hat{h}_t, P_t(q_t))$ where $r_{<t}$ represents all data preceding the time of estimation, $\hat{h}_t = (I - G_t S_t) A \hat{h}_{t-D} + G_t r_t$, $P_t = (I - G_t S_t) R_t$, $R_t = A P_{t-D} A^+ + q_t I$ and G_t is the Kalman gain. Since for any other estimator of the response function, for instance $\hat{h}_t^* = \hat{h}_t(q^{*1} q)$,

$E[(h_t - \hat{h}_t^*)(h_t - \hat{h}_t)] > tr[P_t(q)]$, when the innovation variance is not known exactly, a good estimator of it improves channel response estimation.

2.1 Approximate MAP estimate

The marginal density

$p(q | r_{<t}) \propto \int p(r_t | h_t, q, r_{<t}) p(h_t | q, r_{<t}) p(q | r_{<t}) dq$ leads to a MAP estimate of q given $r_{<t}$ as

$$\hat{q}_{t} = \arg \max_q \log \int N(r_t | S_t A \hat{h}_{t-D}, A P_{t-D} A^+ + q I + S_t \Sigma) p(q | r_{<t}) dq$$

Estimates based on approximations to this criteria can be used to augment a Kalman recursion for improved estimation of the response h_t . Figure 3 presents estimates based on the MAP principle above for q_{t} for the 8 phone array displayed relative to phone 4.

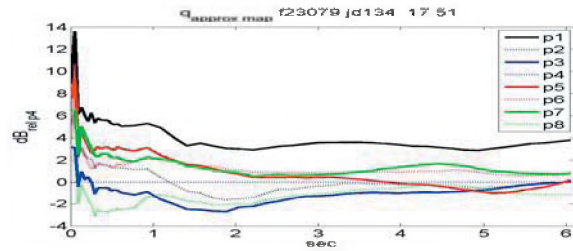


Figure 3. Approximate MAP estimates of innovation variance relative to phone 4.

3. RESULTS

Figure 4 displays a channel response function and a

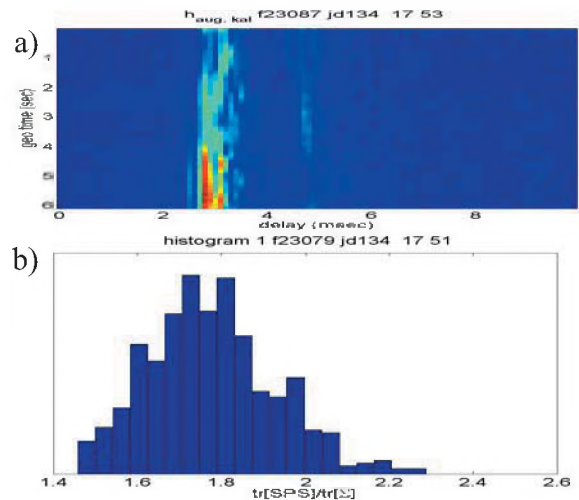


Figure 4 a) Estimated acoustic response function. b) Histogram of ratios of channel estimation error power $tr[S_t P_t S_t^beta]$ to ambient noise power $tr[S]$.

histogram of $tr[S_t P_t S_t^beta] / tr[S]$ which measures adversity of response estimation uncertainty relative to ambient noise variance. The probing interval is of duration 6.25 seconds at a range of approximately 500m. The channel uncertainty is two times as adverse to communications than the noise variance.

REFERENCES

- [1] Gendron Paul J. (2005) An empirical Bayes estimator for in-scale adaptive filtering, IEEE Trans. on Signal Processing, Vol. 53. No. 5, May 2005.
- [2] Garry J. Heard, I. Schumacher, Time Compression of M-sequence transmissions in a very long waveguide with a moving source and receiver. J. Acoust. Soc. Am. 99 (6) June 1996.
- [3] Paul J. Gendron and T.C. Yang, Doppler estimation via low-complexity prior, J. Acoust. Soc. Am. 110 (5) Nov. 2001.

ACKNOWLEDGEMENT

This work is supported by the Office of Naval Research, ONR 321 US.

**PYROK ACOUSTEMENT
ACOUSTICAL PLASTERS
CEILING AND WALL
FINISHES**

Designers and owners choose Pyrok Acoustement for their school and university projects because Pyrok provides:

- Decorative plaster finishes
- Superior sound absorbing performance
- Resistance to damage
- Low life cycle cost
- Non-combustible formulation



Perrot Memorial Library, Old Greenwich, CT

CONTACT:
Howard Podolsky, Pyrok, Inc.
914-777-7070
E-mail: info@pyrokinc.com or
www.pyrokinc.com



William Hart High School, Newhall, CA



High School for Physical City,
New York, NY



Carmel Valley Recreation Center,
San Diego, CA

Accuracy & Low Cost— Scantek Delivers Sound & Vibration Instruments

Scantek offers two integrating sound level meters and real-time octave-band analyzers from CESVA that make measurements quickly and conveniently. The easy to use SC-30 and SC-160 offer a single dynamic range of 100dB, eliminating any need for range adjustments. They simultaneously measure all the functions with frequency weightings A, C and Z. Other features include a large back-lit screen for graphical and numerical representation and a large internal memory.

The SC-30 is a Type 1 precision analyzer while the SC-160 Type 2 analyzer offers the added advantages of lower cost and NC analysis for real-time measurement of equipment and room noise. Prices starting under \$2,000, including software.

Scantek delivers more than just equipment. We provide solutions to today's complex noise and vibration problems with unlimited technical support by acoustical engineers that understand the complex measurement industry.

Scantek

Sound and Vibration
Instrumentation & Engineering

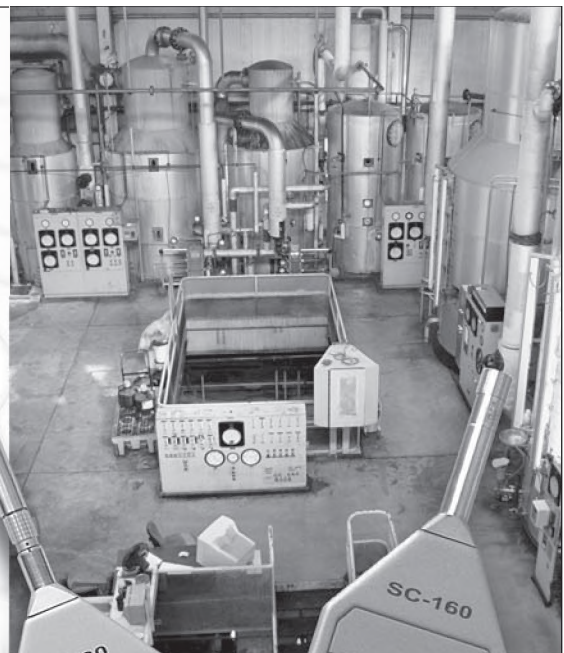
7060 Oakland Mills Road • Suite L
Columbia, MD 21046
800•224•3813
www.scantekinc.com
info@scantekinc.com

SC-30 / SC-160 Applications

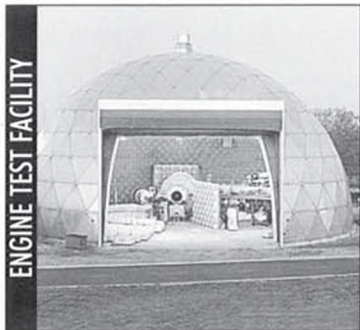
- Machinery Noise
- Community Noise
- HVAC Acoustics
- Room Acoustics & Reverb Time
- Noise Criteria (NC) (SC-160)

CESVA

We sell, rent, service, and calibrate sound and vibration instruments.

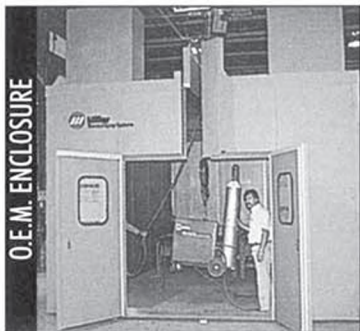


ENGINE TEST FACILITY

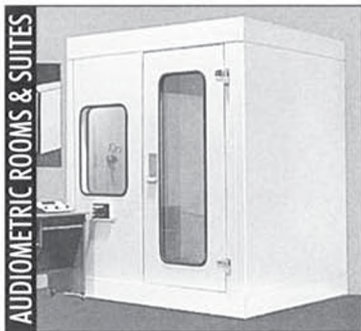


ECKOUSTIC FUNCTIONAL PANELS

O.E.M. ENCLOSURE

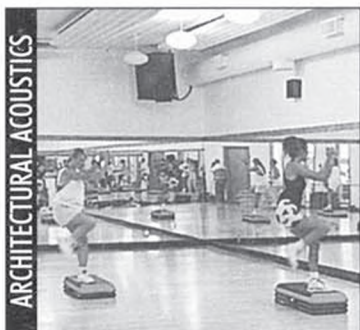


AUDIOMETRIC ROOMS & SUITES

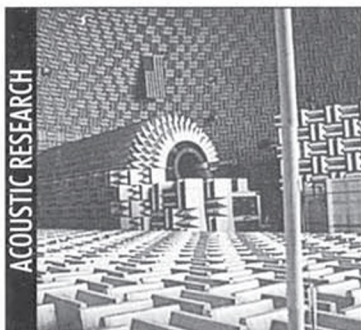


SOUND SOLUTIONS FOR THE FUTURE

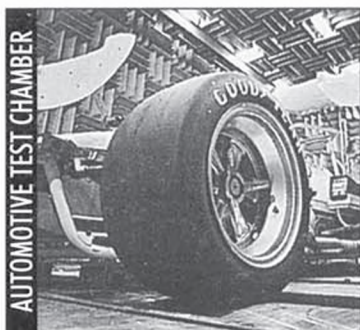
ARCHITECTURAL ACOUSTICS



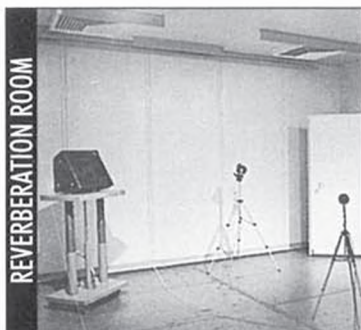
ACOUSTIC RESEARCH



AUTOMOTIVE TEST CHAMBER



REVERBERATION ROOM

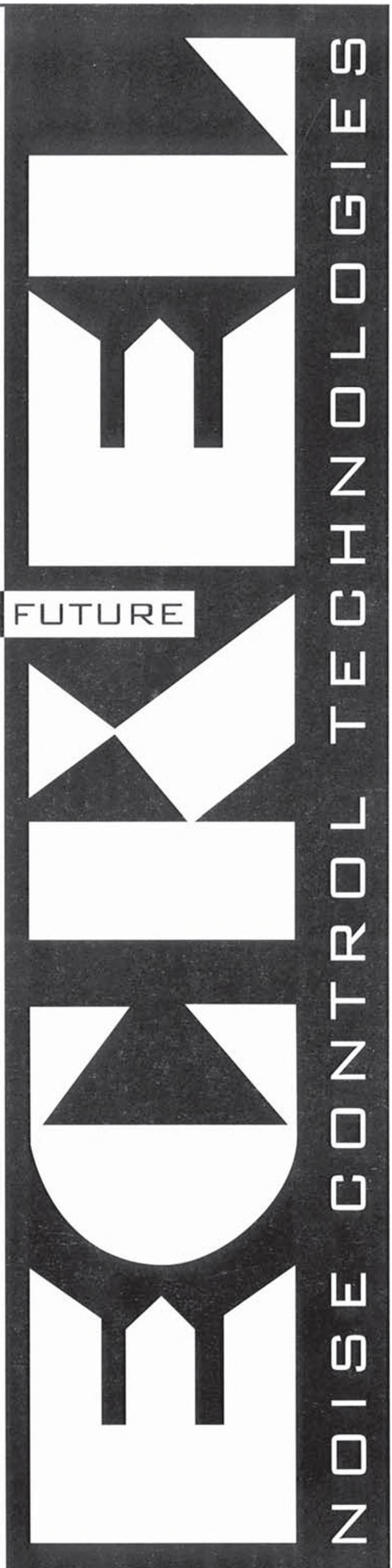


ECKEL

NOISE CONTROL TECHNOLOGIES

CANADIAN OFFICE

Box 776 100 Allison Avenue Morrisburg ON K0C 1X0
Tel: 613-543-2967 800-563-3574 Fax: 613-543-4173
Web site: www.eckel.ca/eckel e-mail: eckel@eckel.ca



ABSTRACTS FOR PRESENTATIONS WITHOUT SUMMARY PAPERS

Plenary

Variability in speech production and consequences for theories of speech perception

Michael Kieffe, School of Human Communication Disorders, Dalhousie University

Our ability to produce and understand speech is most often taken for granted but would otherwise appear to be highly complex processes. A simple vowel such as “ee” in “heed” can be produced in an infinite variety of ways: it can be spoken aloud, whispered, or sung at a number of different pitches and still be understood unambiguously by the casual listener. The processes involved in perceiving this vowel are not very well understood. In fact, the task seems daunting. For example, a vowel sung by a small child at a high pitch bears very little resemblance acoustically to the same vowel whispered by an adult male. Nevertheless, they are perceived as the same speech sound. Human listeners’ ability to reliably identify speech sounds in the face of such variability poses a difficult problem for researchers in speech perception. A substantial portion of related research ignores this variability by focusing solely on, for example, speech from a single phonation type (e.g., voiced versus whispered), gender, or dialect. Recent research has found that the problem is further complicated by the role that the acoustic environment plays in speech perception. This talk discusses research that examines variability observed in speech production from the point of view of speaker, dialect, and phonation type with a special emphasis on dialectal variation in Nova Scotia. In addition recent research that attempts to uncover how human listeners identify speech sounds will be described.

Architectural Acoustics

Noise Control Provisions in Canada’s Building Codes

J.D. Quirt and T.R.T. Nightingale

National Research Council Canada, Ottawa

In 2005, NRC published the new “objective-based” version of the National Building Code of Canada; provincial and territorial codes based on this model will come into use over the next year. Some comparison with regulations in other countries and with studies of occupant annoyance will provide a frame of reference. This talk will then explain how the Codes have changed in the context of noise control in multi-dwelling buildings, and indicate some further changes possible in the next cycle of revisions (which is already underway). These changes have implications for both the research and standards development community, and for design professionals including acoustical consultants.

Bio-Acoustics

A remotely-piloted acoustic array for studying sperm whale vocal behaviour

Tyler Schulz¹, Luke Rendell², and Hal Whitehead¹

¹Department of Biology, Dalhousie University

²Sea Mammal Research Unit, St. Andrew’s University

The inability to attribute clicks to individual sperm whales in a social group has limited our understanding of how these animals use clicks and codas in vocal interactions. In an effort to address this problem, an acoustic array consisting of small remotely-piloted vessels (RPVs) was developed to record and localize the vocalizations of individual sperm whales in traveling social clusters. Each RPV, as well as a larger research platform, is equipped with a hydrophone and a global positioning system (GPS) receiver and logger. The acoustic signals from the remotely-piloted vessels are broadcast by FM transmitters and received by radios onboard the research platform where they are digitally recorded in synchrony, thereby allowing subsequent localization. GPS data, including pseudo-range and phase information, are received by low-cost single-frequency GPS receivers, logged to flash memory cards and downloaded after recovery. Once deployed, the vessels can be piloted to establish and maintain favourable array geometry, provided focal animals are not moving too rapidly. Although GPS error is the primary source of error in our localization accuracy, the smoothing of GPS positions over time greatly improves relative receiver positioning. By using this smoothing, calibration trials with sound sources of a known separation distance have revealed accuracy in acoustic localization of up to 0.5 metres, which is more than adequate to distinguish the vocalizations of neighbouring whales. We have deployed the system several times at sea in the Northwest Atlantic and are currently analyzing recordings to localize the social signals of sperm whales.

Estimating the Acoustic Exposure of Marine Mammals to Underwater Noise

Scott Carr¹, and Adam Frankel²

¹JASCO Research Ltd. and ²Marine Acoustics, Inc

Underwater noise modelling has matured into a reliable tool for predicting the acoustic noise footprints of maritime operations including military training activities, geophysical exploration and production, shipping and marine construction. Given sufficient knowledge of the acousto-physical properties of the water column and the seabed, it is possible to estimate the acoustic transmission loss for individual sound frequencies and hence the overall attenuation of a spectrally described source at any range. In combination with numerical models that provide reliable estimates of the source’s acoustic pulse

properties and spatial pattern, wave propagation modelling provides the means to fully characterize the ensonification of an area, allowing the potential impact on the marine animals to be assessed. The prediction of noise level footprints, however, is only a step in the process of estimating the acoustic impacts on marine life. The interaction between the sound and the animal is also influenced by the animal's frequency-dependent auditory sensitivity relative to the frequency content of the sounds to which it is exposed. The degree to which sounds are audible to an animal can be quantified by subtracting the audiogram thresholds, in decibels, from the respective frequency-dependent band levels of the sounds prior to summing the band levels. The degree of impact is also dependent on the behavioural response to the detected noise which may also be modelled. This presentation outlines a new approach for predicting potential noise impacts on inhabitants of the marine environment that meets current and anticipated future regulatory impact criteria.

Comparing cricket ears

Glenn K. Morris

Biology Dept., University of Toronto at Mississauga, Miss. ON, L5L 1C6, Canada

Cricket males make sounds to attract females for mating or to repel rivals. Their ears are on their forelegs, right and left eardrums backed by internal air tubes opening via spiracles on the thorax. Being very small, yet communicating by low-frequency sinusoidal sounds of long wavelength (~4.5 kHz), crickets are unable to fix the position of a distant caller by body-created side to side differences in sound intensity. Instead common field crickets, *Gryllus*, conduct sound within dedicated internal air tubes, across their body, so that sound waves reach the front and back of each eardrum at different times after travelling different path lengths. Midbody a special tissue spans the trachea and serves to alter phase. As the cricket turns, right and left path lengths change and the changing sound interaction gives usable binaural eardrum differences. More than 3000 cricket species have been named, divided into 11 subfamilies. All these species must have the same localization problem of size relative to wavelength. I am now making a comparative study of the internal waveguides of different representative cricket species and discovering a diversity of adaptive mechanisms. For example, *Allonemobius* spp. utilize a mid-body chamber with two phase shifters in parallel. I report on the morphology of these tracheal structures whose acoustic function remains obscure.

Comparison of algorithms for the automatic recognition of Balaenopterid whale calls in noisy environment

Xavier Mouy¹, Mohammed Bahoura², and Yvan Simard¹

1-Institut des Sciences de la Mer, Université du Québec à Rimouski & 2- Dépt. de Mathématiques Informatique et Génie, Université du Québec à Rimouski

Automatic recognition of animal calls is a useful tool for investigating their seasonal distribution, relative abundance and

behavior in their natural habitat. The performance of signal processing methods is however dependent of vocalization types (frequency band, time-frequency pattern variability) and environmental characteristics (noise, propagation effects). This paper compares several time-frequency methods for detection and identification of blue (*Balaenoptera musculus*) and fin whale (*Balaenoptera physalus*) calls in the St. Lawrence. Three calls of these balaenopterids are regular patterns of stereotypical infrasounds (< 30 Hz) and another one is of a higher-frequency (30–110 Hz), irregular and variable in both frequency and duration (1–5 s). Because of the high traffic, bathymetric and physical characteristics of the St. Lawrence seaway, the majority of calls are polluted by strong low-frequency noise and warped by multipaths. All methods begin with the computation of a high-resolution spectrogram followed by noise removal using image processing techniques. Then, the first approach consists in binarizing the spectrogram and computing the coincidence with a binary time-frequency image template, via a 'and' operation. The second approach consists in selecting local maxima for each time steps of the spectrogram and extract frequency contours of the calls using a tracking algorithm. Then, three recognition methods are tested to classify these contours, Dynamic Time Warping (DTW), Vector Quantization (VQ) and discriminant analysis. The methods' performance is tested on representative call series extracted from continuous recordings collected in the area and their relative advantages and limitations are discussed.

ROCCA: A new tool for real-time acoustic species identification of delphinid whistles

Julie Oswald¹, Shannon Rankin², Jay Barlow², and Marc Lammer³

1- Scripps Institution of Oceanography/JASCO Research Ltd.; 2 - Southwest Fisheries Science Center, National Marine Fisheries Service, NOAA and 3 - Hawaii Institute of Marine Biology

Acoustic species identification studies generally focus on post-processing of field recordings to develop classification algorithms. The ability to identify delphinid vocalizations in real-time would be an asset during shipboard surveys. A new automated system, Real-time Odontocete Call Classification Algorithm (ROCCA), has been developed to allow real-time acoustic species identification in the field. This matlab-based tool automatically extracts 10 variables (beginning, end, minimum and maximum frequencies, duration, slope of the beginning and end sweep, number of inflection points, number of steps, and presence/absence of harmonics) from whistles manually selected from a real-time scrolling spectrograph (ISHMAEL software) and runs classification and regression tree analysis (CART) and discriminant function analysis (DFA) to identify whistles to species. Schools of dolphins are classified based on running tallies of individual whistle classifications. Overall, 46% of schools were correctly classified for seven species and one genus (*Tursiops truncatus*, *Stenella attenuata*, *S. longirostris*, *S. coeruleoalba*, *Steno bredanensis*, *Delphinus* species, *Pseudorca crassidens*, and *Globicephala*

macrorhynchus). This new tool provides a method for identifying schools that are difficult to approach and observe, allows species distribution data to be collected when visual efforts are compromised, reduces the bottleneck of post-cruise analysis, and is valuable for processing data collected using sea-floor mounted acoustic recorders.

Hearing Conservation

In-depth Analysis of Workplace Noise Utilizing a Computer-based Process

Gordon Whitehead, Dalhousie University (retired)

Acoustical professionals have long relied on the sound level meter for analyzing noise in the workplace for purposes of hearing conservation. This presenter has been analyzing such noise for intensity, frequency content, duration, and reflection characteristics utilizing (predominantly) a laptop computer and sound analysis software, for the past 8 years. In the non-clean work environment, the noise has been recorded on a digital auditory tape recorder, for subsequent computer analysis. This approach has proven to be less time consuming than traditional methods, and has provided significantly more acoustical information, as well as the potential for "re-visiting" the acoustical event after it has occurred. Hazardous noise exposures have been identified that may have remained unidentified using only a sound level meter and/or dosimeter. This computer-based process has improved the quality of the hearing conservation effort. During this presentation, the analysis process will be demonstrated, and examples of noise from various industries thus analyzed will be presented.

HF Acoustics and Communications

High frequency acoustic observations of episodic mixing events in Lunenburg Bay

Douglas J. Schillinger and Alex E. Hay
Dalhousie University

Episodic wind and wave forcing events observed over the 4-year life of the Lunenburg Bay Observing System cause bubble injection at the surface, and sediment resuspension at the seabed. The resulting enhanced concentrations of scatterers in the water column have proved to be readily detectable in the backscatter amplitudes registered by the Acoustic Doppler Profilers at the three buoy nodes, and indicate penetration of bubbles to the bottom, and suspended sediment rising to mid-depth during the stronger forcing events. Acoustic backscatter amplitudes show enhanced scattering over a range of frequencies (0.6 to 5 MHz). Times of enhanced scattering coincide with large variances in the horizontal and vertical components of velocity. Bubble concentrations in the sub-surface (top 2 m) and near-surface ($4.5\text{m} > d > 2\text{m}$) layers are correlated with the magnitude of local wind speed, while resuspended sediment concentrations are correlated with significant wave height. Spectra of the near-bottom vertical velocity ($H=0.25\text{m}$) have slopes of $-5/3$ during periods of high

near bottom backscatter indicating that turbulence plays a role in the resuspension of sediment. Backscatter profiles show 2 minute duration bubble plumes extending to 5-10 m depth. Preliminary investigation of these plumes using data from each of the ADPs three beams is consistent with the advection of Langmuir cells over the instrument. The depth of the 70 dB contour, used to demarcate the boundary of these plumes, shows that the depth of penetration of bubbles is related to wind speed. Comparisons of the depth of enhanced scattering to predicted depths of a turbulent dissipation layer shows that turbulent dissipation contributes to the vertical distribution of bubbles.

High-frequency acoustic imaging of bio-degradation of wave-formed sand ripples on the inner continental shelf

Alex E. Hay

Department of Oceanography, Dalhousie University

Continuous in situ observations of orbital-scale sand ripple degradation were made during the Sediment Acoustics Experiment (SAX04) in 15-m water depth on the inner shelf of the Gulf of Mexico following Tropical Storm Mathew in October 2004. The dominant ripple wavelength was 50-60 cm. The sand median grain size was 350 microns. Bed elevation profiles and planform images of the ripple field were obtained at cm-resolution using rotary sonars operating primarily at 2.25 MHz. Tidal and other low-frequency currents, wave orbital velocities, and nearbed turbulence were monitored simultaneously with co-located instruments. Over the 20-d duration of the record, the variance in the primary ripple band decayed by a factor of 10. In contrast, the variance at high spatial frequencies remained nearly constant. Physical forcing in the nearbed region was relatively weak (rms wave orbital velocities ~ 5 cm/s), but non-negligible (turbulent kinetic energy dissipation rates $\sim 10\text{-}6$ W/m²). The dominant mechanism driving ripple decay was biological: specifically, pitting of the seabed by fish. The observed rates of decay the bed roughness spectrum and azimuthally-integrated backscatter amplitudes are compared to models constructed from diffusive dissipation of small-scale roughness.

Music Cognition and Musical Acoustics

Agerian music: Genre classification

Lamya Fergani and Amrane Houacine

Informatic and Electronic Faculty of Algiers, Algeria

Searching and organizing growing musical collections for the Algerian radio requires classifying the music signals into a hierarchy of genres to structure them. Musical genres are defined as categorical labels that auditors use to characterize pieces of music. So, a musical genre can be characterized by a set of common perceptive parameters shared by its members. These perceptive parameters are closely related to the instrumentation, rhythmic structure and also harmonic content of the music. An automatic genre classification would actually be very helpful to replace or complete human genre annotation,

which is actually used. In this paper, we explore the automatic genre classification of a musical Algerian database. More specifically, two feature sets composed of signal objective descriptors and which are closely related to perceptive ones (timbre, rhythm) are proposed. The automatic classification of this database is then evaluated through three classifiers: K-nearest neighbors, Gaussian mixture models and neural networks. We thus obtain scores of 60% to 80% for eight genres. Interesting comparative results are reported and commented.

Index Terms— audio classification, feature extraction, musical genre classification, music information retrieval

Noise Control

Atténuation effective apportée par l'utilisation d'une double protection auditive

Jérémie Voix¹, Frédéric Laville¹, and Hugues Nélisse²

1 - Département de génie mécanique, École de technologie supérieure, Montréal (QC), & 2 - Institut de recherche Robert Sauvé en santé et sécurité du travail, Montréal (QC)

Cette étude vise l'évaluation de l'atténuation effective de la double protection auditive portée par des travailleurs en milieu extrêmement bruyant. La procédure de mesure utilisée découle des travaux de recherche en cours à l'ÉTS en collaboration avec l'IRSST, le Conseil de recherche en sciences naturelles et en génie du Canada (CRSNG) et la compagnie SONOMAX. Il s'agit de mesurer le niveau de pression acoustique dans le canal auditif, entre le bouchon et la coquille et à l'extérieur de la coquille et d'estimer à partir de ces mesures l'atténuation effective de la double protection et aussi de chaque protecteur. Les enregistrements ont été effectués au cours d'une même journée de travail sur l'ensemble des travailleurs pendant des durées de l'ordre de cinq minutes sur plusieurs périodes de travail représentatives de diverses conditions de travail rencontrés. Les enregistrements ont été analysés par la suite en laboratoire pour déterminer les niveaux d'exposition ainsi que l'atténuation effective par bande d'octave et en valeur global pondérée A pour les différentes situations de travail mesurées. Les conclusions de l'étude, similaires à d'autres, font apparaître des performances des coquilles grandement diminuées en présences de fuites acoustiques (cheveux, branches de lunettes de sécurité, etc.), mais ouvrent également des pistes intéressantes pour l'étude de l'efficacité en temps réel des bouchons d'oreille.

CSA Z107.10 Acoustical Standards in Canada

Cameron Sherry

Les Consultants LBCD Inc.

Why did the CSA Z107 committee decide that there should be a Canadian acoustical standard, Z107.10. There are many acoustical standards available within the world but which ones should be used and which should not? If we use an acoustical standard are there any limitations? What terms should we use when talking or writing about acoustics and how are they defined? The answers to some of these questions should be

apparent in this paper and the ones that follow.

Exact acoustical analysis of sound radiation from free vibration of rectangular Mindlin plates

Korosh Khorshidi, Shahrokh Hosseini-Hashemi, and Ali Sadeghi

Iran University of Science and Technology (IUST)

In this study, acoustic radiation of a Mindlin rectangular plate was investigated. The boundary condition of the plate is simply supported (S-S-S). The variational method was utilized to formulate plate vibration. Meanwhile it was assumed that no fluid loading occurs in the structure. The dimensionless equations of motion was derived based on the Mindlin plate theory to study the transverse vibration of moderately thick rectangular plates (in terms of the stress resultant with consideration of transverse shear deformation and rotatory inertia) without any approximate method (S. Hosseini-Hashemi et. al. (2005)). Incorporating structural-acoustic coupling was implemented for vibrating plate models. The radiation field of a plate vibrating with a specified distribution of velocity on the surface can be computed by Rayleigh integral. In the present work, the acoustic pressure distribution of the radiator was analytically obtained in its far field. Numerical results were presented for a wide range of aspect ratio and thickness ratio and their effects on the sound pressure were studied in more detail. It is worth noting that this theory and its results can be applied for thin plates. S.H.Hashemi, M.Arsanjani, 2005” Exact characteristic equations for some of classical boundary conditions of vibrating moderately thick rectangular plates”, International Journal of Solid and Structures, v 42, 819-853.

Physical Acoustics/Ultrasound

An environmental noise impact assessment and forecasting tool for military training activities

Scott Carr, Rob Racca, and Dave Hannay

JASCO Research Ltd.

When military training activities are to be undertaken near populated or ecologically sensitive areas, reliable forecasting of the associated sound levels is often necessary to allow effective noise management planning and to satisfy permitting requirements. The Impulse Noise Propagation Model (INPM) was developed by JASCO as an environmental impact assessment and forecasting tool for military training activities. The package models airborne noise from impulsive sources including on-land explosions, underwater detonations transmitted to air, weapons firing (from small arms to artillery) and shock waves from supersonic shells in flight. INPM enables the estimation of aggregate noise levels from complex operations involving multiple concurrent activities. The location, time period and repetition rate of each activity are user specifiable. The current or forecast atmospheric conditions are automatically imported. The software's architecture includes a specially adapted Parabolic Equation propagation model, an expandable database of measured or computed spectral source

levels from a wide range of activities, a run module that coordinates modelling and summing of sound from multiple sources, and a GIS interface for the definition of operational layouts and the display of noise level contours on area maps. The software computes a variety of metrics commonly used in impact assessment including Leq, Ldn and LAFmax for impulsive noise, based on broadband levels calculated from modelled results in individual frequency bands. Tabular reports of noise levels at any number of receiver locations and modelled times can be automatically sent to e-mail accounts or wireless devices. This presentation will provide an overview of the INPM software and its use at Canadian Forces bases.

Magnetic Resonance Imaging of Acoustic Streaming in Gases

Ben Newling, Duncan MacLean, and Igor Mastikhin, University of New Brunswick

Acoustic streaming (AS) is a time-independent fluid motion generated by a sound field. Rayleigh acoustic streaming, first described by Lord Rayleigh, is circular flow from node to antinode that occurs when a standing wave is set up inside an enclosure. In gases, the AS dynamics can be extraordinarily sensitive. Conventional measurement methods, such as particle imaging velocimetry, are prone to perturbing the flow field. Magnetic resonance imaging (MRI) offers the possibility of non-invasively obtaining three-dimensional quantification of advective velocity and mechanical dispersion of a gas during acoustic streaming. MRI is well-established as a powerful clinical tool, but MRI measurements in a gas are more difficult than in a patient. The density of MRI-active nuclei is ~ 1000 times lower and MRI signal durations are often two or three orders of magnitude shorter in a gas than in a person. Unconventional MRI methods, some of which were developed at the UNB MRI Centre, are required. We have tested several MRI methods for the detection of acoustic streaming in gases. Detection of slow gas motion caused by sound pressure is possible within reasonable acquisition time (minutes). The acquired spatially-resolved velocity spectra show the expected velocity distributions for the case of developed Rayleigh streaming.

Dynamics of the sonoluminescing bubble

Borko Djurkovic, Igor Mastikhin, and Dennis Tokaryk, University of New Brunswick

When bubbles suspended in a fluid are exposed to high power sound pressure, they begin to emit light. This phenomenon is termed sonoluminescence. The study of a single light emitting bubble, known as Single Bubble Sonoluminescence (SBSL), can provide us with a better and more controlled method to study sonoluminescence in an attempt to explain many of its interesting and unique characteristics. To produce SBSL, a sinusoidal ultrasound signal is applied to a water-filled flask at its resonant frequency. The pressure gradient

across the bubble forces it towards the pressure antinode. The bubble undergoes nonlinear radial oscillations caused by the pressure swings of the acoustic field. During the compression phase, the bubble experiences violent collapse which results in an emission of light with spectrum that is continuous into the ultraviolet region. The maximum of the spectrum is still unknown due to the absorption of light by water in this spectral region. In our work, we have discovered that by introducing a sinusoidal modulation to the amplitude of the acoustic signal, it is possible to control the bubble motion. Such control can be used to estimate effects of other physical fields on the conditions inside the bubble. We will compare experimental measurements of bubble motion to numerical simulations.

Molecular dynamics simulation of the response of a gas to a spherical piston: Implications for sonoluminescence

Steven Ruuth¹, Alexander Bass², Seth Putterman², and Barry Merriman²

1 - Simon Fraser University & 2 - UCLA

Sonoluminescence is the phenomena of light emission from a collapsing gas bubble in a liquid. Theoretical explanations of this extreme energy focusing are controversial and difficult to validate experimentally. In this talk hard sphere molecular dynamics simulations of the collapsing gas bubble are used to clarify the energy focusing mechanism, and determine physical parameters that restrict theories of the light emitting mechanism. Our model shows strong energy focusing within the bubble, including the formation of shocks and strong ionization. Our calculations show that the gas-liquid boundary interaction has a strong effect on the internal gas dynamics, and that the gas passes through states where the mean free path is greater than the characteristic distance over which the temperature varies.

Spatially resolved NMR relaxation of cavitating liquid

Igor Mastikhin and Benedict Newling, Physics Department, University of New Brunswick

Information on processes in the boundary layer of cavitating bubbles is very important for a better understanding of the phenomenon of cavitation. The boundary layer regulates delivery of reaction products into the bulk and limits gas exchange between cavitating gaseous bubbles and the surrounding liquid. Obtaining information on boundary layers is remarkably difficult. In this work, we attempt to get access to such information by using nuclear magnetic resonance relaxation measurements of cavitating liquid. Nuclei can serve as tiny sensors sensitive to changes in their molecular environment such as a presence of paramagnetic particles, hot temperature and microflows. Measurements were performed both for the liquid phase and for a dissolved gas: a fluorinated gas was dissolved in water prior to the experiment, and its relaxation parameters were recorded.

Speech and Hearing Sciences

An acoustic study of the African Nova-Scotian English vowel systems in North Preston and North Halifax

Melissa Moloissa, Michael Kiefté, and Elizabeth Kay-Raining Bird, Dalhousie University

An acoustic study of the African Nova-Scotian English vowel systems in North Preston and North Halifax Melissa Moloissa, Michael Kiefté, Ph.D., Elizabeth Kay-Raining Bird, Ph.D. The English dialect spoken by African Nova Scotians (ANSE) has never been described phonetically or acoustically despite the fact that it is very distinct from other dialects spoken in Canada. This paper presents a comparative acoustic analysis of the vowel systems of ANSE spoken in two communities of Nova Scotia: North Preston and North Halifax. The distinctiveness of both dialects can be traced back to African-American ancestry, post-slavery settlement history, the long-standing geographical isolation of African Nova Scotian settlements, and social segregation from mainstream Nova Scotia (Grant, 2002; Poplack & Tagliamonte, 2001). It has also been suggested that ANSE retains some features from early African American English (Poplack & Tagliamonte, 2001). Eleven vowels were sampled from 12 speakers from each community. Samples were obtained via the following tasks: a vowel elicitation task that targets the production of each vowel within seven phonetic CVC contexts (/h_d/, /h_t/, /h_l/, /h_nd/, /h_g/, and /d_d/); a reading of a phonetically-balanced text; and a monologue. Frequency values were measured for f0, F1, F2, and F3 as well as formant transitions for all vowels.

Objective Speech Quality Evaluation Using Markov Chain Monte Carlo Methods

Guo Chen and Vijay Parsa

University of Western Ontario

Objective Speech quality evaluation is highly desirable and beneficial in the field of speech processing. A key issue in objective speech quality evaluation is the determination of the relationship between the extracted features and the subjective quality scores. Typically, an optimal regression model is expected to perform this mapping and the order (hence complexity) of the regression model is highly dependent on the number of training samples, amount of noise in the samples and the complexity of the underlying function being estimated. Choosing a model with the right complexity is a challenging problem as a model with low complexity will not accurately model the underlying relationship and a model with a high complexity will result in over-fitting. In this study we investigated a Bayesian evaluation method using Markov chain Monte Carlo (MCMC) sampling, which elegantly handles the model complexity problem. In the proposed method the loudness patterns extracted from the speech signals are employed as the speech quality features. The speech quality is predicted using the Bayesian linear model and MCMC sampling. The unknown degree of freedom of the regres-

sion model is handled by defining non-informative priors for the parameters that determine the model complexity, and the resulting quality estimation is averaged over all model complexities weighted by their posterior probability given the data samples. The effectiveness of the proposed method is demonstrated through comparisons with the current standardized speech quality metric (ITU-T P.862) using seven subjective speech quality databases of the ITU-T P-series Supplementary 23.

Pitch perception of young cochlear implant users and normal hearing peers

Amy McKinnon and Michael Kiefté

School of Human Communication Disorders, Dalhousie University

Research in pitch perception by cochlear implant users has focused primarily on post-lingually deafened adults. Little is currently known regarding the pitch perception abilities of those who are implanted at a very early age, yet many children receive cochlear implants when they are less than two years old. Given the effects of brain plasticity early in life, it is conceivable that pitch perception by early cochlear implant users may be much better than that of their older counterparts. This study examines pitch discrimination thresholds of young cochlear-implant users between the ages of 4 and 16. A two-alternative forced choice design is used to determine difference limens at three referent tones: 100 Hz, 200 Hz and 400 Hz. Stimuli consist of speech-shaped complex periodic tones with -6 dB/octave roll-off. Two different tasks are employed: pitch-discrimination, which asks whether two stimuli are same or different, and pitch ranking in which participants determine which of two stimuli is higher in pitch. Normal hearing matches are tested to control for maturational effects, and adult cochlear implant users are also tested to compare findings with other studies. Possible implications for age of implantation will be discussed. [This research is funded by the Nova Scotia Health Research Foundation]

Making young ears old (and old ears even older): Simulating a loss of synchrony

Ewen MacDonald¹, Kathy Pichora-Fuller², Bruce Schneider², and Willy Wong¹

1 - Institute of Biomaterials and Biomedical Engineering, University of Toronto, 2 - Department of Psychology, University of Toronto at Mississauga

Age-related changes in the auditory system have been attributed to three independent factors: OHC damage, changes in endocochlear potentials, and loss of neural synchrony. While loss of neural synchrony has little effect on audiometric thresholds, it is thought to contribute to difficulties understanding speech in noise. Young and old adults with good audiograms in the speech range were presented with SPIN-R sentences in two SNR and three processing conditions: intact, jitter, and smear. The parameters of the jittering algorithm were chosen to simulate a loss of synchrony consistent with

prior psychoacoustic and speech experiments on auditory aging. The parameters of smearing algorithm were chosen to match the spectral distortion produced by jitter algorithm. For both age groups, the jitter condition resulted in a significant decline in word identification. However, the smear condition resulted in a significant decline only for the older age group but the decline was not as large as that in the jitter condition. Since a difference in performance between jitter and smear must be due to phase distortion (i.e. a simulated loss of synchrony), the results for both age groups suggest that a loss of synchrony can have a deleterious affect on speech intelligibility in noise. Furthermore, the performance of the young in the jitter conditions was similar to that of the older adults in the intact conditions for low context sentences. Thus, the jitter condition appears to simulate this neural aspect of auditory aging in healthy young ears.

Underwater Acoustics

A Preliminary Study on the Geoacoustic Parameters of Gassy Sediments in St. Margaret's Bay, Nova Scotia
 Marie-Noël R. Matthews, Francine Desharnais, David J. Thomson, Gordon R. Ebbeson, and Garry J. Heard, DRCD Atlantic

The St. Margaret's Bay environment is characterized by a

superficial layer of gassy sediment in the deepest area of the bay. The effect of this layer on the propagation of sound at low frequencies (below 500 Hz) has been shown to be important, influencing results from localization algorithms that rely heavily on accurate predictions of transmission loss (TL). Since the 1970's, major progress has been made in understanding the effect of gassy sediment on the acoustic field. However, the literature concentrates almost exclusively on the effect of gas at high frequencies. Very little has been published on the comparison between theory and in situ measurements of the geoacoustic parameters at frequencies below 1 kHz. This preliminary study on gassy sediment compares measured and predicted TL versus range to estimate the geoacoustic parameters of the sediment layers in St. Margaret's Bay. The TL measurements were calculated from recordings of underwater narrowband sources on a vertical line array deployed in St. Margaret's Bay. The predicted TL were obtained with a parabolic equation propagation model. Estimated values of compressional and shear speed, attenuation, density and layer thickness are presented for the gassy layer and compared to the theoretical values. This preliminary study reveals that some of the estimated geoacoustic values, such as compressional sound speed, are higher than predicted by the theory.

West Caldwell Calibration Laboratories, Inc.
 uncompromised calibration
 Web site: www.wccl.com E-mail: info@wccl.com

Head Office: 1575 State Route 96, Victor, NY 14564
 Phone: 585-586-3900 Fax: 585-586-4327
 Branch Office: 220 Rutherford Rd. S. Suite 210, Brampton, ON L6W 3J6
 Phone: 905-595-1107 Fax: 905-595-1108

A SINGLE SOURCE LABORATORY

for Calibration and Repair of Sound, Vibration, and Electronic Test Instrumentation

SPECIALIZING IN:

- Accelerometers
- Microphones
- Sound Level Meters
- Field Calibrators
- Audiometric Equipment
- Vibration Meters
- Frequency Analyzers
- Vibration Test Equipment

OUR AUTOMATED FACILITY ASSURES YOU OF:

- Calibrations Traceable to N.I.S.T.
- Certification: ISO 9001:2000
- Accreditation: ISO/IEC 17025:2005
- Compliance: ISO 10012-1, MIL-STD-45662A, ANSI/NC SL 2540-1-1994
- Superior Workmanship
- Complete Test Documentation
- Quick Turnaround time:
 - 48 Hour Calibration Service Available for an Additional Fee
 - 5-10 Days Standard Turnaround

OTHER SERVICES INCLUDE:

- Custom System Integration



Authorized Calibration and Repair Center for

- Rion
- Ono-Sokki
- Scantek Inc.

We service equipment manufactured by:

- ACO Pacific*
- Brüel & Kjær*
- CEL*
- Dytran*
- Endevco*
- Fluke
- G.R.A.S.*
- Hewlett-Packard
- Larson Davis*
- Metrosonics*
- Norsonic*
- Norwegian Electric*
- PCB*
- Rion*
- Simpson
- Syminex*
- Quest
- and others

FREE INITIAL OR NEXT CALIBRATIONS COMPLIMENTS FROM WCCL

Your cost of the instrument will be manufacturers list price.

* We will be pleased to order any instrument for you from the manufacturers marked with an ***

Modular Platform

Type 2250's combination of software modules and innovative hardware makes the analyzer a dedicated solution for high-precision measurement tasks, in environmental, occupational and industrial noise application areas.

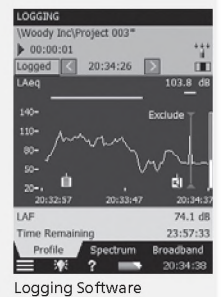
New software modules can easily be added, thus giving you the option of adding more functionality as your measurement requirements change. This way the platform ensures that your investment is securely protected now and in the future.

Currently available applications include:

- **Frequency Analysis Software** – for real-time analysis of 1/1- and 1/3-octave bands
- **Logging Software** – log broadband data and spectra at intervals from 1s to 24 h
- **Enhanced Logging Software** – for continuous monitoring and logging of periodic reports
- **Sound Recording Option** – record measurements signals to identify and document sound sources

Type 2250 has been designed in co-operation with users to be easy, safe and clever.

For more information please contact your local sales representative or go to www.type2250.com



HEADQUARTERS: DK-2850 Nærum · Denmark · Telephone: +4545800500
Fax: +4545801405 · www.bksv.com · info@bksv.com

USA: 2815 Colonnades Court · Norcross, GA 30071
Toll free (800) 332-2040 · www.BKhome.com · bkinfo@bksv.com

Hand-held Analyzer *Type 2250*

Brüel & Kjær 

NEWS / INFORMATIONS

CONFERENCES

If you have any news to share with us, send them by mail or fax to the News Editor (see address on the inside cover), or via electronic mail to stevenb@aciacoustical.com

2006

13-15 September: Autumn Meeting of the Acoustical Society of Japan. Web: www.asj.gr.jp/index-en.html

17-21 September: Interspeech 2006 - ICSLP. Web: www.interspeech2006.org

18-20 September: International Conference on Noise and Vibration Engineering (ISMA2006). Leuven, Belgium. Web: www.isma-isaac.be

18-20 September: ACTIVE 2006, 6th International Symposium on Active Noise and Vibration Control. University of Adelaide, South Australia, Australia. Web: www.active2006.com

18-20 September: 12th International Conference on Low Frequency Noise and Vibration and its control. Bristol, UK. Web: www.lowfrequency2006.org

18-21 September: INTERSPEECH 2006 - ICSLP. Pittsburgh, PA, USA. Web: www.interspeech2006.org

03-06 October: IEEE International Ultrasonics Symposium. Vancouver, Canada. Web: www.ieee-ultrasonics2006.org

11-13 October: Annual Conference of the Canadian Acoustical Association, Halifax, Nova Scotia. Web: <http://www.caa-aca.ca/halifax-2006.html>

16-17 October. Institute of Acoustics Autumn Conference.. Oxford, UK. Web: www.ioa.org.uk/viewupcoming.asp

18-20 October: 37th Spanish Congress on Acoustics. Joint with Iberian Meeting on Acoustics, Gandia-Valencia, Spain. Web: <http://www.ia.csic.es/sea/index.html>

25-28 October: 5th Iberoamerican Congress on Acoustics. Satiago, Chile. Web: www.fia2006.cl

2-3 November: Autumn Meeting of the Swiss Acoustical Society. Luzern Switzerland. Web: www.sga-ssa.ch

20-22 November: Joint Australia/New Zealand Acoustical Conference. Christchurch, New Zealand. Web: www.acoustics.org.nz

28 November – 2 December: 152nd meeting, 4th Joint Meeting of the Acoustical Society of America and the Acoustical Society of Japan, Honolulu, Hawaii. Contact: Acoustical Society of America, Suite 1NO1, 2 Huntington Quadrangle, Melville, NY 11747-4502; Tel: 516-576-2360; Fax: 516-576-2377; E-mail: asa@aip.org; Web: asa.aip.org

3 - 6 December: INTER-NOISE 2006, Honolulu HA, USA (Same Hotel at ASA meeting the week preceding. Web: www.inceusa.org

CONFÉRENCES

Si vous avez des nouvelles à nous communiquer, envoyez-les par courrier ou fax (coordonnées incluses à l'envers de la page couverture), ou par courriel à stevenb@aciacoustical.com

2006

13-15 septembre: Autumn Meeting de l'Acoustical Society du Japon. Web: www.asj.gr.jp/index-en.html

17-21 septembre: Interspeech 2006 - ICSLP. Web: www.interspeech2006.org

18-20 septembre: International Conference sur Noise et Vibration Engineering (ISMA2006). Leuven, Belgium. Web: www.isma-isaac.be

18-20 septembre: ACTIVE 2006, 6th International Symposium sur Active Noise et Vibration Control. University d'Adelaide, South Australia, Australia. Web: www.active2006.com

18-20 septembre: 12th International Conference sur Low Frequency Noise et Vibration et control. Bristol, UK. Web: www.lowfrequency2006.org

18-21 septembre: INTERSPEECH 2006 - ICSLP. Pittsburgh, PA, USA. Web: www.interspeech2006.org

03-06 octobre: IEEE International Ultrasonics Symposium. Vancouver, Canada. Web: www.ieee-ultrasonics2006.org

11-13 octobre: Annual Conference de l'Association Acoustical Canadienne, Halifax, Nova Scotia. Web: <http://www.caa-aca.ca/halifax-2006.html>

16-17 octobre. Institute d'Acoustics Autumn Conference.. Oxford, UK. Web: www.ioa.org.uk/viewupcoming.asp

18-20 octobre: 37th Spanish Congress sur Acoustics. Joint avec Iberian Meeting sur Acoustics, Gandia-Valencia, Spain. Web: <http://www.ia.csic.es/sea/index.html>

25-28 octobre: 5th Iberoamerican Congress sur Acoustics. Satiago, Chile. Web: www.fia2006.cl

2-3 novembre: Autumn Meeting de l'Acoustical Society Swiss. Luzern Switzerland. Web: www.sga-ssa.ch

20-22 novembre: Joint Australia/New Zealand Acoustical Conference. Christchurch, New Zealand. Web: www.acoustics.org.nz

28 novembre – 2 decembre: 152^e rencontre, 4^e Rencontre acoustique jointe de l'Acoustical Society of America, et l'Acoustical Society of Japan, Honolulu, Hawaii. Info: Acoustical Society of America, Suite 1NO1, 2 Huntington Quadrangle, Melville, NY 11747-4502; Tél.: 516-576-2360; Fax: 516-576-2377; Courriel: asa@aip.org; Web: asa.aip.org

3 - 6 decembre: INTER-NOISE 2006, Honolulu HA, USA (Same Hotel at ASA meeting the week preceding). Web: www.inceusa.org

2007

10-12 April. 4th International Conference on Bio-Acoustics. Loughboro, UK. Web: www.ioa.org.uk
17-20 April. IEEE International Congress on Acoustics, Speech, and Signal Processing (IEEE ICASSP 2007). Honolulu, HI, USA. Web: <http://www.icassp2007.org>
16-20 May: IEEE International Conference on Acoustics, Speech, and Signal Processing (IEEE ICASSP 2007). Honolulu, HI, USA. Web: www.icassp2007.org
04-08 June: 153rd Meeting of the Acoustical Society of America. Salt Lake City, Utah, USA. Web: www.asa.aip.org
9-12 July: 14th International Congress on Sound and Vibration (ICSV14). Cairns, Australia. Email: n.kessissoglou@unsw.edu.au
26-29 August: Inter-noise 2007. Istanbul, Turkey. Web: www.internoise2007.org.tr
27-31 August: Interspeech 2007. E-mail: conf@isca-speech.org
2-7 September 19th International Congress on Acoustics (ICA2007), Madrid Spain. (SEA, Serrano 144, 28006 Madrid, Spain; Web: www.ica2007madrid.org
9-12 September: ICA2007 Satellite Symposium on Musical Acoustics (ISMA2007). Barcelona, Spain. Web: www.isma2007.org
9-12 September: ICA2007 Satellite Symposium on Room Acoustics (ISMA2007). Sevilla, Spain. Web: www.isra2007.org
November 27 - December 02: 154th Meeting of the Acoustical Society of America. New Orleans, LA, USA. Web: www.asa.aip.org

2008

29 June - 04 July: Joint Meeting of European Acoustical Association, Acoustical Society of America, and Acoustical Society of France. Paris, France. Web: www.sfa.asso.fr/en/index.htm
7-10 July: 18th International Symposium on Nonlinear Acoustics (ISNA18). Stockholm, Sweden. E-mail: benflo@mech.kth.se
28 July - 1 August: 9th International Congress on Noise as a Public Health Problem. Mashantucket, Pequot Tribal Nation, (CT, USA). Web: www.icben.org
22-26 September: Interspeech 2008 - 10th ICSLP, Brisbane, Australia. Web: www.interspeech2008.org

2010

23-27 August: International Congress on Acoustics 2010. Sydney, Australia. Web: www.acoustics.asn.au

2007

10-12 avril. 4th International Conference sur Bio-Acoustics. Loughboro, UK. Web: www.ioa.org.uk
17-20 avril. IEEE Congress Internationale sur Acoustics, Speech, et Signal Processing (IEEE ICASSP 2007). Honolulu, HI, USA. Web: <http://www.icassp2007.org>
16-20 mai: IEEE International Conference sur Acoustics, Speech, et Signal Processing (IEEE ICASSP 2007). Honolulu, HI, USA. Web: www.icassp2007.org
04-08 juin: 153rd Meeting de l'Acoustical Society d'America. Salt Lake City, Utah, USA. Web: www.asa.aip.org
9-12 juillet: 14th Congress Internationale sur Sound et Vibration (ICSV14). Cairns, Australia. Email: n.kessissoglou@unsw.edu.au
26-29 août: Inter-noise 2007. Istanbul, Turkey. Web: www.internoise2007.org.tr
27-31 août: Interspeech 2007. E-mail: conf@isca-speech.org
2-7 septembre 19^e Congrès international sur l'acoustique (ICA2007), Madrid Spain. (SEA, Serrano 144, 28006 Madrid, Spain; Web: www.ica2007madrid.org
9-12 septembre: ICA2007 Satellite Symposium sur Musical Acoustics (ISMA2007). Barcelona, Spain. Web: www.isma2007.org
9-12 septembre: ICA2007 Satellite Symposium sur Room Acoustics (ISMA2007). Sevilla, Spain. Web: www.isra2007.org
novembre 27 - decembre 02: 154th Meeting de l'Acoustical Society d'America. New Orleans, LA, USA. Web: www.asa.aip.org

2008

29 juin - 04 juillet - 04 July: Joint Meeting d'European Acoustical Association, Acoustical Society d'America, et Acoustical Society du France. Paris, France. Web: www.sfa.asso.fr/en/index.htm
7-10 juillet: 18th International Symposium sur Nonlinear Acoustics (ISNA18). Stockholm, Sweden. E-mail: benflo@mech.kth.se
28 juillet - 1 août: 9th International Congress sur Noise as a Public Health Problem. Mashantucket, Pequot Tribal Nation, (CT, USA). Web: www.icben.org
22-26 septembre: Interspeech 2008 - 10th ICSLP, Brisbane, Australia. Web: www.interspeech2008.org

2010

23-27 août: International Congress sur Acoustics 2010. Sydney, Australia. Web: www.acoustics.asn.au

NEWS

We want to hear from you! If you have any news items related to the Canadian Acoustical Association, please send them. Job promotions, recognition of service, interesting projects, recent research, etc. are what make this section interesting.

EXCERPTS FROM “SCANNING THE JOURNALS”, IN ECHOS, ASA

“**Virtual Acoustic Prototypes:** Listening to Machines that Don’t Exist” is the title of a paper in the December issue of Acoustics Australia. A virtual acoustic prototype (VAP) is a computer representation of a machine such that it can be heard without having to exist as a physical assembly. Whereas visualization tools are well developed in the field of visual design, the analogous tools for auralization are still in their infancy. In order to construct a VAP, a method is needed to represent the excitation and transmission mechanisms. Airborne sound, fluid-borne sound, and structure-borne sound must be considered. This paper was adapted from the keynote lecture at Acoustics 2005.

Physicists have developed a mathematical model to explain the breathing patterns of **canaries when they sing**, according to a paper in the 10 February issue of Physical Review Letters. By treating both a bird’s vocal organ and neurons as nonlinear systems, researchers have found that complex songs, involving notes of many frequencies and lengths, might be produced by surprisingly simple neurological structures and processes. The new model shows that birdsong is produced from the interplay between the air sac and the neural system in contrast to the long-held view in which a nervous system sends instructions to a passive body. This suggests that subharmonic behavior can play an important role in providing a complex variety of responses with minimal neural substrate.

“Sound ideas” is the title of a feature article on **phononic crystals** in the December issue of Physics World. When a wave passes through a periodic structure, interference leads to the formation of “band gaps” that prevent waves with certain frequencies from traveling through the structure. Band gaps are observed for electron waves in semiconductors, electromagnetic waves in photonic crystals, and sound waves in phononic crystals. The periodic variation in the density and speed of sound that is needed to make a phononic crystal can be achieved by making air holes in an otherwise solid structure. Negative refraction in phononic crystals is possible due to multiple scattering of sound waves at the solid-air interfaces. Phononic crystals could provide researchers in acoustics and ultrasonics with new components that offer the same level of control over sound that mirrors and lenses provide over light. [Phononic crystals were reported in Phys. Rev. Letts. **93**, 024301 (July 9, 2004); see Fall 2004 issue of ECHOS].

The **spiral shape of the cochlea** increases sensitivity to low frequency sound, according to a paper in the March 3 issue of Physical Review Letters. Although calculations show that curvature has little effect on the average vibrational energy traveling along the tube, energy increasingly accumulates near the outside edge of the spiral rather than remaining evenly spread across it. Low frequencies travel the furthest into the spiral, so the effect is strongest for them. Concentration of sound intensity translates into higher sensitivity. The researchers liken the sound propagation to the “whispering gallery modes” found in domes such as London’s St. Paul’s Cathedral.

The complex **songs of humpback whales** have their own syntax or grammar, according to an article in the 23 March issue of New Scientist. Male humpback whales produce songs that last anywhere from six to thirty minutes, and these vocalizations vary across the seasons. During breeding periods they are thought to help attract female partners. Now computer programs have been used to analyze complete songs and to demonstrate their hierarchical syntax. Shorter whale songs appear more complex than longer ones. The investigators admit that we are still a long way from understanding the meaning of whale songs, however. Some of the whale songs can be heard at www.newscientist.com/channel/life/dn8886.html.

The **acoustics of the singing voice** is the topic of a review article in the April issue of Physics World. Scientists are now able to record spectra of the human voice using relatively simple equipment, and this is having a major impact on the way singing is learned, performed, and recorded. Displaying the spectral signature of the voice in real time on a computer screen, for example, provides an effective teaching aid. It is possible to detect piracy in commercial recordings and even to synthesize the human voice to recreate lost sounds. Almost all songs recorded nowadays have undergone some degree of pitch shifting, the article claims, to disguise the fact that many pop stars cannot sing very well.

The use of **ultrasonic communication** by the concave-eared torrent frog is reported in the 16 March issue of Nature. Males of this species emit birdlike melodic calls with pronounced frequency modulations that often contain spectral energy in the ultrasonic range. This extraordinary upward extension into the ultrasonic range is likely to have evolved in response to the low-frequency ambient noise near streams.

Regular **didgeridoo** playing has been found to be an effective treatment for patients with obstructive sleep apnea, according to a report in the 23 December issue of the British Medicine Journal. Participants practiced an average of 5.9 days a week for 25.3 minutes.

New digital video technology can reveal **shock waves** as never before according to an article in the January- February issue of American Scientist. Shock waves, like sound waves, are usually as invisible as the air through which they travel. However, schlieren and shadowgraph techniques have been used for flow visualization for at least 100 years. Now high-speed digital cameras with retroreflective screens can record shock position over time and use this information to determine post-shock fluid properties.

“Drowning in Sound” is the title of an article in the April issue of IEEE Spectrum that discusses the **sonar vs. whales** Thomas D. Rossing story. In January 2005 dozens of pilot whales began to run themselves onto the sand beach along North Carolina’s Outer Banks. The U. S. Navy had been conducting a training exercise in the area around the time of the event, and an initial report by the National Marine Fisheries Service listed sonar as a possible cause for the incident. The Navy stated that the exercise took place about 100 kilometers from where the whales beached, too far to have had any effect. More than a year after the stranding, doubts still linger. The sonar controversy has also focused attention on a broader issue: oceans everywhere are getting noisier because of commercial shipping, underwater oil and gas exploration, and other human activity, and scientists have no clear idea what harm these noises have on whales and other sea creatures.

Solitons have been observed in solid crystals for the first time according to a paper in the 29 March issue of Physical Review Letters. Solitons are stable localized waves that propagate through a medium with spreading. They were first observed by the Scottish scientist John Russell in 1834 when he was watching horses drag a barge along a canal. When the boat suddenly stopped, a wave of water continued along the canal without changing shape or slowing down. Now solitons have been observed in crystals of uranium when firing beams of neutrons and X-rays into the material. Vibrations, which have wavelengths as small as the spacing between atoms in the crystal, form randomly throughout the material.

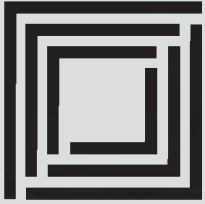
“Nanomechanics of the subreticular space caused by electromechanics of **cochlear outer hair cells**” is the title of a paper in the February 14 Issue of Proceedings of the National Academy of Sciences. The electromechanical properties of the soma of the outer hair cells in a guineapig cochlea was used to generate mechanical force over the entire functionally relevant range of 50 kHz. Vibration responses were measured with a laser Doppler vibrometer. For frequencies up to about 3 kHz, the apical surface of the inner hair cells and the opposing surface of the tectorial membrane were found to vibrate with similar amplitudes but opposite phases. At high frequencies there was little relative motion between these surfaces. For frequencies up to at least 3 kHz there appears to be direct fluid coupling between outer and inner hair cells.

Songbirds may be able to learn grammar, according to a letter in the 27 April issue of Nature. European starlings learned to recognize acoustic patterns defined by a recursive, self-embedding, context-free grammar. The simplest grammar, long thought to be one of the skills that separate man from beast, can be taught to a common songbird, the study suggests.

French physicists say they have cracked the riddle of “**singing sand dunes**” and they are compiling a CD of sand music, according to a note in the 17 September issue of New Scientist. Using sand from Moroccan singing dunes shipped to their laboratory, they found that they could play notes by pushing the sand by hand or with a metal handle. After a month of singing, however, the sands seemed to lose their voice. The singing grains were round with a smooth coating of silicon, iron and manganese, which probably formed on the sand when the dunes once lay beneath an ancient ocean, the researchers said. But in muted grains this coat had been worn away, which explains why only some dunes can sing. What determines frequency is the grain size. However, the role of the coating on the grains is still not well understood. (Ed’s note: some of the sounds can be heard at www.lps.ens.fr/~douady/SongofDunes/ArticleJduC/CD_CNRS/CD_piste3.html).

EDITORIAL BOARD / COMITÉ EDITORIAL

ARCHITECTURAL ACOUSTICS: ACOUSTIQUE ARCHITECTURALE:	Vacant		
ENGINEERING ACOUSTICS / NOISE CONTROL: GÉNIE ACOUSTIQUE / CONTROLE DU BRUIT:	Colin Novak	University of Windsor	(519) 253-3000
PHYSICAL ACOUSTICS / ULTRASOUND: ACOUSTIQUE PHYSIQUE / ULTRASONS:	Werner Richarz	Pinchin Environmental	(905) 712-6397
MUSICAL ACOUSTICS / ELECTROACOUSTICS: ACOUSTIQUE MUSICALE / ELECTROACOUSTIQUE:	Annabel Cohen	University of P. E. I.	(902) 628-4331
PSYCHOLOGICAL ACOUSTICS: PSYCHO-ACOUSTIQUE:	Annabel Cohen	University of P. E. I.	(902) 628-4331
PHYSIOLOGICAL ACOUSTICS: PHYSIO-ACOUSTIQUE:	Robert Harrison	Hospital for Sick Children	(416) 813-6535
SHOCK / VIBRATION: CHOCS / VIBRATIONS:	Li Cheng	Université de Laval	(418) 656-7920
HEARING SCIENCES: AUDITION:	Kathy Pichora-Fuller	University of Toronto	(905) 828-3865
HEARING CONSERVATION: Préservation de L’Oûie:	Alberto Behar	A. Behar Noise Control	(416) 265-1816
SPEECH SCIENCES: PAROLE:	Linda Polka	McGill University	(514) 398-4137
UNDERWATER ACOUSTICS: ACOUSTIQUE SOUS-MARINE:	Garry Heard	DRDC Atlantic	(902) 426-3100
SIGNAL PROCESSING / NUMERICAL METHODS: TRAITMENT DES SIGNAUX / METHODES NUMERIQUES:	David I. Havelock	N. R. C.	(613) 993-7661
CONSULTING: CONSULTATION:	Corjan Buma	ACI Acoustical Consultants Inc.	(780) 435-9172
ADVISOR: MEMBER CONSEILLER:	Sid-Ali Meslioui	Pratt & Whitney Canada	(450) 647-7339



**E.I. Williams
STEEL DIVISION
BUILDING SOUND SOLUTIONS**

Designers & Manufacturers of Noise Enclosures and Industrial Silencers

We specialize in custom-built silencers and noise enclosures for your specific dimensional and operational requirements.

- ◆ Rotary Positive Blower Intake & Discharge Silencers
- ◆ Pod Silencers for Rotary Positive Blowers
- ◆ Combination Silencers for Rotary Positive Blowers
- ◆ Fan Silencers
- ◆ Centrifugal Compressor Silencers
- ◆ Vent Silencers
- ◆ Engine Silencers
- ◆ Noise Enclosures...



Tel: (905) 428-0950 Toll Free: 1-877-840-3347 Fax: (905) 428-8343 Email: info@silencer.biz

**E.I. Williams Industries - 264 Fairall Street, Ajax, Ontario, Canada L1S 1R6
VISIT OUR WEB SITE AT: WWW.SILENCER.BIZ**

SOUND CONTROL SUBFLOOR PANELS



AcustiGuard Subfloor Panels are available for a wide variety of applications including:

- BUILDING CONVERSIONS
- EQUIPMENT & MECHANICAL ROOMS
- HOME THEATRE & MEDIA ROOMS
- AEROBIC & DANCE FLOORS
- GYPSUM OR CONCRETE POUR OVER



WILREP LTD.

Noise & Vibration Control Since 1977

1-888-625-8944

1515 Matheson Blvd. East Unit C-10
Mississauga, Ontario L4W 2P5
905-625-8944

www.wilrep.com
info@wilrep.com

ANNOUNCING A NEW PROGRAM OF MSc/PhD STUDIES IN HEARING SCIENCE
AT THE NATIONAL CENTRE FOR AUDIOLOGY, UNIVERSITY OF WESTERN ONTARIO


Hearing Science is one of ten fields in the new Graduate Program in Health and Rehabilitation Sciences* offered in the Faculty of Health Sciences at The University of Western Ontario.

Hearing Science is the study of normal and impaired auditory sensation and perception, and the technologies and other rehabilitation strategies for persons with hearing loss and other auditory processing disorders. All faculty supervisors are researchers at the National Centre for Audiology (<http://www.uwo.ca/nca/>). Our masters and doctoral programs are available to students interested in a research career in the hearing sciences. We welcome applications and inquiries from persons with diverse educational backgrounds, including engineering science, biosciences, audiology, music, linguistics, psychology, health sciences, and communication sciences.

Program information and on-line applications can be obtained at <http://www.uwo.ca/fhs/>. Contact Dr. Margaret F. Cheesman (cheesman@uwo.ca) for the most current information regarding this exciting new program.

* Pending OCGS approval

**WESTERN
ELECTRO-ACOUSTIC
LABORATORY**

A division of Veneklasen Associates, Inc. 

ACOUSTICAL TESTING & MEASUREMENTS

Laboratory Testing


Sound Transmission Loss, STC	ASTM E-90* (ISO 140*)
Sound Absorption, NRC	ASTM C-423* (ISO 354*)
Calibration of Microphones	ANSI SI-10*
Acoustic Power	ANSI S12-32

Full Anechoic Chamber Measurements also available

Field Testing

Noise Reduction, NIC, FSTC	ASTM E-336*
Impact Sound Transmission, FIIC	ASTM E-1007*
Building Facades	ASTM E-996*

*NVLAP Accredited



TEL: 661.775.3741 FAX: 661.775.3742
25132 Rye Canyon Loop Santa Clarita, CA 91355
www.weal.com

INSTRUCTIONS TO AUTHORS FOR THE PREPARATION OF MANUSCRIPTS

Submissions: The original manuscript and two copies should be sent to the Editor-in-Chief.

General Presentation: Papers should be submitted in camera-ready format. Paper size 8.5" x 11". If you have access to a word processor, copy as closely as possible the format of the articles in *Canadian Acoustics* 18(4) 1990. All text in Times-Roman 10 pt font, with single (12 pt) spacing. Main body of text in two columns separated by 0.25". One line space between paragraphs.

Margins: Top - title page: 1.25"; other pages, 0.75"; bottom, 1" minimum; sides, 0.75".

Title: Bold, 14 pt with 14 pt spacing, upper case, centered.

Authors/addresses: Names and full mailing addresses, 10 pt with single (12 pt) spacing, upper and lower case, centered. Names in bold text.

Abstracts: English and French versions. Headings, 12 pt bold, upper case, centered. Indent text 0.5" on both sides.

Headings: Headings to be in 12 pt bold, Times-Roman font. Number at the left margin and indent text 0.5". Main headings, numbered as 1, 2, 3, ... to be in upper case. Sub-headings numbered as 1.1, 1.2, 1.3, ... in upper and lower case. Sub-sub-headings not numbered, in upper and lower case, underlined.

Equations: Minimize. Place in text if short. Numbered.

Figures/Tables: Keep small. Insert in text at top or bottom of page. Name as "Figure 1, 2, ..." Caption in 9 pt with single (12 pt) spacing. Leave 0.5" between text.

Line Widths: Line widths in technical drawings, figures and tables should be a minimum of 0.5 pt.

Photographs: Submit original glossy, black and white photograph.

Scans: Should be between 225 dpi and 300 dpi. Scan: Line art as bitmap tiffs; Black and white as grayscale tiffs and colour as CMYK tiffs;

References: Cite in text and list at end in any consistent format, 9 pt with single (12 pt) spacing.

Page numbers: In light pencil at the bottom of each page. Reprints: Can be ordered at time of acceptance of paper.

DIRECTIVES A L'INTENTION DES AUTEURS PREPARATION DES MANUSCRITS

Soumissions: Le manuscrit original ainsi que deux copies doivent être soumis au rédacteur-en-chef.

Présentation générale: Le manuscrit doit comprendre le collage. Dimensions des pages, 8.5" x 11". Si vous avez accès à un système de traitement de texte, dans la mesure du possible, suivre le format des articles dans *l'Acoustique Canadienne* 18(4) 1990. Tout le texte doit être en caractères Times-Roman, 10 pt et à simple (12 pt) interligne. Le texte principal doit être en deux colonnes séparées d'un espace de 0.25". Les paragraphes sont séparés d'un espace d'une ligne.

Marges: Dans le haut - page titre, 1.25"; autres pages, 0.75"; dans le bas, 1" minimum; latérales, 0.75".

Titre du manuscrit: 14 pt à 14 pt interligne, lettres majuscules, caractères gras. Centré.

Auteurs/adresses: Noms et adresses postales. Lettres majuscules et minuscules, 10 pt à simple (12 pt) interligne. Centré. Les noms doivent être en caractères gras.

Sommaire: En versions anglaise et française. Titre en 12 pt, lettres majuscules, caractères gras, centré. Paragraphe 0.5" en alinéa de la marge, des 2 cotés.

Titres des sections: Tous en caractères gras, 12 pt, Times-Roman. Premiers titres: numéroter 1, 2, 3, ..., en lettres majuscules; sous-titres: numéroter 1.1, 1.2, 1.3, ..., en lettres majuscules et minuscules; sous-sous-titres: ne pas numéroter, en lettres majuscules et minuscules et soulignés.

Equations: Les minimiser. Les insérer dans le texte si elles sont courtes. Les numéroter.

Figures/Tableaux: De petites tailles. Les insérer dans le texte dans le haut ou dans le bas de la page. Les nommer "Figure 1, 2, 3, ..." Légende en 9 pt à simple (12 pt) interligne. Laisser un espace de 0.5" entre le texte.

Largeur Des Traits: La largeur des traits sur les schémas technique doivent être au minimum de 0.5 pt pour permettre une bonne reproduction.

Photographies: Soumettre la photographie originale sur papier glacé, noir et blanc.

Figures Scanées: Doivent être au minimum de 225 dpi et au maximum de 300 dpi. Les schémas doivent être scannés en bitmaps tif format. Les photos noir et blanc doivent être scannées en échelle de gris tifs et toutes les photos couleurs doivent être scannées en CMYK tifs.

Références: Les citer dans le texte et en faire la liste à la fin du document, en format uniforme, 9 pt à simple (12 pt) interligne.

Pagination: Au crayon pâle, au bas de chaque page. Tirés-à-part: Ils peuvent être commandés au moment de l'acceptation du manuscrit.

The Canadian Acoustical Association l'Association Canadienne d'Acoustique



Application for Membership

CAA membership is open to all individuals who have an interest in acoustics. Annual dues total \$60.00 for individual members and \$20.00 for Student members. This includes a subscription to *Canadian Acoustics*, the Association's journal, which is published 4 times/year. New membership applications received before August 31 will be applied to the current year and include that year's back issues of *Canadian Acoustics*, if available. New membership applications received after August 31 will be applied to the next year.

Subscriptions to *Canadian Acoustics* or Sustaining Subscriptions

Subscriptions to *Canadian Acoustics* are available to companies and institutions at the institutional subscription price of \$60.00. Many companies and institutions prefer to be a Sustaining Subscriber, paying \$250.00 per year, in order to assist CAA financially. A list of Sustaining Subscribers is published in each issue of *Canadian Acoustics*.

Subscriptions for the current calendar year are due by January 31. New subscriptions received before August 31 will be applied to the current year and include that year's back issues of *Canadian Acoustics*, if available.

Please note that electronic forms can be downloaded from the CAA Website at caa-aca.ca

Address for subscription / membership correspondence:

Name / Organization _____
 Address _____
 City/Province _____ Postal Code _____ Country _____
 Phone _____ Fax _____ E-mail _____

Address for mailing *Canadian Acoustics*, if different from above:

Name / Organization _____
 Address _____
 City/Province _____ Postal Code _____ Country _____

Areas of Interest: (Please mark 3 maximum)

- | | | |
|--|---|--|
| 1. Architectural Acoustics | 5. Psychological / Physiological Acoustic | 9. Underwater Acoustics |
| 2. Engineering Acoustics / Noise Control | 6. Shock and Vibration | 10. Signal Processing /
Numerical Methods |
| 3. Physical Acoustics / Ultrasound | 7. Hearing Sciences | 11. Other |
| 4. Musical Acoustics / Electro-acoustics | 8. Speech Sciences | |

For student membership, please also provide:

 (University) (Faculty Member) (Signature of Faculty Member) (Date)

I have enclosed the indicated payment for:
 CAA Membership \$ 60.00
 CAA Student Membership \$ 20.00
 Institutional Subscription \$ 60.00
 Sustaining Subscriber \$ 250.00
 includes subscription (4 issues /year)
 to *Canadian Acoustics*.

Payment by: Cheque
 Money Order
 VISA credit card (Only VISA accepted)

For payment by VISA credit card:

Card number _____
 Name of cardholder _____
 Expiry date _____

Mail application and attached payment to: _____

(Signature) (Date)

D. Quirt, Secretary, Canadian Acoustical Association, PO Box 74068, Ottawa, Ontario, K1M 2H9, Canada



Formulaire d'adhésion

L'adhésion à l'ACA est ouverte à tous ceux qui s'intéressent à l'acoustique. La cotisation annuelle est de 60.00\$ pour les membres individuels, et de 20.00\$ pour les étudiants. Tous les membres reçoivent *'Acoustique Canadienne'*, la revue de l'association. Les nouveaux abonnements reçus avant le 31 août s'appliquent à l'année courante et incluent les anciens numéros (non-épuisés) de *'Acoustique Canadienne'* de cette année. Les nouveaux abonnements reçus après le 31 août s'appliquent à l'année suivante.

Abonnement pour la revue *Acoustique Canadienne* et abonnement de soutien

Les abonnements pour la revue *Acoustique Canadienne* sont disponibles pour les compagnies et autres établissements au coût annuel de 60.00\$. Des compagnies et établissements préfèrent souvent la cotisation de membre bienfaiteur, de 250.00\$ par année, pour assister financièrement l'ACA. La liste des membres bienfaiteurs est publiée dans chaque issue de la revue *Acoustique Canadienne*. Les nouveaux abonnements reçus avant le 31 août s'appliquent à l'année courante et incluent les anciens numéros (non-épuisés) de *'Acoustique Canadienne'* de cette année. Les nouveaux abonnements reçus après le 31 août s'appliquent à l'année suivante.

Pour obtenir des formulaires électroniques, visitez le site Web: caa-aca.ca

Pour correspondance administrative et financière:

Nom / Organisation _____

Adresse _____

Ville/Province _____ Code postal _____ Pays _____

Téléphone _____ Téléc. _____ Courriel _____

Adresse postale pour la revue Acoustique Canadienne

Nom / Organisation _____

Adresse _____

Ville/Province _____ Code postal _____ Pays _____

Cocher vos champs d'intérêt: (maximum 3)

- | | | |
|---|-------------------------------|--|
| 1. Acoustique architecturale | 5. Physio / Psycho-acoustique | 9. Acoustique sous-marine |
| 2. Génie acoustique / Contrôle du bruit | 6. Chocs et vibrations | 10. Traitement des signaux / Méthodes numériques |
| 3. Acoustique physique / Ultrasons | 7. Audition | 11. Autre |
| 4. Acoustique musicale / Electro-acoustique | 8. Parole | |

Prière de remplir pour les étudiants et étudiantes:

(Université) (Nom d'un membre du corps professoral) (Signature du membre du corps professoral) (Date)

Cocher la case appropriée:

- Membre individuel \$ 60.00
- Membre étudiant(e) \$ 20.00
- Abonnement institutionnel \$ 60.00
- Abonnement de soutien \$ 250.00
(comprend l'abonnement à *L'acoustique Canadienne*)

Méthode de paiement:

- Chèque au nom de l'Association Canadienne d'Acoustique
- Mandat postal
- VISA (Seulement VISA)

Pour carte VISA: Carte n° _____

Nom _____

Date d'expiration _____

Prière d'attacher votre paiement au formulaire d'adhésion. Envoyer à :

(Signature)

(Date)

Secrétaire exécutif, Association Canadienne d'Acoustique, Casier Postal 74068, Ottawa, K1M 2H9, Canada

The Canadian Acoustical Association l'Association Canadienne d'Acoustique



PRESIDENT PRÉSIDENT

Stan Dosso
University of Victoria
Victoria, British Columbia
V8W 3P6
(250) 472-4341
sdosso@uvic.ca

PAST PRESIDENT PRÉSIDENT SORTANT

John Bradley
IRC, NRCC
Ottawa, Ontario
K1A 0R6
(613) 993-9747
john.bradley@nrc-cnrc.gc.ca

SECRETARY SECRÉTAIRE

David Quirt
P. O. Box 74068
Ottawa, Ontario
K1M 2H9
(613) 993-9746
dave.quirt@nrc-cnrc.gc.ca

TREASURER TRÉSORIER

Dalila Giusti
Jade Acoustics
545 North Rivermede Road, Suite 203
Concord, Ontario
L4K 4H1
(905) 660-2444
dalila@jadeacoustics.com

EDITOR-IN-CHIEF RÉDACTEUR EN CHEF

Ramani Ramakrishnan
Dept. of Architectural Science
Ryerson University
350 Victoria Street
Toronto, Ontario
M5B 2K3
(416) 979-5000 #6508
rramakri@ryerson.ca
ramani@aiolos.com

WORLD WIDE WEB HOME PAGE: <http://www.caa-aca.ca>

Dave Stredulinsky
(902) 426-3100

ASSISTANT EDITOR RÉDACTEUR ADJOINT

Ralph Baddour
Department of Medical Biophysics
University of Toronto
rbaddour@uhnres.utoronto.ca

DIRECTORS DIRECTEURS

Alberto Behar
(416) 265-1816
behar@sympatico.ca

Nicole Collison
(902) 426-3100, Ext. 94
nicole.collison@drdc-rddc-gc.ca

Vijay Parsa
(519) 661-2111 Ex. 88947
parsa@nce.uwo.ca

Corjan Buma
(780) 435-9172
bunacj@superiway.net

Christian Giguère
613-562-5800 Ext. 3071
cgigure@UOTTAWA.CA

Richard Peppin
(410) 290-7726
peppinr@scantekinc.com

Mark Cheng
(604) 276-6366
mark_cheng@yvr.ca

Anita Lewis
(403) 297-3793
anita.lewis@gov.ab.ca

SUSTAINING SUBSCRIBERS / ABONNES DE SOUTIEN

The Canadian Acoustical Association gratefully acknowledges the financial assistance of the Sustaining Subscribers listed below. Annual donations (of \$250.00 or more) enable the journal to be distributed to all at a reasonable cost. Sustaining Subscribers receive the journal free of charge. Please address donation (made payable to the Canadian Acoustical Association) to the Secretary of the Association.

L'Association Canadienne d'Acoustique tient à témoigner sa reconnaissance à l'égard de ses Abonnés de Soutien en publiant ci-dessous leur nom et leur adresse. En amortissant les coûts de publication et de distribution, les dons annuels (de \$250.00 et plus) rendent le journal accessible à tous nos membres. Les Abonnés de Soutien reçoivent le journal gratuitement. Pour devenir un Abonné de Soutien, faites parvenir vos dons (chèque ou mandat-poste fait au nom de l'Association Canadienne d'Acoustique) au secrétaire de l'Association.

ACI Acoustical Consultants Inc.

Mr. Steven Bilawchuk - (780) 414-6373
stevenb@aciacoustical.com - Edmonton, AB

Acoustik GE Inc.

M. Gilles Elhadad - (514) 487 7159
ge@acoustikge.com - Cote St Luc, QC

Dalimar Instruments Inc.

Mr. Daniel Larose - (514) 424-0033
daniel@dalimar.ca - Vaudreuil-Dorion, QC

Eckel Industries of Canada Ltd.

Mr. Blake Noon - (613) 543-2967
eckel@eckel.ca - Morrisburg, ON

HGC Engineering Ltd.

Mr. Bill Gastmeier - (905) 826-4044
info@hgcengineering.com - Mississauga, ON

J.E. Coulter Associates Ltd.

Mr. John Coulter - (416) 502-8598
jcoulter@on.aibn.com - Toronto, ON

JASCO Research Ltd.

Mr. Scott Carr - (902) 491-4489
scott@jasco.com - Halifax, NS

Novel Dynamics Test Inc.

Mr. Andy Metelka - (519) 853-4495
metelka@aztec-net.com - Acton, ON

Peutz & Associés

M. Marc Asselineau +33 1 45230500
marc.asselineau@club-internet.fr
Paris, FRANCE

Pyrok Inc.

Mr. Howard Podolsky, (914) 777-7770
info@pyrokinc.com - Mamaroneck, NY

SILEX Innovations Inc.

Mr. Mehmood Ahmed - (905) 612-4000
mehmooda@silex.com - Mississauga, ON

Solutions Acoustiques Inc.

Sylvain Larivière - (514) 793-3767,
sylvainlariviere@solutionsacoustiques.com -
Laval, QC

State of the Art Acoustik Inc.

Dr. C. Fortier - (613) 745-2003
sota@sota.ca - Ottawa, ON

Valcoustics Canada Ltd.

Dr. Al Lightstone - (905) 764-5223
solutions@valcoustics.com - Richmond Hill, ON

Water & Earth Science Assoc. (WESA)

Dejan Zivkovic, M.Sc. - (905) 639-5789 x151
dzivkovic@wesa.ca - Burlington, ON

ACO Pacific Inc.

Mr. Noland Lewis - (650) 595-8588
acopac@acopacific.com - Belmont, CA

Aercoustics Engineering Ltd

Mr. John O'Keefe - (416) 249-3361
aercoustics@aercoustics.com - Rexdale, ON

Dodge-Regupol

Mr. Paul Downey - (416) 440-1094
pcd@regupol.com - Toronto, ON

H.L. Blachford Ltd.

Mr. Dalton Prince - (905) 823-3200
amsales@blachford.ca - Mississauga, ON

Hydro-Quebec

M. Blaise Gosselin - (514) 840-3000x5134
gosselin.blaise@hydro.qc.ca - Montréal, QC

J.L.Richards & Assoc. Ltd.

Mr. Fernando Ribas - (613) 728-3571
mail@jlrichards.ca - Ottawa, ON

Mc SQUARED System Design Group

Mr. Wade McGregor - (604) 986-8181
info@mcsquared.com - North Vancouver, BC

Owens-Corning Canada Inc.

Mr. Keith Wilson - (800) 988-5269
keith.wilson@owenscorning.com - Orillia, ON

Michel Picard

(514) 343-7617; FAX: (514) 343-2115
michel.picard@umontreal.ca - Brossard, QC

Royal Mat Inc

R. Ducharme - (418) 774-3694
R.Ducharme@Royalmat.com, Beauceville, QC

SNC/Lavalin Environment Inc.

M. Jean-Luc Allard - (514) 651-6710
jeanluc.allard@snclavalin.com - Longueuil, QC

SounDivide Inc.

C.W. Roy Bakker - (416) 208-3040
roy.bakker@SounDivide.com - Mississauga, ON

Swallow Acoustic Consultants Ltd.

Mr. John Swallow - (905) 271-7888
jswallow@jsal.ca - Mississauga, ON

Vibro-Acoustics

Mr. Tim Charlton - (800) 565-8401
tcharlton@vibro-acoustics.com - Scarborough

West Caldwell Calibration Labs

Mr. Stanley Christopher - (905) 595-1107
info@wcccl.com - Brampton, ON

Acoustec inc.

Dr. J.G. Migneron - (418) 834-1414
courrier@acoustec.qc.ca - St-Nicolas, QC

Bruel & Kjaer North America Inc.

Mr. Andrew Khoury - (514) 695-8225
andrew.khoury@bksv.com - Pointe-Claire, QC

Earth Tech Canada Inc.

Ms. Deborah Olsen - (905) 886-7022x2209
noisevibration@earthtech.ca - Markham, ON

Hatch Associates Ltd.

Mr. Tim Kelsall - (905) 403-3932
tkelsall@hatch.ca - Mississauga, ON

Integral DX Engineering Ltd.

Mr. Greg Clunis - (613) 761-1565
greg@integraldxengineering.ca - Ottawa, ON

Jade Acoustics Inc.

Ms. Dalila Giusti - (905) 660-2444
dalila@jadeacoustics.com - Concord, ON

MJM Conseillers en Acoustique Inc.

MJM Acoustical Consultants Inc.
M. Michel Morin - (514) 737-9811
mmorin@mjm.qc.ca - Montréal, QC

OZA Inspections Ltd.

Mr. David Williams - (800) 664-8263x25
oza@ozagroup.com - Grimsby, ON

Pinchin Environmental Ltd.

(905) 507-4855; FAX: (905) 507-9151
nwilliams@pinchin.com - Mississauga, ON

Scantek Inc.

Mr. Richard J. Peppin - (410)-290-7726
peppinr@scantekinc.com - Columbia, MD

Soft dB Inc.

M. André L'Espérance - (418) 686-0993
contact@softdb.com - Sillery, QC

Spaarg Engineering Ltd.

Dr. Robert Gaspar - (519) 972-0677
gasparr@kelcom.igs.net - Windsor, ON

Tacet Engineering Ltd.

Dr. M.P. Sacks - (416) 782-0298
mal.sacks@tacet.ca - Toronto, ON

Wakefield Acoustics Ltd.

Mr. Clair Wakefield - (250) 370-9302
nonoise@shaw.ca - Victoria, BC

Wilrep Ltd.

Mr. Don Wilkinson - (905) 625-8944
info@wilrep.com - Mississauga, ON